

Development of methods for the synthesis of large combinatorial libraries of macrocyclic compounds

Présentée le 26 mai 2023

Faculté des sciences de base
Laboratoire de protéines et peptides thérapeutiques
Programme doctoral en chimie et génie chimique

pour l'obtention du grade de Docteur ès Sciences

par

Mischa SCHÜTTEL

Acceptée sur proposition du jury

Prof. K. Sivula, président du jury
Prof. C. Heinis, directeur de thèse
Prof. O. Seitz, rapporteur
Dr H. M. Maric, rapporteur
Prof. G. Turcatti, rapporteur

Acknowledgments

First, I would like to express my utmost gratitude and say “merci viu mau” to my family, namely my parents, Carmen and Jürg, brothers, Dimitri and Olivier, and sister, Noëlla, for their unconditional support. I am pleased and proud to have you all around me; without you, it would not have been possible.

I want to thank my doctoral thesis advisor, Prof. Christian Heinis. Since joining the laboratory, I have been laser focus on helping and developing the macrocycle platform and was inspired by your passion for science and peptide-based drugs. I have very much enjoyed working with and learning from you throughout the last 4.5 years. You offered me an excellent and resourceful environment in an outstanding balance of freedom and guidance to further develop my hypothesizing, problem identification and solving experimental designing and critical thinking, and scientific presentation skills. I would also like to thank senior scientist Dr. Ruud Hovius, who willingly acted as a mentor throughout my studies. In addition, I very much enjoyed teaching the course “Experimental Biochemistry and Biophysics” multiple times with you to help students develop laboratory skills in an educational and enjoyable environment. Regarding my first-year candidacy exam, I thank Prof. Beat Fierz and Prof. Paul Dyson for taking the time and providing me with valuable input for my doctoral thesis during my first-year candidacy exam. Finally, I would like to express my gratitude to the internal and external jury members and president, Prof. Gerardo Turcatti, Prof. Oliver Seitz, Dr. Hans Michael Maric and Prof. Kevin Sivula.

A smooth daily working and study routine at EPFL with delicious sweet surprises would not have been possible without the laboratory’s secretary, Béatrice Bliesener and the administrative assistant of the doctoral program, Anne Lene Odegaard. Thank you both a lot! Moreover, I highly appreciated the well-organized structure of the Institute of Chemical Sciences and Engineering (ISIC) at EPFL, providing access to multiple platforms from which I was able to take full advantage. It comprises the chemical store (Maurizio Maio, Sven André von Rotz, Florent Menoud), mechanical (Guillaume Francey, André Fattet, Florian Pattiny) and electronic (Benjamin Charles Le Geyt, Harald Holze) workshop as well as IT support (Lorenzo Chiriatti), Mass spectroscopy (Daniel Ortiz Trujillo) and nuclear magnetic resonance facility (Aurélien Bornet). Thank you all!

An exceptional thank you goes to all LPPT members who are still enrolled (Anne, Chei-Wei, Edward, Grégoire and Zsolt) or have already graduated (Alessandro, Patrick, Vanessa, Manuel, Gontran and Sevan), current and former (Alexander, Bo, Cristina, Lluc, Ganesh M., Ganesh S., Hang, Jun, Sangram, Xudong, Xinjian, Xingwang and Yuteng) or visited as a project student (Bo, Camilla, Conor, Edouard, Ilaria, Jaijun, Mahdi, Maurice, Pauline and Thomas). Many thanks to Camilla and Mahdi, whom I had the great pleasure of supervising. I have very much appreciated your work and personality. I enjoyed the group's ambiance to share and conceptualize ideas and discuss diverse topics in sound but also in frustrating times when science did not go the anticipated path. In my leisure time, I also had the opportunity to travel to multiple countries worldwide, from Japan to El Salvador over Norway to Denmark and discover Switzerland in greater detail during COVID times. I was super glad to follow and share my hobbies like traveling, photography, wellness, movies, eating, snowboarding, hiking and camping and fishing with many great people. Thank you all (Adi, Alex, Beni, Didi, Fabian, Gontran, Pam and Reto)!

Last but not least, a huge thank you goes to my fantastic girlfriend, Pamela. You always have unconditionally supported me and I am very thankful to have you. You are an awesome girlfriend and I thank you a thousand times for your love and support. Can't wait to spend many more years with you!

Abstract

Macrocycles have raised much interest in the pharmaceutical industry due to their ability to bind challenging targets, while often still being able to cross membranes for reaching intracellular proteins. However, the development of macrocyclic ligands to new disease targets is hindered by the limited availability of large, structurally diverse macrocyclic compound libraries suitable for high-throughput screening. To address this gap, the overall goal of my thesis was to develop methods and tools to synthesize large libraries of structurally diverse macrocyclic compounds.

In my first project, I have investigated the efficiency of a wide range of commercially available bis-electrophilic reagents to cyclize short peptides via two thiol groups. Such reagents are of interest as they allow the synthesis of $m \times n$ macrocyclic compounds if " m " short di-thiol peptides are combinatorially reacted with " n " bis-electrophilic reagents. I have assessed the reaction efficiency of 46 different bis-electrophilic reagents undergoing either S_N2 , Michael addition and epoxide opening reactions. Of these reagents, 35 cyclized peptides with around 50% or greater yield, a bar considered as sufficient for synthesizing and screening combinatorially cyclized peptides as crude products. As a useful guide to di-thiol peptide cyclization reagent selection, I present information about the best performing bis-electrophilic reagents as a "periodic table", organized by number of backbone atoms inserted, reaction efficiency and reaction type.

In my second project, I have developed high-density immobilized tris-(2-carboxyethyl)phosphine (TCEP) beads based on silica support for efficient disulfide bond reduction of di-thiol peptides and subsequent cyclization by bis-electrophile reagents. The immobilization of TCEP on beads allows its efficient removal, which is necessary as it would react with bis-electrophilic cyclization reagents. The generation of "high-density" TCEP beads was required as commercially provided agarose TCEP beads have a rather low reducing capacity, making them unsuitable for disulfide reduction at millimolar peptide concentrations. I tested a wide range of different solid supports and found that conjugation to silica gel offered an 8-fold higher reducing capacity ($129 \pm 16 \mu\text{mol/mL}$ wet beads) compared to commercial agarose TCEP beads.

In my third project, I have modified a commercial 96-well parallel peptide synthesizer so that it can synthesize peptides in 384-well plates. This was achieved by developing hardware parts to hold 384-well plates, a multichannel dispenser unit with 16 channels and a reagents rack that could hold more than hundred different Fmoc amino acids. This allowed the synthesis of peptides in four 384-well reactor plates and thus 1,536 peptides in one run. Moreover, I have designed and developed practical tools for rapid and homogenous resin loading to 96- and 384-well plates. The new synthesizer is now intensively used by several members of the lab and eliminated a major bottleneck of the group's macrocycle library synthesis platform.

In my fourth project, I have tested if microvalves can be used to precisely and rapidly transfer reagents and solvents for parallel solid-phase peptide synthesis. This was of interest as syringe-based dispensing, used in commercial parallel peptide synthesizers, is limited in precision and speed, in particular for the synthesis in 384-well plates. I was able to apply solenoid microvalves for dispensing organic solvents required for peptide synthesis such as DMF or DCM and highly corrosive TFA. I further showed that short peptides can be synthesized by microvalve dispensing in 384-well plates and even in 1,536-well plates, demonstrating the potential of microvalve dispensing in increasing the throughput and miniaturization of parallel peptide synthesis.

In summary, I have developed multiple methods and tools to facilitate the chemical synthesis and production of large libraries of peptide-based macrocycles. Most impactful of the four projects may be the peptide synthesis in 384-well plates that has been applied already by more than eight persons of the lab, who synthesized in total more than 20,000 peptides over the course of the last year. Hopefully, the methods and tools will contribute to the discovery of new macrocyclic ligands against therapeutically important targets and the discovery of drugs for currently unmet medical needs.

Zusammenfassung

Makrozyklen haben großes Interesse in der pharmazeutischen Industrie geweckt, da sie sich an schwierige therapeutische Ziele binden können, während sie oft immer noch in der Lage sind, Membranen zu durchqueren, um intrazelluläre Proteine zu erreichen. Die Entwicklung von makrozyklischen Liganden für neue Krankheitsziele wird jedoch durch die begrenzte Verfügbarkeit von großen, strukturell vielfältigen makrozyklischen Verbindungsbibliotheken behindert, die für das Hochdurchsatz-Screeningverfahren notwendig wären. Das übergeordnete Ziel meiner Doktorarbeit ist es, diese Lücke zu schliessen und Methoden und Werkzeuge zu entwickeln, die zur Herstellung von strukturell unterschiedlichen und makrozyklischen Bibliotheken verhelfen.

In meinem ersten Projekt habe ich die Effizienz einer breiten Palette an kommerziell erhältlichen bis-elektrophile Reagenzien untersucht, um kurze Peptide über zwei Thiolgruppen zu zyklisieren. Solche Reagenzien sind von Interesse, da sie die Synthese von $m \times n$ makrozyklischen Verbindungen ermöglichen, wenn „m“ kurze Dithiolpeptide kombinatorisch mit „n“ bis-elektrophilen Reagenzien umgesetzt werden. Ich habe die Reaktionseffizienz von 46 verschiedenen bis-elektrophilen Reagenzien bewertet, die entweder S_N2 -, Michael-Addition- oder Epoxidöffnungsreaktionen durchlaufen. Von diesen Reagenzien zyklisierten 35 Linkerreagenzien ausreichend. Unser Richtwert von etwa 50% Ausbeute sahen wir als genügend für die Synthese und das Screenen von rohen kombinatorisch zyklisierten Peptiden. Als nützlicher Leitfaden für die Auswahl von Reagenzien für die Dithiol-Peptid-Zyklisierung präsentiere ich die leistungsstärksten gefundenen bis-elektrophilen Reagenzien in Form eines „Periodensystem“, geordnet nach Anzahl der eingefügten Gerüstatomen, Reaktionseffizienz und des Reaktionstyps.

In meinem zweiten Projekt habe ich hochdichte immobilisierte Tris-(2-carboxyethyl)phosphin (TCEP)-Kügelchen auf Basis von Silica-Trägern, für die effiziente Reduktion von Disulfid Bindungen in Dithiolpeptiden und dessen anschließende Zyklisierung durch bis-elektrophile Reagenzien, entwickelt. Die Immobilisierung von TCEP auf Kügelchen ermöglichte seine effiziente Entfernung, was notwendig ist, da es sonst mit den bis-elektrophilen Zyklisierungsreagenzien nebenreagieren kann. Die

Erzeugung von TCEP-Kügelchen mit "hoher Dichte" war erforderlich, da kommerziell bereitgestellte Agarose-TCEP-Kügelchen eine relative geringe Reduktionskapazität aufweisen, welche sich für die Reduktion von millimolaren Peptidkonzentrationen nicht eignen. Ich habe eine breite Palette an diversen Feststoffträgern getestet und festgestellt, dass die Konjugation an Kieselgel eine 8-fache höhere Reduktionskapazität ($129 \pm 16 \mu\text{mol/ml}$ Sediment), im Vergleich zu kommerziellen erhältlichen Agarose-TCEP-Kügelchen bietet.

In meinem dritten Projekt habe ich einen kommerziellen 96-Well-Parallel-Peptid-Synthesizergerät so modifiziert, dass es Peptide in 384-Well-Platten produzieren kann. Dies wurde durch die Entwicklung von Hardwarebestandteilen zur Einspannung von 384-Well-Platten, einen Mehrkanal-Dispensierungseinheit mit 16 Kanälen und einem Reagenzien Gestell ermöglicht, und stellte somit mehr als hundert verschiedene Fmoc-Aminosäuren zur Peptiddiversifizierung bereit. Dies ermöglichte die Peptidsynthese von vier 384-Well-Reaktorplatten und maximal 1'536 einzelne Peptide in einem Durchlauf. Darüber hinaus habe ich praktische Werkzeuge für die schnelle und homogene Beladung von Harz in 96- und 384-Well-Platten entworfen und entwickelt. Der neue Synthesizer wird jetzt von mehreren Labormitgliedern intensiv genutzt und beseitigt einen großen Engpass der von der Gruppe entwickelten Syntheseplattform zur Generierung von makrozyklischen Verbindungsbibliotheken.

In meinem vierten Projekt habe ich überprüft, ob Mikroventile für die parallele Festphasen-Peptidsynthese verwendet werden können, um Reagenzien und Lösungsmittel präzise und schnell zu transferieren. Dies war von grossem Interesse, da die spritzenbasierte Flüssigkeitsabgabe eine begrenzte Präzision und Geschwindigkeit aufweist und insbesondere für die Synthese von Peptiden in 384-Well-Platten problematisch sein kann. Ich konnte erfolgreich Magnet-Mikroventile zum Dosieren von organischen Lösungsmitteln wie DMF oder DCM und hochkorrosives TFA einsetzen, die für die Peptidsynthese benötigt werden. Ich habe aufzeigen können, dass kurze Peptide durch Mikroventil-Dispensierung in 384-Well- und sogar in 1'536-Well-Platten synthetisiert werden können. Das Potenzial der Mikroventil-Dispensierung zur Erhöhung

des Durchsatzes und Miniaturisierung der parallelen Peptidsynthese wurde in dieser Arbeit demonstriert.

Zusammenfassend habe ich mehrere Methoden und Werkzeuge entwickelt, die die chemische Synthese und Produktion großer Peptid-basierten Makrozyklenbibliotheken erleichtert. Die wirkungsvollste der vier Projekte dürfte die Peptidsynthese in 384-Well-Platten sein, die bereits von mehr als acht Labormitarbeitern routinemässige Anwendung findet. Im Laufe des letzten Jahres haben sie insgesamt mehr als 20,000 Peptide synthetisiert. Hoffentlich werden diese entwickelten Methoden und Werkzeuge einen wichtigen Beitrag zur Entdeckung neuer makrozyklischer Liganden gegen therapeutisch relevante Ziele und Arzneimitteln, für derzeit unerfüllte medizinische Bedürfnisse, leisten.

Table of Content

Acknowledgments	2
Abstract	4
Zusammenfassung	6
Table of Content	9
List of abbreviations	11
1. Introduction	14
1.1 Macrocycles as therapeutics	16
1.1.1 Properties of macrocycles	16
1.1.2 Macrocycle drugs	20
1.2 Methods for generating and screening macrocyclic compound libraries	23
1.2.1 Existing macrocycle libraries for high-throughput screening (HTS)	23
1.2.2 One-bead one-compound (OBOC) macrocycle libraries	28
1.2.3 DNA-encoded libraries (DELs) of macrocyclic compounds	30
1.3 Nano-scale synthesis of macrocycle libraries	33
1.3.1 Solid phase synthesis of disulfide-containing peptides	34
1.3.2 Combinatorial synthesis of macrocycle libraries using acoustic dispensing	37
1.3.3 Solid phase synthesis of dithiol peptides	41
1.4 References	44
2. Aim of the thesis	56
3. Reactivity and properties of thiol-thiol peptide cyclization reagents presented as a periodic table	58
3.1 Work contribution	59
3.2 Abstract	60
3.3 Introduction	61
3.4 Results & discussion	67
3.5 Conclusion	72
3.6 Material & methods	73
3.7 Supplementary information	77
3.8 References	111
4. High-density immobilization of TCEP on silica beads for efficient disulfide bond reduction and alkylation	115
4.1 Work contribution	116
4.2 Abstract	118
4.3 Introduction	119
4.4 Results & discussion	122
4.5 Conclusion	131
4.6 Material & methods	132
4.7 Supplementary information	141
4.8 References	145
5. Solid-phase peptide synthesis in 384-well plates	147
5.1 Work contribution	148

5.2	Abstract.....	150
5.3	Introduction	151
5.4	Results & discussion.....	154
5.5	Conclusion	164
5.6	Material & methods	165
5.7	Supplementary information	180
5.8	Reference	200
6.	<i>Use of microvalves for reagent dispensing in solid-phase peptide synthesis.....</i>	203
6.1	Work contribution.....	204
6.2	Abstract.....	206
6.3	Introduction	207
6.4	Results & discussion.....	210
6.5	Conclusion	218
6.6	Material & methods	219
6.7	Supplementary information	227
6.8	References	237
7.	<i>General Conclusion.....</i>	238
8.	<i>Curriculum Vitae.....</i>	240

List of abbreviations

AcOH	Acetic acid
ADE	Acoustic droplet ejection
ALK	Anaplastic lymphoma kinase
AM	Amino methyl
APTES	(3-aminopropyl)triethoxysilane
BBP	2,6-bis(bromomethyl)pyridine
BCP	1,4-bis(chloroacetyl)piperazine
BDT	1,4-butadiene
bRo5	Beyond rule of five
CAD	Computer aided design
CAS	Chemical abstract service
cLogP	Calculated partition coefficient
CNC	Computerized Numerical Control
CNS	Central nervous system
d	Diameter
Da	Dalton
DBM	2,3-dibromomaleimide
DCA	1,3-dichloroacetone
DCM	dichloromethane
DEL	DNA encoded library
DIPEA	Diisopropylethyl amine
DMF	Dimethyl formamide
DMSO	Dimethylsulfoxide
DNA	Deoxyribonucleic acid
DTT	Dithiothreitol
DVS	Divinyl sulfones
DWP	Deep well plate
EBA	<i>N,N'</i> -ethylenebis(acrylamide)
EDC	<i>N</i> -(3-dimethylaminopropyl)- <i>N</i> -ethylcarbodiimide
EM	Exact mass
EPFL	École Polytechnique Fédérale de Lausanne
eRo5	Expanded rule of five
Et ₂ O	Diethyl ether
EtOAc	Ethyl acetate
EVA	Ethylene vinyl acetate
FDA	U.S. Food and Drug Administration
FFKM	Perfluoroelastomer
FK506	Tacrolimus (drug)

FKBP	FK506 binding protein
Fmoc	9-Fluorenylmethoxycarbonyl
FRB	FKBP-rapamycin-binding domain
GPCR	G-protein-coupled receptors
h	Height
HATU	1-[Bis(dimethylamino)methylene]-1 <i>H</i> -1,2,3-triazolo[4,5- <i>b</i>]pyridinium 3-oxid hexafluorophosphate
HBA	Hydrogen bond acceptor
HBD	Hydrogen bond donor
HBTU	<i>N,N,N',N'</i> -Tetramethyl- <i>O</i> -(1 <i>H</i> -benzotriazol-1-yl)uronium hexafluorophosphate
HPLC	High performance liquid chromatography
HT	High-throughput
HTS	High-throughput screening
JAK2	Januskinase 2
K _i	Inhibitor constants (conc. at which 1/2 max inhibition)
KLK5	Tissue Kallikrein related peptidase 5
L	Linker
l	Length
ISIC	Institute of Chemical Sciences and Engineering
LCMS	Liquid chromatography mass spectroscopy
LPPT	Laboratory of therapeutic proteins and peptides
MC	Macrocycle
MDM2	Moused double minute 2 (E3 ubiquitin-protein ligase Mdm2)
Mea	Mercaptoethyl amine
MeCN	Acetonitrile
MeNbz	<i>N</i> -acyl- <i>N'</i> -methyl-benzimidazolinone
MeOH	Methanol
MES	2-(<i>N</i> -morpholino)ethanesulfonic acid
Mpa	3-mercaptopropionic acid
mRNA	messenger RNA
Mw	Molecular weight
n.c.	Not compatible
N.D.	Not determin
NEt ₃	Triethylamine
NHS	<i>N</i> -hydroxysuccinimide
NMM	<i>N</i> -methylmorpholine
NMP	<i>N</i> -methylpyrrolidone
NRotB	Number of freely rotatable bonds
OBOC	One bead one compound
OBTC	One bead two compounds

p53	tumor protein p53
PAMPA	Parallel artificial membrane permeation assay
PCR	Polymerase chain reaction
PE	Polyethylene
PEEK	Polyether ether ketone
PEG	Polyethylene glycol
PEMFinder	Peptidomimetic macrocycles library
PN	Product number
PP	Polypropylene
PPI	Protein-protein interaction
PSA	Polar surface area
PSA	Polystyrene
PTFE	Polytetrafluoroethylene (Teflon)
R	Side chain residue
R&D	Research and development
RCM	Ring-closing metathesis
RNA	Ribonucleic acid
Ro5	Rule of five (Lipinski)
RVC	Rotational vacuum concentrator
SD	Standard deviation
siRNA	small interfering RNA
SPPS	Solid phase peptide synthesis
TCEP	Tris-(2-carboxyethyl)phosphine
TEA	Triethylamine
TFA	Trifluoroacetic acid
THF	Tetrahydrofuran
TIS	Triisopropyl silane
Trt	Trityl
UHPLC-MS	Ultra high performance liquid chromatography mass spectrometry
UV	Ultra violet
w	Width

1. Introduction

Unmet medical needs are present in many areas, such as in neurodegenerative (Alzheimer's), cardiovascular (heart failure, pulmonary hypertension), gynecological (endometriosis) and infectious (bacterial and viral) diseases. The reasons for unmet medical needs are diverse and often caused by the lack of fundamental understanding of the biological cause and unsolved scientific, industrial, regulatory and economic challenges.¹ The cause of a disease may occur through external factors like pathogens or internal factors like a specific dysfunction of one or multiple proteins. The human being is a complex biological system involving about 21'000 different proteins. Roughly 3000 are disease-relevant, and only a subset of 600-1500 protein targets are considered to be druggable with conventional therapeutic modalities like small molecules.² Druggable proteins often have well-defined pockets on their surface, allowing them to develop a drug-like molecule more efficiently with suitable binding and permeability properties.

However, there are other protein classes relevant to drug development, such as those involved in protein-protein interactions (PPI). They were considered to be undruggable due to their large and featureless surfaces. It is difficult for small molecules to form appropriate interactions on such surfaces, mainly because of their small size and shape. Nevertheless, PPIs are an attractive target class since the whole human interactome of proteins is estimated to have ~130,000 – 650,000 different interactions. The numerous options for intervention offer scientists many new opportunities to develop molecules for specific PPI modulation. Nevertheless, the development of such molecules would require more sophisticated methods to develop molecular tools.^{3, 4}

The term of challenging targets shifted from “undruggable” to “difficult-to-drug” and “yet-to-be drugged” due to the more recent development of alternative modalities capable of modulating protein-protein interactions.⁵ For this purpose, molecules with constrained conformations were particularly successful.⁶

Therefore, macrocycles, a type of molecular modality with particular properties explained in greater detail later, have gained much attention in the scientific and industrial community during the past few years. Furthermore, the macrocycle's ability to combine

the best attributes of different modalities, such as from antibodies (size, specificity, affinity) and small molecules (oral availability), allows for the use of these molecules against challenging intracellular targets.⁶ As of 2017, more than 130 publications with over 3000 citations indicate continuous interest in this relatively young field since its inception in the 1990s.⁷ Our laboratory and the work done in this thesis focus on developing methods to generate macrocycles to engineer molecules against difficult-to-drug targets as protein-protein interactions.

1.1 **Macrocycles as therapeutics**

1.1.1 *Properties of macrocycles*

In principle, macrocycles are ring-shaped molecules, which have 12 or more atoms within the backbone.⁸ Many macrocyclic natural products contain 14-, 16 and 18-membered ring systems and often occur in even-numbered ring sizes and, to a lesser extent, in odd ones. Macrocycles with ring systems beyond 50+ atoms have also been found.⁹ The molecular diversity of macrocycles is vast and may comprise crown ethers, calixenes, porphyrins, cyclodextrin, macrolides and macrocyclic peptides. The macrocycle's three most favorable molecular attributes in drug development are their strong affinities against challenging targets, size and cell-permeability.

Firstly, a macrocycles' cyclic structure has a positive, energetic contribution to the binding affinity. The positive binding effect is due to the highly pre-organized structural conformation resulting in a lower entropic barrier, which benefits binding.¹⁰ In comparison, linear molecules with less rigid molecular structures must adapt themselves more extensively to appropriately display their atoms to the protein surface to form specific enthalpic interactions.¹¹ In addition to the macrocycle's backbone, peripheral (small atoms groups directly connected to the backbone) and side chain groups all contribute to the overall binding energy by forming specific interactions.¹²

Secondly, the ligand's size is essential to reach the residues distributed along the protein surface (hot spots), which are required to form sufficient and specific enthalpic intermolecular interactions. A mid-sized macrocycle (500 - 1500 Da)¹³ has a polar surface area (PSA) of ~180 – 280 Å² distributed across a macrocycle surface area of 400 – 800 Å².¹⁴ Typical extended binding sites (e.g., hot spots) in difficult-to-drug targets, such as those found in protein-protein interactions, have a significantly larger surface area and may amount to ~500-3000 Å².¹⁴ In contrast, small molecules have more difficulty reaching the hot spots due to their small size (~500 Da, 140 Å² PSA, 300-500 Å² molecule surface area), but their size is suitable for smaller compact binding sites found in other targets like proteases.^{15, 16}

In the pharmaceutical industry, cell permeability is an essential molecular property for the successful development of drugs when orally administered or applied to an

intracellular target of interest. Traditionally, the Lipinski rules (rule of 5, Ro5) were used to predict the probability of drug-like properties for small molecules to better focus valuable resources on molecules with permeable membrane properties.^{16, 17} Nevertheless, macrocycles were found to still be permeable despite violating standard Lipinski guidelines. A famous example of a permeable mid-sized macrocyclic molecule is cyclosporine A (1203 Da). Cyclosporine A adopts different conformational states depending on the polarity of the surrounding medium. In an apolar environment like a membrane bilayer, the formed intramolecular hydrogen bonding network shields polar residues enabling membrane permeability.¹⁴ This behavior is named the chameleonic effect. Such findings led to the further adaptation of guidelines suitable for larger molecules. Table 1 shows different established guidelines, such as the expanded (eRo5),¹⁸ beyond rule of five (bRo5)¹⁹ and specific for oral and non-oral macrocycles.¹²

Table 1: Overview of different guidelines for small molecules and macrocycles (MC) to evaluate their potential of drug-like behavior. Different values are shown involving molecular weight (Mw), polar surface area (PSA), calculated octanol-water partition coefficient (cLogP), hydrogen bond acceptor (HBA), hydrogen bond donors (HBD) and total freely rotatable bond (NRotB).

Guideline [ref]	Mw (Da)	PSA (Å ²)	cLogP	HBA	HBD	NRotB
Ro5 ¹⁷	<500	< 140	< 5	≤ 10	≤ 5	< 10
eRo5 ¹⁸	500 - 700	< 200	0 - 7.5	≤ 10	≤ 5	≤ 20
bRo5 ¹⁹	700 -1000	>200	<0 or > 7.5	> 10	>5	> 20
oral MC ¹²	600 - 1200	180 - 320	-2 - 6	12 - 16	≤ 12	≤ 15
non-oral MC ¹²	600 - 1300	150 - 500	-7 - 2	9 - 20	≤ 17	≤ 30

In addition to the favorable properties of macrocycles, they often showed better stability against proteolytic degradation in the gut, blood, or tissues. The improved stability is due to the cyclic ring, which shields specific peptide residues away from the metabolic and enzymatic recognition sites necessary for the catalytic cleavage of peptide bonds.²⁰

Besides all the favorable properties, macrocycles' rigidity may also have negative practical implications. In the pharmaceutical industry, compound libraries are tested against multiple therapeutic targets to evaluate the compound's activity against a target of interest. The testing of macrocycle libraries may require an extended library size to

overcome the loss of conformational diversity from the reduced flexibility. The required sizes of compound libraries demand better technological access to purchase or create appropriate macrocycles in sufficient numbers (e.g., hundreds-thousands to millions) for initial high throughput activity screening. In addition to this, lead structure optimization of promising macrocyclic molecules is challenging. The cyclic nature of the macrocycle often means that local changes within the backbone may affect distal structural conformations and may strongly affect binding properties.²¹

In summary, macrocycles are a unique class of molecules with many advantageous properties like binding affinity, specificity, proteolytic stability and the capability to permeate membranes despite their large size and numerous polar groups. These features make them a complimentary and attractive molecular tool to develop therapeutics, particularly against intracellular and difficult-to-drug targets. This is in contrast with other drug modalities like small molecules or biologicals. Figure 1 summarizes why the macrocycle chemical space is so attractive against challenging targets like protein-protein interactions.²²

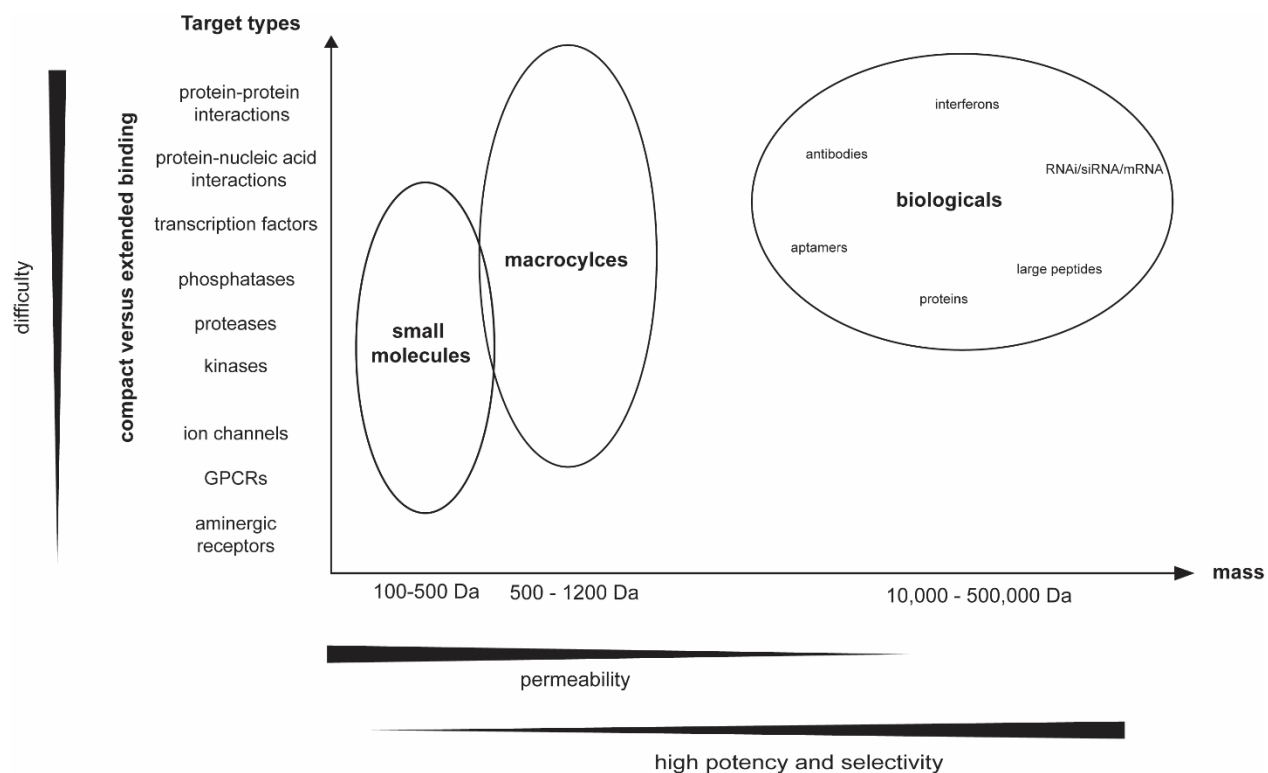


Figure 1: Overview of different drug classes and trends in relation to mass and therapeutic targets.²² Three drug modalities (small molecules, macrocycles and biologicals) are shown. General properties of druggability difficulty from easier (bottom) to most challenging (top) along the y-axis and permeability, potency and selectivity trends on the x-axis are shown.

1.1.2 *Macrocyclic drugs*

Eighty-seven macrocyclic drugs have been approved as of 2021 by the U.S. Food and Drug Administration (FDA) and many more are currently in clinical development.^{23; 24} Typical therapeutic applications of macrocycles are in infectious diseases and cancer-related treatments. Generally, macrocycles can be categorized into multiple classes with specific chemical features and bioactivities. Bioactive macrocycles were often isolated as natural products and originated from bacteria, fungi, or plants. It seems somehow that nature already uses macrocyclic substructures to obtain specific biological functions.²⁵

Macrolides belong perhaps to the most well-known class of orally available macrocycles, mainly used to treat gram-positive bacteria and, to a lower extent, against gram-negative bacteria.²⁶ Examples of macrolide drugs are erythromycin, azithromycin and clarithromycin (Figure 2). They are classified as complex polyketides and have a typical ring size from 14 to 16 atoms cyclized by a lactone with one or more pendant glycosidic residues.²⁷ Their primary mode of action is protein synthesis inhibition by binding to the nascent peptide exit tunnel of the bacterial ribosome subunit 50S.²⁸ This binding mechanism allows it to slow down or even stop bacterial growth. The discovery of the macrolide rapamycin (tacrolimus) was an essential milestone in the field of molecular glues to form neo-protein-protein associations. Rapamycin has specific binding properties towards the mammalian target of rapamycin (mTOR) kinase. This protein kinase is vital for cell growth regulation in mammals.²⁹ Research efforts revealed that rapamycin acts as a “molecular glue” between a specific protein-protein interaction. First, it binds allosterically to the 12 kDa FK506 binding protein (FKBP12). Then it forms a complex at the FKBP-rapamycin-binding (FRB) domain of the mTor receptor at which further downstream kinase activity is inhibited and consequently arrests cell growth. In the 1980s, protein kinases were considered as undruggable targets.³⁰ Rapamycin is used as an acute and chronic immunosuppressant drug in organ transplantations.³¹ Other rapamycin derivatives (everolimus, temsirolimus) obtained FDA approval in 2007 and 2009 for treating advanced renal cancer tumors.³² Structures of the different macrolides are shown in figure 2.

Another important class of antibiotic macrocycles are rifamycins. They differ slightly from macrolides. Their structural characteristics are a lactam bond and aromatic moiety in the backbone. Rifamycins have a mode of action, which differs from macrolides, instead they are inhibiting the bacterial RNA polymerase to interrupt the bacteria's lifecycle. Rifamycins are often applied in tuberculosis therapy.³³

Polymyxins are cationic antimicrobial cyclic heptapeptides carrying a fatty acid tail on the N-terminus. Due to their positive charge, these peptides are able to bind to gram-negative bacteria's outer membrane through electrostatic interactions. It induces cavity formation, causes the membrane to leak and kills the bacteria. Polymyxins are used as a first line of defense against many gram-negative bacteria.³⁴

In addition to the natural product-inspired macrocycles, synthetic macrocycle drugs have also been developed with a particular focus on cancer treatments.³⁵ For example, Lorlatinib is a synthetic macrocyclic drug derived from a small molecule to achieve better selectivity and drug-like properties.³⁶ It was approved in 2018 by the FDA for treating anaplastic lymphoma kinase (ALK). Another synthetic macrocycles drug example is pacritinib used for inhibiting the Janus kinase 2 (JAK2) signaling pathway. This macrocycle showed promising clinical phase III data against myelofibrosis.^{37, 38}

Despite the success of macrocycles in terms of affinity, stability and selectivity, they still represent a small portion of all 1,453 FDA-approved drugs (as of 2013).^{39,40} This underrepresentation is most probably due to their relatively difficult synthesis. This hampers the creation and testing of large macrocycle libraries and the discovery of new lead structures against therapeutically relevant targets. Improved synthetic access to macrocycles would allow the further exploitation of macrocycle's chemical space. The modular synthesis approach of peptides from numerous commercially available amino acid building blocks, the well-established solid phase chemistry, synthesis automatization and the ability of the peptides's backbone (peptide bonds) to form an intermolecular hydrogen bond network with protein surfaces upon an binding event are valuable reasons to focus on peptide based macrocycle libraries when the peptide size is limited (~< 1000 Da) to still have an chance of developing permeable characteristics.

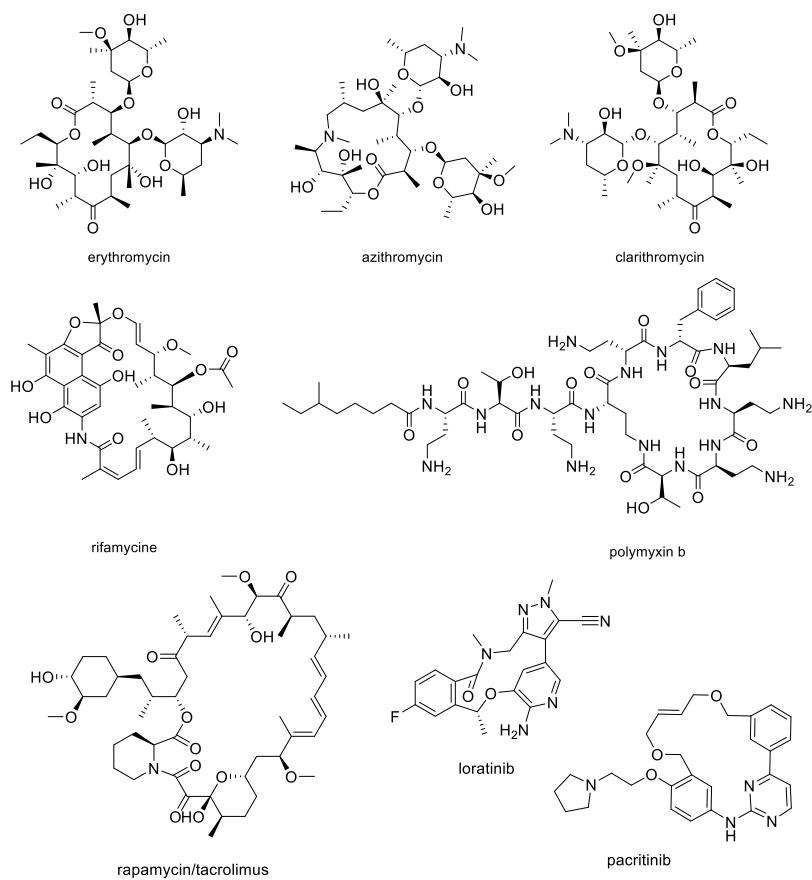


Figure 2: Examples of macrocycles. Erythromycin, azithromycin, clarithromycin and rapamycin are typical macrolides used as antibiotics or immunosuppressant drugs. Rifamycin is a polyketide with a lactam bond. Polymyxin b is a lipided and cyclic macrolactam peptide. Loratinib and pacritinib are small molecule-derived macrocycles.

1.2 *Methods for generating and screening macrocyclic compound libraries*

This chapter discusses three crucial strategies used to create macrocyclic compound libraries. It encompasses the traditional sequential preparation of individual compounds and two combinatorial approaches using beads and DNA for encoding.

1.2.1 Existing macrocycle libraries for high-throughput screening (HTS)

In a high-throughput screening process, individual compounds are tested to assess the molecules' ability to modulate a target of interest. For this, diverse and numerous compounds are required for testing to increase the chance of identifying active structures. The establishment of a compound collection is realized by either individually synthesizing and purifying compounds in-house or purchasing them from a commercial source. These compounds are usually stored and managed at a central location using automatized infrastructure in order to be able to cope with the logistics of so many compounds. Only a small fraction of the actual compound stock solution is used for testing and usually lasts for many rounds of screening.

The most crucial component of high throughput screening is the compound libraries themselves. As of 2019, commercial compound library suppliers have steadily grown their collections, offering over 16 million different and individually purified substances.⁴¹ However, the individual synthesis and purification of such compounds in high numbers and sufficient quantities (milligrams per compound) is cost-intensive and intensify even more when complex chemical structures are built. Generating a compound library requires enormous resources costing between \$ 0.4 to 2 billion for one million compounds.⁴²

The limited availability of macrocycle libraries is due to their complex chemical structure. To synthesize macrocycles, a linear precursor is often prepared before cyclization. The cyclization is an entropically unfavorable process⁴³ and is usually performed under diluted conditions to omit the risk of intermolecular oligomerization.⁴⁴ Macrolides are particularly complex and require more sophisticated, labor-intensive chemical procedures involving inert reaction conditions, stereoselective transformations and numerous tedious purification steps.²⁶ Consequently, the number of available

macrocyclic compounds is somewhat limited with only a few suppliers (table 2). Typically, they are sold in solution (DMSO) at relatively high concentrations (e.g., 10 mM) in microliter volumes (50 μ l/well) directly delivered in standard 384-well storage plates ready-to-use with standard liquid handling instrumentation (Figure 3a). Compound libraries typically have purities above 85%.

Table 2: Commerical suppliers of macrocycle compound libraries.

Supplier	Library size	Library description	Reference
ChemBridge	>20,000	Synthetic macrocycles, < 800 Da, 11-27 ring atoms, scaffolds with and without peptidic backbone elements, a focused subset of 7,000 macrocycles available for CNS	45
Asinex	10,091	Synthetic macrocycles, 250 - 800 Da, peptide-like and non-peptidic chemotypes, >4000 macrocycles tested for permeability (PAMPA)	46
ChemDiv	2,335	Synthetic macrocycles, 200 – 600 Da, 10,12, 14-22 ring atoms, cyclized by lactamization and click chemistry	47
Spexis (Polyphor)	50,000	Synthetic macrocycles, peptidic and non-peptidic, MacroFinder (500-800 Da) & PEMfinder (700-2000 Da) technology platform	48, 49
Enamine	592	Synthetic macrocycles, < 300-800 Da, macrocyclization by RCM, click, ring-enlargement, macrolacton/-lactam, etc.)	50
AnalytiCon	2,368	Natural product-inspired macrocyclic peptides and macrolide-resembling structures	51
Princeton Biomolecular	1,568	180 – 1050 Da, natural product and synthetic macrocycles, various types of cyclization (e.g. disulfide, lacto- and lactamization etc.)	52

Other essential components are required to realize high-throughput screening experiments. To cope with the sheer number of to-be-tested compounds, high-throughput screening infrastructure is required to process hundreds of thousands to millions of individual compounds.⁵³ Microplates are compatible with many commercially available and automated robotic devices comprising liquid handling, sealing, peeling, storage, centrifugation and plate reader instruments. An example of our own HTS liquid handling platform is shown in Figure 3b.

To test a compound, a suitable assay is required. An assay is defined as a wet and signal-amplifiable experimental set-up to ultimately test a compound's ability to modulate a therapeutic target of interest. They are a simplified and artificial representation of

biological processes (e.g. enzymatic activity, Figure 3c.) inside wells of microtiter plates (figure b). Ideally, a screen has a low hit rate of ~0.01-0.14%.⁵⁴ Occasionally, false positive or false negative hits may occur in a screen and lead to resource-intensive hit validation or missed opportunities, respectively. Therefore, a robust and reliable assay is key for successful screening, especially when only single-point measurements are performed to test hundred-thousands of compounds.

The actual assaying of compounds occurs in so-called microtiter plates, standard devices used as consumables in high-throughput screening. One microtiter plate contains many uniform and individual compartments (96, 384 and 1536) named a well. A microplate can have well-formats in 8×12 , 16×24 , or 32×48 arrays, as shown in Figure 3d. Each well corresponds to one test with one single compound usually tested at a specific concentration (e.g., ~10 μM). Volume capacity per well varies from 100 over 20 to 10 μl /well depending on the applied well plate type.

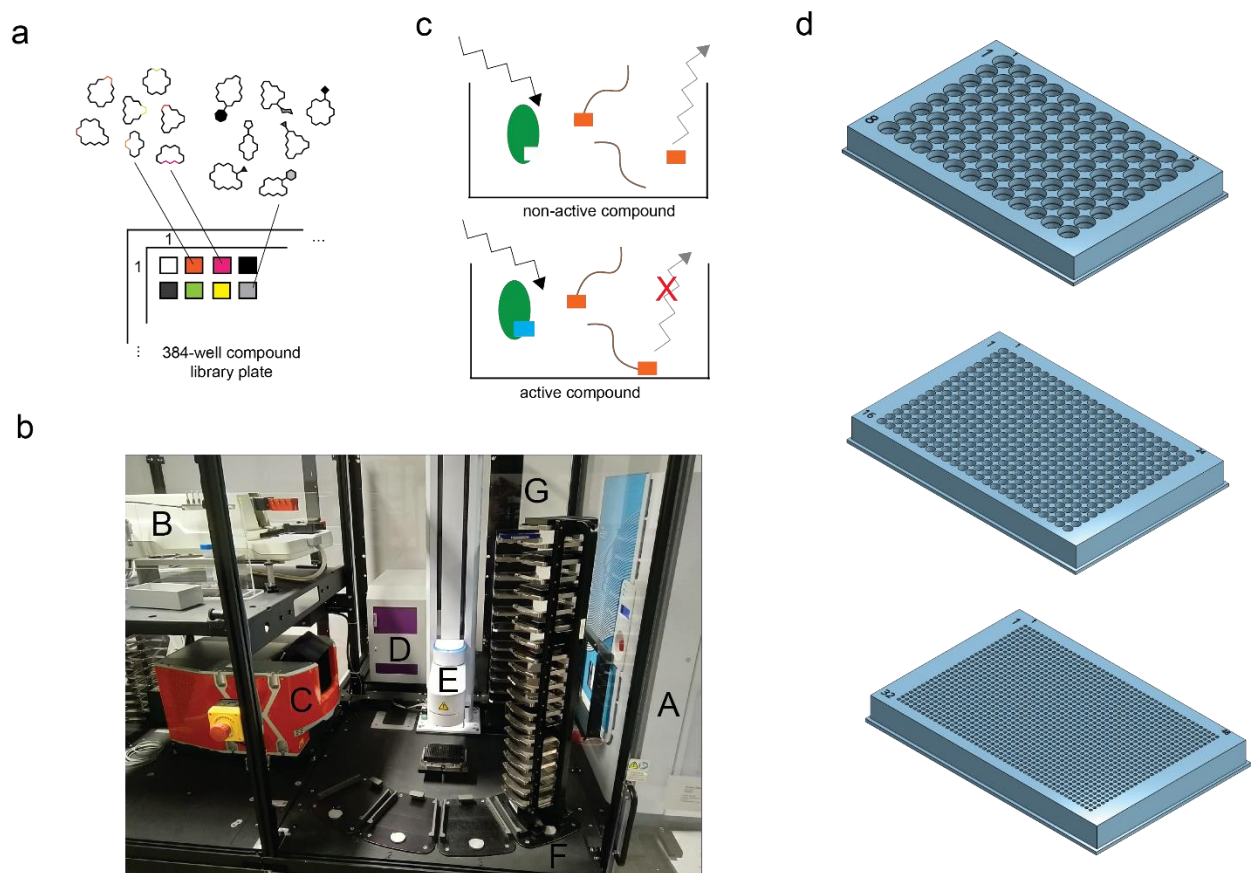


Figure 3: Examples of testing plates, assay, HTS infrastructure and compound library. a) 96-well (top), 384 (middle) and 1536-well microplates (bottom). b) scheme of an enzymatic assay with an enzyme (green), substrate (brown) with a fluorophore (orange) and an active compound (turquoise). Detection occurs with exciting (black) and emitting (grey) light (arrow) at specific wavelengths. c) acoustic droplet ejection dispenser (A), bulk dispenser (B), centrifuge (C), plate reader (D), the robotic arm (E), storage rack for microplates (F) and delidder station (G). d) example of how compounds are stored or purchased from commercial suppliers in liquid handling compatible microplates.

In summary, macrocycles represent only a tiny fraction (<1%) of commercially available compounds. In addition, the individual and sequential compound synthesis and purification strategy to establish chemical libraries are time-consuming and slow down the iterative exploitation of a specific area in the chemical space. Therefore, the development of new methods to generate macrocycle libraries is very desirable. Further miniaturization and automatization of macrocycle synthesis could help to overcome current limitations. The use of existing high-throughput liquid handling infrastructure is not limited to screening. Therefore, synthesizing macrocyclic compounds at lower volumes by using HTS infrastructure could be very attractive. The screening of untagged and non-

immobilized compounds as found in traditional compound libraries has the significant advantage of being compatible with more assay types (e.g., functional and cellular assays),^{55, 56} which is in contrast to more recently developed and complementary compound library strategies briefly described in the following two sub-chapters.

1.2.2 One-bead one-compound (OBOC) macrocycle libraries

The one-bead one compound (OBOC) method allows the construction of large combinatorial compound libraries by a repetitive split and pool procedure, where different building blocks are iteratively coupled onto the resin (Figure 4a). At the end of this process, each bead only contains one type of multiple copies of the same compound. In addition, using beads allows for the simple filtration of excess reagents used during coupling. This combinatorial approach enables the exponential synthesis of different linear peptides. The formation of macrocycles was realized by cyclizing the linear species directly on resin. The principle of the methodology is illustrated in Figure 4a.⁵⁷ Then, the large and diverse macrocycle library can be screened by incubating the beads inside a solution with a protein of interest labeled with a dye. Finally, the hits can be visually identified with a microscope, and the strikingly colored beads are selectively picked by hand for further analysis. Each bead carries multiple copies of the same species, sufficient in quantity to determine the peptide sequence.⁵⁸

The Edman degradation methodology can derive the sequence of the linear active synthesized peptides⁵⁹ by using MS analysis.⁶⁰ However, Edman degradation is only applicable to α -amino acids. It is no longer applicable when non-canonical amino acid building blocks or macrocyclic peptides (no free n-terminus) are used. A potential alternative is using tandem mass spectroscopy to identify peptide sequences. However, when macrocycles are applied, it is often difficult and tedious to determine the peptide sequence from cyclic structures.⁶¹

An alternative solution called one bead two compounds (OBTC) was developed to overcome this problem. The use of orthogonal protecting groups and two different types of linkers allowed the simultaneous synthesis of cyclic and linear peptides on one single bead (as shown in Figure 4b).⁶² The linear peptide is usable for Edman degradation analysis and the macrocycle for testing the affinity binding against a target of interest.⁶³

The OBOC methodology was used to identify nanomolar macrocyclic binders against the K-RAS(G12V)/effector⁶⁴ and TNF α /TNF α -R interactions.⁶⁵ The applied libraries ranged from hundreds of thousands to millions of macrocycles.

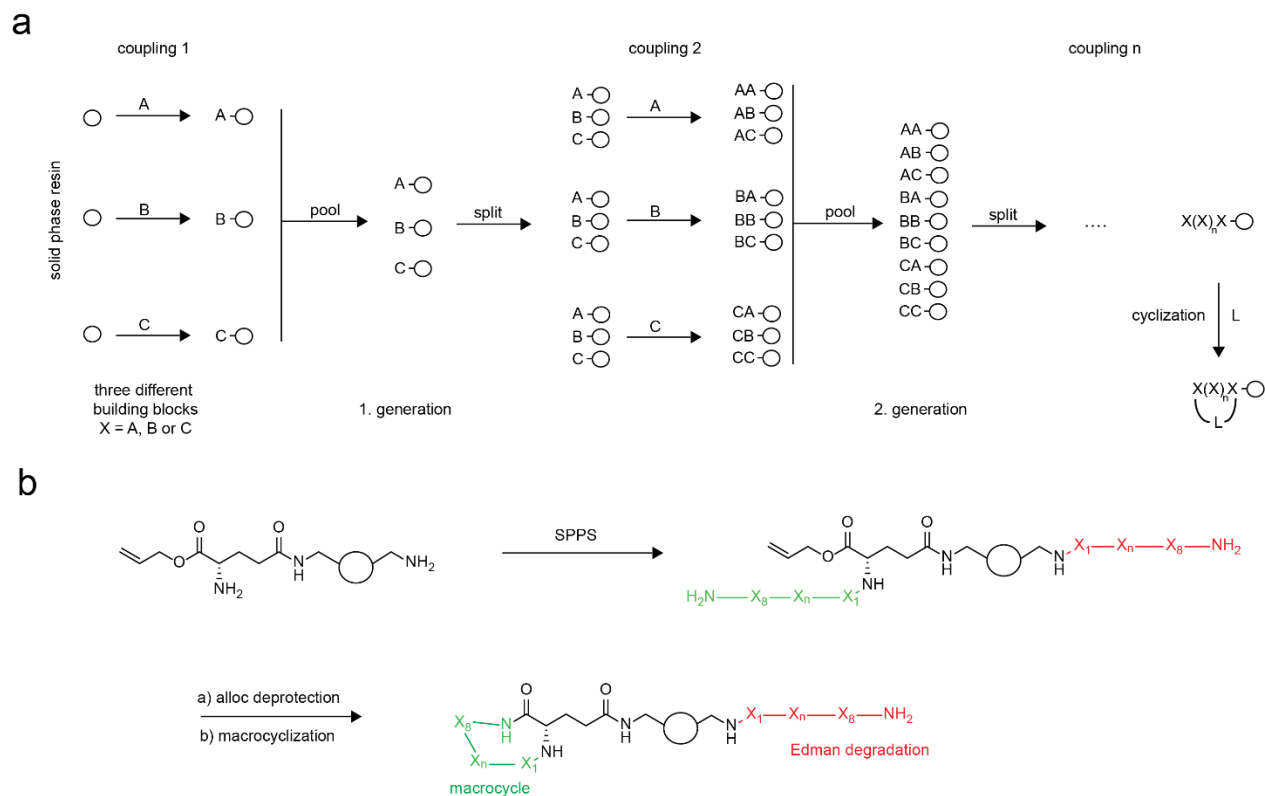


Figure 4: An exemplified overview of the combinatorial split and pool approach in OBOC for macrocycles. a) three different building blocks (A, B, C) are coupled onto spatially separated portions of resin and pool after coupling. A uniform mixed pooled of beads was split into equal spatial separated portions. This corresponds to the first generation. Many generations (rounds) are conductive. In the last step, the peptide is cyclized on resin. b) Alternative approach to have macrocycle and identifier sequence both on the same bead by introducing selective orthogonal protecting groups.

1.2.3 DNA-encoded libraries (DELs) of macrocyclic compounds

The technology of deoxyribonucleic acid (DNA) encoded libraries (DELs) was first proposed by Brenner and Lerner and demonstrated that chemical entities on beads are linkable to individual DNA fragments acting as a barcode.⁶⁶ This approach combines the advantages of chemical diversity from the traditional chemical compound library synthesis with the ability to identify binders by decoding artificially introduced DNA throughout the library generation. Furthermore, the strategy allows synthesizing compounds at a very low scale since DNA is amplifiable later by using polymerase chain reaction (PCR) and compensates for the need for more substance. Finally, using next-generation DNA sequencing decodes the amplified DNA sequences and reveals the supposed structure.⁶⁷

Typically, DEL libraries are screened by affinity selection, where a potential binder sticks onto an immobilized target, and non-binding molecules are washed away through a simple filtration process. As a result of the facile screening procedure, a wide range of DNA encoded libraries was synthesized comprising of small molecules⁶⁸, macrocycles on beads⁶⁹ or in solution⁷⁰ Cyclic structures comprising of peptidic^{71, 72} a natural product inspired⁷³ or nonpeptidic characterized libraries⁷⁴ were also possible to generate.

Commonly, two types of strategies are applied: DNA recording and DNA templated synthesis. As previously discussed, the DNA recording approach follows a split and pool technique, where the first building block is introduced into the backbone under DNA-compatible reaction conditions. The initial starting molecule comprises a reactive group and a double-stranded DNA-starting sequence required to perform the DNA recording strategy. In a subsequent and separate step, a DNA identifier, which represents (encodes) the first building block, is ligated onto the starter DNA to record the first introduced building block onto the DNA barcode. Only afterward, all intermediates are pooled and split. The exponential growth of DNA-encoded macrocycles is achieved by using many more building blocks and multiple iterations (3-5) of split-couple and pool cycles, as shown in figure 5a.⁶⁹

In contrast to the DNA recording approach, DNA templated strategy allows the library synthesis in solution without tethering molecules onto beads. This makes the split and pool processes even more convenient in the laboratory. However, in such a process,

the realization of the library generation slightly differs. The initial modified single-stranded DNA represents the DNA-encoded construction plan for the to-be-synthesized molecules. Adding the building blocks attached to a complementary single-stranded DNA anneals onto the DNA template and reacts with the reaction partner upon close proximity only. Different linker lengths are required to induce a reaction between the building block's single-stranded DNA and chemical moiety. Preparing such DNA-building block conjugates is more time-consuming than the DNA recording strategy. This process is illustrated schematically in figure 5b. For both methods, single-digit micromolar to double-digit nanomolar macrocyclic binders were identified against multiple targets.^{69, 70, 72, 75} This demonstrates the utility of DEL as an alternative source of macrocycle libraries.

Overall, DEL macrocyclic libraries have many advantages. They require only very little infrastructure and are carried out in standard academic and industry laboratories resulting in a “liberating” way to access diverse and large chemical libraries. One million compound collection costs about \$ 0.4 - 2 billion. For DELs, an 800 Mio-membered DELs library amounts to only \$150,000.⁴² Besides the many positive aspects of DEL libraries, such as size, cost, minimal assay development, parallel screening, fast selection process and the possibility of multiple selection cycles for macrocycle enrichments, there are also a few disadvantages. Drawbacks of this technology are low library purities due to limiting coupling efficiencies, verification of successful molecule synthesis, restricted access to DNA compatible and efficient reactions, limited to “simple” affinity-based pull-down assay (no functional assays, e.g., enzymatic), relatively high false hit rate (~50%) and solubility challenges due to the polar encoding entity.^{56, 76} This technology could be of interest to gain information about some initial structural anchor points when other existing solutions are not sufficient. However, establishment of such an approach requires large synthetic efforts, which is for our lab rather difficult to realize.

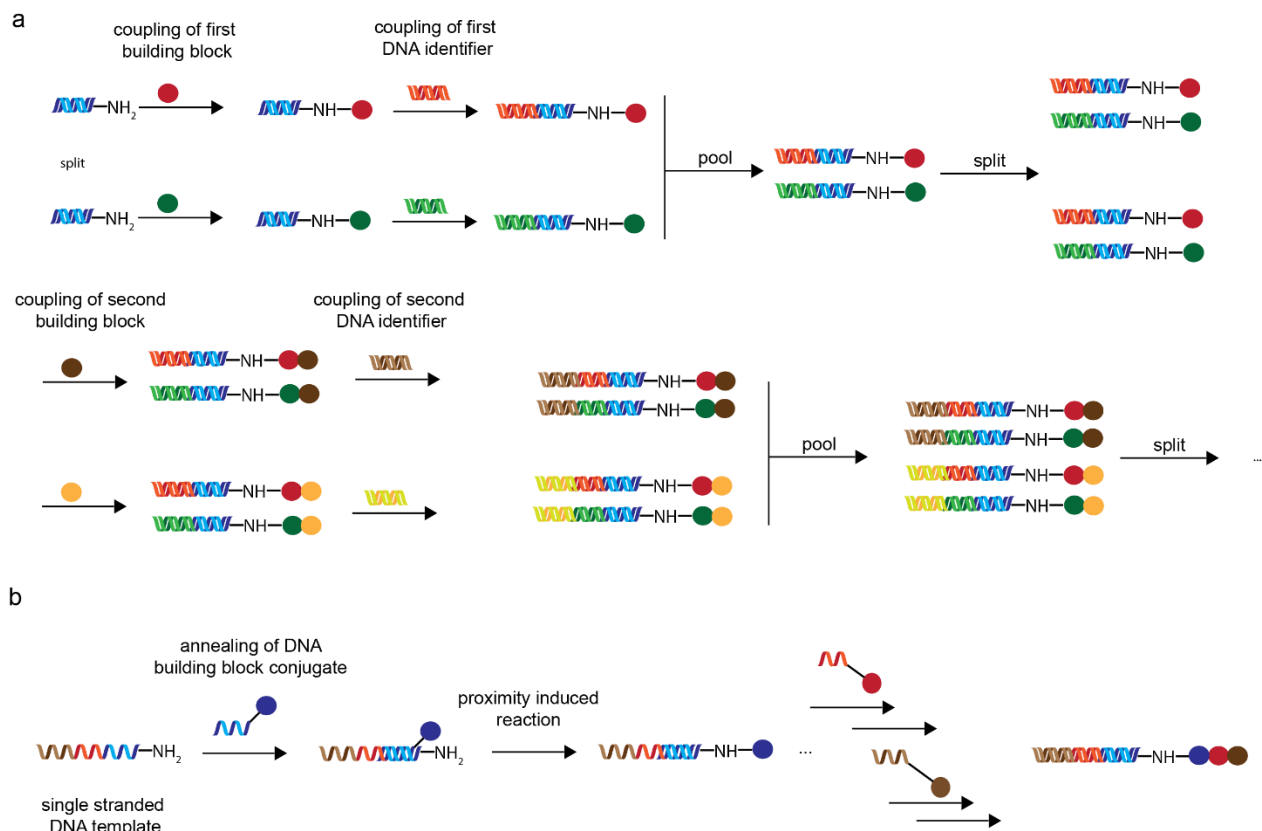


Figure 5: Common strategies for DNA encoded libraries. a) DNA recording methodology: The first building block (red and green) is coupled onto an initial and reactive short DNA sequence (blue), followed by the ligation of a specific DNA sequence (orange) to encode the particular building block being used into the DNA barcode. Usually, the reactions are realized in multiple spatial separated reaction containers, not only two, as illustrated here. Afterward, spatially separated syntheses were all pooled together, homogenized and equally redistributed (split) into new reaction containers. The same procedure was repeated until desired DEL library was achieved. b) DNA templated synthesis: The single-stranded DNA template dictates which complementary single-stranded DNA-building block conjugate with the appropriate linker length reacts with the active group to undergo the proximity-induced reaction. This allows performing DNA templated synthesis in one pot without needing a split and pool.

1.3 *Nano-scale synthesis of macrocycle libraries*

The miniaturization of reaction scales is essential to reduce cost during synthesis and cover a more significant fraction of the chemical space by using the same or fewer resources. This is necessary due to the sheer amount of drug-like opportunities (10^{60}), vastly exceeding human capabilities.⁷⁷ High-throughput experimentation at the nanoscale was implemented into numerous fields of chemistry including reaction discovery and condition optimization, using only micrograms of compound per experiment. However, nanoscale synthesis was only moderately applied to the synthesis of complex molecules and could have an enormous impact on drug discovery.⁷⁸ Combining nanoscale synthesis inside standardized microplates, which are compatible with many existing automated infrastructures, would enable the subsequent, direct assaying of compounds without purification. This is a relatively new concept and may overcome the limitation of restricted access to macrocycle libraries.⁷⁹

In the last few years, our laboratory has established methodologies to iteratively synthesize and screen peptide macrocycles to develop binders against targets.^{79–81} Using efficient chemistry (e.g., SPPS and diversification reaction) with high-yielding outcomes and good compatibility with the following assay is fundamental. Thiols are particularly interesting to use since they can undergo excellent conversions with electrophilic moieties in an aqueous environment. Their use as a diversification vector to generate macrocycle libraries are therefore appealing. However, a combinatorial synthesis approach using the concept of mixing liquid volumes for reaction (component-based) requires high-purity starting materials to avoid misleading screening data by unknown side products. Thus, applying efficient methodologies to obtain such high-quality starting materials are essential, especially when needed to the hundreds or thousands in parallel. A few methods are briefly discussed below. Having efficient, high purity, and high-yielding chemical reactions combined with infrastructure to downsize resource consumption is key to exploiting the chemical space for the iterative hunt of bioactive molecules.⁸²

1.3.1 *Solid phase synthesis of disulfide-containing peptides*

In nature, disulfide bonds have a critical role and are found in numerous proteins and peptides. Disulfide bonds are formed inter-or intramolecularly by building a covalent bond between two sulfhydryl groups from cysteines. These bonds are stable under oxidative conditions and are mainly found in the extracellular space. Typical examples are the heterodimeric peptide hormone insulin⁸³ or the nonapeptide oxytocin.⁸⁴ Under reductive conditions, the disulfide bonds are labile and, therefore, not present in an intracellular environment, except when they are well enough buried and shielded from the environment⁸⁵. The formation of such disulfide bonds helps to constrain peptides to obtain specific functionalities.⁸⁵ They are present in many animals and plants, often found as peptide venom. The bioactivities of these toxic peptides caused great attention and attracted many researchers to investigate their therapeutic potential.⁸⁶ As a consequence of this, methods have been developed to prepare bioactive disulfide peptides to study them. For their synthesis, the invention of the solid phase peptide synthesis (SPPS) by Merrifield,⁸⁷ automation of SPPS synthesis⁸⁸ and fluorenylmethyloxycarbonyl (Fmoc) chemistry⁸⁹ were crucial for the efficient synthesis of individual disulfide bond containing peptides on solid phase.⁹⁰

Recently, our group has developed a methodology that takes advantage of the disulfide bond's reversibility, which is compatible under SPPS Fmoc synthesis strategy conditions and acid-resistant character (figure 6a). In this approach, small macrocyclic disulfide peptides are synthesized in standardized 96-well plates by establishing first the linear peptide through a Fmoc-based SPPS strategy.⁹¹ Deprotection of side chains occurred with trifluoroacetic acid (TFA, 95%) while the peptide remained on the resin. This allows for the washing away of all excess reagents like scavengers and side products without the liberation of the peptide itself. The selective liberation occurs by an intramolecular cyclative release reaction under basic conditions, where the C-terminal sulfhydryl group attacks the resin-tethered disulfide bond. This strategy releases highly pure (>90%) crude peptides in high quantity (54-100% yield) and concentrations (10-15 mM, 200 μ l) using volatile and removable reagents only. In short, this cyclative release strategy made it possible to efficiently form disulfide-based macrocyclic peptides suitable

for library generation with a meaningful synthetic throughput in the hundreds to thousands of macrocycles.

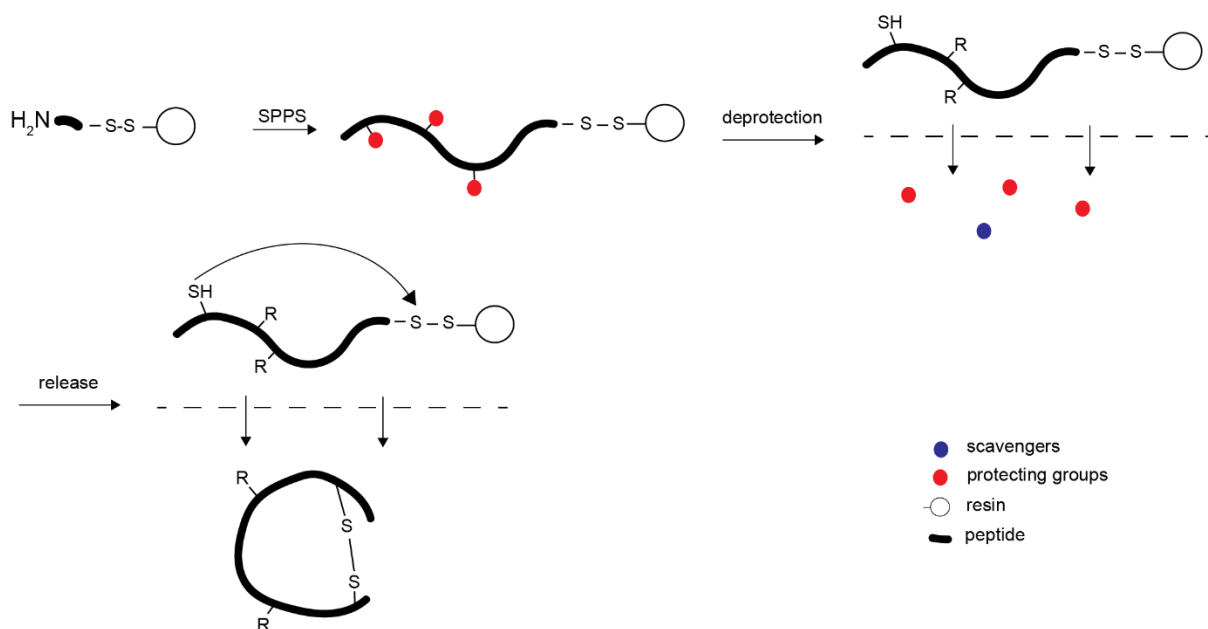
Traditionally, the linear peptide species are synthesized by SPPS using the Fmoc strategy followed by the simultaneous release of the whole crude peptide along with the side chain protecting groups, all in one solution. In the second step, the linear peptide containing two sulfhydryl groups is oxidized under diluted macrocyclization conditions (Figure 6b). Finally, tedious purification steps are necessary to isolate the desired disulfide macrocycles by applying ether precipitation and preparative HPLC.⁹² Such an approach is not convenient for the generation of peptide libraries.

Besides disulfide bond-forming strategies, numerous alternative release strategies have been developed for liberating cyclized peptides by forming different chemical bonds.⁹³ It comprises the following methods: thioester linker,⁹⁴ olefin linkers for ring-closing metathesis⁹⁵ and Dawson's linker system for native chemical ligation⁹⁶ as well as the oxidative release of thioether immobilized peptides on solid supports.^{97, 98} However, all these approaches suffer from low yields and purity or require extensive purification efforts unsuitable for library generation.

In summary, the developed methodology by Habeshian et al. is desirable for library generation since it allows the facilitated production of many pure disulfide macrocycles in microplates without the need for purification. However, these macrocycles are suitable for extracellular but not intracellular targets due to the reversible nature of disulfide bonds in oxidative or reductive environments as found outside or inside cells. The formation of a thioether bond by using thiols and electrophiles could overcome this problem. A traceless reductive methodology to reduce clean and crude disulfide peptides to form linear species could provide an exciting alternative to generate macrocycle libraries suitable to intracellular targets. Additionally, the cyclative release mechanism carries the risk that highly rigid or small peptide backbones cannot undergo an intramolecular cyclative release due to the lack of the peptide's pliability to reach the tethering disulfide bond for liberation. Furthermore, commercially available SPPS synthesizer capabilities, especially for parallel microplate synthesis, are somewhat limited to 96-well plates. This reduces the diversity and size of peptide scaffolds used in macrocycle libraries. Lastly and more

generally, the reversible nature of disulfide bonds could lead to undesired dimer formation when inappropriately stored or under stress (low pH, room temperature, etc.).

a



b

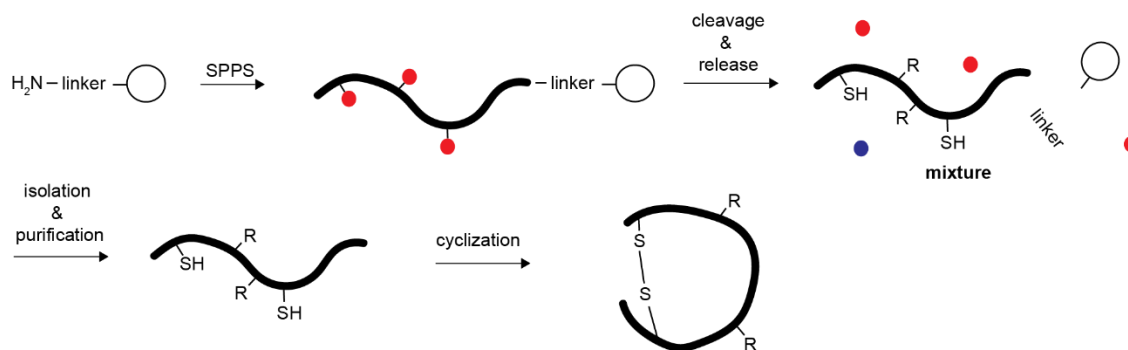


Figure 6: Overview of strategies to synthesize disulfide peptides. a) The cyclative release approach involves resin deprotection enabled by the acid-resistant disulfide bond linker. The selective intramolecular release mechanism allows the isolation of disulfide macrocycles through simple filtration without tedious purification procedures. b) Synthesis of a linear peptide by SPPS. Cleavage and deprotection occur in solution followed by tedious isolation (either precipitation) and purification (preparative HPLC) to yield clean linear peptide for cyclization under low-yielding diluted conditions.

1.3.2 Combinatorial synthesis of macrocycle libraries using acoustic dispensing

Transferring liquid volume on a nanoliter scale is not feasible with traditional pipetting robotics. Consequently, different technologies have been developed to handle fluids. Acoustic droplet ejection (ADE) technology allowed our laboratory to combine both concepts, nano-scaled synthesis and the direct screening of compounds, all in one process inside microplates. Before going into detail about how these macrocycle libraries were generated, it is worth first understanding the ADE technology's principles and advantages.

Historically, the first effects of high-frequency acoustic sound on liquids and their subsequent impact on droplet formation were already described in 1927 by Wood and Loomis.⁹⁹ Engineering efforts led to the technical feasibility of precisely focusing acoustic waves onto a liquid surface. The concentration of sound onto a single point on the liquid's meniscus inside a well allowed for nanoliter-sized droplet ejection in a non-invasive manner. The speed at which the nanoliter droplets are ejected is sufficient to travel a short distance into an opposing well from an inverted microplate as illustrated in figure 7a.¹⁰⁰ This technology turned out to be extremely automation friendly and compatible with many microplate formats (96, 384, 1536), enabling miniaturization to overcome common drawbacks during liquid handling like reproducible nanoliter transfers, invasiveness, use of many consumables (tips), speed and cross-contamination issues.¹⁰¹ This technology quickly found its way into screening facilities around the world and is used for compound library reformatting,¹⁰¹ transfer of compounds for primary assaying and dose-response curves,¹⁰² scouting of chemical reactions¹⁰³ and combinatorial synthesis of small molecules¹⁰⁴ as well as compound synthesis and screening at nanomolar scale¹⁰⁵ are all examples of how acoustic dispensing can be used. A possible disadvantage of current ADE instrumentation is the requirement of constant circulating water to maintain the transducer functionality. The humidity inside the instrument is high (saturated) and precious compound libraries dissolved in DMSO are directly exposed to humidity, which might comprise the quality of compound stock solutions or the quality of crude nano-scaled reactions.

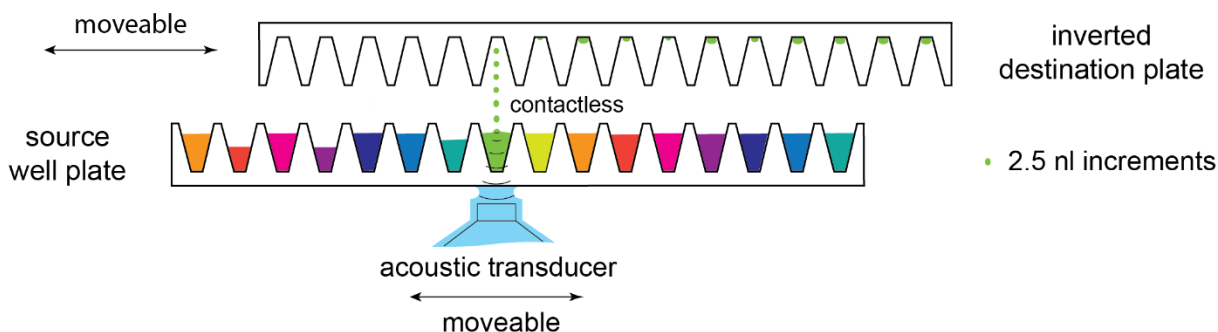
In 2021, Sangouard et al. introduced for the first time a methodology in which ADE was applied to transfer three stepwise reagents for the synthesis of macrocyclic peptides at picomolar (nanoliter) scale for the construction of a 2,700 membered library followed by the direct screening of crude reaction mixtures (Figure 7b).⁷⁹ The three-component-based macrocycle synthesis strategy resulted in submicromolar binders for MDM2. However, a few drawbacks were observed by applying this methodology and involved mainly the following ones: i) reactions yields changed considerably due to the more challenging amine-to-thiol macrocyclization reaction, ii) complex reaction mixtures were obtained due to the implemented tag required for facilitated product precipitation and thiol protection and iii) the low diversity of commercially available bis-electrophilic linkers. These drawbacks reduced the methodology's effectiveness in producing large and diverse macrocycle libraries.

Our group has recently published an alternative methodology to circumvent some of the drawbacks mentioned above. The established macrocycle library was based on disulfide macrocycles. Habeshian et al. developed a method in which numerous (192) small disulfide bond-containing macrocycles were chemically modified with many carboxylic acids (104) by late-stage-amidation of amines situated along the cyclic backbone as shown in figure 7 c.⁸¹ The formed 19,968-membered macrocycle library allowed the discovery of potent double-digit nanomolar inhibitors for the protease thrombin ($K_i = 44$ nM) and the MDM2:p53 ($K_i = 43$ nM) protein-protein interaction. In addition, this work demonstrated the proof of concept of performing nano-scaled reactions (picomolar) for the iterative macrocycle synthesis combined with directly assaying to rapidly explore the chemical space for potent nanomolar inhibitors.

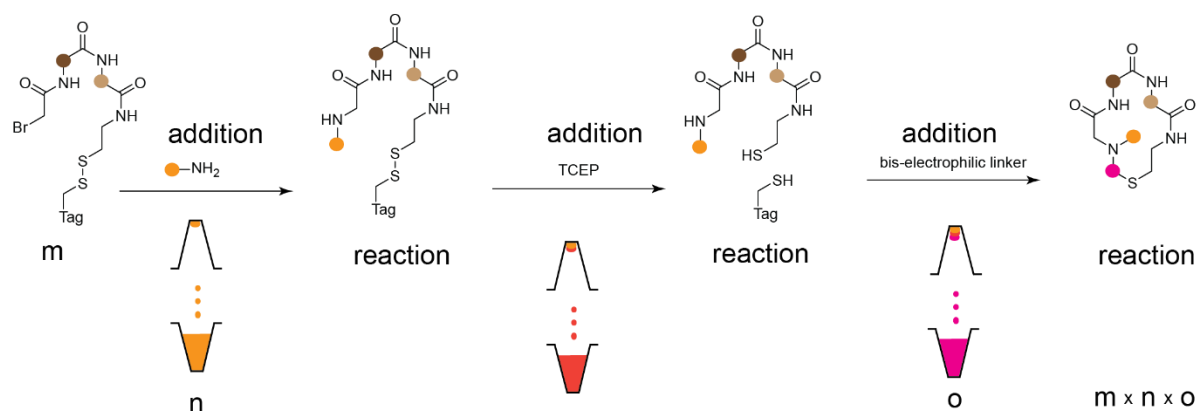
Despite the fact that the method demonstrated its potential, a major disadvantage of using disulfide bond-containing macrocycles is their instability towards reductive conditions, which becomes especially relevant when intracellular protein targets for drug development are tested. In addition, the two component-based synthesis strategy established by Habeshian et al. has a relatively low scaffold diversity with only 192 different peptide macrocycles. The low throughput of initial macrocycles synthesized by SPSS might limit future successes in finding potent inhibitors against more difficult-to-drug targets. The initially established cyclative release methodology requiring no need for

purification is basically only limited by the low throughput of the current microplate-based parallel SPPS synthesizer using 96-well plates only. It would be very valuable to overcome this bottleneck to cover a more significant fraction of the chemical space by being able to have more diverse scaffolds for nanoscale modification.

a



b



c

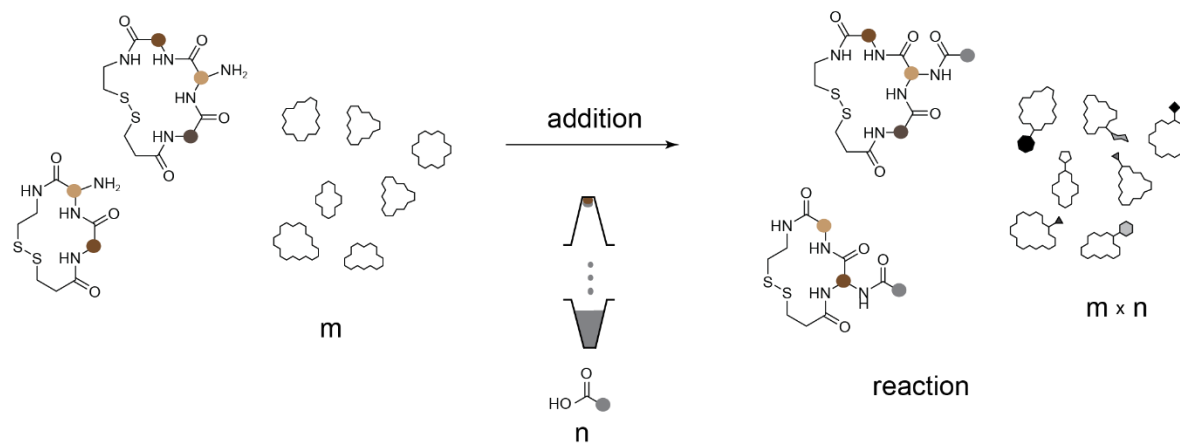


Figure 7: Overview of acoustic dispensing principle and methodologies for generating macrocycle libraries at picomolar scale using ADE. a) The movable acoustic transducer focuses the acoustic waves to the liquid surface of an ECHO-qualified source plate well to eject 2.5 nl droplet increments into a well from an inverted destination plate (e.g., 384-well microplate) located closely above the source plate (e.g., 384-well). b) The three-component-based macrocycle library generation strategy uses a tag (Mpa-SGRY) to facilitate purification and thiol protection, followed by a thiol-to-amine cyclization strategy. c) A two-component-based synthesis strategy involving many different disulfide

bonds, including scaffolds with one diamino acid building block per macrocycle, were modified by an amidation as a late-stage chemical transformation at picomolar scale followed by direct assaying.

1.3.3 *Solid phase synthesis of dithiol peptides*

Traditional synthetic SPPS procedures can produce dithiol-containing peptides by first conducting the linear peptide synthesis followed by the simultaneous cleavage, side chain deprotection and peptide liberation. Usually, this involves tedious isolation protocols such as ether precipitation and chromatographic purification (Figure 8a).⁹² If applied to peptide libraries, the workload may become cumbersome and overwhelming, especially when libraries comprise thousands of peptides.

The previously discussed cyclative release strategy from Habeshian et al. would overcome the peptide isolation and purification problem but still require additional steps and reagents to reduce the disulfide macrocycles to obtain dithiol peptides⁹¹ (Figure 8b). Applying a sufficiently dense immobilized reducing reagent on solid support would allow traceless reduction of disulfide peptides to form dithiol-containing peptides. However, such chemical tools are commercially not available, and if so, only with limited, reducing capacity and solvent compatibility.

Recently, our laboratory developed an alternative method to selectively circumvent many of the aforementioned challenges to form dithiol peptides for monocyclic peptides.¹⁰⁶ This method is handy when applied at scale in microtiter plates. Zsolt et al. synthesized a linear peptide *via* an acid-resistant disulfide linker. The side chain deprotection occurred on the resin, followed by a reductive release using the reagent 1,4-butadiene (BDT) under basic conditions (triethylamine, TEA) in dimethylformamide (DMF). All implemented reagents are volatile and straightforward to remove (Figure 8c). The side-product of BDT during reduction is its 6-membered oxidized disulfide ring, which is also volatile and, therefore, easily removable. The abolition of all used reagents was performed using a rotational vacuum concentrator. However, the fully reduced peptides may carry the risk of peptide oligomerization during the concentration process. In order to suppress this oxidation, the release solution was acidified and concentrated under mild thermal (30°C) conditions resulting in highly pure dithiol peptides applicable to peptides with various lengths (1 to 10 amino acid building blocks) in satisfactory yields and ready-

to-use stock solutions (double digit millimolar) for alkylation with good storable properties. Suppose the stock solution contains partial or fully oxidized peptide. This protocol allows an easy and fast regeneration of the reduced peptide state inside the wells of microplates.

Despite the substantial procedural improvements to circumvent tedious isolation and purification steps, they all share a common limitation for peptide library generation. The restricted throughput of commercially available parallel synthesizers (thousands) limits the establishment of more diverse scaffolds (ten-thousands). Label-free and unconjugated peptides in sufficient numbers, quantity and concentration would allow the group to further exploit the in-house developed iterative macrocycle synthesis platform at picomolar scale coupled with direct assaying. Additionally, the variety of so far applied diversification reagents (bis-electrophilic linkers) for cyclizing dithiol peptides are rather low.⁷⁹ It would be beneficial to have a more extensive toolbox available to increase the diversity of macrocycles by typical thiol alkylation. Numerous peptides and diversification reagents are needed to cover a larger chemical space to hopefully discover more frequently new macrocycles with unique bioactivities that are more suitable for intracellular targets.

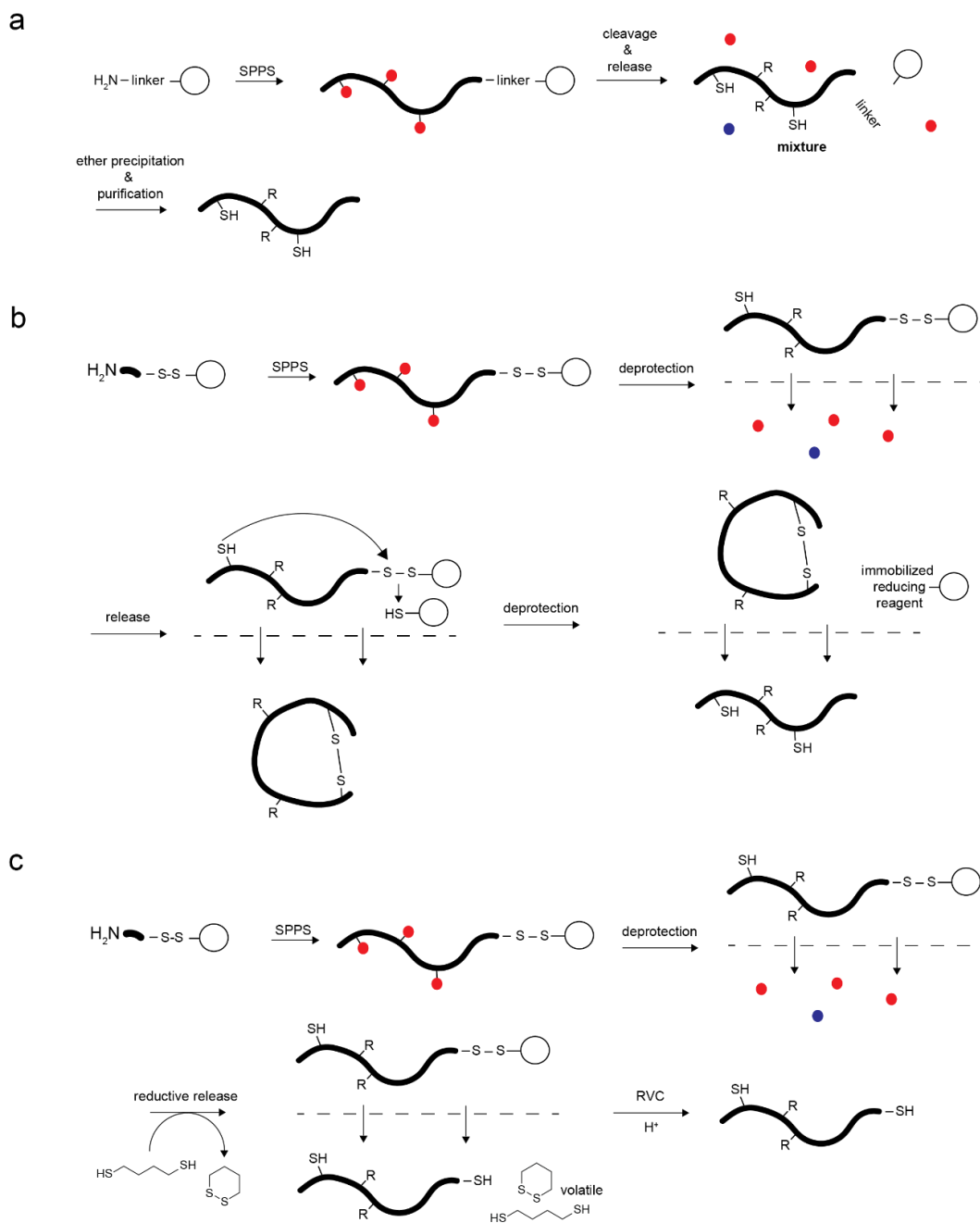


Figure 8: Schematic overview of strategies to obtain free thiol peptides. a) Traditional approach by synthesizing the linear peptide on an acid-labile linker. Ether precipitation and purification are required for the pure isolation of dithiol peptides. b) In-house established cyclative release strategy using a disulfide bond linker for the synthesis, side chain deprotection on resin followed by a nucleophilic and intramolecular cyclative release mechanism to form macrocyclic disulfide peptides. A traceless reduction method would be required to obtain free dithiol peptides to omit further purification steps. c) In-house developed reductive release methodology by reducing the linker disulfide bond with liquid and volatile reducing reagent BDT with a subsequent rotational vacuum concentration (RVC) step under acidic conditions to maintain both thiols and omit oxidation.

1.4 References

- (1) Joshua Cohen. Unmet Medical Needs Persists across Many Diseases. *Forbes* **2018**.
- (2) Hopkins, A. L.; Groom, C. R. The Druggable Genome. *Nat. Rev. Drug Discov.* **2002**, 1 (9), 727–730. <https://doi.org/10.1038/nrd892>.
- (3) Stumpf, M. P. H.; Thorne, T.; de Silva, E.; Stewart, R.; An, H. J.; Lappe, M.; Wiuf, C. Estimating the Size of the Human Interactome. *Proc. Natl. Acad. Sci.* **2008**, 105 (19), 6959–6964. <https://doi.org/10.1073/pnas.0708078105>.
- (4) Venkatesan, K.; Rual, J.-F.; Vazquez, A.; Stelzl, U.; Lemmens, I.; Hirozane-Kishikawa, T.; Hao, T.; Zenkner, M.; Xin, X.; Goh, K.-I.; Yildirim, M. A.; Simonis, N.; Heinzmann, K.; Gebreab, F.; Sahalie, J. M.; Cevik, S.; Simon, C.; de Smet, A.-S.; Dann, E.; Smolyar, A.; Vinayagam, A.; Yu, H.; Szeto, D.; Borick, H.; Dricot, A.; Klitgord, N.; Murray, R. R.; Lin, C.; Lalowski, M.; Timm, J.; Rau, K.; Boone, C.; Braun, P.; Cusick, M. E.; Roth, F. P.; Hill, D. E.; Tavernier, J.; Wanker, E. E.; Barabási, A.-L.; Vidal, M. An Empirical Framework for Binary Interactome Mapping. *Nat. Methods* **2009**, 6 (1), 83–90. <https://doi.org/10.1038/nmeth.1280>.
- (5) Coleman, N.; Rodon, J. Taking Aim at the Undruggable. *Am. Soc. Clin. Oncol. Educ. Book* **2021**, No. 41, e145–e152. https://doi.org/10.1200/EDBK_325885.
- (6) Morrison, C. Constrained Peptides' Time to Shine? *Nat. Rev. Drug Discov.* **2018**, 17 (8), 531–533. <https://doi.org/10.1038/nrd.2018.125>.
- (7) Vinogradov, A. A.; Yin, Y.; Suga, H. Macrocyclic Peptides as Drug Candidates: Recent Progress and Remaining Challenges. *J. Am. Chem. Soc.* **2019**, 141 (10), 4167–4181. <https://doi.org/10.1021/jacs.8b13178>.
- (8) Yudin, A. K. Macrocycles: Lessons from the Distant Past, Recent Developments, and Future Directions. *Chem. Sci.* **2015**, 6 (1), 30–49. <https://doi.org/10.1039/C4SC03089C>.
- (9) Frank, A. T.; Farina, N. S.; Sawwan, N.; Wauchope, O. R.; Qi, M.; Brzostowska, E. M.; Chan, W.; Grasso, F. W.; Haberfield, P.; Greer, A. Natural Macrocyclic Molecules Have a Possible Limited Structural Diversity. *Mol. Divers.* **2007**, 11 (3–4), 115–118. <https://doi.org/10.1007/s11030-007-9065-5>.
- (10) Claveria-Gimeno, R.; Vega, S.; Abian, O.; Velazquez-Campoy, A. A Look at Ligand Binding Thermodynamics in Drug Discovery. *Expert Opin. Drug Discov.* **2017**, 12 (4), 363–377. <https://doi.org/10.1080/17460441.2017.1297418>.

- (11) DeLorbe, J. E.; Clements, J. H.; Whiddon, B. B.; Martin, S. F. Thermodynamic and Structural Effects of Macrocyclic Constraints in Protein–Ligand Interactions. *ACS Med. Chem. Lett.* **2010**, *1* (8), 448–452. <https://doi.org/10.1021/ml100142y>.
- (12) Villar, E. A.; Beglov, D.; Chennamadhavuni, S.; Porco, J. A.; Kozakov, D.; Vajda, S.; Whitty, A. How Proteins Bind Macrocycles. *Nat. Chem. Biol.* **2014**, *10* (9), 723–731. <https://doi.org/10.1038/nchembio.1584>.
- (13) Iqbal, E. S.; Hartman, M. C. T. Shaping Molecular Diversity. *Nat. Chem.* **2018**, *10* (7), 692–694. <https://doi.org/10.1038/s41557-018-0095-7>.
- (14) Whitty, A.; Zhong, M.; Viarengo, L.; Beglov, D.; Hall, D. R.; Vajda, S. Quantifying the Chameleonic Properties of Macrocycles and Other High-Molecular-Weight Drugs. *Drug Discov. Today* **2016**, *21* (5), 712–717. <https://doi.org/10.1016/j.drudis.2016.02.005>.
- (15) Jones, S.; Thornton, J. M. Principles of Protein-Protein Interactions. *Proc. Natl. Acad. Sci.* **1996**, *93* (1), 13–20. <https://doi.org/10.1073/pnas.93.1.13>.
- (16) Veber, D. F.; Johnson, S. R.; Cheng, H.-Y.; Smith, B. R.; Ward, K. W.; Kopple, K. D. Molecular Properties That Influence the Oral Bioavailability of Drug Candidates. *J. Med. Chem.* **2002**, *45* (12), 2615–2623. <https://doi.org/10.1021/jm020017n>.
- (17) Lipinski, C. A. Drug-like Properties and the Causes of Poor Solubility and Poor Permeability. *J. Pharmacol. Toxicol. Methods* **2000**, *44* (1), 235–249. [https://doi.org/10.1016/S1056-8719\(00\)00107-6](https://doi.org/10.1016/S1056-8719(00)00107-6).
- (18) Doak, B. C.; Over, B.; Giordanetto, F.; Kihlberg, J. Oral Druggable Space beyond the Rule of 5: Insights from Drugs and Clinical Candidates. *Chem. Biol.* **2014**, *21* (9), 1115–1142. <https://doi.org/10.1016/j.chembiol.2014.08.013>.
- (19) DeGoey, D. A.; Chen, H.-J.; Cox, P. B.; Wendt, M. D. Beyond the Rule of 5: Lessons Learned from AbbVie's Drugs and Compound Collection: Miniperspective. *J. Med. Chem.* **2018**, *61* (7), 2636–2651. <https://doi.org/10.1021/acs.jmedchem.7b00717>.

- (20) Nielsen, D. S.; Shepherd, N. E.; Xu, W.; Lucke, A. J.; Stoermer, M. J.; Fairlie, D. P. Orally Absorbed Cyclic Peptides. *Chem. Rev.* **2017**, *117* (12), 8094–8128. <https://doi.org/10.1021/acs.chemrev.6b00838>.
- (21) Appavoo, S. D.; Huh, S.; Diaz, D. B.; Yudin, A. K. Conformational Control of Macrocycles by Remote Structural Modification: Focus Review. *Chem. Rev.* **2019**, *acs.chemrev.8b00742*. <https://doi.org/10.1021/acs.chemrev.8b00742>.
- (22) Terrett, N. K. Methods for the Synthesis of Macrocyclic Libraries for Drug Discovery. *Drug Discov. Today Technol.* **2010**, *7* (2), e97–e104. <https://doi.org/10.1016/j.ddtec.2010.06.002>.
- (23) Giordanetto, F.; Kihlberg, J. Macrocyclic Drugs and Clinical Candidates: What Can Medicinal Chemists Learn from Their Properties? *J. Med. Chem.* **2014**, *57* (2), 278–295. <https://doi.org/10.1021/jm400887j>.
- (24) Sun, D. Recent Advances in Macrocyclic Drugs and Microwave-Assisted and/or Solid-Supported Synthesis of Macrocycles. *Molecules* **2022**, *27* (3), 1012. <https://doi.org/10.3390/molecules27031012>.
- (25) Begnini, F.; Poongavanam, V.; Over, B.; Castaldo, M.; Geschwindner, S.; Johansson, P.; Tyagi, M.; Tyrchan, C.; Wissler, L.; Sjö, P.; Schiesser, S.; Kihlberg, J. Mining Natural Products for Macrocycles to Drug Difficult Targets. *J. Med. Chem.* **2021**, *64* (2), 1054–1072. <https://doi.org/10.1021/acs.jmedchem.0c01569>.
- (26) Seiple, I. B.; Zhang, Z.; Jakubec, P.; Langlois-Mercier, A.; Wright, P. M.; Hog, D. T.; Yabu, K.; Allu, S. R.; Fukuzaki, T.; Carlsen, P. N.; Kitamura, Y.; Zhou, X.; Condakes, M. L.; Szczypiński, F. T.; Green, W. D.; Myers, A. G. A Platform for the Discovery of New Macrolide Antibiotics. *Nature* **2016**, *533* (7603), 338–345. <https://doi.org/10.1038/nature17967>.
- (27) Katz, L. Manipulation of Modular Polyketide Synthases. *Chem. Rev.* **1997**, *97* (7), 2557–2576. <https://doi.org/10.1021/cr960025+>.
- (28) Myers, A. G.; Clark, R. B. Discovery of Macrolide Antibiotics Effective against Multi-Drug Resistant Gram-Negative Pathogens. *Acc. Chem. Res.* **2021**, *54* (7), 1635–1645. <https://doi.org/10.1021/acs.accounts.1c00020>.

- (29) Liu, G. Y.; Sabatini, D. M. MTOR at the Nexus of Nutrition, Growth, Ageing and Disease. *Nat. Rev. Mol. Cell Biol.* **2020**, *21* (4), 183–203. <https://doi.org/10.1038/s41580-019-0199-y>.
- (30) Schreiber, S. L. The Rise of Molecular Glues. *Cell* **2021**, *184* (1), 3–9. <https://doi.org/10.1016/j.cell.2020.12.020>.
- (31) Dumont, F. J.; Su, Q. Mechanism of Action of the Immunosuppressant Rapamycin. *Life Sci.* **1995**, *58* (5), 373–395. [https://doi.org/10.1016/0024-3205\(95\)02233-3](https://doi.org/10.1016/0024-3205(95)02233-3).
- (32) Li, J.; Kim, S. G.; Blenis, J. Rapamycin: One Drug, Many Effects. *Cell Metab.* **2014**, *19* (3), 373–379. <https://doi.org/10.1016/j.cmet.2014.01.001>.
- (33) Campbell, E. A.; Korzheva, N.; Mustaev, A.; Murakami, K.; Nair, S.; Goldfarb, A.; Darst, S. A. Structural Mechanism for Rifampicin Inhibition of Bacterial RNA Polymerase. *Cell* **2001**, *104* (6), 901–912. [https://doi.org/10.1016/S0092-8674\(01\)00286-0](https://doi.org/10.1016/S0092-8674(01)00286-0).
- (34) Poirel, L.; Jayol, A.; Nordmann, P. Polymyxins: Antibacterial Activity, Susceptibility Testing, and Resistance Mechanisms Encoded by Plasmids or Chromosomes. *Clin. Microbiol. Rev.* **2017**, *30* (2), 557–596. <https://doi.org/10.1128/CMR.00064-16>.
- (35) Amrhein, J. A.; Knapp, S.; Hanke, T. Synthetic Opportunities and Challenges for Macrocyclic Kinase Inhibitors. *J. Med. Chem.* **2021**, *64* (12), 7991–8009. <https://doi.org/10.1021/acs.jmedchem.1c00217>.
- (36) Kong, X.; Pan, P.; Sun, H.; Xia, H.; Wang, X.; Li, Y.; Hou, T. Drug Discovery Targeting Anaplastic Lymphoma Kinase (ALK). *J. Med. Chem.* **2019**, *62* (24), 10927–10954. <https://doi.org/10.1021/acs.jmedchem.9b00446>.
- (37) William, A. D.; Lee, A. C.-H.; Blanchard, S.; Poulsen, A.; Teo, E. L.; Nagaraj, H.; Tan, E.; Chen, D.; Williams, M.; Sun, E. T.; Goh, K. C.; Ong, W. C.; Goh, S. K.; Hart, S.; Jayaraman, R.; Pasha, M. K.; Ethirajulu, K.; Wood, J. M.; Dymock, B. W. Discovery of the Macrocyclic 11-(2-Pyrrolidin-1-yl-Ethoxy)-14,19-Dioxo-5,7,26-Triaza-Tetracyclo[19.3.1.1(2,6).1(8,12)]Heptacos-1(25),2(26),3,5,8,10,12(27),16,21,23-Decaene (SB1518), a Potent Janus Kinase 2/Fms-Like Tyrosine Kinase-3 (JAK2/FLT3) Inhibitor for the Treatment of Myelofibrosis and Lymphoma. *J. Med. Chem.* **2011**, *54* (13), 4638–4658. <https://doi.org/10.1021/jm200326p>.

- (38) Mesa, R. A.; Vannucchi, A. M.; Mead, A.; Egyed, M.; Szoke, A.; Suvorov, A.; Jakucs, J.; Perkins, A.; Prasad, R.; Mayer, J.; Demeter, J.; Ganly, P.; Singer, J. W.; Zhou, H.; Dean, J. P.; te Boekhorst, P. A.; Nangalia, J.; Kiladjian, J.-J.; Harrison, C. N. Pacritinib versus Best Available Therapy for the Treatment of Myelofibrosis Irrespective of Baseline Cytopenias (PERSIST-1): An International, Randomised, Phase 3 Trial. *Lancet Haematol.* **2017**, *4* (5), e225–e236. [https://doi.org/10.1016/S2352-3026\(17\)30027-3](https://doi.org/10.1016/S2352-3026(17)30027-3).
- (39) Kinch, M. S.; Haynesworth, A.; Kinch, S. L.; Hoyer, D. An Overview of FDA-Approved New Molecular Entities: 1827–2013. *Drug Discov. Today* **2014**, *19* (8), 1033–1039. <https://doi.org/10.1016/j.drudis.2014.03.018>.
- (40) Driggers, E. M.; Hale, S. P.; Lee, J.; Terrett, N. K. The Exploration of Macrocycles for Drug Discovery — an Underexploited Structural Class. *Nat. Rev. Drug Discov.* **2008**, *7* (7), 608–624. <https://doi.org/10.1038/nrd2590>.
- (41) Volochnyuk, D. M.; Ryabukhin, S. V.; Moroz, Y. S.; Savych, O.; Chuprina, A.; Horvath, D.; Zabolotna, Y.; Varnek, A.; Judd, D. B. Evolution of Commercially Available Compounds for HTS. *Drug Discov. Today* **2019**, *24* (2), 390–402. <https://doi.org/10.1016/j.drudis.2018.10.016>.
- (42) Goodnow, R. A.; Dumelin, C. E.; Keefe, A. D. DNA-Encoded Chemistry: Enabling the Deeper Sampling of Chemical Space. *Nat. Rev. Drug Discov.* **2017**, *16* (2), 131–147. <https://doi.org/10.1038/nrd.2016.213>.
- (43) Bechtler, C.; Lamers, C. Macrocyclization Strategies for Cyclic Peptides and Peptidomimetics. *RSC Med. Chem.* **2021**, *12* (8), 1325–1351. <https://doi.org/10.1039/D1MD00083G>.
- (44) White, C. J.; Yudin, A. K. Contemporary Strategies for Peptide Macrocyclization. *Nat. Chem.* **2011**, *3* (7), 509–524. <https://doi.org/10.1038/nchem.1062>.
- (45) <https://chembridge.com/screening-compounds/macrocycles/> (17.01.2023).
- (46) <https://www.asinex.com/macrocycles> (17.01.2023).

- (47) <https://www.chemdiv.com/catalog/focused-and-targeted-libraries/macrocycles-library/> (17.01.2023).
- (48) Batur, G.; Ermert, P.; Zimmermann, J.; Obrecht, D. Macrocycle Therapeutics to Treat Life-Threatening Diseases. *CHIMIA* **2021**, 75 (6), 508. <https://doi.org/10.2533/chimia.2021.508>.
- (49) <https://spexisbio.com/macrocycle-discovery-platform/> (17.01.2023).
- (50) <https://enamine.net/compound-collections/macrocycles> (17.01.2023).
- (51) https://ac-discovery.com/wp-content/uploads/ACD_Flyer-NATx-Macrocycles-1805-02-WEB.pdf (17.01.2023).
- (52) <https://princetonbio.com/products/macrocycles> (17.01.2023).
- (53) Mayr, L. M.; Fuerst, P. The Future of High-Throughput Screening. *SLAS Discov.* **2008**, 13 (6), 443–448. <https://doi.org/10.1177/1087057108319644>.
- (54) Zhu, T.; Cao, S.; Su, P.-C.; Patel, R.; Shah, D.; Chokshi, H. B.; Szukala, R.; Johnson, M. E.; Hevener, K. E. Hit Identification and Optimization in Virtual Screening: Practical Recommendations Based on a Critical Literature Analysis: Miniperspective. *J. Med. Chem.* **2013**, 56 (17), 6560–6572. <https://doi.org/10.1021/jm301916b>.
- (55) Inglese, J.; Shamu, C. E.; Guy, R. K. Reporting Data from High-Throughput Screening of Small-Molecule Libraries. *Nat. Chem. Biol.* **2007**, 3 (8), 438–441. <https://doi.org/10.1038/nchembio0807-438>.
- (56) Ottl, J.; Leder, L.; Schaefer, J. V.; Dumelin, C. E. Encoded Library Technologies as Integrated Lead Finding Platforms for Drug Discovery. *Molecules* **2019**, 24 (8), 1629. <https://doi.org/10.3390/molecules24081629>.
- (57) Lam, K. S.; Salmon, S. E.; Hersh, E. M.; Hruby, V. J.; Kazmierski, W. M.; Knapp, R. J. A New Type of Synthetic Peptide Library for Identifying Ligand-Binding Activity. *Nature* **1991**, 354 (6348), 82–84. <https://doi.org/10.1038/354082a0>.

- (58) Lam, K. S.; Lebl, M.; Krchňák, V. The “One-Bead-One-Compound” Combinatorial Library Method. *Chem. Rev.* **1997**, *97* (2), 411–448. <https://doi.org/10.1021/cr9600114>.
- (59) Edman, P.; Högfeldt, E.; Sillén, L. G.; Kinell, P.-O. Method for Determination of the Amino Acid Sequence in Peptides. *Acta Chem. Scand.* **1950**, *4*, 283–293. <https://doi.org/10.3891/acta.chem.scand.04-0283>.
- (60) Miyashita, M.; Presley, J. M.; Buchholz, B. A.; Lam, K. S.; Lee, Y. M.; Vogel, J. S.; Hammock, B. D. Attomole Level Protein Sequencing by Edman Degradation Coupled with Accelerator Mass Spectrometry. *Proc. Natl. Acad. Sci.* **2001**, *98* (8), 4403–4408. <https://doi.org/10.1073/pnas.071047998>.
- (61) Mohimani, H.; Yang, Y.-L.; Liu, W.-T.; Hsieh, P.-W.; Dorrestein, P. C.; Pevzner, P. A. Sequencing Cyclic Peptides by Multistage Mass Spectrometry. *PROTEOMICS* **2011**, *11* (18), 3642–3650. <https://doi.org/10.1002/pmic.201000697>.
- (62) Thakkar, A.; Trinh, T. B.; Pei, D. Global Analysis of Peptide Cyclization Efficiency. *ACS Comb. Sci.* **2013**, *15* (2), 120–129. <https://doi.org/10.1021/co300136j>.
- (63) *Peptide Libraries: Methods and Protocols*; Derda, R., Ed.; Methods in Molecular Biology; Springer New York: New York, NY, 2015; Vol. 1248. <https://doi.org/10.1007/978-1-4939-2020-4>.
- (64) Wu, X.; Upadhyaya, P.; Villalona-Calero, M. A.; Briesewitz, R.; Pei, D. Inhibition of Ras–Effector Interactions by Cyclic Peptides. *MedChemComm* **2013**, *4* (2), 378–382. <https://doi.org/10.1039/C2MD20329D>.
- (65) Lian, W.; Upadhyaya, P.; Rhodes, C. A.; Liu, Y.; Pei, D. Screening Bicyclic Peptide Libraries for Protein–Protein Interaction Inhibitors: Discovery of a Tumor Necrosis Factor- α Antagonist. *J. Am. Chem. Soc.* **2013**, *135* (32), 11990–11995. <https://doi.org/10.1021/ja405106u>.
- (66) Brenner, S.; Lerner, R. A. Encoded Combinatorial Chemistry. *Proc. Natl. Acad. Sci.* **1992**, *89* (12), 5381–5383. <https://doi.org/10.1073/pnas.89.12.5381>.

- (67) Decurtins, W.; Wichert, M.; Franzini, R. M.; Buller, F.; Stravs, M. A.; Zhang, Y.; Neri, D.; Scheuermann, J. Automated Screening for Small Organic Ligands Using DNA-Encoded Chemical Libraries. *Nat. Protoc.* **2016**, *11* (4), 764–780. <https://doi.org/10.1038/nprot.2016.039>.
- (68) Franzini, R. M.; Ekblad, T.; Zhong, N.; Wichert, M.; Decurtins, W.; Nauer, A.; Zimmermann, M.; Samain, F.; Scheuermann, J.; Brown, P. J.; Hall, J.; Gräslund, S.; Schüler, H.; Neri, D. Identification of Structure-Activity Relationships from Screening a Structurally Compact DNA-Encoded Chemical Library. *Angew. Chem. Int. Ed.* **2015**, *54* (13), 3927–3931. <https://doi.org/10.1002/anie.201410736>.
- (69) Koesema, E.; Roy, A.; Paciaroni, N. G.; Coito, C.; Tokmina-Roszyk, M.; Kodadek, T. Synthesis and Screening of a DNA-Encoded Library of Non-Peptidic Macrocycles**. *Angew. Chem. Int. Ed.* **2022**, *61* (18). <https://doi.org/10.1002/anie.202116999>.
- (70) Usanov, D. L.; Chan, A. I.; Maianti, J. P.; Liu, D. R. Second-Generation DNA-Templated Macrocyclic Libraries for the Discovery of Bioactive Small Molecules. *Nat. Chem.* **2018**, *10* (7), 704–714. <https://doi.org/10.1038/s41557-018-0033-8>.
- (71) Li, Y.; De Luca, R.; Cazzamalli, S.; Pretto, F.; Bajic, D.; Scheuermann, J.; Neri, D. Versatile Protein Recognition by the Encoded Display of Multiple Chemical Elements on a Constant Macrocyclic Scaffold. *Nat. Chem.* **2018**, *10* (4), 441–448. <https://doi.org/10.1038/s41557-018-0017-8>.
- (72) Onda, Y.; Bassi, G.; Elsayed, A.; Ulrich, F.; Oehler, S.; Plais, L.; Scheuermann, J.; Neri, D. A DNA-Encoded Chemical Library Based on Peptide Macrocycles. *Chem. – Eur. J.* **2021**, *27* (24), 7160–7167. <https://doi.org/10.1002/chem.202005423>.
- (73) Stress, C. J.; Sauter, B.; Schneider, L. A.; Sharpe, T.; Gillingham, D. A DNA-Encoded Chemical Library Incorporating Elements of Natural Macrocycles. *Angew. Chem. Int. Ed.* **2019**, *58* (28), 9570–9574. <https://doi.org/10.1002/anie.201902513>.
- (74) Shin, M. H.; Lee, K. J.; Lim, H.-S. DNA-Encoded Combinatorial Library of Macrocyclic Peptoids. *Bioconjug. Chem.* **2019**, *30* (11), 2931–2938. <https://doi.org/10.1021/acs.bioconjchem.9b00628>.
- (75) Seigal, B. A.; Connors, W. H.; Fraley, A.; Borzilleri, R. M.; Carter, P. H.; Emanuel, S. L.; Fargnoli, J.; Kim, K.; Lei, M.; Naglich, J. G.; Pokross, M. E.; Posy, S. L.; Shen,

H.; Surti, N.; Talbott, R.; Zhang, Y.; Terrett, N. K. The Discovery of Macrocyclic XIAP Antagonists from a DNA-Programmed Chemistry Library, and Their Optimization To Give Lead Compounds with in Vivo Antitumor Activity. *J. Med. Chem.* **2015**, *58* (6), 2855–2861. <https://doi.org/10.1021/jm501892g>.

- (76) Fitzgerald, P. R.; Paegel, B. M. DNA-Encoded Chemistry: Drug Discovery from a Few Good Reactions. *Chem. Rev.* **2021**, *121* (12), 7155–7177. <https://doi.org/10.1021/acs.chemrev.0c00789>.
- (77) Reymond, J.-L. The Chemical Space Project. *Acc. Chem. Res.* **2015**, *48* (3), 722–730. <https://doi.org/10.1021/ar500432k>.
- (78) Zickermann, V.; Wirth, C.; Nasiri, H.; Siegmund, K.; Schwalbe, H.; Hunte, C.; Brandt, U. Mechanistic Insight from the Crystal Structure of Mitochondrial Complex I. *Science* **2015**, *347* (6217), 44–49. <https://doi.org/10.1126/science.1259859>.
- (79) Sangouard, G.; Zorzi, A.; Wu, Y.; Ehret, E.; Schüttel, M.; Kale, S.; Díaz-Perlas, C.; Vesin, J.; Bortoli Chapalay, J.; Turcatti, G.; Heinis, C. Picomole-Scale Synthesis and Screening of Macrocyclic Compound Libraries by Acoustic Liquid Transfer. *Angew. Chem.* **2021**, *133* (40), 21870–21875. <https://doi.org/10.1002/ange.202107815>.
- (80) Kale, S. S.; Bergeron-Brlek, M.; Wu, Y.; Kumar, M. G.; Pham, M. V.; Bortoli, J.; Vesin, J.; Kong, X.-D.; Machado, J. F.; Deyle, K.; Gonschorek, P.; Turcatti, G.; Cendron, L.; Angelini, A.; Heinis, C. Thiol-to-Amine Cyclization Reaction Enables Screening of Large Libraries of Macrocyclic Compounds and the Generation of Sub-Kilodalton Ligands. *Sci. Adv.* **2019**, *5* (8), eaaw2851. <https://doi.org/10.1126/sciadv.aaw2851>.
- (81) Habeshian, S.; Merz, M. L.; Sangouard, G.; Mothukuri, G. K.; Schüttel, M.; Bognár, Z.; Díaz-Perlas, C.; Vesin, J.; Bortoli Chapalay, J.; Turcatti, G.; Cendron, L.; Angelini, A.; Heinis, C. Synthesis and Direct Assay of Large Macrocyclic Diversities by Combinatorial Late-Stage Modification at Picomole Scale. *Nat. Commun.* **2022**, *13* (1), 3823. <https://doi.org/10.1038/s41467-022-31428-8>.
- (82) Gesmundo, N. J.; Sauvagnat, B.; Curran, P. J.; Richards, M. P.; Andrews, C. L.; Dandliker, P. J.; Cernak, T. Nanoscale Synthesis and Affinity Ranking. *Nature* **2018**, *557* (7704), 228–232. <https://doi.org/10.1038/s41586-018-0056-8>.

- (83) Marglin, B.; Merrifield, R. B. The Synthesis of Bovine Insulin by the Solid Phase Method ¹. *J. Am. Chem. Soc.* **1966**, 88 (21), 5051–5052. <https://doi.org/10.1021/ja00973a068>.
- (84) du Vigneaud, V.; Ressler, C.; Swan, J. M.; Roberts, C. W.; Katsoyannis, P. G. The Synthesis of Oxytocin ¹. *J. Am. Chem. Soc.* **1954**, 76 (12), 3115–3121. <https://doi.org/10.1021/ja01641a004>.
- (85) Swaisgood, H. E. The Importance of Disulfide Bridging. *Biotechnol. Adv.* **2005**, 23 (1), 71–73. <https://doi.org/10.1016/j.biotechadv.2004.09.004>.
- (86) Lewis, R. J.; Garcia, M. L. Therapeutic Potential of Venom Peptides. *Nat. Rev. Drug Discov.* **2003**, 2 (10), 790–802. <https://doi.org/10.1038/nrd1197>.
- (87) Merrifield, R. B. Solid Phase Peptide Synthesis. I. The Synthesis of a Tetrapeptide. *J. Am. Chem. Soc.* **1963**, 85 (14), 2149–2154. <https://doi.org/10.1021/ja00897a025>.
- (88) Merrifield, R. B.; Stewart, J. M. Automated Peptide Synthesis. *Nature* **1965**, 207 (4996), 522–523. <https://doi.org/10.1038/207522a0>.
- (89) Carpino, L. A.; Han, G. Y. 9-Fluorenylmethoxycarbonyl Amino-Protecting Group. *J. Org. Chem.* **1972**, 37 (22), 3404–3409. <https://doi.org/10.1021/jo00795a005>.
- (90) Postma, T. M.; Albericio, F. Disulfide Formation Strategies in Peptide Synthesis: Disulfide Formation Strategies in Peptide Synthesis. *Eur. J. Org. Chem.* **2014**, 2014 (17), 3519–3530. <https://doi.org/10.1002/ejoc.201402149>.
- (91) Habeshian, S.; Sable, G. A.; Schüttel, M.; Merz, M. L.; Heinis, C. Cyclative Release Strategy to Obtain Pure Cyclic Peptides Directly from the Solid Phase. *ACS Chem. Biol.* **2022**, 17 (1), 181–186. <https://doi.org/10.1021/acscchembio.1c00843>.
- (92) Gonschorek, P.; Zorzi, A.; Maric, T.; Le Jeune, M.; Schüttel, M.; Montagnon, M.; Gómez-Ojea, R.; Vollmar, D. P.; Whitfield, C.; Reymond, L.; Carle, V.; Verma, H.; Schilling, O.; Hovnanian, A.; Heinis, C. Phage Display Selected Cyclic Peptide Inhibitors of Kallikrein-Related Peptidases 5 and 7 and Their *In Vivo* Delivery to the Skin. *J. Med. Chem.* **2022**, 65 (14), 9735–9749. <https://doi.org/10.1021/acs.jmedchem.2c00306>.

- (93) Ganesan, A. Cyclative Cleavage as a Solid-Phase Strategy. In *Linker Strategies in Solid-Phase Organic Synthesis*; Scott, P. J. H., Ed.; John Wiley & Sons, Ltd: Chichester, UK, 2009; pp 135–149. <https://doi.org/10.1002/9780470749043.ch4>.
- (94) Marsault, E.; Hoveyda, H. R.; Gagnon, R.; Peterson, M. L.; Vézina, M.; Saint-Louis, C.; Landry, A.; Pinault, J.-F.; Ouellet, L.; Beauchemin, S.; Beaubien, S.; Mathieu, A.; Benakli, K.; Wang, Z.; Brassard, M.; Lonergan, D.; Bilodeau, F.; Ramaseshan, M.; Fortin, N.; Lan, R.; Li, S.; Galaud, F.; Plourde, V.; Champagne, M.; Doucet, A.; Bhérer, P.; Gauthier, M.; Olsen, G.; Villeneuve, G.; Bhat, S.; Foucher, L.; Fortin, D.; Peng, X.; Bernard, S.; Drouin, A.; Déziel, R.; Berthiaume, G.; Dory, Y. L.; Fraser, G. L.; Deslongchamps, P. Efficient Parallel Synthesis of Macrocyclic Peptidomimetics. *Bioorg. Med. Chem. Lett.* **2008**, *18* (16), 4731–4735. <https://doi.org/10.1016/j.bmcl.2008.06.085>.
- (95) Guo, Z.; Hong, S. Y.; Wang, J.; Rehan, S.; Liu, W.; Peng, H.; Das, M.; Li, W.; Bhat, S.; Peiffer, B.; Ullman, B. R.; Tse, C.-M.; Tarmakova, Z.; Schiene-Fischer, C.; Fischer, G.; Coe, I.; Paavilainen, V. O.; Sun, Z.; Liu, J. O. Rapamycin-Inspired Macrocycles with New Target Specificity. *Nat. Chem.* **2019**, *11* (3), 254–263. <https://doi.org/10.1038/s41557-018-0187-4>.
- (96) Gless, B. H.; Olsen, C. A. Direct Peptide Cyclization and One-Pot Modification Using the MeDbz Linker. *J. Org. Chem.* **2018**, *83* (17), 10525–10534. <https://doi.org/10.1021/acs.joc.8b01237>.
- (97) Rietman, B. H.; Smulders, R. H. P. H.; Eggen, I. F.; Vliet, A.; Werken, G.; Tesser, G. I. Protected Peptide Disulfides by Oxidative Detachment from a Support. *Int. J. Pept. Protein Res.* **2009**, *44* (3), 199–206. <https://doi.org/10.1111/j.1399-3011.1994.tb00161.x>.
- (98) Zoller, T.; Ducep, J.-B.; Tahtaoui, C.; Hibert, M. Cyclo-Release Synthesis of Cyclic Disulfides on Solid Phase. *Tetrahedron Lett.* **2000**, *41* (51), 9989–9992. [https://doi.org/10.1016/S0040-4039\(00\)01852-9](https://doi.org/10.1016/S0040-4039(00)01852-9).
- (99) Wood, R. W.; Loomis, A. L. XXXVIII. *The Physical and Biological Effects of High-Frequency Sound-Waves of Great Intensity*. *Lond. Edinb. Dublin Philos. Mag. J. Sci.* **1927**, *4* (22), 417–436. <https://doi.org/10.1080/14786440908564348>.

- (100) Hadimioglu, B.; Stearns, R.; Ellson, R. Moving Liquids with Sound: The Physics of Acoustic Droplet Ejection for Robust Laboratory Automation in Life Sciences. *SLAS Technol.* **2016**, *21* (1), 4–18. <https://doi.org/10.1177/2211068215615096>.
- (101) Ellson, R.; Mutz, M.; Browning, B.; Lee, L.; Miller, M. F.; Papen, R. Transfer of Low Nanoliter Volumes between Microplates Using Focused Acoustics—Automation Considerations. *JALA J. Assoc. Lab. Autom.* **2003**, *8* (5), 29–34. <https://doi.org/10.1016/S1535-5535-03-00011-X>.
- (102) Griffith, D.; Northwood, R.; Owen, P.; Simkiss, E.; Brierley, A.; Cross, K.; Slaney, A.; Davis, M.; Bath, C. Implementation and Development of an Automated, Ultra-High-Capacity, Acoustic, Flexible Dispensing Platform for Assay-Ready Plate Delivery. *SLAS Technol.* **2012**, *17* (5), 348–358. <https://doi.org/10.1177/2211068212457159>.
- (103) Shaabani, S.; Xu, R.; Ahmadianmoghaddam, M.; Gao, L.; Stahorsky, M.; Olechno, J.; Ellson, R.; Kossenjans, M.; Helan, V.; Dömling, A. Automated and Accelerated Synthesis of Indole Derivatives on a Nano-Scale. *Green Chem.* **2019**, *21* (2), 225–232. <https://doi.org/10.1039/C8GC03039A>.
- (104) Wang, Y.; Shaabani, S.; Ahmadianmoghaddam, M.; Gao, L.; Xu, R.; Kurpiewska, K.; Kalinowska-Tluscik, J.; Olechno, J.; Ellson, R.; Kossenjans, M.; Helan, V.; Groves, M.; Dömling, A. Acoustic Droplet Ejection Enabled Automated Reaction Scouting. *ACS Cent. Sci.* **2019**, *5* (3), 451–457. <https://doi.org/10.1021/acscentsci.8b00782>.
- (105) Gao, K.; Shaabani, S.; Xu, R.; Zarganes-Tzitzikas, T.; Gao, L.; Ahmadianmoghaddam, M.; Groves, M. R.; Dömling, A. Nanoscale, Automated, High Throughput Synthesis and Screening for the Accelerated Discovery of Protein Modifiers. *RSC Med. Chem.* **2021**, *12* (5), 809–818. <https://doi.org/10.1039/D1MD00087J>.
- (106) Bognar, Z.; Mothukuri, G. K.; Nielsen, A. L.; Merz, M. L.; Pânzar, P. M. F.; Heinis, C. Solid-Phase Peptide Synthesis on Disulfide-Linker Resin Followed by Reductive Release Affords Pure Thiol-Functionalized Peptides. *Org. Biomol. Chem.* **2022**, *20* (29), 5699–5703. <https://doi.org/10.1039/D2OB00910B>.

2. Aim of the thesis

Macrocycles have raised much interest in the pharmaceutical industry due to their ability to bind to challenging targets such as protein-protein interactions and their ability to cross membranes. However, the high throughput development of synthetic macrocyclic ligands to new disease targets is hindered by the limited availability of large, structurally diverse macrocyclic compound libraries. The overall goal of my thesis was to develop methods to increase the throughput and diversity of macrocycle libraries used in HTS to ultimately increase the chances to identify new bioactive structures against challenging targets.

A first goal of my thesis was to apply acoustic dispensing to generate large macrocycle libraries by combinatorially cyclizing " m " short di-thiol peptides with " n " bis-electrophilic reagents, and to screen the $m \times n$ macrocyclic compounds as crude products in 384-well plates. This approach turned out to be more difficult than thought due to oxidation of di-thiol peptides that formed disulfide-cyclized peptides or even dimeric peptides. Despite the problems, the project yielded valuable results such as the side-by-side comparison of a wide range of bis-electrophilic reagents for the cyclization of di-thiol peptides.

A second goal was to develop a strategy in which partially oxidized di-thiol peptides can be fully reduced, wherein the reducing reagent could be removed so that it did not interfere with the cyclization reaction. Towards this end, I proposed to develop TCEP that is immobilized at high density on a solid phase so that it could be removed by filtration or centrifugation. This project led to the generation of silica TCEP beads that have a high density of TCEP allowing reduction of di-thiol peptides at double-digit nanomolar concentrations.

A third goal of my thesis was to increase the throughput of parallel peptide synthesis for generating larger numbers of di-thiol peptides, needed for generating macrocycle libraries. Towards this end, I proposed to expand solid-phase peptide synthesis from the established 96-well format to synthesis in 384-well reactor plates. This project required development of several hardware parts for the modification of a commercial peptide synthesizer. A second action I proposed to further increase peptide synthesis throughput

was the use of microvalves for the dispensing of small volumes in solid-phase peptide synthesis. This project was motivated to perform more efficiently peptide synthesis in 384-well plates and potentially even in 1,536-well plates.

3. Reactivity and properties of thiol-thiol peptide cyclization reagents presented as a periodic table

3.1 *Work contribution*

Reactivity and properties of thiol-thiol peptide cyclization reagents presented as a periodic table

Mischa Schüttel,¹ Xinjian Ji,¹ Mahdi Assari,¹ Mark Daniel Nolan,¹ Sevan Habeshian,¹ Anne Sofie Zarda,¹ Alexander Lund Nielsen¹ and Christian Heinis^{1,*}

¹Institute of Chemical Sciences and Engineering, School of Basic Sciences, École Polytechnique Fédérale de Lausanne (EPFL), CH-1015 Lausanne, Switzerland.

Keywords

alkyl halide, alpha-haloactetyl, bromomethyl benzene, cyclization, cyclic peptide, cysteine, electrophile, peptide, stapling, thiol, skeletal diversity

Author contribution: I and Christian Heinis conceptualized the idea of using more diverse linkers. The idea of a “periodic table” representation came from Christian Heinis. I and Xinjian Ji conducted the experimental work (linker study) and performed the search of bis-electrophilic linkers in the two databases. I performed all experiments for the synthesized bis-electrophilic linkers. The manuscript was drafted and edited by me, Christian Heinis and Mark Nolan. I and Christian Heinis prepared and edited the figures. Mahdi Assari, Sevan Habeshian, Anne Sofie Zarda and Alexander Lund Nielsen contributed by suggesting additional individual linkers for testing.

This chapter is based on a manuscript prepared for publication and was supported by an SNSF grant (192368). Mark Nolan is supported by SFI SSPC (12/RC/2275_P2) and the European Peptide Society.

3.2 *Abstract*

The efficient and selective reaction of cysteine thiols with electrophilic groups such as alkyl halides or Michael acceptors is widely applied for the cyclization of peptides. Many compounds containing two electrophilic groups, termed herein bis-electrophiles, can cyclize peptides in aqueous solution and at ambient temperature. The thiol-reactive bifunctional reagents are used for example, for generating photoswitchable peptides, cyclic peptides that mimic protein epitopes, stapling α -helical peptides, or for screening large libraries of cyclic peptides by phage display or as crude reactions in microwell plates. Herein, we review the different classes of bis-electrophilic reagents used and perform a side-by-side comparison of the peptide cyclization efficiency for 39 commercially available compounds and seven herein newly synthesized ones. We display the most suited reagents in a “periodic table” in which they are ordered according to the linker length, the peptide cyclization efficiency and the type of reaction, as a guide to choose reagents for thiol-thiol peptide cyclization in future work.

3.3 *Introduction*

From bioconjugations to macrocyclizations, the reaction of a native cysteine residue or other thiol with an electrophile has proved both a valuable and facile technique. This reaction takes advantage of the relative nucleophilicity of the cysteine thiol for selective modification of unprotected sequences, a key advantage for applications at the protein or peptide level. Diverse electrophiles, including maleimides, α -halocarbonyls, benzylhalides, acrylamides and vinylsulfones are suited for this reaction in aqueous environment. The thiol alkylations proceed well in mildly basic conditions and are operationally simple, providing a highly accessible approach that has been shown to be efficient, with good reaction profile in numerous applications, ranging from labeling proteins with fluorophores or other tags, over protein and peptide immobilization reactions, to protein dimerization and antibody-drug conjugation.¹⁰⁷

The efficient and clean reaction of thiols with the various electrophiles has been exploited much also for the cyclization of peptides, wherein functional reagents are used that contain two electrophilic groups in order to connect a pair of thiol groups in peptides.^{43, 108} These bispecific molecules, termed in the following bis-electrophilic reagents or simply bis-electrophiles, have found wide application for peptide cyclization with different applications in mind, ranging from mimicking protein epitopes and stabilizing secondary structures to generating and screening large libraries of cyclic peptides. An early example for peptide cyclization via cysteines is the stabilization of peptide conformations by photoswitchable linkers functionalized with α -haloacetamides (Figure 9a).^{109, 110} Another application is the mimicking of protein epitopes based such as protein surface loops by peptides cyclized with benzyl halide-type reagents (Figure 9b).¹¹¹ Further, bis-electrophilic reagents were used to stabilize α -helices in their helical conformation by cyclizing helical peptides or helical sequences taken from protein structures (Figure 9c).^{108, 112} Our laboratory has extensively used bis-electrophiles to generate and screen large libraries of cyclic peptides by phage display (Figure 9d).¹¹³ More recently, we have used structurally diverse bis-electrophiles to generate and screen combinatorial libraries of macrocyclic compounds in microwell plates (Figure 9e). In addition to the bis-specific reagents, chemicals with more than two electrophilic groups were used, for example, in early studies

for mimicking non-linear epitopes¹¹¹ and subsequently for the phage display selection of bicyclic peptides (Figure 9f).¹¹⁴

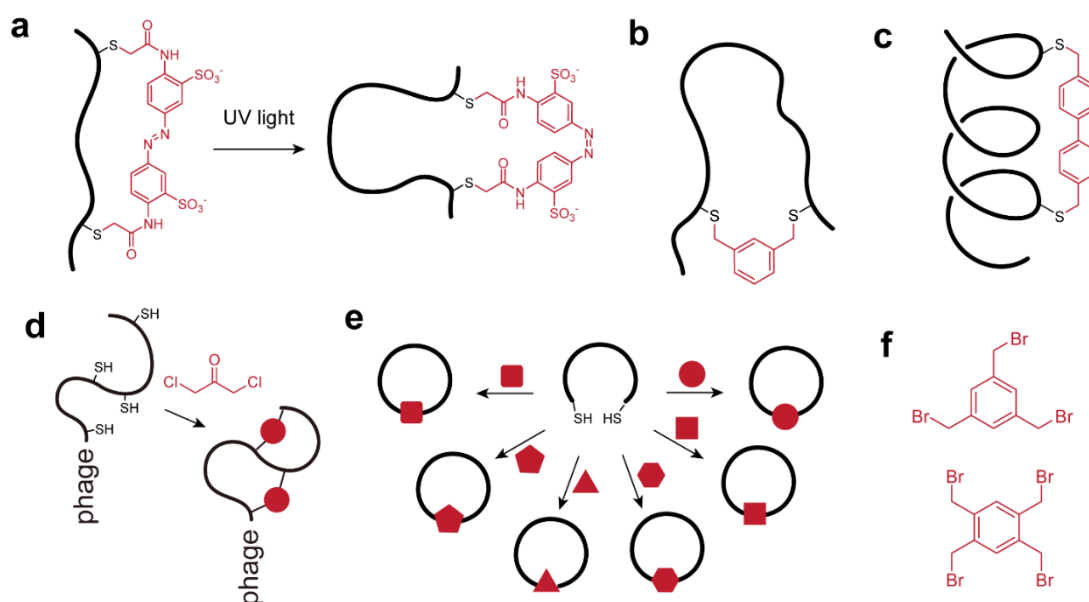


Figure 9: Applications in which peptides are cyclized via a pair of cysteine in aqueous solvent. (a) Peptide cyclized with a diazobenzene linker. UV exposure switches the linker into a trans-conformation that may impose a different conformation into the peptide. (b) Cyclization of a peptide by bromomethylbenzene-type reagent was applied to mimic protein epitopes. (c) Cyclization of peptides to favor an α -helical conformation. (d) Cyclization of cysteine-rich peptides on phage allows the screening of billions of different (bi)cyclic peptides. (e) Cyclization of short peptides via two thiol groups with diverse linkers in a combinatorial fashion allows screening of libraries without purification. (f) Reagents with three or four thio-reactive groups for the generation of bi- and tri-cyclic peptides.

Due in part to the vast utility of this chemistry, a large number of bis-electrophiles suited for peptide cyclization have been identified or developed. The electrophile types most widely used for peptide cyclization may be broadly categorized into two groups, the alkyl halides and the Michael acceptors, following two key mechanisms, the S_N2 substitution and Michael addition, respectively (Figure 10a). Within these groupings, subgroups shown in Figure 10b (alkyl halides) and Figure 10c (Michael acceptors) become apparent and are discussed in detail in the following two paragraphs. Additional thiol-thiol conjugation reagents, not falling into the above groups, are epoxides (Figure 10d, top left) (ref epoxide cyclization), perfluoroaromatic structures (Figure 10d, top right)¹¹⁵, hypervalent iodine reagents (Figure 10d, bottom left)^{116, 117} and unsaturated phosphinates (Figure 10d, bottom right).^{118, 119, 120} Of these bi-functional reagents in Figure

10c, the perfluoroaromatic structures and the hypervalent iodines were already successfully applied in peptide cyclization / helix stapling.^{115, 116, 117}

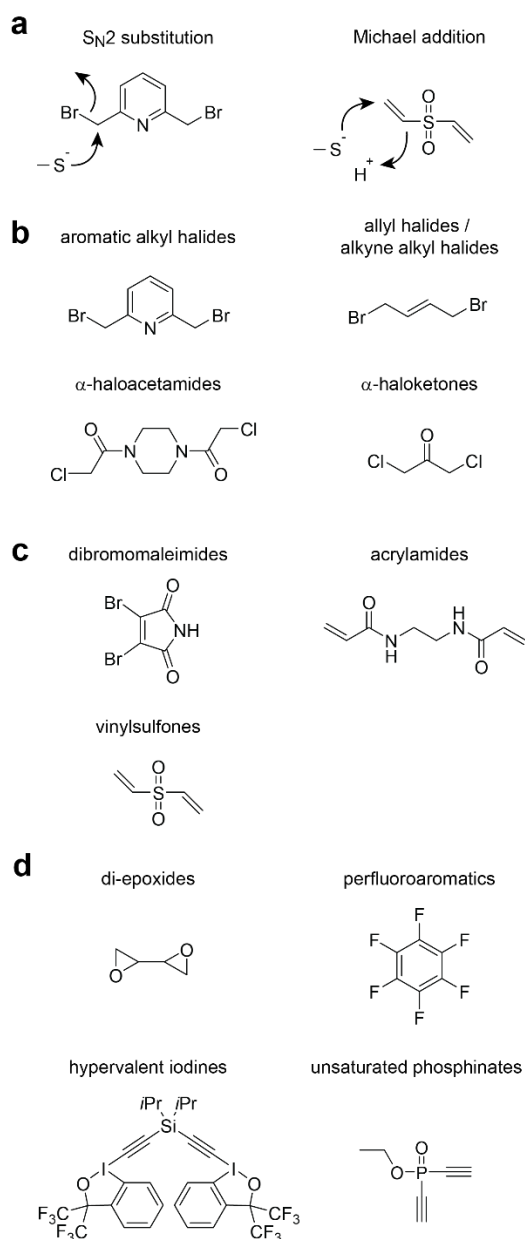


Figure 10: Bivalent reagents for thiol-thiol cyclizations. (a) Most bis-electrophilic reagents follow the indicated two types of reactions. (b) Alkyl halide bis-electrophilic reagents are divided into four sub-classes. For each class, a particularly well-performing reagent is shown. (c) Michael acceptor-based bis-electrophilic reagents are divided into three sub-classes. For each class, one example reagent is shown. (d) Additional classes of bis-electrophile reagents, of which some have only recently been introduced for thiol-thiol cyclization of peptides.

Among the alkyl halides, aromatic structures functionalized with two bromomethyl groups represent probably the largest and structurally most diverse group of reagents applied for peptide cyclization. The broad use of this class of reagents was triggered following a report by Timmerman and co-workers that bromomethylbenzene-type reagents react efficiently and selectively in aqueous conditions and at ambient temperature. The first such reagents were based on benzenes carrying two, three or even four electrophilic bromomethyl groups, including also those in Figure 9f, and were applied for generating mono-, bi- or tri-cyclic peptides.¹¹¹ An example for a bis-electrophile reagent of this group is 2,6-bis(bromomethyl)pyridine (BBP) (Figure 10b, top left). A large number of such or related structures were used for stapling α -helical peptides,^{108, 112} phage display selection of cyclic peptides,¹¹³ or for the combinatorial synthesis of large cyclic peptide libraries.^{79,80} Related structures can be generated by using heteroaromatic groups as cores. Figure 11b shows a wide range of bis-electrophiles having two halomethyl groups linked to aromatic cores (**1**, **5**, **6**, **8**, **9**, **11**, **14**, **15**, **16**, **20**, **26**, **31**, **33**, **34**, **35**, **36**, **37** and **43**). Bis-electrophilic reagents that are related in terms of the structure and reaction mechanism are aryl halides and alkyne alkyl halides, that are typically composed of two chloromethyl or bromomethyl groups conjugated to an alkene or alkyne core, as for example *trans*-1,4-dibromo-2-butene (DBB) (Figure 10b, top right). More examples of this class are shown in Figure 11b (**7**, **10**, **22**, **27**, **38**).

Another large group of the alkyl halide-based cyclization reagents are the α -halocarbonyl compounds, that can be divided further into the α -haloacetamides such as 1,4-bis(chloroacetyl)piperazine (BCP) (Figure 10b, bottom left) and α -haloketone compounds such as dichloroacetone (DCA) (Figure 10b, bottom right). Bis-electrophiles based on α -haloacetamide functional groups were used for generating photoswitchable peptides as shown in Figure 9a. Diazobenzene core structures functionalized at the ends with α -haloacetamide groups, such iodo-, bromo- and chloro-acetamide proved suitable for the generation of photoswitchable cyclic peptides.^{109, 121} Some of these reagents were applied for the phage display selection of photoswitchable peptides.^{122, 123} Several examples of bispecific α -halocarbonyl reagent without photoswitchable group are shown in Figure 11b (**2**, **12**, **21**, **24**). The second sub-class of α -halocarbonyl bis-electrophiles

are the α -haloketones. Dawson and co-workers found that the small reagent dichloroacetone (DCA) (Figure 10b, bottom right) is suited for efficiently cyclizing peptides via two thiol groups or a thiol and an amino group.¹²⁴ The reagent was subsequently used in various peptide cyclization applications, including the phage display selection of double-bridged peptides.¹¹³ In the latter and subsequent studies, DCA stood out when used in parallel with a panel of other bis-electrophiles as it yielded the best binders many having nanomolar affinities for protein targets. Derda and co-workers introduced the related diketone reagent 1,5-dichloropentane-2,4-dione for thiol-thiol peptide cyclization and applied it in phage display selections.¹²⁵ This reagent could further be used as a handle for attaching via the bioorthogonal Knorr pyrazole reaction hydrazine-functionalized compounds to the cyclized peptides.

Peptide cyclization reagents of the Michael acceptor group can be divided into the dibromomaleimides such as 2,3-dibromomaleimide (DBM) (Figure 10c, top left), the acrylamides as for example *N,N'*-ethylenebis(acrylamide) (EBA) (Figure 10c, top right) and the vinylsulfones such as divinylsulfones (DVS) (Figure 10c, bottom left). The thiol-Michael addition reaction is a type of conjugate addition in which a nucleophilic attack on the β -carbon of an α,β -unsaturated carbonyl results in a negatively charged enolate intermediate that subsequently yields the Michael adduct.¹²⁶ While maleimides are much used in bioconjugation reactions such as protein modifications via cysteines, they did not find broad use as bifunctional reagents for peptide cyclization, possibly due to product mixtures resulting from the newly formed stereocenters. The recently introduced dibromomaleimides offer reversible peptide cyclization reagents that benefit from the Michael addition reactivity, but can then eliminate a bromide to reform the Michael acceptor system, allowing for a second addition and thus peptide cyclization with one maleimide unit.¹²⁷ Vinylsulfones such as the DVS are slightly more reactive than most electrophiles described above and can cyclize peptides efficiently already at low micromolar concentrations. They proved efficient for generating and screening cyclic peptide libraries by phage display^{113, 128} and as crude reactions in microwell plates.⁸⁰

To date, a comprehensive study of the comparative reaction efficiency of bis-electrophile reagents for thiol-thiol macrocyclisation in aqueous environment is not available. In this work, we have investigated the efficiency of a range of commercially

available bis-electrophilic reagents of each of the aforementioned major classes. Efficiencies were evaluated through reaction with a model peptide (Figure 11a). The results obtained were used to develop a periodic table of *bis*-electrophilic linkers, in which such commercial compounds are ordered according to the number of atoms and their macrocyclization efficiency. This provides an invaluable tool for chemists and biologists to select the most appropriate and efficient bis-electrophilic reagents for their many applications.

3.4 Results & discussion

We aimed at comparing side-by-side the cyclization efficiency of a wide range of bis-electrophilic reagents. For the study, we used the peptide Mpa-Tyr-Leu-Mea that contains the two building blocks 3-mercaptopropionic acid (Mpa) and mercaptoethylamine (Mea) that introduce thiol groups at each end (Figure 11a). We performed the reactions in a volume of 25 μ l, applying the peptide at a concentration of 1 mM and the bis-electrophilic reagents in a 4-fold molar excess (4 mM) for higher conversion. As solvents, we chose a mixture of 50% of ammonium bicarbonate (removable under reduced pressure by decomposition into water, carbon dioxide and ammonia) buffer and 50% acetonitrile. Acetonitrile was used in the reaction due to the limited solubility of some of the reagents at high concentration. Ammonium carbonate as buffer (85 mM final conc.) to ensure a constant pH of 8 where the peptide's sulfhydryl groups are largely deprotonated. The same solvent mixture and buffer have previously been found suited for peptide cyclizations with many bis-electrophilic reagents.^{80, 111, 113} We first added to the reaction tube the buffer, then the bis-electrophilic reagent, and then the peptide, and incubated the reactions over night at room temperature.

As bis-electrophilic reagents, we chose 19 compounds that were previously used by us or others and proved to efficiently cyclize peptides.^{111, 113, 127, 129} These reagents were 6 aromatic alkyl halides (**8**, **14**, **20**, **26**, **34**, **37**), 3 allyl halides (**7**, **10**, **27**), 1 alkyne alkyl halide (**22**), 1 α -haloacetamide (**21**), 2 α -haloketones (**17**, **23**), 2 dibromomaleimides reagents (**28**, **30**), 1 dibromonaphthoquinone (**3**), 1 acrylamide (**25**) and 2 vinylsulfones (**4**, **13**) (Figure 11b and Supplementary Table 1). In addition, we included in the study 19 additional reagents that were not used for peptide cyclization before, but that contained electrophilic groups suited for reactions with thiols. For choosing these additional reagents, we searched the databases SciFinder and Reaxys for chemicals that contain two of the above-described thiol-reactive functional groups. As additional criteria for the search, we requested that the compounds are commercially available in stock and affordable (< \$1000/g). The search of the SciFinder database by the first author of this study identified 108 different compounds and the search of the Reaxys by the second author identified 58 different compounds as well as 25 common structures identified by

both authors in addition to the 19 reagents that we had chosen above (Supplementary Table 2). Comparison of the compounds showed a rather small overlap of 25 compounds for the two searches, which likely resulted from different search strategies applied by the two persons and the use of different databases. Of the total of 211 compounds, we ordered 20 compounds that differed in length and geometry compared to the already chosen 19 reagents. These additional reagents were 8 aromatic alkyl halides (**1**, **5**, **9**, **11**, **16**, **33**, **35**, **36**), 1 allyl halide (**38**), 3 α -haloketones (**32**, **46**), 3 alkyl halides (**39**, **40**, **42**), 4 epoxides (**18**, **19**, **29**, **44**), and 1 phosphine oxide (**41**) as well as 1 perfluorated benzene (**45**) as a negative control (Figure 11b and Supplementary Table 1). In addition to the purchased compounds, we synthesized seven new bis-electrophile reagents that introduced linker structures into peptides that were structurally particularly attractive as they were different from the others, including linkers with spiro structures, fused aliphatic rings or five-membered rings. These reagents were 4 aromatic alkyl halides (**6**, **15**, **31**, **43**) and 3 α -haloacetamides (**2**, **12**, **24**) (Figure 11b and Supplementary Table 1).

We assessed the reaction efficiency of a total of 46 bis-electrophilic reagents by performing the reactions twice by two persons (first and second author of this work) who prepared the reagents, performed the reactions, and analyzed the products completely independently. We quantified the percent of peptide converted into product by integrating the area under the substrate, product, and side-product peaks recorded at 220 nm, and ranked the bis-electrophiles based on the average of the two independently performed tests (Figure 11c). For seven of the 46 reactions, a larger difference (> 30%) was found for the two independently performed experiments, and we thus repeated the seven reactions. The large differences were found for the compounds **25**, **28**, **30**, **36**, **37**, **39** and **40**. Out of the 46 reagents 35 cyclized 50% or more of the peptide.

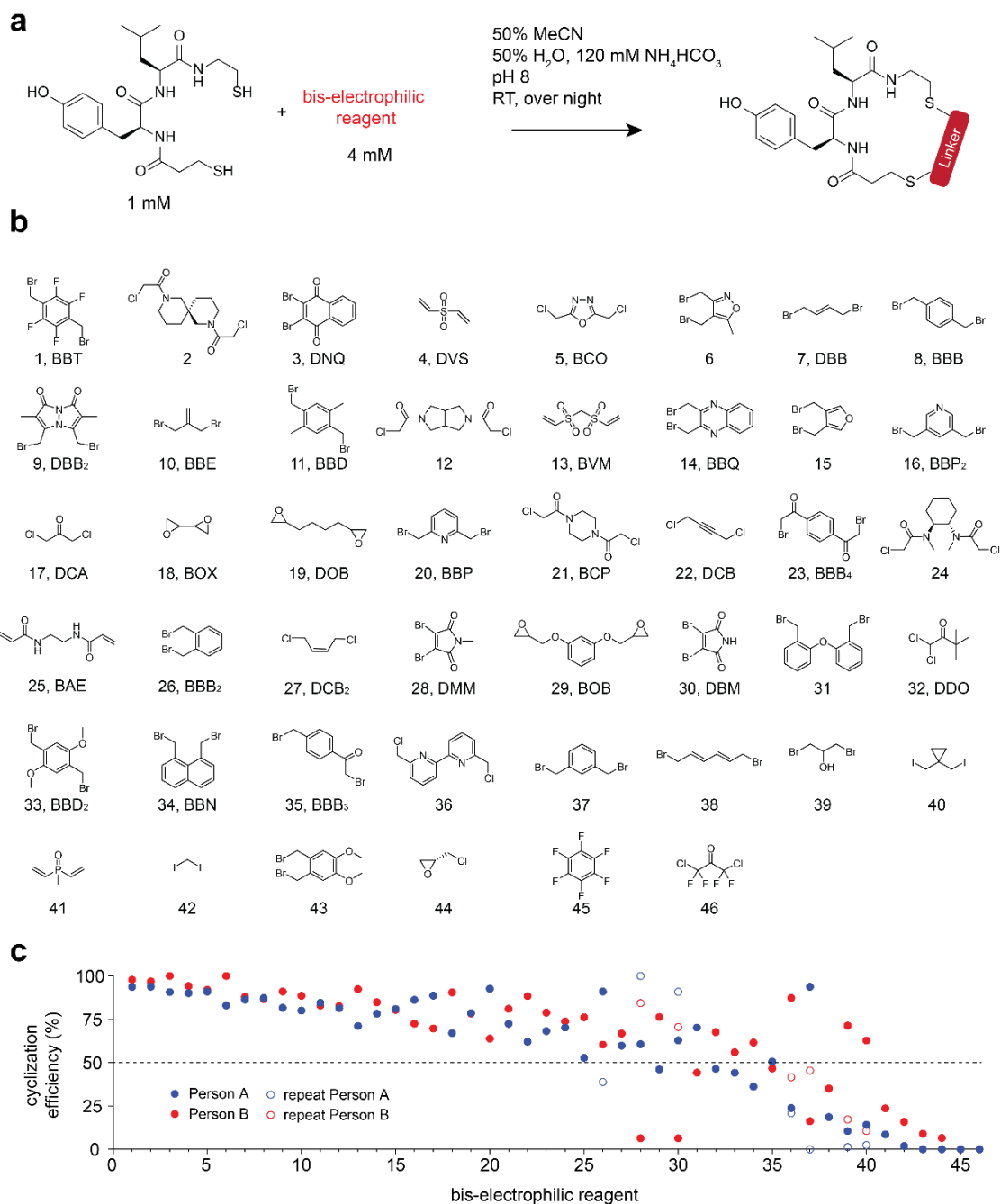


Figure 11: Side-by-side comparison of 46 bis-electrophilic reagents for peptide cyclization. (a) Model peptide and applied conditions (solvent, pH, reagent concentrations, temperature, time). The reagents were prepared, and the peptide cyclization was tested independently by two persons. (b) Bis-electrophile reagents are arranged in the order of performance in the cyclization reaction (best reagents first). Reagents cyclizing the peptide with more than 50% yield, and being commercially available, are given a 3-letter abbreviation that is also used in Figure 12. (c) Cyclization efficiency for the 46 tested reagents as determined by LC-MS. If the cyclization efficiency different largely between the two independently performed experiments, the reactions were repeated (open circles). The reagents are ordered according to the cyclization yield (average of two or four measurements).

To highlight the high-yielding and thus most suited bis-electrophilic reagents (>50% cyclization), we established a periodic table to visually summarize the obtained results (Figure 4). The best-performing bis-electrophilic linkers are sorted left to right according to the number of atoms the linker adds to the cyclic peptide backbone. The bis-electrophilic linkers are listed from the top of each column in order of descending cyclization yield. We included in the “periodic table” only compounds that are commercially accessible, but not five bis-electrophiles that showed greater than 50% cyclization and that require chemical synthesis (**2**, **6**, **12**, **15**, **25**). Therefore, the column with nine atoms

number of atoms in linker										
1	2	3	4	5	6	7	8	9	10	11
DDO ●●●○ 57% 189.0 C ₈ H ₉ Cl ₂ O 98.07 1,1-dichloro-3,3-dimethylbutan-2-one	DNQ ●●●● 95% 315.9 C ₁₀ H ₅ Br ₂ O ₃ 126.0 2,3-dibromo-naphthoquinone	BBE ●●●● 84% 213.9 C ₈ H ₇ Br ₂ 54.09 3-bromo-2-bromomethyl-1-propene	DBB ●●●● 87% 213.9 C ₈ H ₇ Br ₂ 54.09 trans-1,4-dibromo-2-butene	DVS ●●●● 92% 118.2 C ₄ H ₄ O ₂ S 120.8 divinyl sulfone	BBT ●●●● 96% 335.9 C ₁₀ H ₆ Br ₂ F ₄ 176.1 Br 1,4-bis(bromomethyl)-2,3,5,6-tetrafluorobenzene	BVM ●●●● 82% 196.2 C ₈ H ₆ O ₂ S ₂ 198.3 bis(vinylsulfonyl)-methane	DOB ●●●○ 79% 142.2 C ₈ H ₈ O ₂ 144.2 1,4-dioxiran-2-yl)-butane		BAE ●●●○ 65% 168.2 C ₇ H ₇ N ₃ O ₃ 170.2 1,2-bis(acrylamide)-ethane	BOB ●●●○ 61% 222.2 C ₁₀ H ₈ O ₂ 224.1 1,3-bisoxirane-2-ylmethoxybenzene
DMM ●●●○ 63% 268.9 C ₁₀ H ₇ Br ₂ NO ₂ 108.0 2,3-dibromo-N-methylmaleimide	DCA ●●●○ 79% 126.0 C ₃ H ₂ Cl ₂ O 56.06 1,3-dichloroacetone	BBQ ●●●● 82% 316.0 C ₁₀ H ₆ Br ₂ N ₂ 156.2 2,3-bis(bromomethyl)-quinoxaline	BCO ●●●● 92% 167.0 C ₈ H ₄ Cl ₂ N ₂ O 96.09 2,5-bis(chloromethyl)-1,3,4-oxadiazole	BBB ●●●● 87% 264.0 C ₉ H ₆ Br ₂ 104.2 1,4-bis(bromomethyl)-benzene	BBB3 ●●●○ 49% 292.0 C ₁₀ H ₆ Br ₂ O 132.2 1-bromomethyl-4-bromoacetylbenzene	BCP ●●●○ 77% 239.1 C ₁₀ H ₆ Cl ₂ N ₂ O ₂ 168.2 1,4-bis(chloroacetyl)-piperazine				
DBM ●●●○ 58% 254.9 C ₈ H ₆ Br ₂ NO ₂ 95.00 2,3-dibromomaleimide		BOX ●●●○ 79% 86.09 C ₃ H ₂ O ₂ 88.05 2,2'-bioxirane	DBB2 ●●●○ 86% 350.0 C ₁₀ H ₆ Br ₂ N ₂ O ₂ 190.2 dibromobimane	BBD ●●●○ 84% 292.0 C ₁₀ H ₆ Br ₂ 132.2 Br 1,4-bis(bromomethyl)-2,5-dimethylbenzene		BBB4 ●●●○ 74% 320.2 C ₁₀ H ₆ Br ₂ O ₂ 160.2 1,4-bis(bromoacetyl)-benzene				
		DCB ●●●○ 75% 123.0 C ₄ H ₄ Cl ₂ 52.08 1,4-dichloro-2-butyne	BBP2 ●●●○ 79% 265.0 C ₁₀ H ₆ Br ₂ N 105.1 3,5-bis(bromomethyl)pyridine	BBD2 ●●●○ 50% 324.0 C ₁₀ H ₆ Br ₂ O ₂ 164.1 Br 1,4-bis(bromomethyl)-2,5-dimethoxybenzene						
		DCB2 ●●●○ 63% 125.0 C ₄ H ₄ Cl ₂ 54.09 cis-1,4-dichloro-2-butene	BBP ●●●○ 78% 265.0 C ₁₀ H ₆ Br ₂ N 105.1 2,6-bis(bromomethyl)pyridine							
		BBB2 ●●●○ 63% 264.0 C ₁₀ H ₆ Br ₂ 104.1 1,2-bis(bromomethyl)benzene	BBN ●●●○ 49% 314.0 C ₁₀ H ₆ Br ₂ 154.1 Br 1,8-bis(bromomethyl)naphthalene							

aromatic alkyl halide
 allyl halide and alkyne alkyl halide
 α-haloacetamide
 α-haloketone
 dibromomaleimide
 dibromonaphthoquinone
 acrylamide
 vinylsulfone
 epoxide

molecular weight
 exact mass of incorporated linker atoms
 cyclization yield
 trivial or UPAC name

BBP ●●●○ 78%
 265.0 C₁₀H₆Br₂N
 105.1

 2,6-bis(bromomethyl)pyridine

Figure 12: Commercially available bis-electrophilic compounds that cyclized 50% or more of the model peptide in aqueous solvent, presented as a "periodic table". The compounds are arranged left to right according to the number of atoms the introduced chemical linker contributes to the backbone of the cyclic peptide. The best performing reagents (cyclization yield) are display in the top. The colors indicate the reaction type. For each compound, a 3-letter abbreviation is proposed. For compounds having the same abbreviation, a number was added to allow their discrimination in this work.

remains empty. The table overview should provide a simple guide to choose suitable bis-electrophilic linkers from a diverse structural range for thiol-thiol peptide cyclization applications.

3.5 *Conclusion*

We have successfully evaluated the cyclization efficiency of many bis-electrophilic linkers with a model peptide. Of the 46 tested reagents, 35 cyclized peptides with around 50% or greater yield, a bar that we consider as sufficient for most of the applications discussed, such as peptide stapling, phage display selection of cyclic peptides, and screening combinatorially cyclized peptides as crude products. These best-performing bis-electrophilic reagents contain a large diversity of functional groups, being either alkyl halides, Michael acceptors or epoxides. Most of them are compounds with two bromomethyl groups linked to aromatic core structures. Other bis-electrophile groups that performed particularly well are allyl halides, alkyne alkyl halides, α -haloacetamides, α -haloketones, dibromomaleimides, acrylamides and vinylsulfones. While some of the tested compounds did not display sufficient reactivity at the conditions applied, they are likely to work efficiently too if solvent, pH, temperature or concentration conditions were tailored to their specific chemistry and nature. As a useful guide to peptide cyclization reagent selection, we present information about the best performing commercially accessible bis-electrophilic reagents as a “periodic table”, organized by the number of backbone atoms inserted, reaction efficiency, and reaction type.

3.6 *Material & methods*

General considerations

Unless otherwise noted, all reagents were purchased from commercial sources and used without additional purification. The solvents were not anhydrous, nor were they dried prior to use. The following abbreviations for solvents standard reagents are used in this article: AcOH (acetic acid), DCM (dichloromethane), DMSO (dimethylsulfoxide), Et₂O (diethyl ether), EtOAc (ethyl acetate), HATU (1-[Bis(dimethylamino)methylene]-1H-1,2,3-triazolo[4,5-b]pyridinium 3-oxide hexafluorophosphate) HCHO (paraformaldehyde), MeCN (acetonitrile), NEt₃ (triethylamine), NMM (*N*-methylmorpholine), THF (tetrahydrofuran), TIS (triisopropylsilane).

Quality of chemicals

Acetic acid (Merck KGaA, 100%), ammonium bicarbonate (Sigma-Aldrich, 99-101%), MeCN (Fisher Chemical, >99.8%), 1,4-bis(bromoacetyl)benzene (Molbase, 95%), 1,2-bis(bromomethyl)benzene (Sigma-Aldrich, 95%), 1,3-bis(bromomethyl)benzene (Apollo Scientific, 97%), 1,4-bis(bromomethyl)benzene (Sigma-Aldrich, 97%), 1,4-bis(bromomethyl)-2,5-dimethylbenzene (Sigma-Aldrich, 98%), 1,4-bis(bromomethyl)-2,3,5,6-tetrafluorobenzene (Sigma-Aldrich, 98%), 1,4-bis(bromomethyl)-2,5-dimethoxybenzene (Sigma-Aldrich, 95%), 1,8-bis(bromomethyl)naphthalene (Sigma Aldrich, 98%), 3,5-bis(bromomethyl)pyridine hydrobromide (Enamine, 95%), 2,6-bis(bromomethyl)pyridine (Sigma-Aldrich, 98%), 2,3-bis(bromomethyl)quinoxaline (Sigma-Aldrich, 98%), bis(chloromethyl)-1,3,4-oxadiazole (Enamine, 95%), 6,6'-bis(chloromethyl)2,2'-bipyridyl (TCI, 98%), 3,4-bis(hydroxymethyl)furan (Sigma-Aldrich, 98%), 1,3-bis(oxiran-2-ylmethoxy)benzene (Sigma-Aldrich, 95%), bis(vinylsulfonyl) methane (TCI, ≥98%), 1,1-bis(iodomethyl)cyclopropane (CombiBlocks, 95%), 1-bromomethyl-4-bromoacetylbenzene (Enamine, 95%), 2,2'-bioxirane (Sigma-Aldrich, 97%), chloroacetylchloride (Sigma-Aldrich, 99%), 3-bromo-2-bromomethyl-1-propene (Sigma-Aldrich, 95%), (2*E*,4*E*)-1,6-dibromohex-2,4-diene (Enamine, 95%), 2,3-dibromomaleimide (TCI, 98%), 2,3-dibromo-1,4-naphthoquinone (Sigma-Aldrich, 97%), 1,3-dibromo-2-propanol (Sigma-Aldrich, 98%), 1,4-bis(chloroacetyl)piperazine (abcr, 95%), dibromobimane (Sigma-Aldrich, 95%), *cis*-1,4-dichloro-2-butene (Sigma-Aldrich,

95%), 3-(chloromethyl)-5-methyl-1,2-oxazole (Enamine, 95%), 2,3-dibromo-*N*-methylmaleimide (Sigma-Aldrich, 99%), 1,4-(dibromoacetyl)benzene (Molbase, 95%), 1,3-dichloroacetone (Sigma-Aldrich, 98%), 1,3-dichlorotetrafluoroacetone (TCI, 98%), 1,4-dichloro-2-butyne (Sigma-Aldrich, 98%), 1,1-dichloro-3,3-dimethylbutan-2-one (CombiBlocks, 95%), dichloromethane (Sigma-Aldrich, >99.9%), 1,1-diiodomethane (Sigma-Aldrich, 99%), 1,2-diiodoethane (Enamine, 99%), diethyl ether (Honeywell Riedel-de Häen, >99.8%), 1,2-dimethoxybenzene (Sigma-Aldrich, 98%), dimethyl formamide (Biosolve Chimie Sarl, >99.5%), DMSO (Sigma-Aldrich, >99.5%), 2,8-diazaspiro[5.5]undecane (Enamine, 95%), divinyl sulfone (TCI, 97%), [ethenyl(methyl)phosphoryl]ethane (Enamine, 95%), ethyl acetate (Thommen Furler AG, 98%), 1,2-bis(acrylamide)ethane (Alfa Aesar, 96%), 1-Chloro-2,3-epoxypropane (Merck KGaA, 98%), fluorenylmethoxycarbonyl (Fmoc) amino acids and derivatives (GL Biochem Shanghai Ltd, >99%), HATU (GL Biochem Shanghai Ltd, >99%), hexafluorobenzene (Sigma-Aldrich, 98%), hexane (Merck KGaA, >99%), hydrobromide (VWR chemicals, 47%), 3-(tritylthio)propionic acid (Combiblock, 95%), NEt₃ (Fluka Analytical, >98%), *N*-methylimidazole (Sigma-Aldrich, 99%), NMM (Sigma-Aldrich, >98%), 1,4-di(oxiran-2-yl)-butane (TCI, 97%), octahydropyrrolo[3.4-*C*]pyrrole (Fluorochem, 95%), 2,2'-oxybis-benzenemethanol (TCI, >98%), paraformaldehyde (Sigma-Aldrich, 95%), phosphorous tribromide (Sigma-Aldrich, 97%), silica gel (Silicycle, SiliaFlash® P60), sodium bicarbonate (Merck KGaA, 99.5-100.5%), sodium chloride (Fisher Chemicals, >99.5%), sodium sulfate (Reactolab, 98%), TFA (Sigma-Aldrich, >99%), THF (Fisher Chemical, 99.8%), *trans*-1,4-dibromo-2-butene (Sigma-Aldrich, 99%), *trans*-(1*S*, 2*S*)-*N,N'*-bismethyl-1,2-cycloheanediamine (Fluorochem, 98%), trimethylamine (Roth AG, >99.5%), 1,3,5-trioxane (Sigma-Aldrich, >99%), water (MilliQ).

Search of commercially available bis-electrophilic reagents

The two data bases SciFinder and Reaxys were searched each by one person for bis-electrophilic reagents. Search criteria were i) that the compounds contain exactly two electrophilic groups that promised to react with thiols in aqueous solvent and at room temperature, ii) were commercially offered and in stock, and iii) did not exceed a price of 1000 US dollar per gram. The identified compounds were ordered according to the number of backbone atoms they contributed to a cyclized peptide.

Synthesis of model peptide

The model peptide was produced by solid-phase peptide synthesis (SPPS) at a 500 μmol scale using a 20 ml PP syringe with PE frit (CEM, 99.278). Cysteamine-4-methoxy trityl polystyrene resin (284 mg, 460 μmol , 1.00 equiv., 1.62 mmol/g, Novabiochem, 8.56087) was pre-swelled with DMF (10 ml) for 20 min and filtered before SPPS. Coupling was performed by dissolving the Fmoc amino acid derivative (1.38 mmol, 3 equiv.) and HATU (525 mg, 1.38 mmol, 3 equiv.) in DMF (10 ml) followed by the addition of DIPEA (0.469 ml, 2.76 mmol, 6 equiv.) for 1 min pre-activation prior to addition to the swelled and free N-terminal resin inside the column reactor. The syringe was closed and incubated for 45 min under rotation at 25 rpm (Stuart rotator). Fmoc-L-Tyr(*t*Bu)-OH (634 mg, 1.38 mmol, 3 equiv.), Fmoc-L-Leu-OH (488 mg, 1.38 mmol, 3 equiv.) and 3-(tritylthio)propionic acid (481 mg, 1.38 mmol, 3 equiv.) were used as Fmoc derivatives and double couplings were conducted to ensure full conversion. After each double coupling step, the resin was washed with DMF (3×10 ml) followed by Fmoc deprotection with 20% piperidine (10 ml, 27 mmol, 20 equiv.) for 5 min. Fmoc deprotection was conducted twice before washing with DMF (3×10 ml) for each coupling cycle. After the last coupling step with 3-(tritylthio)propionic acid, no Fmoc deprotection with piperidine was applied. A final resin wash with DCM (3×10 ml) was performed and the resin was dried under air. To cleave the peptide from the resin, a cleavage cocktail (20 ml, TFA:H₂O:TIS, 95:2.5:2.5, v/v/v) was added and incubated for 3 h at room temperature before filtering into a 50 ml falcon tube (greiner bio-one, 227 261). Nearly all TFA was evaporated with a continuous stream of nitrogen before re-dissolving in solvent (20 ml, MeCN:H₂O, 50:50) for lyophilisation. The lyophilized solid residue was purified by RP-HPLC using a Waters HPLC system (2489 UV detector, 2535 pump, Fraction Collector III), a 19 mm \times 250 mm Waters Xterra MS C18 OBD preparative column (125 Å pore, 10 μm particle), solvents A (H₂O, 0.1% v/v TFA) and B (MeCN, 0.1% v/v TFA), and a gradient of 0 – 40% solvent B over 30 min with UV detection at 220 nm. The fractions with the desired product were lyophilized to a white powder of pure (>99%, UHPLC-MS) model peptide (8.66 mg, 19.6 μmol , 4%).

Cyclization with bis-electrophilic reagents

Reactions were performed in volumes of 25 μl in PP LC-MS vials (Shimadzu, 961-10020-15) closed with caps (Shimadzu, 961-10020-15). Solvent, bis-electrophile reagent and peptide were added in this order within 1 minute. The solvent was prepared by first dissolving NH_4HCO_3 in water to obtain a concentration of 170 mM NH_4HCO_3 having a pH of around 8. To this buffer, an equal volume of MeCN was added to obtain a solvent mixture of 50% NH_4HCO_3 and 50% MeCN and a NH_4HCO_3 concentration of 85 mM. The pH was measured to verify that it was 8.0. Of this solvent, 17.5 μl were added to the tube. Bis-electrophile reagent was dissolved in 100% MeCN to reach a concentration of 40 mM, followed by adding an equal volume of water. Of this 20 mM reagent in 50% MeCN and 50% water, 5 μl were added to the reaction tube (100 nmol, 4 equiv.). Model peptide was dissolved in 100% MeCN to reach a concentration of 20 mM, followed by addition of an equal volume of water. Of this 10 mM peptide in 50% MeCN and 50% water, 2.5 μl was added to the reaction tube (25 nmol, 1 equiv.). The reagents were mixed by pipetting and by vortexing. The final reaction concentration was 1 mM model peptide, 4 mM bis-electrophilic reagent and 60 mM NH_4HCO_3 concentration in a solvent mixture of 50% MeCN and 50% water. Bis-electrophilic reagents that were not soluble in 50% acetonitrile and 50% water were dissolved in 50% DMSO and 50% water (compounds **3**, **14**, **29**, **31**). The reagent preparation (bis-electrophiles), the reactions and the reaction analysis were performed twice independently by two persons.

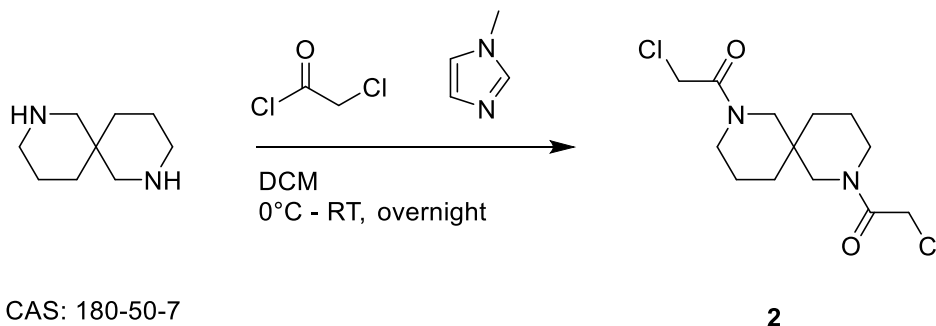
LC-MS analysis of reactions

Peptide samples were analyzed by LC-MS analysis with a UHPLC and single quadrupole MS system (Shimadzu LCMS-2020) using a C18 reversed phase column (Phenomenex Kinetex 2.1 mm \times 50 mm C18 column, 100 Å pore, 2.6 μm particle) and a linear gradient of solvent (MeCN, 0.05% formic acid) over solvent A (H_2O , 0.05% formic acid) at a flow rate of 1 ml/min. For all samples, a gradient of 0 - 60% MeCN within 5 min was applied and absorbance was recorded at 220 nm. Mass analysis was performed in a positive ion mode. 100 μl PP HPLC microvial (Shimadzu, 961-10030-14) with silicon and teflon caps (Shimadzu, 961-10020-15) were used for all samples. For analysing the peptide cyclization reactions, 1 μl of the undiluted sample was injected.

3.7 Supplementary information

Preparation of bis-electrophilic reagent 2

The reagent 2 was prepared following a similar procedure as described in Nawaz et al..¹³⁰

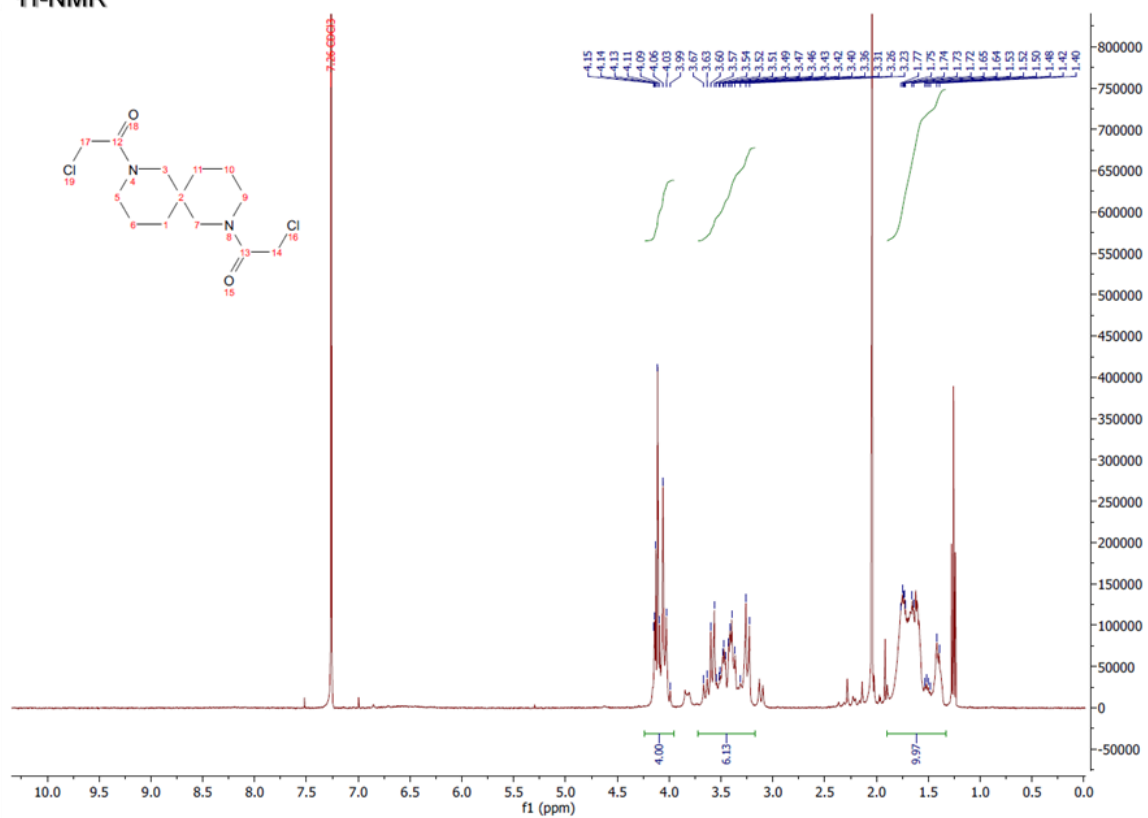


2,8-Diazaspiro[5.5]undecane (0.250 g, 1.54 mmol, 1.00 equiv.) was dissolved in DCM (8.0 ml) followed by the addition of 1-methylimidazole (0.37 ml, 4.6 mmol, 3.0 equiv.). The reaction mixture was cooled down with an ice bath under inert atmosphere (nitrogen) and chloroacetyl chloride (0.27 ml, 1.4 mmol, 2.2 equiv.) was added dropwise. The slightly yellow reaction solution was stirred overnight at room temperature. Afterward, the reaction mixture was extracted with aqueous 0.1 M HCl (3 × 10 ml), the organic phase was washed with brine (3 × 10 ml) until neutral pH 7 and dried over Na₂SO₄, filtered and concentrated under reduced pressure (40°C, 600-2 mbar) to afford pale yellow sticky oil as a crude product (334 mg). The crude product was purified via flash column chromatography (10 g silica gel) using the solvents DCM and EtOAc and a gradient from 0 to 50% EtOAc in 25% incremental steps. The combined organic fractions were concentrated under reduced pressure (40°C, 600 – 2 mbar) to afford a pale brown oil as the desired product **2** (354 mg, 1.15 mmol, 75% yield) after drying under high vacuum over the weekend. The product was stored under nitrogen at 4°C to prevent hydrolysis, which was observed to occur rapidly by NMR (Additional peaks in ¹³C-NMR). Cyclization product with model peptide yielded clean product with a desired mass difference.

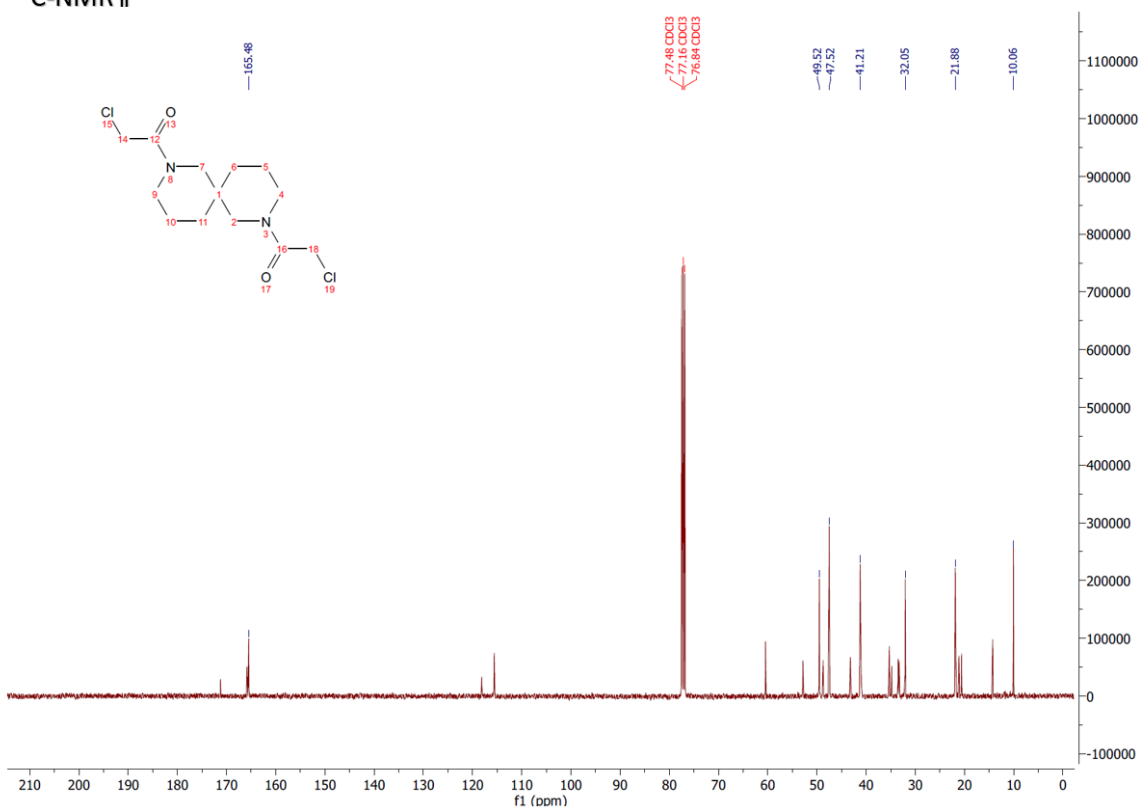
¹H NMR (400 MHz, CDCl₃) δ = 4.23 - 4.00 (m, 4H), 3.71 – 3.04 (m, 6H), 1.86 – 1.35 (m, 10H) ppm; **¹³C{¹H}-NMR** (101 MHz, CDCl₃) δ = 165.48 (2C), 49.52 (2C), 47.52 (2C), 41.21 (2C), 32.05 (1C), 21.88 (2C), 10.06 (2C) ppm; **UHPLC-MS** (ESI), calc'd for [M+H]⁺ = [C₁₃H₂₁Cl₂N₂O₂]⁺ = 307.0975 m/z, found = 307.1 m/z, 94% purity (peak area, 220 nm); **HRMS** (nanochip-based ESI/LTQ-Orbitrap), calc'd for [M+H]⁺ = C₁₃H₂₁Cl₂N₂O₂⁺ =

307.0975 m/z, found = 307.0971 m/z (deviation: 0.7 ppm); R_f = 0.27 (one spot, DCM:EtOAc, 1:1, UV & KMnO₄).

¹H-NMR

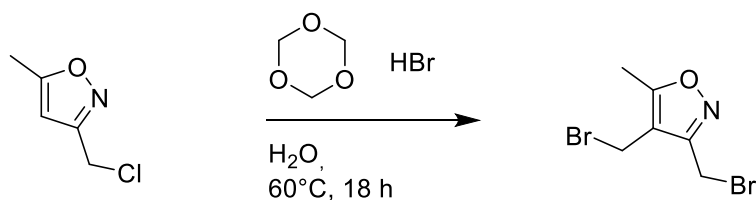


¹³C-NMR



Preparation of bis-electrophilic reagent 6

The reagent 6 was prepared following the procedure of Madsen et al..¹³¹



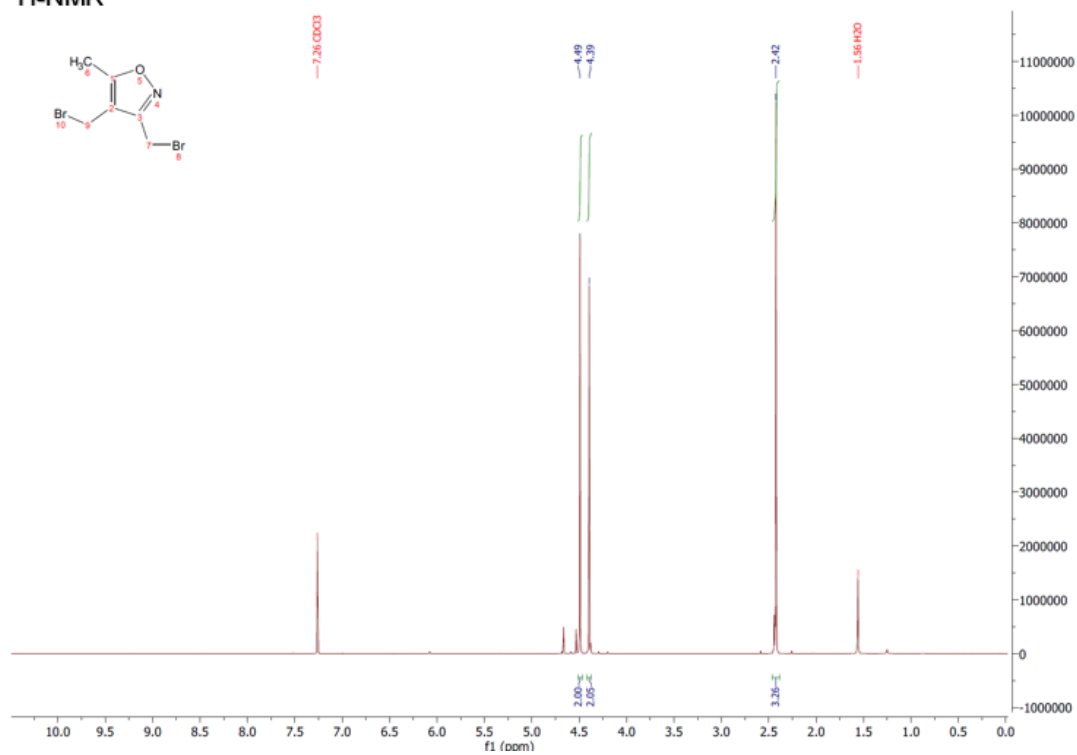
CAS: 35166-37-1

6

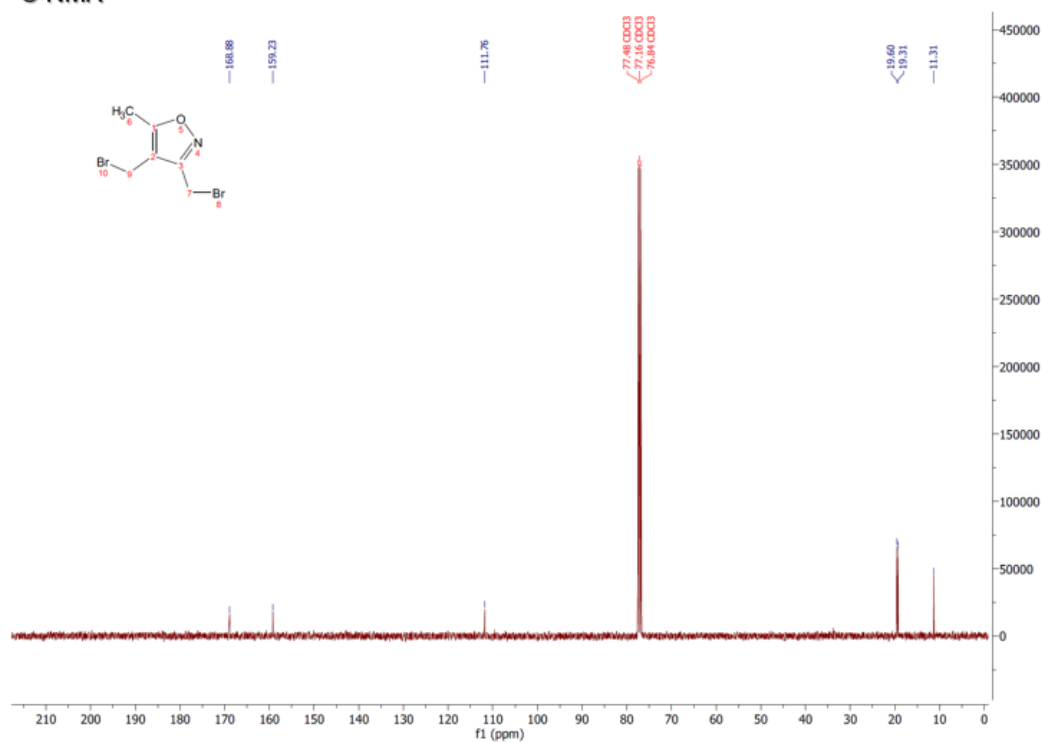
3-(Chloromethyl)-5-methyl-1,2-oxazole (0.50 g, 3.7 mmol, 1.0 equiv.) and 1,3,5-trioxane (0.50 g, 5.5 mmol, 1.5 equiv.) were introduced into a 20 ml microwave high-pressure vial followed by the addition of 48% HBr_(Aq) (5.1 ml, 44 mmol, 12 equiv.). The vial was sealed and stirred overnight at 60°C. After cooling down to room temperature, the reaction mixture was extracted with DCM (2 × 10 ml). The combined organic phase was washed with brine (3 × 10 ml), dried over Na₂SO₄, filtered and concentrated under reduced pressure to afford crude product (0.747 g). The crude product was purified via flash column chromatography (24 g silica gel) using the solvents DCM and hexane and a gradient from 20 to 50% DCM with 10% incremental increase of DCM. The combined organic fractions were concentrated under reduced pressure and dried under vacuum to afford the desired product **6** (0.645 g, 62% yield).

¹H NMR (400 MHz, CDCl₃) δ = 4.49 (s, 2H), 4.39 (s, 2H), 2.42 (s, 3H) ppm; **¹³C{¹H}-NMR** (101 MHz, CDCl₃) δ = 168.88 (1C), 159.23 (1C), 111.76 (1C), 19.60 (1C), 19.31 (1C), 11.31 (1C) ppm; **UHPLC-MS** (ESI), calc'd for [M+H]⁺ = [C₆H₈Br₂NO]⁺ = 267.8967 m/z, found = 267.8 m/z, 96% purity (peak area, 220 nm); **HRMS** (nanochip-based ESI/LTQ-Orbitrap), calc'd for [M+H]⁺ = C₆H₈Br₂NO⁺ = 267.8967 m/z, found = 267.8965 m/z (deviation: 0.7 ppm); **R_f** = 0.30 (one spot, DCM:hexane, 1:1, UV & KMnO₄).

¹H-NMR



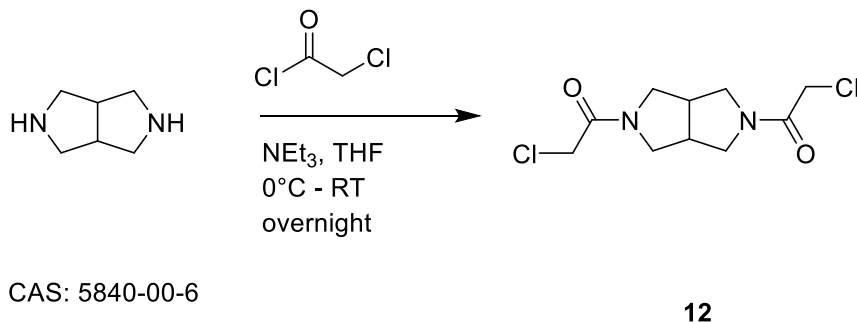
¹³C-NMR



Preparation of bis-electrophilic reagent 12

The reagent 12 was prepared following a similar procedure as published by Lizza et al..

132

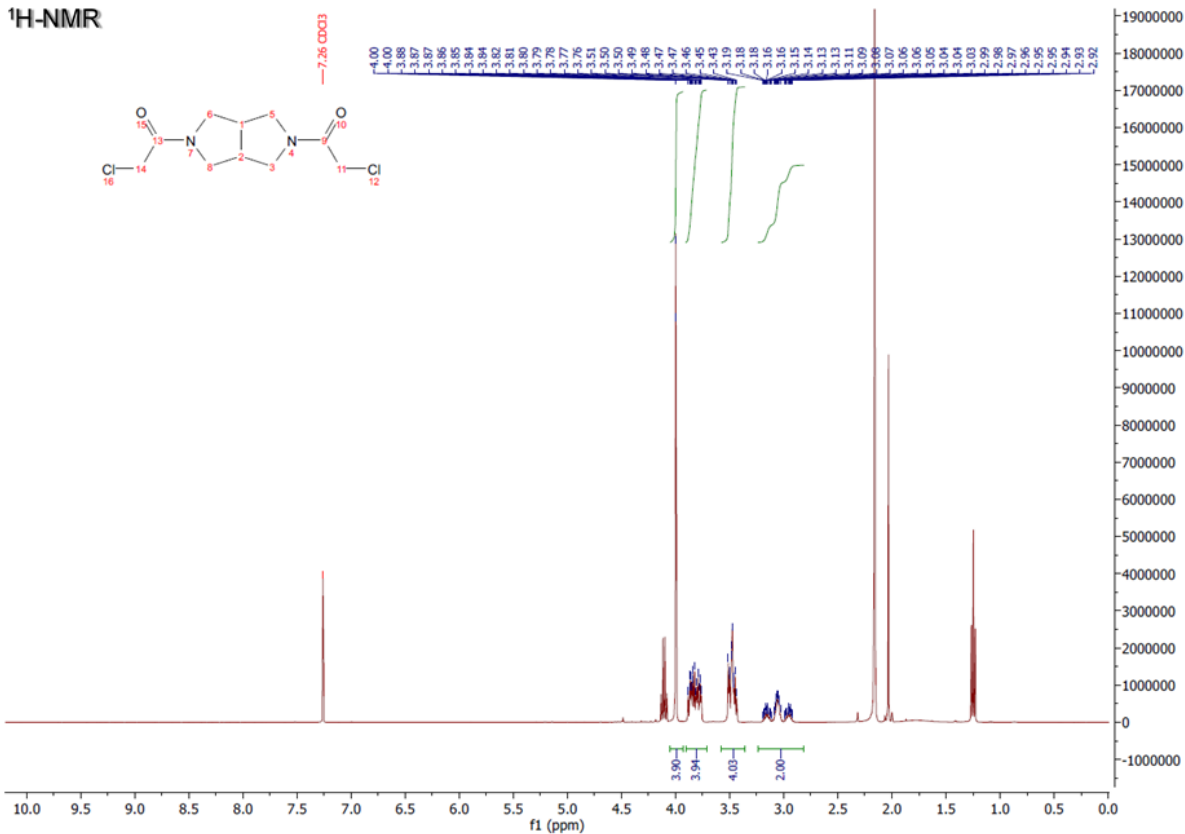


To a stirring solution of chloroacetyl chloride (0.51 ml, 6.35 mmol, 3.00 equiv.) and triethyl amine (0.80 ml, 5.7 mmol, 2.7 equiv.) in THF (18 ml) at 0°C was added dropwise octahydropyrrolo[3.4-C]pyrrole (0.25 g, 2.2 mmol, 1.0 equiv.) as a solution in THF (3.0 mL) over 20 minutes. The mixture was allowed to room temperature and stirred overnight. The reaction mixture was quenched with 4 M dioxane (1.5 ml, 6.0 mmol, 2.8 equiv.) followed by the removal of all volatiles under reduced pressure. The residue was dissolved in DCM (10 ml) and washed with 0.1 M HCl (3 × 10 ml, pH 1), aqueous saturated NaHCO₃ (3 × 10 ml, pH 9) and brine (3 × 10 ml, pH 7). The organic phase was dried over Na₂SO₄, filtered and concentrated under reduced pressure to afford a dark brown viscous oil (159 mg). The residue was purified by flash column chromatography (8.0 g silica gel) using the solvents DCM and EtOAc and a gradient from 0 to 100% EtOAc in 25% incremental steps to afford the desired product **12** (72 mg, 0.27 mmol, 13% yield) as a dark brown sticky oil after high vacuum drying over the weekend. The final product was stored under argon and in the fridge to prevent hydrolysis.

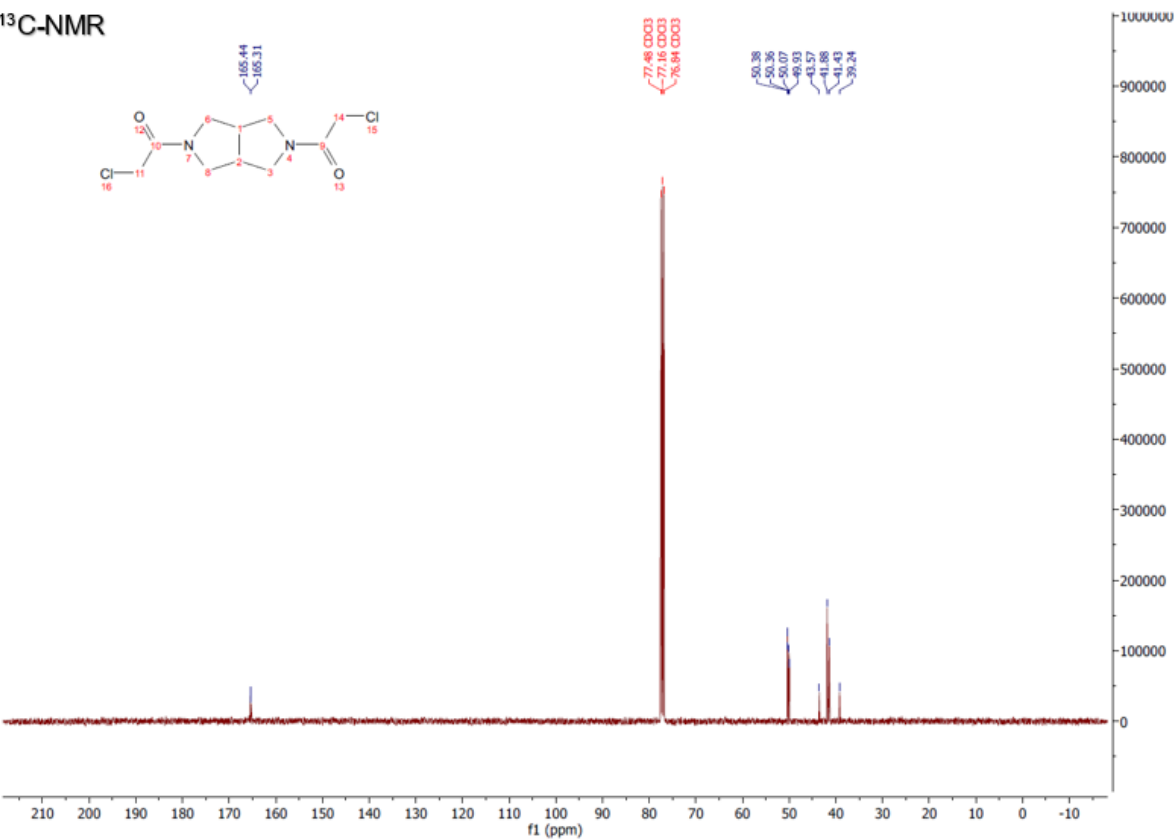
¹H NMR (400 MHz, CDCl₃) δ = 4.00 (s, 4H), 3.91 – 3.71 (m, 4H), 3.58 – 3.36 (m, 4H), 3.24 – 2.81 (m, 2H) ppm; **¹³C{¹H}-NMR** (101 MHz, CDCl₃) δ = 165.44 (1C), 165.31 (1C), 50.38 (1C), 50.36 (1C), 50.07 (1C), 49.93 (1C), 43.57 (1C), 41.88 (1C), 41.43 (1C), 39.24 (1C) ppm; **UHPLC-MS** (ESI), calc'd for [M+H]⁺ = [C₁₀H₁₅Cl₂N₂O₂]⁺ = 265.05 m/z, found = 264.95 m/z, 99% purity (peak area, 220 nm); **HRMS** (nanochip-based ESI/LTQ-Orbitrap),

calc'd for $[M+H]^+ = C_{10}H_{15}Cl_2N_2O_2^+ = 265.0505$ m/z, found = 265.0502 m/z (deviation: 1 ppm); $R_f = 0.12$ (one spot, DCM:EtOAc, 1:1, UV & $KMnO_4$).

¹H-NMR

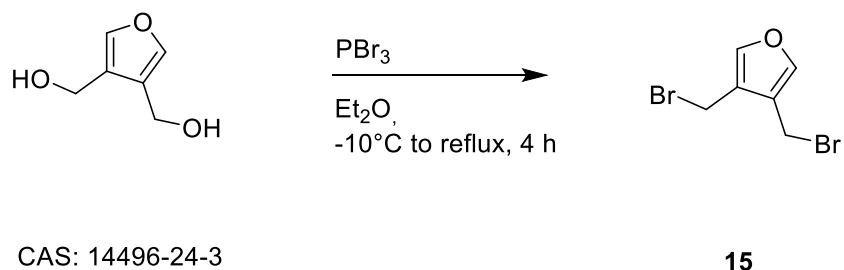


¹³C-NMR



Preparation of bis-electrophilic reagent **15**

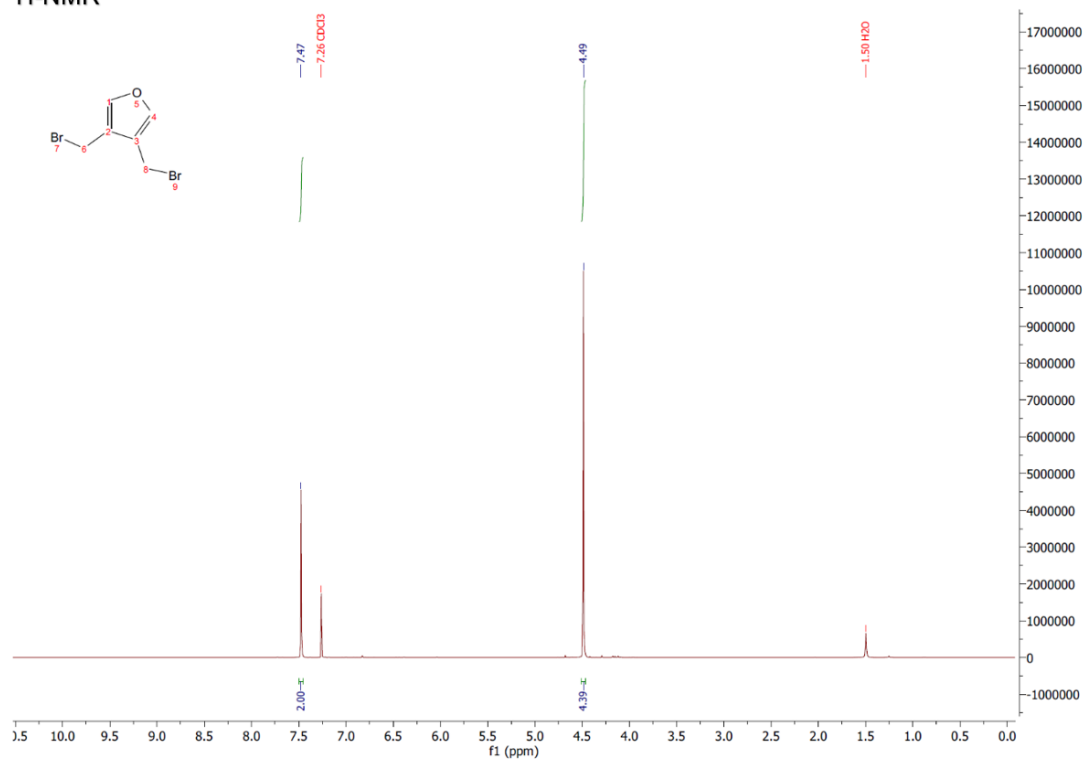
The reagent **15** was prepared following the procedure of Cervantes-Reyes et al..¹³³



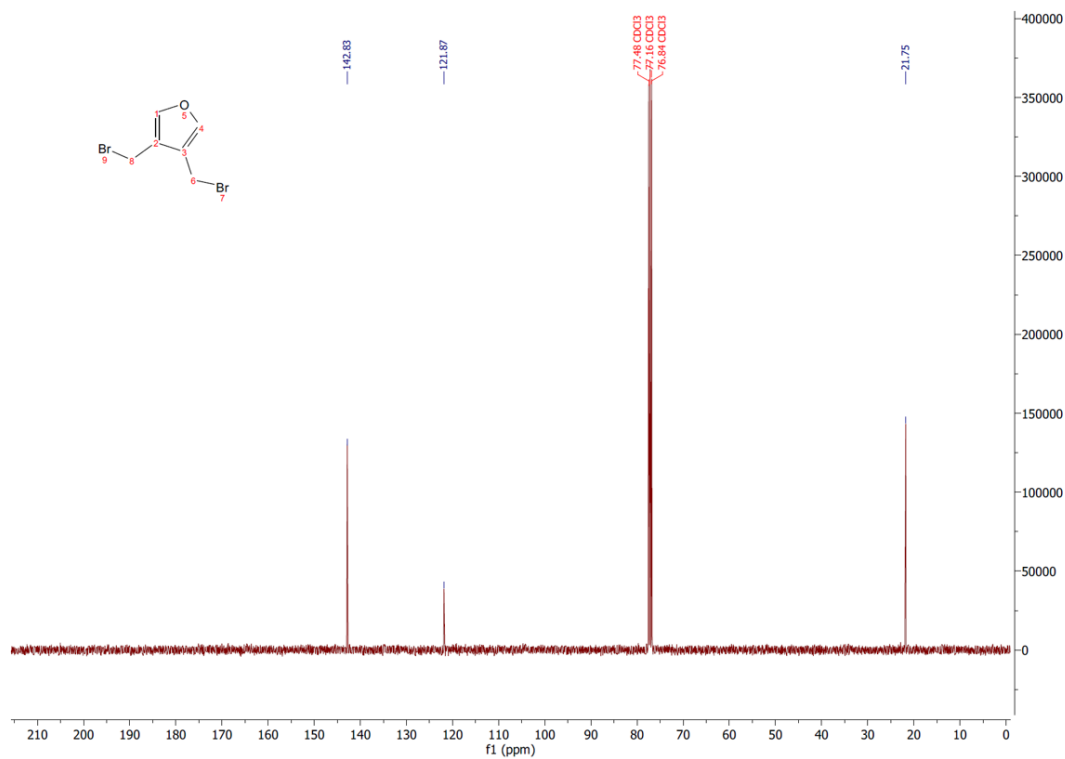
Phosphorous tribromide (0.230 ml, 2.45 mmol, 0.98 equiv.) was added dropwise to a solution of 3,4-bis(hydroxymethyl)furan (0.257 ml, 2.50 mmol, 1.00 equiv.) in dry diethyl ether (11.3 ml) at -10°C during 45 min under inert atmosphere (nitrogen). The reaction mixture was allowed to room temperature and then refluxed for 4 h at 45°C. Afterward, the reaction mixture was poured onto crushed ice (25 ml) and stirred for 1 h after which chloroform (10 ml) was added. The organic layer was separated and the aqueous layer was extracted once more with chloroform (10 mL). The combined organic phases were washed with a saturated aqueous solution of NaHCO₃, dried over Na₂SO₄, filtered and concentrated under reduced pressure to afford a brown liquid crude product (0.83 g). The crude product was purified via flash column chromatography using the solvents DCM and hexane with an isocratic mixture (10% DCM). The combined organic fractions were concentrated under reduced pressure to afford a slightly yellow-colored liquid as the desired product **15** (0.533 g, 2.10 mmol, 84% yield).

¹H NMR (400 MHz, CDCl₃) δ = 7.47 (s, 2H), 4.49 (s, 4H) ppm; **¹³C{¹H}-NMR** (101 MHz, CDCl₃) δ = 142.83 (2C), 121.87 (2C), 21.75 (2C) ppm; **UHPLC-MS** (ESI), calc'd for [M+H]⁺ = [C₆H₇Br₂O]⁺ = 252.8858 m/z, found = non, 99% purity (peak area, 220 nm); **HRMS** (nanochip-based ESI/LTQ-Orbitrap), calc'd for [M+H]⁺ = C₆H₇Br₂O⁺ = 252.8858 m/z, found = 252.8859 m/z (deviation: -0.4 ppm); **R_f** = 0.36 (one spot, DCM:hexane, 1:9, UV & KMnO₄).

¹H-NMR

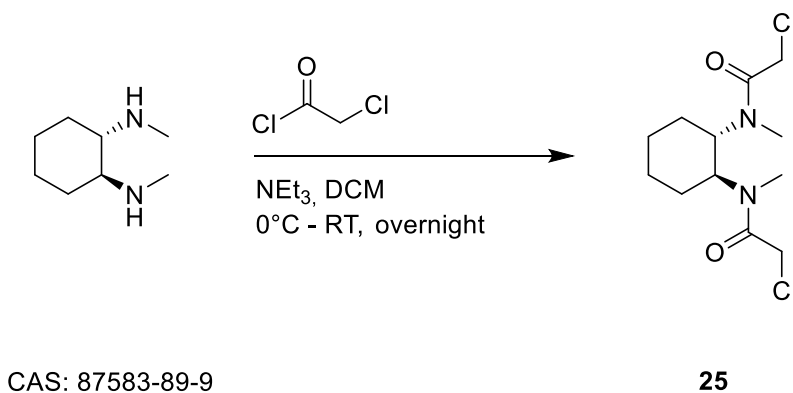


¹³C-NMR



Preparation of bis-electrophilic reagent 25

The reagent 25 was prepared following a procedure similar to Lizza et al..¹³²

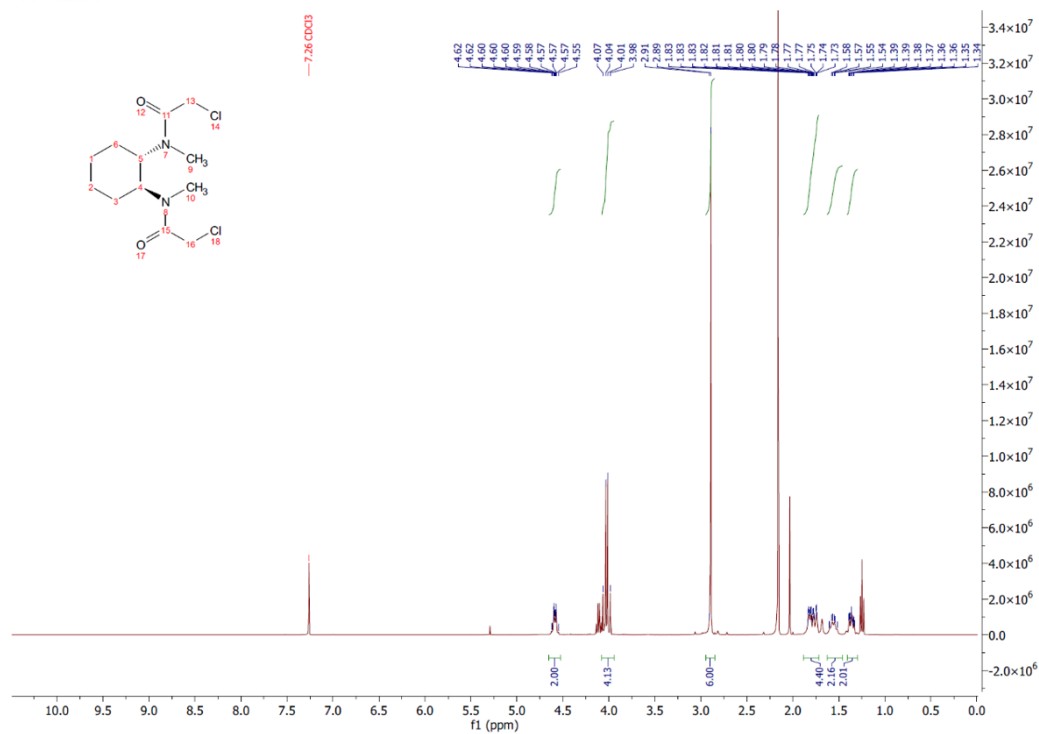


To a solution of chloroacetyl chloride (0.52 ml, 6.5 mmol, 3.0 equiv.) and triethylamine (0.80 mL, 5.7 mmol, 2.7 equiv.) in THF (18 ml) at 0°C was added portionwise *trans*-(1*S*,2*S*)-*N,N*-bismethyl-1,2-cyclohexanediamine (0.25 g, 2.2 mmol, 1.0 equiv.). The reaction mixture was allowed to warm to room temperature after the complete addition and stirred overnight. Afterward, the reaction mixture was quenched with 4 M dioxane (1.5 ml, 6.0 mmol, 2.8 equiv.) followed by the removal of all volatiles under reduced pressure. The residue was dissolved in DCM (10 ml) and washed with aqueous 0.1 M HCl (3 × 10 ml, pH 1), aqueous saturated NaHCO₃ (3 × 10 ml, pH 9) and brine (3 × 10 ml, pH 7). The organic phase was dried over Na₂SO₄, filtered and concentrated under reduced pressure to afford a dark brown viscous oil (279 mg). The crude product was purified via flash column chromatography (11 g silica gel) using the solvents DCM and EtOAc and a gradient from 0 to 50% EtOAc with 10% incremental steps. The combined organic fractions were concentrated under reduced pressure and dried under vacuum to afford the desired product **25** (154 mg, 0.521 mmol, 24% yield) as a dark brown sticky oil after drying at high vacuum over the weekend. Residual ethyl acetate was still found despite high vacuum drying.

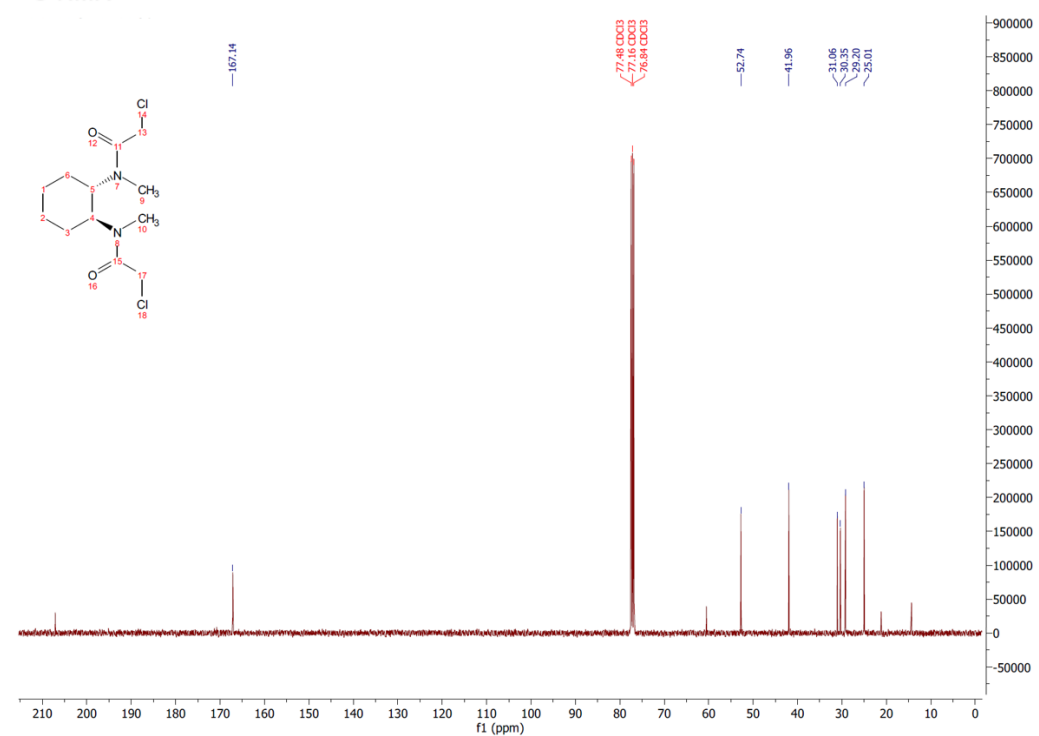
¹H NMR (400 MHz, CDCl₃) δ = 4.66 - 4.53 (m, 2H), 4.07 – 3.95 (m, 4H), 2.89 (s, 6H), 1.78 (m, 4H), 1.56 (m, 2H), 1.44 – 1.29 (m, 2H) ppm; **¹³C{¹H}-NMR** (101 MHz, CDCl₃) δ = 167.14 (2C), 52.74 (2C), 41.96 (2C), 31.06 (1C), 30.35 (1C), 29.20 (2C), 25.01 (2C) ppm; **UHPLC-MS** (ESI), calc'd for [M+H]⁺ = [C₁₂H₂₁Cl₂N₂O₂]⁺ = 295.0975 m/z, found = 295.0 m/z, 99% purity (peak area, 220 nm); **HRMS** (nanochip-based ESI/LTQ-Orbitrap), calc'd

for $[M+H]^+ = C_{12}H_{21}Cl_2N_2O_2^+ = 295.0975$ m/z, found = 295.0973 m/z (deviation: 0.7 ppm);
 $R_f = 0.48$ (one spot, DCM:EtOAc, 1:1, UV & $KMnO_4$).

¹H-NMR

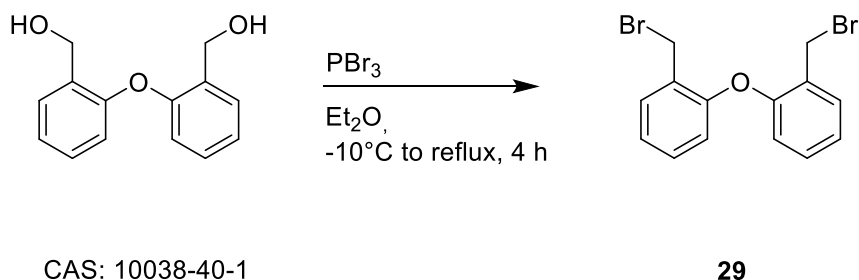


¹³C-NMR



Preparation of bis-electrophilic reagent 29

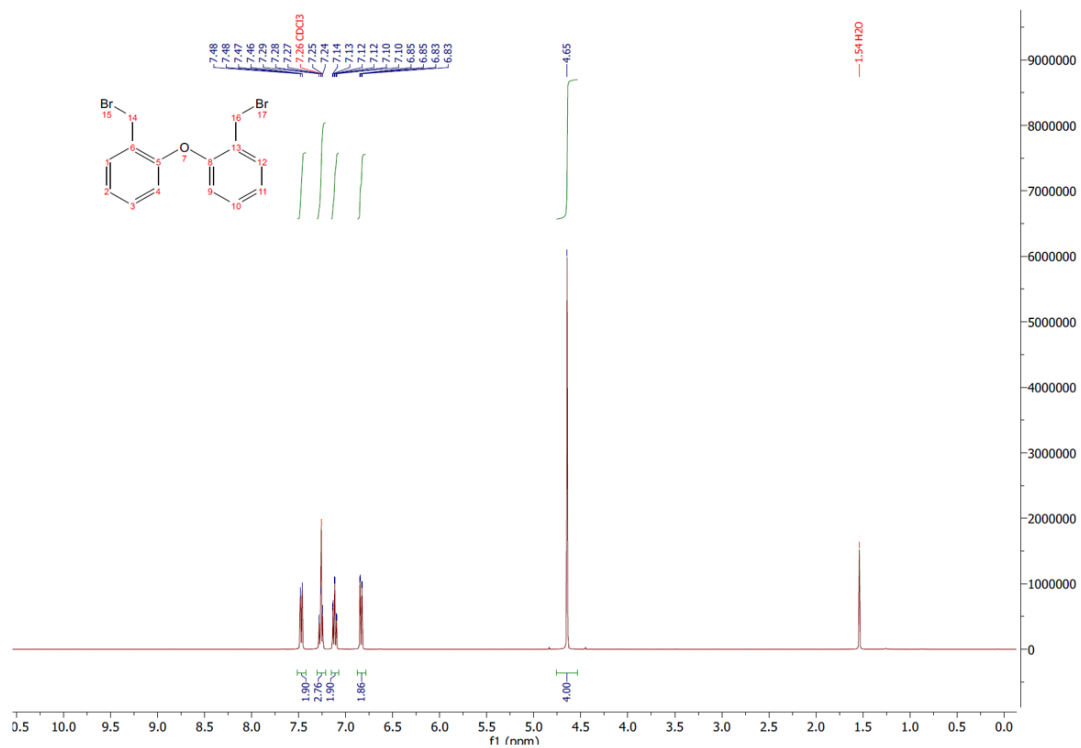
The reagent 29 was prepared following the procedure of Cervantes-Reyes et al..¹³³



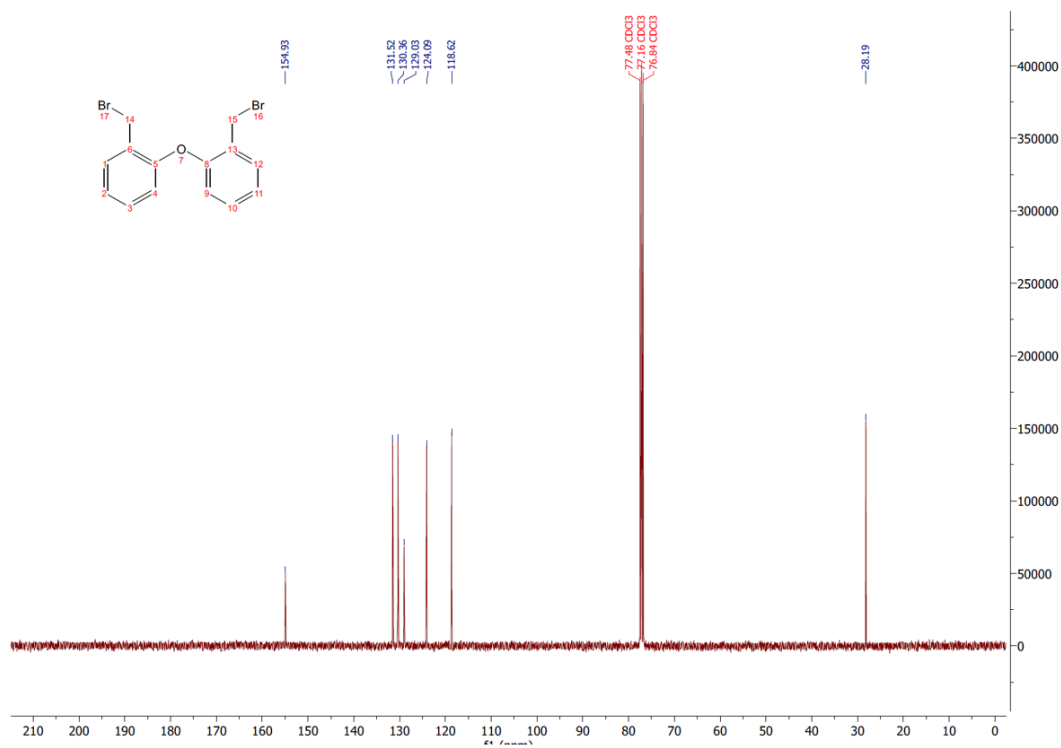
Phosphorous tribromide (0.230 ml, 2.45 mmol, 0.98 equiv.) was added dropwise to a solution of 2,2'-oxybis-benzenemethanol (576 mg, 2.50 mmol, 1.00 equiv.) in dry diethyl ether (11.3 ml) under inert atmosphere (nitrogen) at -10°C during 45 min. The reaction mixture was allowed to room temperature and refluxed at 45°C. Afterward, the reaction mixture was poured onto crushed ice (~25 ml) and stirred for 1 h after which chloroform (10 ml) was added. The organic layer was separated and the aqueous layer was further extracted with chloroform (1 × 10 ml). The combined organic phases were washed with saturated aqueous NaHCO₃ (2 × 10 ml), dried over Na₂SO₄, filtered and concentrated under reduced pressure to afford a crude pure white solid as the desired product **29** (0.58 g, 1.63 mmol, 65% yield) as a bright beige solid.

¹H NMR (400 MHz, CDCl₃) δ = 7.47 (dd, *J* = 7.6, 1.7 Hz, 2H), 7.30 – 7.21 (m, 2H), 7.12 (td, *J* = 7.6, 1.2 Hz, 2H), 6.84 (d, *J* = 8.2, 1.2 Hz, 2H), 4.65 (s, 4H) ppm; **¹³C{¹H}-NMR** (101 MHz, CDCl₃) δ = 154.93 (2C), 131.52 (2C), 130.36 (2C), 129.03 (2C), 124.09 (2C), 118.62 (2C), 28.19 (2C) ppm; **UHPLC-MS** (ESI), calc'd for [M+H]⁺ = [C₁₄H₁₃Br₂O]⁺ = 354.9328 m/z, found = non (not ionizable), 99% purity (peak area, 220 nm); **HRMS** (Sicrit Plasma/LTQ-Orbitrap), calc'd for [M-Br]⁺ = C₁₄H₁₂BrO⁺ = 275.0066 m/z, found = 275.0068 m/z (deviation: -0.7 ppm); **R_f** = 0.28 (one spot, DCM:hexane, 1:9, UV & KMnO₄).

¹H-NMR

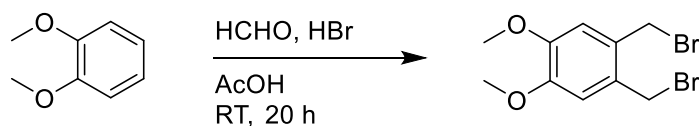


¹³C-NMR



Preparation of bis-electrophilic reagent 43

The reagent 43 was prepared following the procedure of Stubba et al..¹³⁴



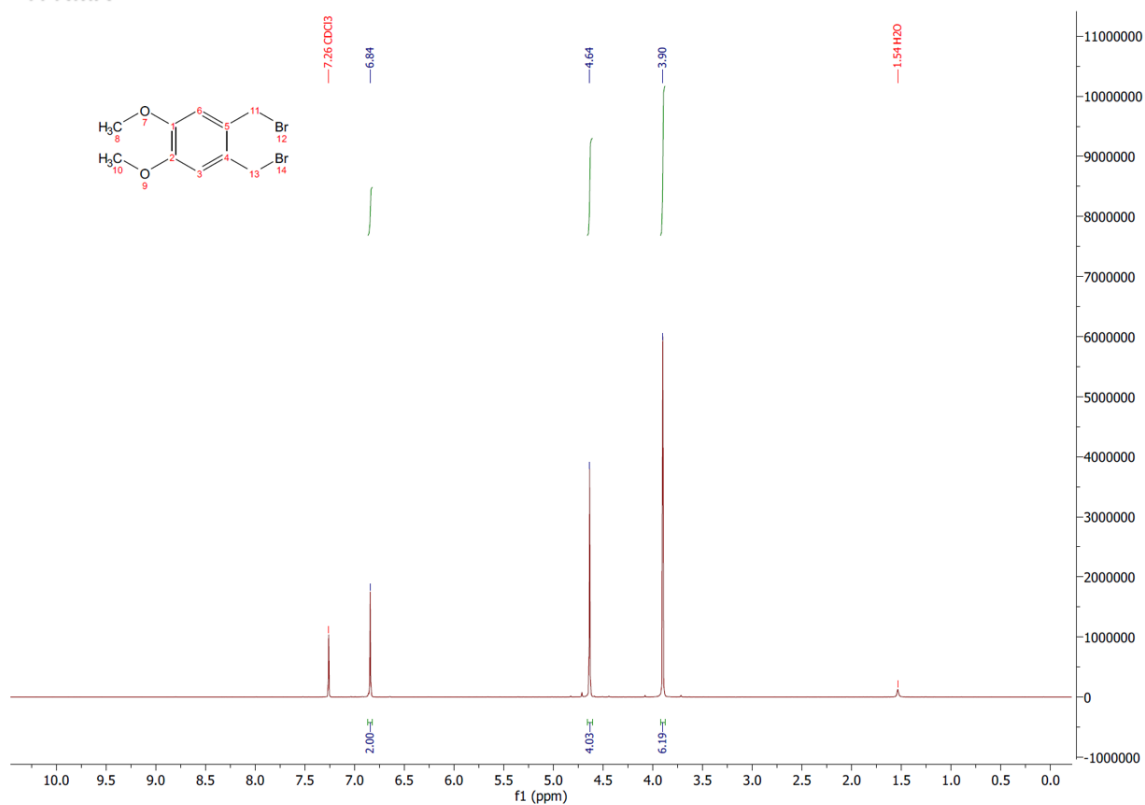
CAS: 91-16-7

43

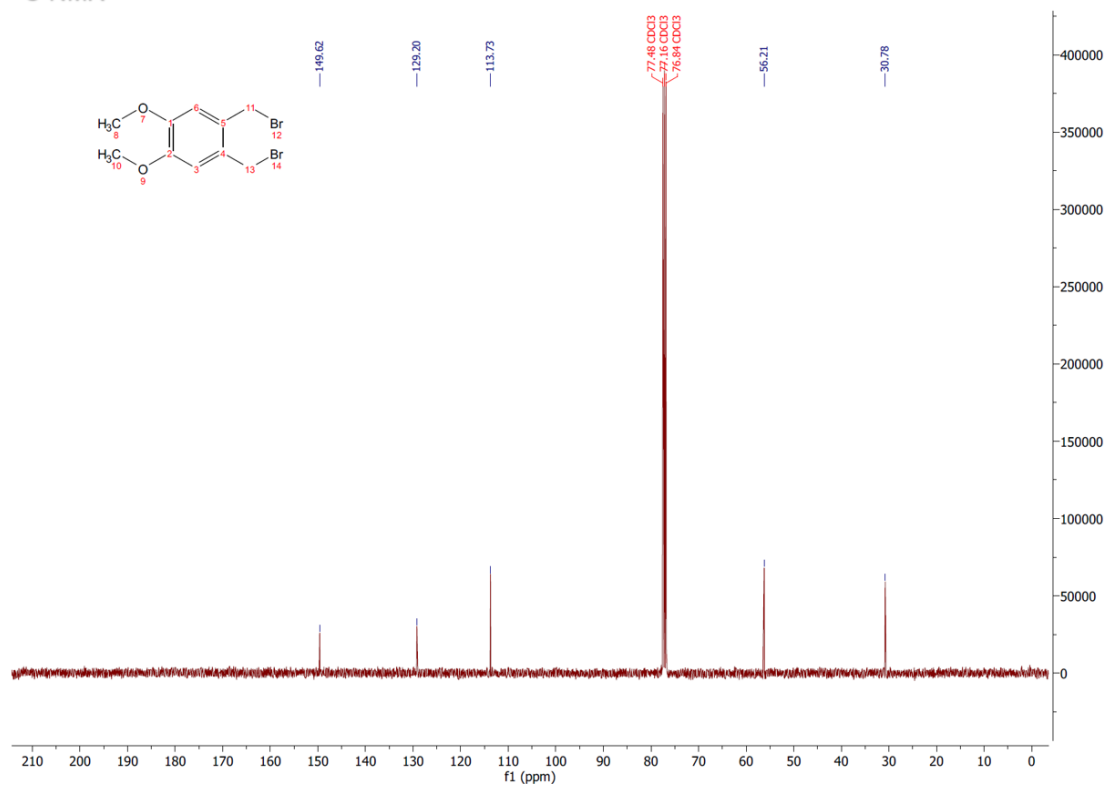
To a solution of 1,2-dimethoxybenzene (1.02 mL, 8.00 mmol, 1.00 equiv.) and paraformaldehyde (0.480 g, 16.0 mmol, 2.00 equiv.) in acetic acid (4.8 ml) inside a round bottom flask, it was slowly added a solution of 33% HBr (4.00 mL, 18.8 mmol, 2.35 equiv.) in acetic acid (3.4 ml) at 0°C. The reaction mixture was stirred for 20 h at room temperature, followed by heating up for one hour at 65°C. After cooling down to room temperature, the mixture was poured on ice (~25 ml). The resulting dark brown, sticky precipitate was filtered off and washed with water (3 × 10 ml) to afford crude product. The crude product was re-dissolved in DCM (2 ml) and absorbed onto silica gel by slurrying with silica gel and removing DCM under reduced pressure. The crude product was purified via flash column chromatography (30 g silica gel) using the solvents DCM and hexane with a gradient from 50 to 100% DCM. The desired combined organic fractions were concentrated under reduced pressure (35°C, 621 mbar) to afford the desired product **43** (0.623 g, 1.90 mmol, 24% yield) as a bright beige solid.

¹H NMR (400 MHz, CDCl₃) δ = 6.84 (s, 2H), 4.64 (s, 4H), 3.90 (s, 6H) ppm; **¹³C{¹H}-NMR** (101 MHz, CDCl₃) δ = 149.61 (2C), 129.19 (2C), 113.73 (2C), 56.20 (2C), 30.76 (2C) ppm; **UHPLC-MS** (ESI), calc'd for [M+H]⁺ = [C₁₀H₁₃Br₂O₂]⁺ = 322.9277 m/z, found = non, 99% purity (peak area, 220 nm); **R_f** = 0.64 (one spot, DCM, 100%, UV & KMnO₄).

¹H-NMR



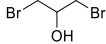

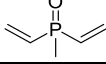
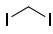
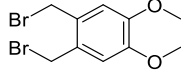
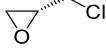
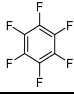
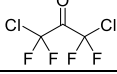
¹³C-NMR



Supplementary Table 1: Overview of 46 bis-electrophilic reagents that were tested for their efficiency in cyclizing the model peptide. Reagents that were successfully used for thiol-thiol peptide cyclization in aqueous solvent are indicated with one asterisk (*). Newly synthesized reagents are indicated with two asterisks (**)

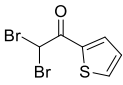
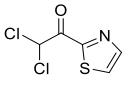
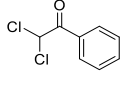
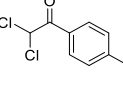
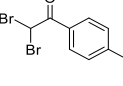
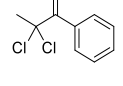
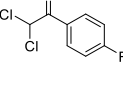
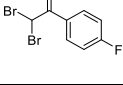
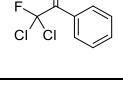
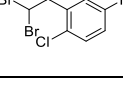
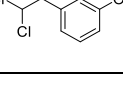
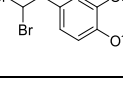
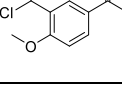
#	Chemical structure	Name	Abbreviation	Mw compound	Exact mass linker	CAS number
1*		1,4-bis(bromomethyl)-2,3,5,6-tetrafluorobenzene	BBT	335.9	176.1	776-40-9
2**		1,1'-(2,8-diazaspiro[5.5]undecane-2,8-diyl)bis(2-chloroethan-1-one)	-	307.2	236.3	Not registered
3*		2,3-dibromonaphthoquinone	DNQ	315.9	126.0	13243-65-7
4*		divinyl sulfone	DVS	118.2	120.8	77-77-0
5*		2,5-bis(chloromethyl)-1,3,4-oxadiazole	BCO	167.0	96.09	541540-90-3
6**		3,4-bis(bromomethyl)-5-methyl isoxazole	-	268.9	188.0	266341-64-4
7*		<i>trans</i> -1,4-dibromo-2-butene	DBB	213.9	54.09	821-06-7
8*		1,4-bis(bromomethyl) benzene	BBB	264.0	104.2	623-24-5
9*		dibromobimane	DBB ₂	350.0	190.2	68654-25-1
10*		3-bromo-2-bromomethyl-1-propene	BBE	213.9	54.09	15378-31-3
11*		1,4-bis(bromomethyl)-2,5-dimethylbenzene	BBD	292.0	132.2	35168-62-8
12**		1,1'-(tetrahydropyrrolo[3,4-c]pyrrole-2,5(1H,3H)-diyl)bis(2-chloroethan-1-one)	-	265.1	194.2	Not registered
13*		bis(vinylsulfonyl)methane	BVM	196.0	198.0	3278-22-6
14*		2,3-bis(bromomethyl)quinoxaline	BBQ	316.0	156.2	3138-86-1
15**		3,4-bis(bromomethyl)furan	-	253.9	94.11	146604-80-0
16*		3,5-bis(bromomethyl)pyridine	BBP ₂	265.0	105.1	1118754-56-5
17*		1,3-dichloroacetone	DCA	126.0	56.06	534-07-6

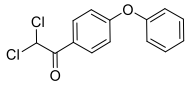
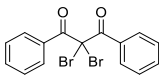
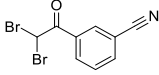
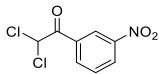
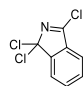
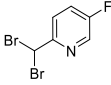
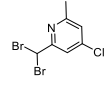
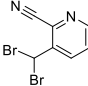
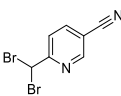
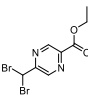
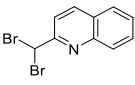
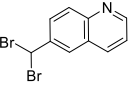
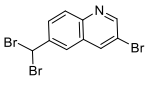
18*		2,2'-bioxirane	BOX	88.05	86.04	1464-53-5
19*		1,4-di(oxiran-2-yl)-butane	DOB	142.2	144.2	2426-07-5
20*		2,6-bis(bromomethyl)pyridine	BBP	265.0	105.1	7703-74-4
21*		1,4-bis(chloroacetyl)piperazine	BCP	239.1	168.2	1703-23-7
22*		1,4-dichloro-2-butyne	DCB	123.0	52.08	821-10-3
23*		1,4-bis(bromoacetyl)benzene	BBB ₄	320.0	160.2	946-03-2
24**		<i>N,N</i> -((1 <i>S</i> ,2 <i>S</i>)-cyclohexane-1,2-diyl)bis(2-chloro- <i>N</i> -methylacetamide)	-	294.1	224.3	499205-02-6
25*		1,2-bis(acrylamide)ethane	BAE	168.2	170.2	2956-58-3
26*		1,2-bis(bromomethyl)benzene	BBB ₂	264.0	104.1	91-13-4
27*		<i>cis</i> -1,4-dichloro-2-butene	DCB ₂	125.0	54.09	1476-11-5
28*		2,3-dibromo- <i>N</i> -methylmaleimide	DMM	268.9	109.0	3005-27-4
29*		1,3-bis(oxiran-2-ylmethoxy)benzene	BOB	222.2	224.1	101-90-6
30*		2,3-dibromomaleimide	DBM	254.9	95.00	1122-10-7
31**		bis(2-bromomethylphenyl)ether	-	356.1	196.3	10038-41-2
32*		1,1-dichloro-3,3-dimethylbutan-2-one	DDO	169.0	98.07	22591-21-5
33*		1,4-bis(bromomethyl)-2,5-dimethoxybenzene	BBD ₂	324.0	164.1	50874-27-6
34*		1,8-bis(bromomethyl)naphthalene	BBN	314.0	154.1	2025-95-8
35*		1-bromomethyl-4-bromoacetylbenzene	BBB ₃	292.0	132.2	62546-51-4
36		6,6'-bis(chloromethyl)-2,2'-bipyridine	-	253.1	182.2	74065-64-8
37		1,3-bis(bromomethyl)benzene	-	264.0	104.1	626-15-3
38		(2 <i>E</i> ,4 <i>E</i>)-1,6-dibromohexa-2,4-diene	-	240.0	80.13	63621-95-4

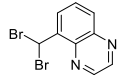
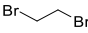
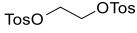
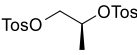
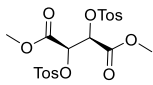
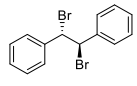
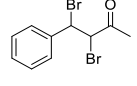
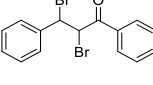
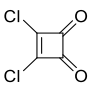
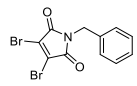
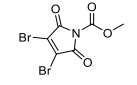
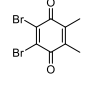
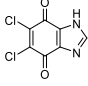
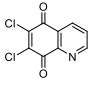
39		1,3-dibromopropan-2-ol	-	215.9	58.08	96-21-9
40		1,1-bis(iodomethyl) cyclopropane	-	321.9	68.12	83321-23-7
41		methyldivinylphosphine oxide	-	116.1	118.1	945460-42-4
42		diiodomethane	-	267.8	14.02	75-11-6
43**		1,2-bis(bromomethyl)-4,5- dimethoxybenzene	-	324.0	164.1	945460-42-4
44		(+)-epichlorhydrin	-	92.52	58.04	67843-74-7
45		perfluorobenzene	-	186.1	148.0	392-56-3
46		1,3-dichloro-1,1,3,3- tetrafluoropropan-2-one	-	198.9	128.2	127-21-9

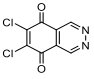
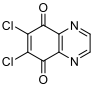

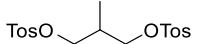

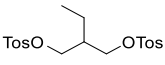
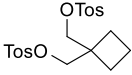
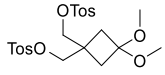
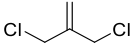
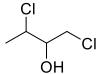
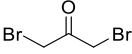
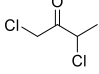
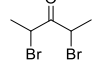
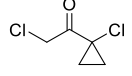
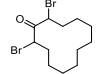
Supplementary Table 2: A list of 191 commercially provided reagents found in the databases SciFinder and Reaxys that promise to be suited for thiol-thiol peptide cyclization in aqueous solution based on their reactive groups. Only reagents with a price of less than 1000 US \$ were included. The table does not include the bis-electrophile reagents shown in Supplementary Table 1.

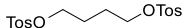
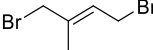

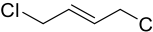
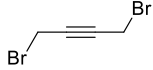
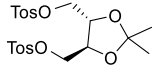
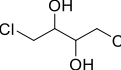
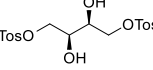
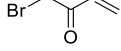
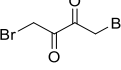
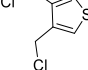
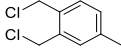
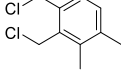
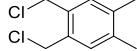
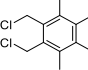
#	Number of linker atoms	Chemical Structure	Name	Abbreviation	Mw (reagent)	Exact mass (linker)	CAS number
47	1		methylene bis(4-methylbenzenesulfonate)	-	356.4	14.02	24124-59-2
48	1		1,1-dichloropropan-2-one	-	127.0	56.02	513-88-2
49	1		1,1-dibromo-3,3-dimethylbutan-2-one	-	258.0	98.07	30263-65-1
50	1		1-(1-adamantyl)-2,2-dibromoethanone	-	336.1	176.1	26525-25-7
51	1		1,1-dibromo-3,3-difluoropropan-2-one	-	251.9	92.01	1309602-53-6
52	1		3,3-dichloro-1,1,1-trifluoropropan-2-one	-	180.9	110.0	126266-75-9
53	1		2,2-dichloroacetamide	-	128.0	57.02	683-72-7
54	1		2,2-dichloro-1-(pyrrolidin-1-yl)ethan-1-one	-	182.0	111.1	20266-01-7
55	1		1-(azepan-1-yl)-2,2-dichloroethan-1-one	-	210.0	139.1	64661-12-7
56	1		2,2-Dichloro-1-(4-morpholinyl)ethanone	-	198.0	127.1	39205-49-7
57	1		2,2,6-tribromo-3,4-dihydronaphthalen-1(2H)-one	-	382.9	222.0	1632285-90-5

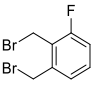
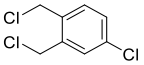
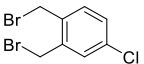
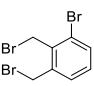
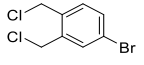
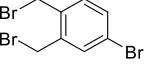
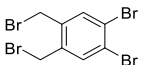
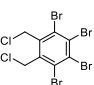
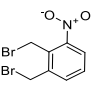
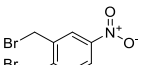
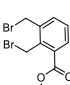
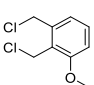
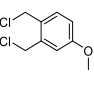
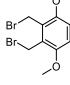
58	1		2,2-dibromo-1-(thiophen-2-yl)ethanone	-	284.0	124.0	68672-88-8
59	1		2,2-dichloro-1-(1,3-thiazol-2-yl)ethanone	-	196.1	125.0	79265-41-1
60	1		2,2-dichloro-1-phenylethan-1-one	-	189.0	118.0	2648-61-5
61	1		2,2-dichloro-1-(4-methylphenyl)ethan-1-one	-	203.1	132.4	4974-59-8
62	1		2,2-dibromo-1-(p-tolyl)ethan-1-one	-	292.0	132.4	13664-98-7
63	1		2,2-dichloro-1-phenylpropan-1-one	-	203.1	132.4	57169-51-4
64	1		2,2-dichloro-1-(4-fluorophenyl)ethan-1-one	-	207.0	136.3	5157-58-4
65	1		2,2-dibromo-1-(4-fluorophenyl)ethanone	-	296.0	136.0	7542-64-5
66	1		2,2-dichloro-2-fluoro-1-phenylethan-1-one	-	207.0	136.0	384-66-7
67	1		2,2-dibromo-1-(2,6-dichloro-3-fluorophenyl)ethanone	-	364.8	204.0	1820604-17-8
68	1		2,2-dichloro-1-(3-hydroxyphenyl)ethan-1-one	-	205.0	134.3	85299-04-3
69	1		2,2-dibromo-1-(3,4-dimethoxyphenyl)ethan-1-one	-	338.0	178.1	63987-72-4
70	1		1-(3-(dichloromethyl)-4-methoxyphenyl)ethan-1-one	-	233.1	162.1	1823212-44-7

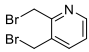
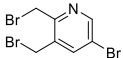
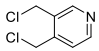
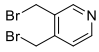
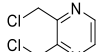
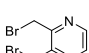
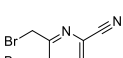
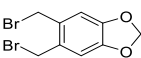
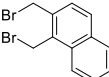
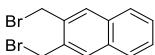
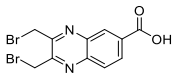
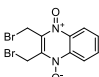
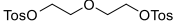
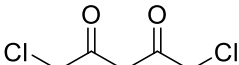
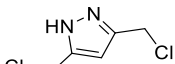
71	1		2,2-dichloro-1-(4-phenoxyphenyl)ethan-1-one	-	281.1	210.1	59867-68-4
72	1		2,2-dibromo-1,3-diphenylpropane-1,3-dione	-	382.1	222.1	16619-55-9
73	1		3-(2,2-dibromoacetyl)benzonitrile	-	303.0	143.0	212374-08-8
74	1		2,2-dichloro-1-(3-nitrophenyl)ethan-1-one	-	234.0	164.0	27700-44-3
75	1		1,1,3-trichloro-1H-isoindole	-	220.5	149.0	21021-41-0
76	1		2-(dibromomethyl)-5-fluoropyridine	-	268.9	109.0	1000343-67-8
77	1		4-chloro-2-(dibromomethyl)-6-methylpyridine	-	299.4	139.0	856851-76-8
78	1		3-(dibromomethyl)picolinonitrile	-	275.9	116.0	126570-65-8
79	1		6-(dibromomethyl)nicotinonitrile	-	275.9	116.0	1189128-09-3
80	1		ethyl 5-(dibromomethyl)pyrazine-2-carboxylate	-	309.9	150.0	866327-72-2
81	1		2-(dibromomethyl)quinoline	-	301.0	141.1	53867-81-5
82	1		6-(dibromomethyl)quinoline	-	301.0	141.1	872264-38-5
83	1		3-bromo-6-(dibromomethyl)quinoline	-	379.9	310.9	860758-00-5

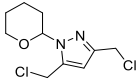
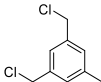
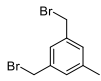
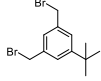
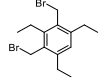
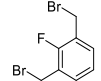
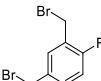
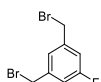
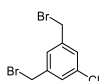
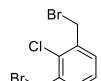
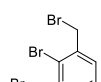
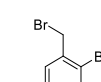
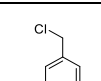
84	1		5-(dibromomethyl)quinoxaline	-	302.0	142.1	958994-25-7
85	2		1,2-dibromoethane	-	185.9	28.03	106-93-4
86	2		ethane-1,2-diyl bis(4-methylbenzenesulfonate)	-	370.4	28.03	6315-52-2
87	2		(S)-propane-1,2-diyl bis(4-methylbenzenesulfonate)	-	384.5	42.28	60434-71-1
88	2		dimethyl (2R,3R)-2,3-bis(tosyloxy)succinate	-	486.5	144.0	1773493-87-0
89	2		1,2-Dibromo-1,2-diphenylethane	-	340.1	180.1	13440-24-9
90	2		3,4-dibromo-4-phenylbutan-2-one	-	306.0	146.1	6310-44-7
91	2		2,3-dibromo-1,3-diphenylpropan-1-one	-	368.1	208.1	611-91-6
92	2		3,4-dichlorocyclobut-3-ene-1,2-dione	-	150.9	79.99	2892-63-9
93	2		1-benzyl-3,4-dibromo-1H-pyrrole-2,5-dione	-	345.0	185.0	91026-0-5
94	2		methyl 3,4-dibromo-2,5-dioxo-2,5-dihydro-1H-pyrrole-1-carboxylate	-	312.9	153.0	1442447-48-4
95	2		2,3-dibromo-5,6-dimethylcyclohexa-2,5-diene-1,4-dione	-	293.9	134.0	38969-08-3
96	2		5,6-dichloro-1H-benzo[d]imidazole-4,7-dione	-	217.0	146.0	34674-41-4
97	2		6,7-dichloroquinoline-5,8-dione	-	228.0	157.0	6541-19-1

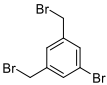
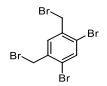
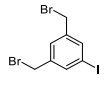
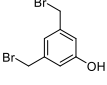
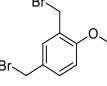
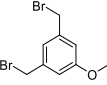
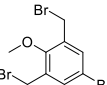
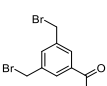
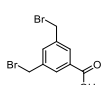
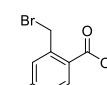
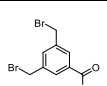
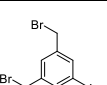
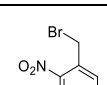
98	2		6,7-dichlorophthalazine-5,8-dione	-	229.0	158.0	102072-85-5
99	2		6,7-dichloroquinoxaline-5,8-dione	-	229.0	158.0	102072-82-2
100	3		propane-1,3-diyl bis(4-methylbenzenesulfonate)	-	384.5	42.05	5469-66-9
101	3		2-methylpropane-1,3-diyl bis(4-methylbenzenesulfonate)	-	398.5	56.06	24330-53-8
102	3		2,2-dimethylpropane-1,3-diyl bis(4-methylbenzenesulfonate)	-	412.5	70.08	22308-12-9
103	3		2-ethylpropane-1,3-diyl bis(4-methylbenzenesulfonate)	-	412.5	70.08	24330-55-0
104	3		cyclobutane-1,1-diylbis(methylene) bis(4-methylbenzenesulfonate)	-	424.5	82.08	22308-09-4
105	3		(3,3-dimethoxycyclobutane-1,1-diyl)bis(methylene) bis(4-methylbenzenesulfonate)	-	484.6	142.1	1023815-74-8
106	3		1,1-bis(chloromethyl)ethylene	-	125.0	54.05	1871-57-4
107	3		1,3-dichlorobutan-2-ol	-	143.0	72.06	116529-72-7
108	3		1,3-dibromopropan-2-one	-	215.9	56.03	816-39-7
109	3		1,3-dichlorobutan-2-one	-	141.0	70.04	16714-77-5
110	3		2,4-dibromopentan-3-one	-	243.9	84.06	815-60-1
111	3		2-chloro-1-(1-chlorocyclopropyl)ethan-1-one	-	153.0	110.1	120983-72-4
112	3		2,12-dibromocyclododecan-1-one	-	340.1	180.2	28148-04-1

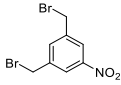
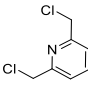
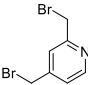
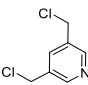
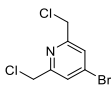
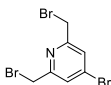
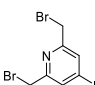
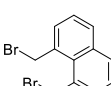
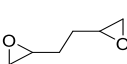
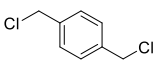
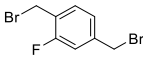
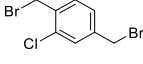
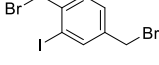
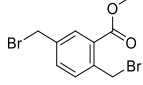
113	4		butane-1,4-diyl bis(4-methylbenzenesulfonate)	-	398.5	56.06	4724-56-5
114	4		<i>trans</i> -1,4-dibromo-2-methylbut-2-ene	-	227.9	68.06	18860-95-2
115	4		<i>cis</i> -1,4-dibromobut-2-ene	-	213.9	54.05	18866-73-4
116	4		<i>trans</i> -1,4-dichlorobut-2-ene	-	125.0	54.05	110-57-6
117	4		1,4-dibromo-2-butyne	-	211.9	52.03	2219-66-1
118	4		((4 <i>S</i> ,5 <i>S</i>)-2,2-dimethyl-1,3-dioxolane-4,5-diyl)bis(methylene) bis(4-methylbenzenesulfonate)	-	470.6	128.1	37002-45-2
119	4		1,4-dichlorobutane-2,3-diol	-	159.0	88.05	2419-73-0
120	4		(2 <i>S</i> ,3 <i>S</i>)-2,3-dihydroxybutane-1,4-diyl bis(4-methylbenzenesulfonate)	-	430.5	88.05	57495-46-5
121	4		1-bromobut-3-en-2-one	-	149.0	70.04	155622-69-8
122	4		1,4-dibromo-2,3-butanedione	-	243.9	84.02	6305-43-7
123	4		3,4-bis(chloromethyl)thiophene	-	181.1	110.0	18448-62-9
124	4		1,2-bis(chloromethyl)-4-methylbenzene	-	189.1	118.1	2735-06-0
125	4		1,2-bis(chloromethyl)-3,4-dimethylbenzene	-	203.1	132.1	951793-37-6
126	4		1,2-bis(chloromethyl)-4,5-dimethylbenzene	-	203.1	132.1	2362-16-5
127	4		1,2-bis(chloromethyl)-3,4,5,6-tetramethylbenzene	-	231.2	160.1	29002-55-9

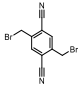
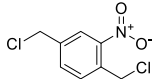
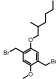
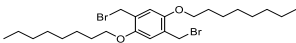
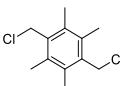
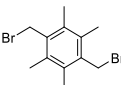
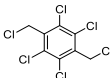
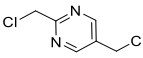
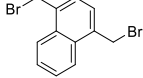
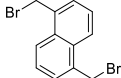
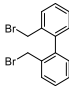
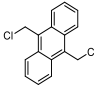
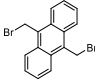
128	4		1,2-bis(bromomethyl)-3-fluorobenzene	-	282.0	122.1	62590-16-3
129	4		4-chloro-1,2-bis(chloromethyl)benzene	-	209.5	138.0	212755-99-2
130	4		1,2-bis(bromomethyl)-4-chlorobenzene	-	298.4	138.0	31684-14-7
131	4		1-bromo-2,3-bis(bromomethyl)benzene	-	342.9	182.0	127168-82-5
132	4		4-bromo-1,2-bis(chloromethyl)benzene	-	253.9	182.0	934011-79-7
133	4		4-bromo-1,2-bis(bromomethyl)benzene	-	342.9	182.0	69189-19-1
134	4		1,2-dibromo-4,5-bis(bromomethyl)benzene	-	421.8	273.9	6425-67-8
135	4		1,2,3,4-tetrabromo-5,6-bis(chloromethyl)benzene	-	490.6	415.7	62785-15-3
136	4		1,2-bis(bromomethyl)-3-nitrobenzene	-	309.0	149.1	66126-16-7
137	4		1,2-bis(bromomethyl)-4-nitrobenzene	-	309.0	149.1	6425-66-7
138	4		methyl 2,3-bis(bromomethyl)benzoate	-	322.0	319.9	127168-91-6
139	4		1,2-bis(chloromethyl)-3-methoxybenzene	-	205.1	134.1	90047-44-2
140	4		1,2-bis(chloromethyl)-4-methoxybenzene	-	205.1	134.1	4685-45-4
141	4		2,3-bis(bromomethyl)-1,4-dimethoxybenzene	-	324.0	164.1	19164-83-1

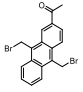
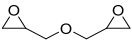
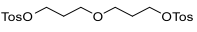
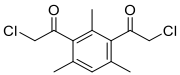
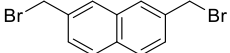
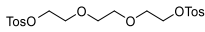
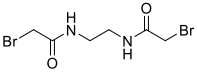
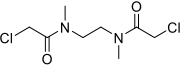
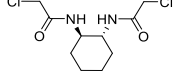
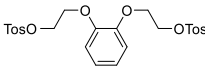
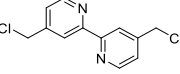
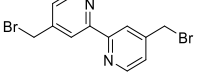
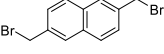
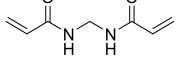
142	4		2,3-bis(bromomethyl)pyridine	-	264.9	105.1	917476-19-8
143	4		5-bromo-2,3-bis(bromomethyl)pyridine	-	343.8	182.0	905273-34-9
144	4		3,4-bis(chloromethyl)pyridine	-	176.0	83.02	38070-81-4
145	4		3,4-bis(bromomethyl)pyridine	-	176.0	83.02	1803611-21-3
146	4		2,3-bis(chloromethyl)pyrazine	-	265.9	106.1	51043-75-5
147	4		2,3-bis(bromomethyl)pyrazine	-	265.9	106.1	282528-30-7
148	4		5,6-bis(bromomethyl)pyrazine-2,3-dicarbonitrile	-	316.0	156.0	189701-21-1
149	4		5,6-bis(bromomethyl)benzo[d][1,3]dioxole	-	308.0	148.1	114394-68-2
150	4		1,2-bis(bromomethyl)naphthalene	-	314.0	246.1	59882-98-3
151	4		2,3-bis(bromomethyl)naphthalene	-	314.0	246.1	38998-33-3
152	4		2,3-bis(bromomethyl)quinoxaline-6-carboxylic acid	-	360.0	200.1	32602-11-2
153	4		2,3-bis(bromomethyl)quinoxaline-1,4-dioxide	-	348.0	188.1	18080-67-6
154	5		oxybis(ethane-2,1-diyl) bis(4-methylbenzenesulfonate)	-	414.5	72.06	7460-82-4
155	5		1,5-dichloropentane-2,4-dione		169.0	98.04	40630-12-4
156	5		3,5-bis(chloromethyl)-1H-pyrazole	-	165.0	94.05	780712-04-1

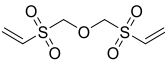
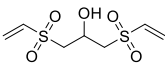
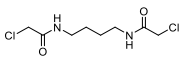
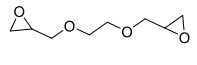
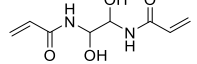
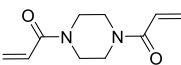
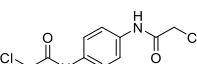
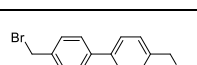
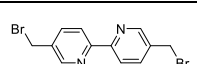
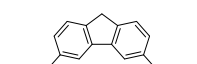
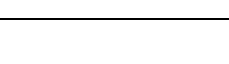
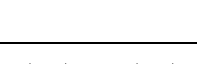
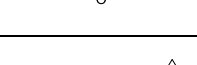
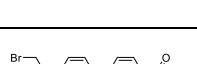
157	5		3,5-bis(chloromethyl)-1-(oxan-2-yl)pyrazole	-	249.1	178.1	252334-30-8
158	5		1,3-bis(chloromethyl)-5-methylbenzene	-	189.1	118.1	79539-14-3
159	5		1,3-bis(bromomethyl)-5-methylbenzene	-	278.0	118.1	19294-04-3
160	5		1,3-bis(bromomethyl)-5-(tert-butyl)benzene	-	320.1	160.1	64726-28-9
161	5		2,4-bis(bromomethyl)-1,3,5-triethylbenzene	-	348.1	188.2	190779-61-4
162	5		1,3-bis(bromomethyl)-2-fluorobenzene	-	282.0	122.1	25006-86-4
163	5		2,4-bis(bromomethyl)-1-fluorobenzene	-	282.0	122.1	1379366-74-1
164	5		1,3-bis(bromomethyl)-5-fluorobenzene	-	282.0	122.1	19254-80-9
165	5		1,3-bis(bromomethyl)-5-chlorobenzene	-	298.4	203.9	781616-32-8
166	5		1,3-bis(bromomethyl)-2-chlorobenzene	-	298.4	203.9	25006-87-5
167	5		2-bromo-1,3-bis(bromomethyl)benzene	-	342.9	183.2	25006-88-6
168	5		1-bromo-2,4-bis(bromomethyl)benzene	-	342.9	183.2	35510-04-4
169	5		1-bromo-3,5-bis(chloromethyl)benzene	-	254.0	182.0	108835-03-6

170	5		1-bromo-3,5-bis(bromomethyl)benzene	-	342.9	183.2	51760-23-7
171	5		1,5-dibromo-2,4-bis(bromomethyl)benzene	-	421.8	259.9	35510-03-3
172	5		1,3-bis(bromomethyl)-5-iodobenzene	-	389.9	295.8	107164-93-2
173	5		3,5-bis(bromomethyl)phenol	-	280.0	185.9	135990-12-4
174	5		2,4-bis(bromomethyl)-1-methoxybenzene	-	294.0	134.1	83020-58-0
175	5		1,3-bis(bromomethyl)-5-methoxybenzene	-	294.0	134.1	19254-79-6
176	5		5-bromo-1,3-bis(bromomethyl)-2-methoxybenzene	-	372.9	212.0	118249-11-9
177	5		1-(3,5-bis(bromomethyl)phenyl)ethan-1-one	-	306.0	146.1	544467-01-8
178	5		3,5-bis(bromomethyl)benzoic acid	-	308.0	148.1	94111-75-8
179	5		methyl 2,4-bis(bromomethyl)benzoate	-	322.0	162.1	63112-94-7
180	5		methyl 3,5-bis(bromomethyl)benzoate	-	322.0	162.1	29333-41-3
181	5		3,5-bis(bromomethyl)benzonitrile	-	289.0	129.1	74163-48-7
182	5		1,3-bis(bromomethyl)-2-nitrobenzene	-	309.0	149.0	55324-01-1

183	5		1,3-bis(bromomethyl)-5-nitrobenzene	-	309.0	149.0	51760-20-4
184	5		2,6-bis(chloromethyl)pyridine	-	176.0	105.1	3099-28-3
185	5		2,4-bis(bromomethyl)pyridine	-	264.9	105.1	1003294-47-0
186	5		3,5-bis(chloromethyl)pyridine	-	176.0	105.1	41711-38-0
187	5		4-bromo-2,6-bis(chloromethyl)pyridine	-	254.9	183.0	120491-87-4
188	5		4-bromo-2,6-bis(bromomethyl)pyridine	-	343.8	183.0	106967-42-4
189	5		2,6-bis(bromomethyl)-4-iodopyridine	-	390.8	231.0	106967-33-3
190	5		1,8-bis(bromomethyl)naphthalene	-	314.0	154.1	2025-95-8
191	6		1,2:5,6-diepoxyhexane	-	114.1	116.1	1888-89-7
192	6		1,4-bis(chloromethyl)benzene	-	175.1	104.1	623-25-6
193	6		1,4-bis(bromomethyl)-2-fluorobenzene	-	282.0	122.1	69857-33-6
194	6		1,4-bis(bromomethyl)-2-chlorobenzene	-	298.4	138.0	10221-09-7
195	6		1,4-bis(bromomethyl)-2-iodobenzene	-	389.9	230.0	60017-02-9
196	6		methyl 2,5-bis(bromomethyl)benzoate	-	322.0	162.1	74725-06-7

197	6		1,4-bis(bromomethyl)-2,5-dicyanobenzene	-	314.0	154.1	64746-04-9
198	6		1,4-bis(chloromethyl)-2-nitrobenzene	-	220.1	149.1	16255-50-8
199	6		1,4-bis(bromomethyl)-2-methoxy-5-((2-methylhexyl)oxy)benzene	-	408.2	248.2	209625-37-6
200	6		1,4-bis(bromomethyl)-2,5-bis(octyloxy)benzene	-	520.4	360.3	147274-72-4
201	6		1,4-bis(chloromethyl)-2,3,5,6-tetramethylbenzene	-	231.2	160.1	3022-16-0
202	6		1,4-bis(bromomethyl)-2,3,5,6-tetramethylbenzene	-	231.2	160.1	35168-64-0
203	6		1,2,4,5-tetrachloro-3,6-bis(chloromethyl)benzene	-	312.8	239.9	1079-17-0
204	6		2,5-bis(chloromethyl)pyrimidine	-	177.0	106.1	126504-87-8
205	6		1,4-bis(bromomethyl)naphthalene	-	364.1	204.1	34373-96-1
206	6		1,5-bis(bromomethyl)naphthalene	-	364.1	204.1	21646-18-4
207	6		2,2'-bis(bromomethyl)-1,1'-biphenyl	-	340.1	180.1	38274-14-5
208	6		9,10-bis(chloromethyl)anthracene	-	275.1	204.1	10387-13-0
209	6		9,10-bis(chloromethyl)anthracene	-	364.1	204.1	34373-96-1

210	6		1-(9,10-bis(bromomethyl)anthracen-2-yl)ethan-1-one	-	406.1	246.1	790257-33-9
211	7		2,2'-(oxybis(methylene))bis(oxirane)	-	130.1	132.1	2238-07-5
212	7		oxybis(propane-3,1-diyl) bis(4-methylbenzenesulfonate)	-	442.5	100.1	55005-96-4
213	7		2-chloro-1-[3-(2-chloroacetyl)-2,4,6-trimethylphenyl]ethanone	-	273.2	202.1	156641-43-9
214	7		2,7-bis(bromomethyl)naphthalene	-	314.0	154.1	38309-89-6
215	8		(ethane-1,2-diylbis(oxy))bis(ethane-2,1-diyl) bis(4-methylbenzenesulfonate)	-	458.5	166.1	19249-03-7
216	8		N,N'-ethyldienebis(2-bromoacetamide)	-	302.0	142.1	4960-81-0
217	8		2-chloro-N-[2-(2-chloro-N-methylacetamido)ethyl]-N-methylacetamide	-	241.1	170.1	36784-59-5
218	8		N,N'-((1R,2R)-cyclohexane-1,2-diyl)bis(2-chloroacetamide)	-	267.2	196.1	150576-46-8
219	8		(1,2-phenylenebis(oxy))bis(ethane-2,1-diyl) bis(4-methylbenzenesulfonate)	-	506.6	164.1	54535-06-7
220	8		4,4'-bis(chloromethyl)-2,2'-bipyridine	-	253.1	182.1	138219-98-4
221	8		4,4'-bis(bromomethyl)-2,2'-bipyridine	-	342.0	182.1	134457-14-0
222	8		2,6-bis(bromomethyl)naphthalene	-	314.0	154.1	4542-77-2
223	9		N,N'-methylenediacrylamide	-	154.2	156.1	110-26-9

224	9		bis(vinylsulfonylmethyl) ether	-	226.3	228.0	26750-50-5
225	9		1,3-bis(ethenylsulfonyl)propan-2-ol	-	240.2	242.0	67006-32-0
226	10		N,N'-(butane-1,4-diyl)bis(2-chloroacetamide)	-	241.1	170.1	33619-34-0
227	10		1,2-bis(oxiran-2-ylmethoxy)ethane	-	174.2	176.1	2224-15-9
228	10		N,N'-(1,2-dihydroxyethane-1,2-diyl)diacrylamide	-	200.2	202.1	868-63-3
229	10		1,1'-(piperazine-1,4-diyl)bis(prop-2-en-1-one)	-	194.2	196.1	6342-17-2
230	10		N,N'-(1,4-phenylene)bis(2-chloroacetamide)	-	261.1	190.1	2653-08-9
231	10		4,4'-bis(bromomethyl)-1,1'-biphenyl	-	340.1	180.1	20248-86-6
232	10		5,5'-bis(Bromomethyl)-2,2'-Bipyridine	-	342.0	182.2	92642-09-6
233	10		1,1'-(9H-fluorene-3,6-diyl)bis(2-chloroethan-1-one)	-	319.2	248.1	726156-98-5
234	11		((oxybis(ethane-2,1-diyl))bis(oxy))bis(ethane-2,1-diyl)bis(4-methylbenzenesulfonate)	-	502.6	160.1	37860-51-8
235	11		4,4'-oxybis((Bromomethyl)Benzene)	-	356.1	196.1	4542-75-0
236	12		1,4-bis(oxiran-2-ylmethoxy)butane	-	202.3	204.1	2425-79-8
237	12		1,1'-([1,1'-biphenyl]-4,4'-diyl)bis(2-bromoethan-1-one)	-	396.1	236.1	4072-67-7

3.8 References

- (42) Goodnow, R. A.; Dumelin, C. E.; Keefe, A. D. DNA-Encoded Chemistry: Enabling the Deeper Sampling of Chemical Space. *Nat. Rev. Drug Discov.* **2017**, *16* (2), 131–147. <https://doi.org/10.1038/nrd.2016.213>.
- (80) Kale, S. S.; Bergeron-Brele, M.; Wu, Y.; Kumar, M. G.; Pham, M. V.; Bortoli, J.; Vesin, J.; Kong, X.-D.; Machado, J. F.; Deyle, K.; Gonschorek, P.; Turcatti, G.; Cendron, L.; Angelini, A.; Heinis, C. Thiol-to-Amine Cyclization Reaction Enables Screening of Large Libraries of Macrocyclic Compounds and the Generation of Sub-Kilodalton Ligands. *Sci. Adv.* **2019**, *5* (8), eaaw2851. <https://doi.org/10.1126/sciadv.aaw2851>.
- (107) Spicer, C. D.; Davis, B. G. Selective Chemical Protein Modification. *Nat. Commun.* **2014**, *5* (1), 4740. <https://doi.org/10.1038/ncomms5740>.
- (108) Jo, H.; Meinhardt, N.; Wu, Y.; Kulkarni, S.; Hu, X.; Low, K. E.; Davies, P. L.; DeGrado, W. F.; Greenbaum, D. C. Development of α -Helical Calpain Probes by Mimicking a Natural Protein–Protein Interaction. *J. Am. Chem. Soc.* **2012**, *134* (42), 17704–17713. <https://doi.org/10.1021/ja307599z>.
- (109) Kumita, J. R.; Smart, O. S.; Woolley, G. A. Photo-Control of Helix Content in a Short Peptide. *Proc. Natl. Acad. Sci.* **2000**, *97* (8), 3803–3808. <https://doi.org/10.1073/pnas.97.8.3803>.
- (110) Woolley, G. A. Photocontrolling Peptide α Helices. *Acc. Chem. Res.* **2005**, *38* (6), 486–493. <https://doi.org/10.1021/ar040091v>.
- (111) Timmerman, P.; Beld, J.; Puijk, W. C.; Meloen, R. H. Rapid and Quantitative Cyclization of Multiple Peptide Loops onto Synthetic Scaffolds for Structural Mimicry of Protein Surfaces. *ChemBioChem* **2005**, *6* (5), 821–824. <https://doi.org/10.1002/cbic.200400374>.
- (112) Muppidi, A.; Wang, Z.; Li, X.; Chen, J.; Lin, Q. Achieving Cell Penetration with Distance-Matching Cysteine Cross-Linkers: A Facile Route to Cell-Permeable Peptide Dual Inhibitors of Mdm2/Mdmx. *Chem. Commun.* **2011**, *47* (33), 9396. <https://doi.org/10.1039/c1cc13320a>.

- (113) Kale, S. S.; Villequey, C.; Kong, X.-D.; Zorzi, A.; Deyle, K.; Heinis, C. Cyclization of Peptides with Two Chemical Bridges Affords Large Scaffold Diversities. *Nat. Chem.* **2018**, *10* (7), 715–723. <https://doi.org/10.1038/s41557-018-0042-7>.
- (114) Heinis, C.; Rutherford, T.; Freund, S.; Winter, G. Phage-Encoded Combinatorial Chemical Libraries Based on Bicyclic Peptides. *Nat. Chem. Biol.* **2009**, *5* (7), 502–507. <https://doi.org/10.1038/nchembio.184>.
- (115) Spokoyny, A. M.; Zou, Y.; Ling, J. J.; Yu, H.; Lin, Y.-S.; Pentelute, B. L. A Perfluoroaryl-Cysteine S_NAr Chemistry Approach to Unprotected Peptide Stapling. *J. Am. Chem. Soc.* **2013**, *135* (16), 5946–5949. <https://doi.org/10.1021/ja400119t>.
- (116) Allouche, E. M. D.; Grinhagena, E.; Waser, J. Hypervalent Iodine-Mediated Late-Stage Peptide and Protein Functionalization. *Angew. Chem. Int. Ed.* **2022**, *61* (7). <https://doi.org/10.1002/anie.202112287>.
- (117) Ceballos, J.; Grinhagena, E.; Sangouard, G.; Heinis, C.; Waser, J. Cys–Cys and Cys–Lys Stapling of Unprotected Peptides Enabled by Hypervalent Iodine Reagents. *Angew. Chem. Int. Ed.* **2021**, *60* (16), 9022–9031. <https://doi.org/10.1002/anie.202014511>.
- (118) Baumann, A. L.; Schwagerus, S.; Broi, K.; Kemnitz-Hassanin, K.; Stieger, C. E.; Trieloff, N.; Schmieder, P.; Hackenberger, C. P. R. Chemically Induced Vinylphosphonothiolate Electrophiles for Thiol–Thiol Bioconjugations. *J. Am. Chem. Soc.* **2020**, *142* (20), 9544–9552. <https://doi.org/10.1021/jacs.0c03426>.
- (119) Kasper, M.; Lassak, L.; Vogl, A. M.; Mai, I.; Helma, J.; Schumacher, D.; Hackenberger, C. P. R. Bis-ethynylphosphonamidates as an Modular Conjugation Platform to Generate Multi-Functional Protein- and Antibody-Drug-Conjugates. *Eur. J. Org. Chem.* **2022**, *2022* (10). <https://doi.org/10.1002/ejoc.202101389>.
- (120) Stieger, C. E.; Franz, L.; Körlin, F.; Hackenberger, C. P. R. Diethynyl Phosphinates for Cysteine-Selective Protein Labeling and Disulfide Rebridging. *Angew. Chem. Int. Ed.* **2021**, *60* (28), 15359–15364. <https://doi.org/10.1002/anie.202100683>.
- (121) Zhang, F.; Sadoski, O.; Xin, S. J.; Woolley, G. A. Stabilization of Folded Peptide and Protein Structures via Distance Matching with a Long, Rigid Cross-Linker. *J. Am. Chem. Soc.* **2007**, *129* (46), 14154–14155. <https://doi.org/10.1021/ja075829t>.

- (122) Jafari, M. R.; Deng, L.; Kitov, P. I.; Ng, S.; Matochko, W. L.; Tjihung, K. F.; Zeberoff, A.; Elias, A.; Klassen, J. S.; Derda, R. Discovery of Light-Responsive Ligands through Screening of a Light-Responsive Genetically Encoded Library. *ACS Chem. Biol.* **2014**, *9* (2), 443–450. <https://doi.org/10.1021/cb4006722>.
- (123) Bellotto, S.; Chen, S.; Rentero Rebollo, I.; Wegner, H. A.; Heinis, C. Phage Selection of Photoswitchable Peptide Ligands. *J. Am. Chem. Soc.* **2014**, *136* (16), 5880–5883. <https://doi.org/10.1021/ja501861m>.
- (124) Assem, N.; Ferreira, D. J.; Wolan, D. W.; Dawson, P. E. Acetone-Linked Peptides: A Convergent Approach for Peptide Macrocyclization and Labeling. *Angew. Chem. Int. Ed.* **2015**, *54* (30), 8665–8668. <https://doi.org/10.1002/anie.201502607>.
- (125) Ekanayake, A. I.; Sobze, L.; Kelich, P.; Youk, J.; Bennett, N. J.; Mukherjee, R.; Bhardwaj, A.; Wuest, F.; Vukovic, L.; Derda, R. Genetically Encoded Fragment-Based Discovery from Phage-Displayed Macrocyclic Libraries with Genetically Encoded Unnatural Pharmacophores. *J. Am. Chem. Soc.* **2021**, *143* (14), 5497–5507. <https://doi.org/10.1021/jacs.1c01186>.
- (126) Nair, D. P.; Podgórski, M.; Chatani, S.; Gong, T.; Xi, W.; Fenoli, C. R.; Bowman, C. N. The Thiol-Michael Addition Click Reaction: A Powerful and Widely Used Tool in Materials Chemistry. *Chem. Mater.* **2014**, *26* (1), 724–744. <https://doi.org/10.1021/cm402180t>.
- (127) Smith, M. E. B.; Schumacher, F. F.; Ryan, C. P.; Tedaldi, L. M.; Papaioannou, D.; Waksman, G.; Caddick, S.; Baker, J. R. Protein Modification, Bioconjugation, and Disulfide Bridging Using Bromomaleimides. *J. Am. Chem. Soc.* **2010**, *132* (6), 1960–1965. <https://doi.org/10.1021/ja908610s>.
- (128) Kong, X.-D.; Moriya, J.; Carle, V.; Pojer, F.; Abriata, L. A.; Deyle, K.; Heinis, C. De Novo Development of Proteolytically Resistant Therapeutic Peptides for Oral Administration. *Nat. Biomed. Eng.* **2020**, *4* (5), 560–571. <https://doi.org/10.1038/s41551-020-0556-3>.
- (129) Greenbaum, D.; Medzihradszky, K. F.; Burlingame, A.; Bogoy, M. Epoxide Electrophiles as Activity-Dependent Cysteine Protease Profiling and Discovery Tools. *Chem. Biol.* **2000**, *7* (8), 569–581. [https://doi.org/10.1016/S1074-5521\(00\)00014-4](https://doi.org/10.1016/S1074-5521(00)00014-4).

- (130) Nawaz, H.; Pires, P. A. R.; El Seoud, O. A. Kinetics and Mechanism of Imidazole-Catalyzed Acylation of Cellulose in LiCl/N,N-Dimethylacetamide. *Carbohydr. Polym.* **2013**, *92* (2), 997–1005. <https://doi.org/10.1016/j.carbpol.2012.10.009>.
- (131) Madsen, U. Ionotropic Excitatory Amino Acid Receptor Ligands. Synthesis and Pharmacology of a New Amino Acid AMPA Antagonist. *Eur. J. Med. Chem.* **2000**, *35* (1), 69–76. [https://doi.org/10.1016/S0223-5234\(00\)00104-5](https://doi.org/10.1016/S0223-5234(00)00104-5).
- (132) Lizza, J. R.; Patel, S. V.; Yang, C. F.; Moura-Letts, G. Direct Synthesis of Cyanopyrrolidinyl β -Amino Alcohols for the Development of Diabetes Therapeutics: Direct Synthesis of Cyanopyrrolidinyl β -Amino Alcohols for the Development of Diabetes Therapeutics. *Eur. J. Org. Chem.* **2016**, *2016* (30), 5160–5168. <https://doi.org/10.1002/ejoc.201600969>.
- (133) Cervantes-Reyes, A.; Rominger, F.; Rudolph, M.; Hashmi, A. S. K. Gold(I) Complexes Stabilized by Nine- and Ten-Membered N-Heterocyclic Carbene Ligands. *Chem. – Eur. J.* **2019**, *25* (50), 11745–11757. <https://doi.org/10.1002/chem.201902458>.
- (134) Stubba, D.; Lahm, G.; Geffe, M.; Runyon, J. W.; Arduengo, A. J.; Opatz, T. Xylochemistry-Making Natural Products Entirely from Wood. *Angew. Chem. Int. Ed.* **2015**, *54* (47), 14187–14189. <https://doi.org/10.1002/anie.201508500>.

4. High-density immobilization of TCEP on silica beads for efficient disulfide bond reduction and alkylation

4.1 *Work contribution*

High-density immobilization of TCEP on silica beads for efficient disulfide bond reduction and alkylation

Mischa Schüttel¹ and Christian Heinis^{1,*}

¹Institute of Chemical Sciences and Engineering, School of Basic Sciences, École Polytechnique Fédérale de Lausanne (EPFL), CH-1015 Lausanne, Switzerland.

*Correspondence should be addressed to C.H. E-mail: christian.heinis@epfl.ch

Keywords

cyclic peptide, disulfide bridge, disulfide reduction, immobilized TCEP, reduction, TCEP, TCEP-agarose

Author contributions: I, along with Christian Heinis conceptualized the method and developed the strategy. I performed proof-of-concept experiments, synthesis of model peptides and TCEP immobilized beads on various solid supports as well as developed the assay to evaluate the bead's reductive capacity. I helped to make all figures, wrote the first draft of the manuscript, and contributed to editing. Christian Heinis reviewed and edited the manuscript.

Acknowledgment: Alexander Lund Nielsen provided constructive feedback on the first initial draft of the manuscript.

This chapter is based on a manuscript prepared for publication and was supported by an Innosuisse grant (Grant 192368).

4.2 ***Abstract***

Tris-(2-carboxyethyl)phosphine (TCEP) linked to agarose beads is widely used for reducing disulfide bridges in proteins and peptides. The immobilization on beads allows efficient removal after reduction to prevent interference of TCEP with conjugation reagents. However, a limitation of the agarose-TCEP is its rather low reducing capacity per milliliter wet beads (up to 15 $\mu\text{mol/ml}$), making it unsuitable for reducing disulfides of molecules at millimolar concentrations. In this work, we tested the immobilization of TCEP to a range of different solid supports and found that conjugation to silica gel offers TCEP beads with about 8-fold higher reduction capacity ($129 \pm 16 \mu\text{mol/ml}$ wet beads). We show that it allows reducing disulfide-cyclized peptides at millimolar concentrations for subsequent cyclization by bis-electrophile linker reagents. Given the substantially higher reduction capacity, the robust performance in different solvents, the low cost of the silica gel and the ease of functionalization with TCEP, the silica gel-TCEP is suited for reducing disulfide bridges in essentially any peptide and is particularly useful for reducing peptides at higher concentrations.

4.3 Introduction

TCEP is a powerful reagent widely used for reducing disulfide bonds in proteins, peptides and other disulfide bond-containing molecules.^{135, 136, 137} Its strong irreversible reductive capability towards disulfide bonds at a wide pH range (1.5-8.5), its high solubility and good stability in aqueous solutions, its compatibility with many functional groups present in the biological systems and its odorless nature are critical features for TCEP's success.^{137,138,139} Due to the interference of TCEP with peptide and protein labeling and modification agents (e.g. maleimides, haloacetic acid),^{135,140} the reducing agent needs to be removed in many applications, which is cumbersome if done by dialysis or chromatographic purification. TCEP immobilized to solid supports offers an efficient and convenient solution to this problem as it can be removed by centrifugation, filtration, or even by magnetic capture. For example, several providers commercially offer TCEP immobilized on agarose beads and it is used in many applications.^{141, 142, 143} Immobilized TCEP is also used in case reducing agents are incompatible with analytical techniques, as in some types of gel electrophoresis or mass spectrometric analysis.

A limitation of TCEP-agarose is the relatively low reducing capacity per volume of wet agarose beads. Commercial providers promise for their products that they reduce at least 8 μmol disulfide bonds per milliliter of wet agarose. Given that TCEP is typically applied in large excess over the biomolecules to reduce peptide bonds quantitatively and that the beads should not occupy more than half the volume of a reaction, the application is restricted to protein and peptide concentrations well below 1 mM. In our laboratory, we regularly reduce disulfide bridges in peptides containing two or more thiol groups to subsequently cyclize them by bis- or tris-electrophile reagents.^{79, 80} A preferred peptide concentration for such cyclization reactions is 1 mM, but such high concentrations of reduced peptide can currently not be obtained using agarose-TCEP due to the described low reducing capacity. Reduction of thiol groups in peptides at millimolar concentrations would be of great interest in many other applications too, including for peptide labeling by fluorophores, for crosslinking, or for immobilization to surfaces.

TCEP has been immobilized to other supports than agarose with diverse applications in mind, the solid supports being polyethylene glycol (PEG) polymers,¹⁴¹ silica beads,¹⁴⁴ and magnetic cobalt beads.¹⁴³ Subra and co-workers have conjugated TCEP to hydrophilic PEG-based beads to efficiently reduce disulfide bonds in aqueous and organic solvents and under microwave irradiation.¹⁴¹ They conjugated TCEP via a carboxylic acid to amino-functionalized PEG using O-benzotriazole-*N,N,N',N'*-tetramethyl-uronium-hexafluoro-phosphate (HBTU) as coupling agent. The TCEP-PEG resin was efficiently applied to reduce disulfide bonds in peptides at concentrations of around 100 μ M. The reducing capacity of the PEG-TCEP was not reported but is likely higher than that of agarose-TCEP based on the quantity of immobilized TCEP molecules. Alzahrani and Welham have immobilized TCEP on monolithic silica for the reduction of proteins in microfluidic chips.¹⁴⁴ They achieved this by silanisation of the silica surface with (3-aminopropyl)triethoxysilane (APTES), followed by coupling of TCEP via a carboxylic acid to the amine using N-(3-dimethylaminopropyl)-N-ethylcarbodiimide (EDC) and sulfo-N-hydroxysuccinimide (NHS) as coupling agents. The monolithic silica-TCEP was characterized in depth by various analytical methods and successfully applied to reduce the disulfide bonds in insulin that was run through the microchip, but the reduction capacity was not quantified. Most recently, Stark and co-workers immobilized TCEP on magnetic carbon-coated cobalt nanoparticles, which allows fast and efficient removal of the reducing agent with a magnet. The TCEP was conjugated to PEG on cobalt beads by esterification using EDC. The beads were applied to quantitatively reduce disulfide bonds of bovine insulin at a concentration of 400 μ M. The reduction capacity of the cobalt beads was quantified to be 70 μ mol functional TCEP per gram of beads, which is substantially higher than that of the commercially available agarose-TCEP.

Herein, we aimed at producing immobilized TCEP that has a reduction capacity per volume of solid support that is sufficiently high to reduce disulfide bonds in peptides at millimolar concentrations. An important goal was also that the production of the TCEP beads is relatively cheap in order to afford reducing disulfides in peptides at milligram scale and/or reducing large numbers of different peptides at microgram scale. We further wished that the immobilized TCEP is compatible with aqueous as well as diverse organic solvents. Towards this end, we coupled TCEP to a range of commercially accessible,

inexpensive solid supports, quantified their reduction capacity and studied in depth the performance and properties of the immobilized TCEP that had the highest reduction capacity.

4.4 *Results & discussion*

We first established a standardized procedure to quantify the reduction capacity of immobilized TCEP. Such a method was needed in order to accurately and reproducibly determine the performance of commercial and newly developed immobilized TCEP. We chose to quantify the reducing capacity by comparing it to the reducing capacity of free TCEP (assuming that one molecule of free TCEP can reduce one disulfide bridge), and we expressed this in " μmol of functional TCEP per ml wet resin". For quantifying the reducing capacity of free and immobilized TCEP, we incubated both with Ellman's reagent in parallel and quantified the amount of reduced reagents by measuring absorbance at 412 nm, as described before.¹³⁹ With the method, we quantified the reducing capacity of two commercially provided agarose-immobilized TCEP, one being the Pierce™ Immobilized TCEP Disulfide Reducing Gel (ThermoFisher) and the other one being G-Biosciences TCEP Reducing Resin (G-Biosciences). The two agarose-TCEP resins displayed reducing capacities of 15.3 ± 1.3 and 10.4 ± 3.7 μmol of functional TCEP per ml wet resin (Figure 13b).

Compared to free TCEP, which can be dissolved in multiple solvents including H_2O , dimethylsulfoxide (DMSO) and dimethylformamide (DMF), and applied at high millimolar concentrations, these reduction capacities were substantially lower, showing the limit of agarose-immobilized TCEP. In order to visualize the limit of the reducing capacity for commercially provided immobilized TCEP, we added increasing volumes of agarose-TCEP to a typical sample volume of 40 μl . The largest volume of wet agarose-TCEP that could still be mixed with the 40 μl sample was around 50 μl and corresponded to the reducing capacity of 0.8 μmol free TCEP (Figure 13c). The relatively low value was likely due to the limited loading density, but certainly also due to the extensive swelling found for the agarose beads, which takes a larger space in reaction tubes and reduces the capacity per volume.

We next assessed the capacity of commercial agarose-TCEP to quantitatively reduce disulfide-cyclized peptides, an important need of our laboratory when synthesizing (bi)cyclic peptides for drug development.^{79,80} We synthesized three model peptides of the format Mpa-Xaa-Xaa-Mea, with Xaa being random amino acids and Mpa and Mea being

mercaptopropionic acid and mercaptoethylamine, both building blocks containing a thiol group that could oxidize to form disulfide-cyclized peptides (Figure 13d). We incubated the peptides (0.4 μmol) in 400 μl water (1 mM final conc.) with different quantities of agarose-TCEP. The reducing capacity of the applied quantities corresponded to those of 2, 4, 8, or 16-fold molar excess free TCEP over the peptide. Analysis of the peptides by LC-MS showed that at least eight equivalents were required to completely (>99%) reduce the peptides in three hours at room temperature. Together with the reducing capacity of agarose-TCEP, and the maximal volume of agarose-TCEP that can fit into a given volume (if the agarose beads are allowed to occupy around half the volume), this result indicated that the maximal concentration of peptide that agarose-immobilized TCEP could reduce was around 1 mM, and thus is rather low (Figure 13e).

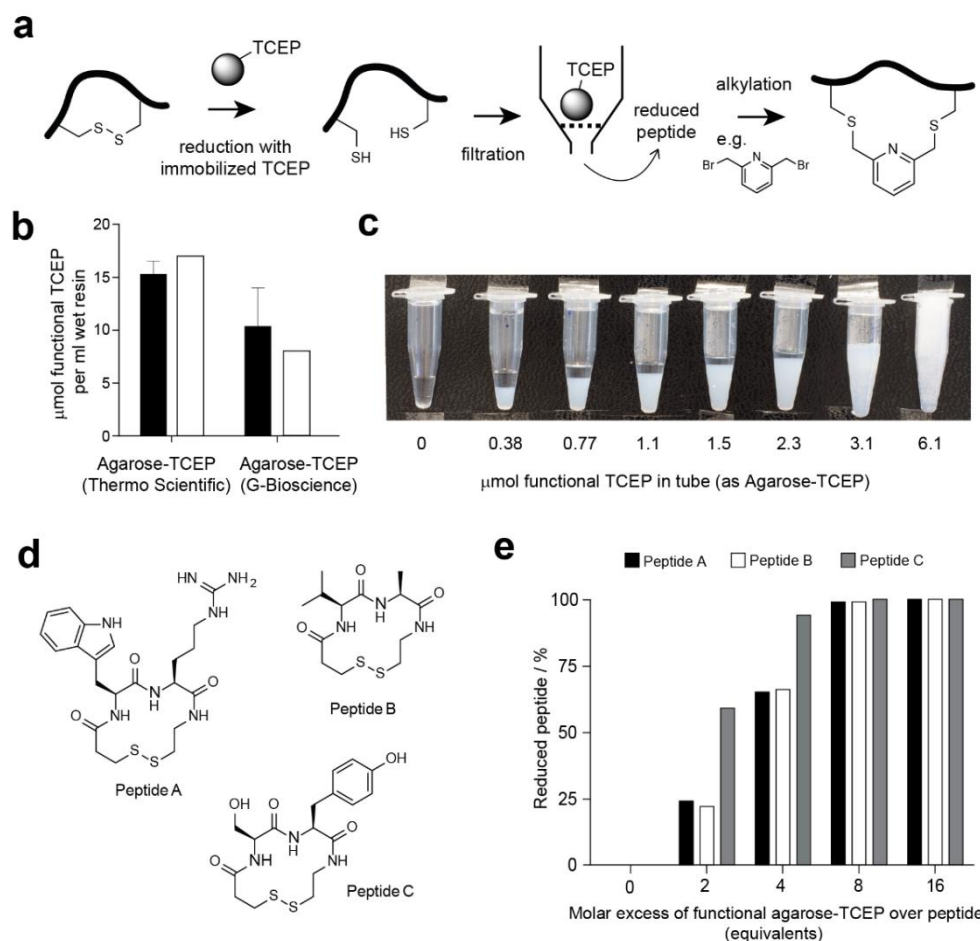


Figure 13: Disulfide bond reduction by immobilized TCEP. (a) Schematic depiction of strategy for reducing disulfide bonds, removal of immobilized TCEP by filtration, and alkylation of reduced thiol groups, shown for a cyclization reaction. (b) Capacity of commercially provided agarose-TCEP to reduce Ellman's reagent. The capacity is indicated as μmol of

functional TCEP per mL wet resin, determined using Ellman's reagent and using free TCEP as a reference. The black bars show the mean values of three independent measurements. SDs are indicated. The white bars indicate the reduction capacity indicated by the commercial provider. (c) Visual presentation of the volume occupied by TCEP immobilized on agarose beads in a volume of 40 μ L water (beads from Thermo Fisher, 15.3 ± 1.3 μ mol functional TCEP per mL wet resin). The quantity of functional TCEP (as agarose-TCEP beads) is indicated. (d) Model peptides cyclized by disulfide bridges were used to test the reduction capacity of immobilized TCEP. (e) Model peptides (0.4 μ mol) in 400 μ L water (1 mM final conc.) were incubated with the indicated molar excess of functional agarose-TCEP (from ThermoFisher, 15.3 ± 1.3 μ mol functional TCEP per mL wet resin determined by Ellman's reagent) for 3 h at RT, and analyzed by HPLC.

We next set out to identify a solid phase to which TCEP could be immobilized more densely so that disulfide bridges in higher concentrated peptide samples could be reduced. We aimed at coupling TCEP to solid surfaces via one of its carboxylic acid through an amide bond with an amino group present on the solid phase. We applied seven amine-functionalized resins used for solid-phase peptide synthesis, one agarose solid phase that is used as chromatography support, and silica gel that is used for flash chromatography. For immobilizing TCEP on the silica gel, we first functionalized the material with amino groups by silanization with APTES (Figure 14a). For TCEP immobilization through amidation on all solid supports, we applied the coupling agent EDC and an excess of TCEP over the number of accessible amino groups.

Comparison of the reducing capacity of all TCEP-functionalized solid supports using the above-described Ellman's assay showed that silica gel-TCEP was far superior to all other supports, including the commercially offered agarose-TCEP (Figure 14b). One ml wet resin of the silica gel-TCEP had a reducing capacity equivalent to 129 ± 16 μ mol of free TCEP (mean value and SD of five silica gel-TCEP batches produced over the course of the project). Compared to the better one of the two commercial agarose-TCEP products, the silica gel-TCEP had thus an 8.3-fold higher reducing capacity. Working with the different solid phases, we realized another strength of the silica gel is the limited swelling, which limits the volume taken by the solid phase and thus a maximal reducing capacity. To illustrate the maximal reducing capacity, we added increasing volumes of the silica gel-TCEP to a typical sample volume of 40 μ L. The largest volume of wet silica gel-TCEP (mean value) that could still be mixed with the 40 μ L sample was 50 μ L and

corresponded to a reducing capacity of 6.4 μmol free TCEP (Figure 14c). This value is 8-fold larger than the one found for agarose-TCEP.

In initial applications of the silica gel-TCEP, we observed an unexpected product with a mass that was 32 Da smaller than the reduced peptides. Based on the mass, we speculated that the product might result from eliminating one of the sulfur groups. This side product was substantially reduced or completely suppressed if silica gel-TCEP was acidified prior to use (Supplementary Figure 1). For all subsequent experiments, we thus acidified the silica-TCEP prior to application.

We quantified the reducing performance of the silica gel-TCEP with the three model peptides described above. We incubated the peptides (0.4 μmol) in 40.0 μl DMSO (10 mM final conc.) with different quantities of silica gel-TCEP. The reducing capacity of the applied quantities corresponded to those of 1, 2, 4, or 8-fold molar excess free TCEP over the peptide. Four equivalents were needed to reduce peptides maximally in three hours at room temperature (>96% reduced peptide; Figure 14d). Based on the reducing capacity, the excess needed for quantitative reduction of model peptides, and the maximal volume of silica gel-TCEP that can fit into a given volume, we calculated the maximal concentration of peptide that could be reduced by silica gel-TCEP being 40 mM, and thus 16-fold higher than for agarose-TCEP.

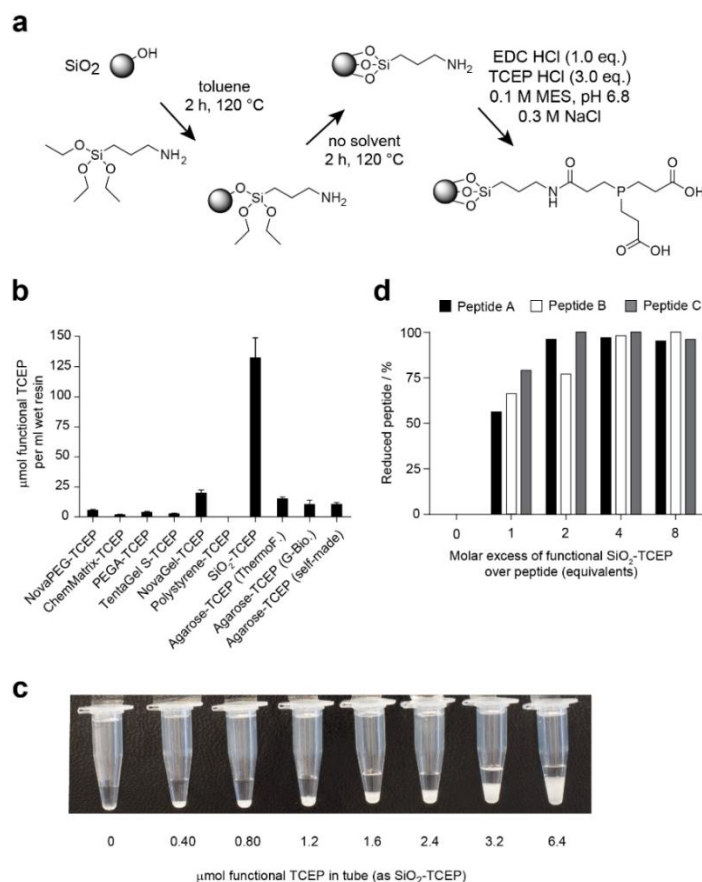


Figure 14: Immobilization of TCEP on silica beads and characterization. (a) Strategy for functionalizing silica with amino groups and subsequent functionalization with TCEP. (b) Reduction capacity of ten different TCEP-functionalized solid supports. Six of the solid supports are peptide synthesis resins, one is silica gel, and three are based on agarose beads (two commercial, one custom-made). The capacity is indicated as μmol of functional TCEP per ml wet resin, determined using Ellman's reagent and using free TCEP as a reference. Mean values and SDs of three measurements (technical replicates) are shown. For silica gel-TCEP, the mean value and SD is shown for five different batches (Supplementary table 1). (c) Visual presentation of the volume occupied by TCEP immobilized on silica gel in a volume of 40 μL DMSO (131 ± 16 μmol functional TCEP per mL wet beads). (d) Model peptides (0.4 μmol) in 40 μL DMSO (10 mM final conc.) were incubated with the indicated molar excess of functional SiO₂-TCEP (batch reducing capacity: 131 ± 16 μmol functional TCEP per ml wet resin determined by Ellman's reagent) for 3 h at RT, and analyzed by HPLC.

We next tested if the thiol groups of the reduced peptides could be alkylated after removing the silica gel. As a reaction, we chose the cyclization by the bis-electrophilic reagent **1** as shown in Figure 13a, which involved two consecutive reactions of which the second one is intramolecular. The reaction of the peptides in volumes of 20 μL at a concentration of 1 mM with four equivalents of **1** in ammonium carbonate buffer/DMSO

(1:1, v/v, pH 8) for 3 h led to quantitative cyclization (Figure 15). No disulfide-cyclized peptide was observed, indicating that the peptides were quantitatively reduced and did not partially oxidize back during the alkylation reaction.

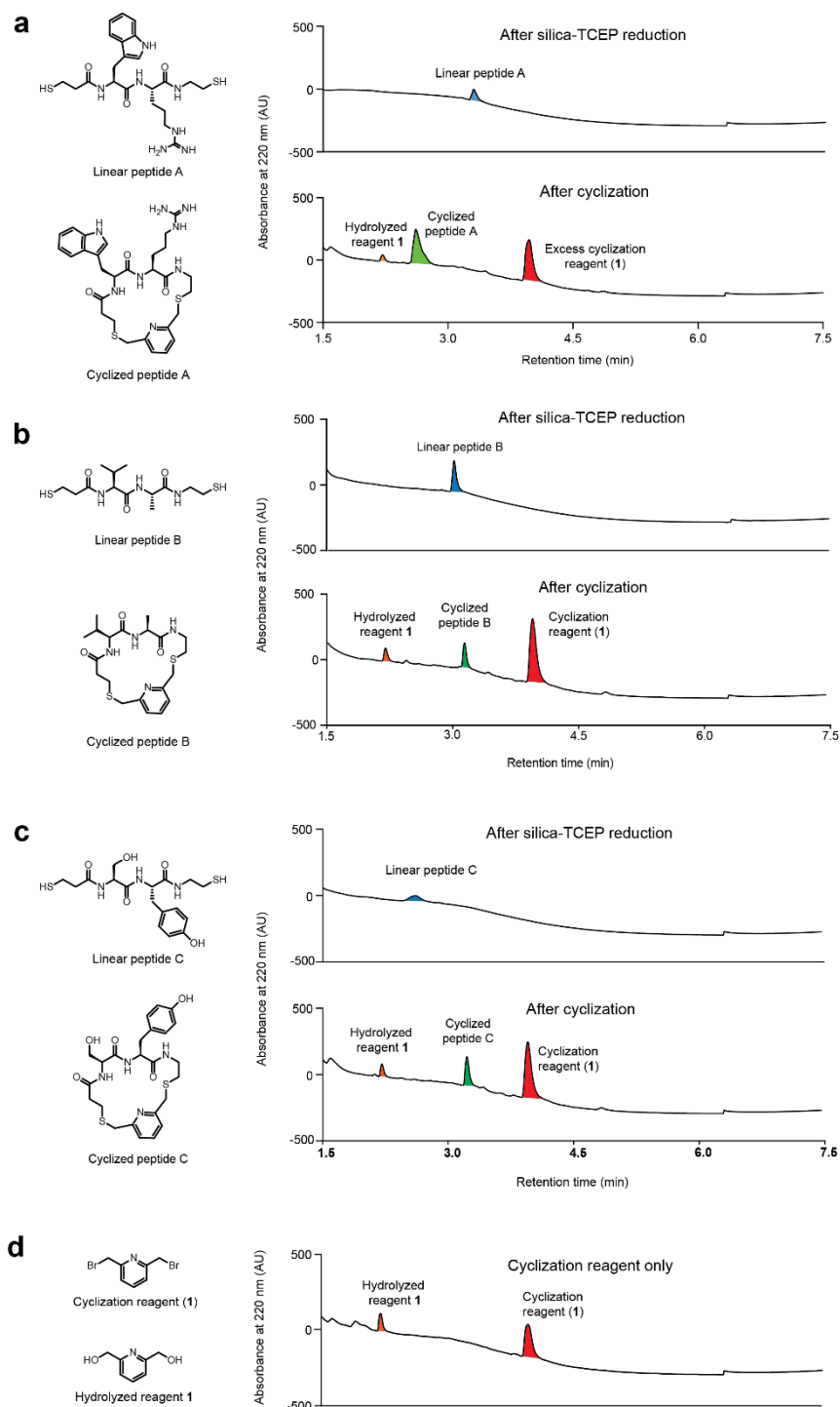


Figure 15: Alkylation of thiols after reduction with silica-TCEP beads. Three model peptides were reduced and cyclized with the bis-electrophilic reagent 2,5-bis(bromomethyl)pyridine. Peptides were analyzed by LC-MS before and

after alkylation. (a) Peptide A. (b) Peptide B. (c) Peptide C. (d) LC-MS analysis of cyclization reagent without peptide. Peaks of linear peptides (blue), cyclized peptides (green), cyclization reagent (red) and hydrolyzed cyclization reagent (yellow) are highlighted with color.

Depending on the chemical reaction and the reagents needed for chemically modifying the reduced thiol groups, specific solvents may be required, and we thus tested the performance of silica gel-TCEP in a range of different solvents. We dissolved lyophilized model peptides in 40 μ l water, methanol (MeOH), acetonitrile (MeCN), DMSO or DMF at a concentration of 10 mM (0.4 μ mol) or as high as the solubility allowed, incubated the peptides with 12 μ l wet silica gel-TCEP (corresponding to a reducing capacity of 1.6 μ mol free TCEP, 4 equiv.) for 3 h at room temperature, and analyzed the peptidic species by LC-MS before and after reduction. The peptide was reduced with an efficiency between 96 and 100% (Figure 16a), showing that the silica-immobilized TCEP can flexibly be applied in many different solvents.

After the removal of immobilized TCEP from peptides, the thiols may partially oxidize back, which would lead to incomplete modification of the peptides. The risk of back-oxidation is particularly high for peptides containing two or more thiol groups as they can react intramolecularly. For the synthesis of cyclic peptides, as shown in the example above, partial back-oxidation would lead to product mixtures of linker-cyclized peptide and disulfide-cyclized peptide. In order to assess the propensity of dithiol peptides to oxidize and to find conditions that limit oxidation, we tested the stability of a peptide in different solvents and at different pHs (Figure 16b). As solvents, we used water containing either 10% DMSO, 10% DMF or 20% acetonitrile, which are mixtures that are suited for dissolving most peptides and compatible with thiol-alkylation reactions. For testing different pH conditions, we added HCl to the solvent/buffer mixtures to reach a pH of 6, 4 or 2. We followed back-oxidation by LC-MS analysis of samples taken over a time span of 24 hours. While the model peptide fully oxidized in 10% DMSO at all pH values, it remained reduced at pH 2 in 10% DMF and 20% MeCN (Figure 16b). We subsequently tested the back-oxidation of two additional peptides to test if the effects of different solvents and pH are peptide sequence-dependent. The two additional peptides neither back-oxidized at low pH and in 10% DMF or 20% MeCN and thus behaved similarly (Supplementary Figure 2).

We tested further measures for preventing rapid back-oxidation of the dithiol peptides, this time over several days, one being the storage of the peptide solutions at -20°C and one the closing of the microwell plates containing the peptides by DMSO-soaked micro clime lids at room temperature simulating experimental screening conditions. For this experiment, we incubated a model peptide in DMSO for six days and analyzed samples at different time points by LC-MS (Figure 16c). In this experiment, we also tested the influence of peptide concentration on oxidation (1 mM, 5 mM, 10 mM, 20 mM). We simultaneously monitored water uptake into the DMSO samples and the increase in the sample volumes (Supplementary Figure 3). At room temperature and without a lid on the microtiter plate, thiol oxidation took place already on the first day to a large extent, and the peptide was fully oxidized after six days. At room temperature and covered with a lid, a small quantity of oxidized peptide was observed after 1-2 days, and around 25% of the peptide remained reduced after six days. Peptides covered with a lid and stored at -20°C oxidized only marginally over the first two days, and more than 75% was still reduced after six days. Taken these results together, dithiol peptides do rapidly oxidize after removal of the TCEP beads if no precaution is taken, but the oxidation can be controlled to a large extent if peptides are kept in an appropriate solvent or away from humidity and at low temperature. If the application allows, it is best to remove the TCEP beads only immediately before the thiol is to be chemically modified.

Finally, we assessed the stability of the silica gel-TCEP beads at different conditions to find out how they are best kept for short periods and stored over longer times. We kept the beads at different temperatures (room temperature, 4°C, -20°C) and under different atmospheres (air, nitrogen, vacuum) for more than 100 days and tested the reducing capacity with Ellman's reagent (Figure 16d). The temperature had the strongest effect, wherein storage at -20°C was best and retained around 80% of the reducing capacity after 112 days. Without any storage precautions (room temperature and air in tubes), the beads still kept more than 50% of their reducing capacity, showing that they are rather stable and that no particular storage measures need to be taken when using the beads over several days.

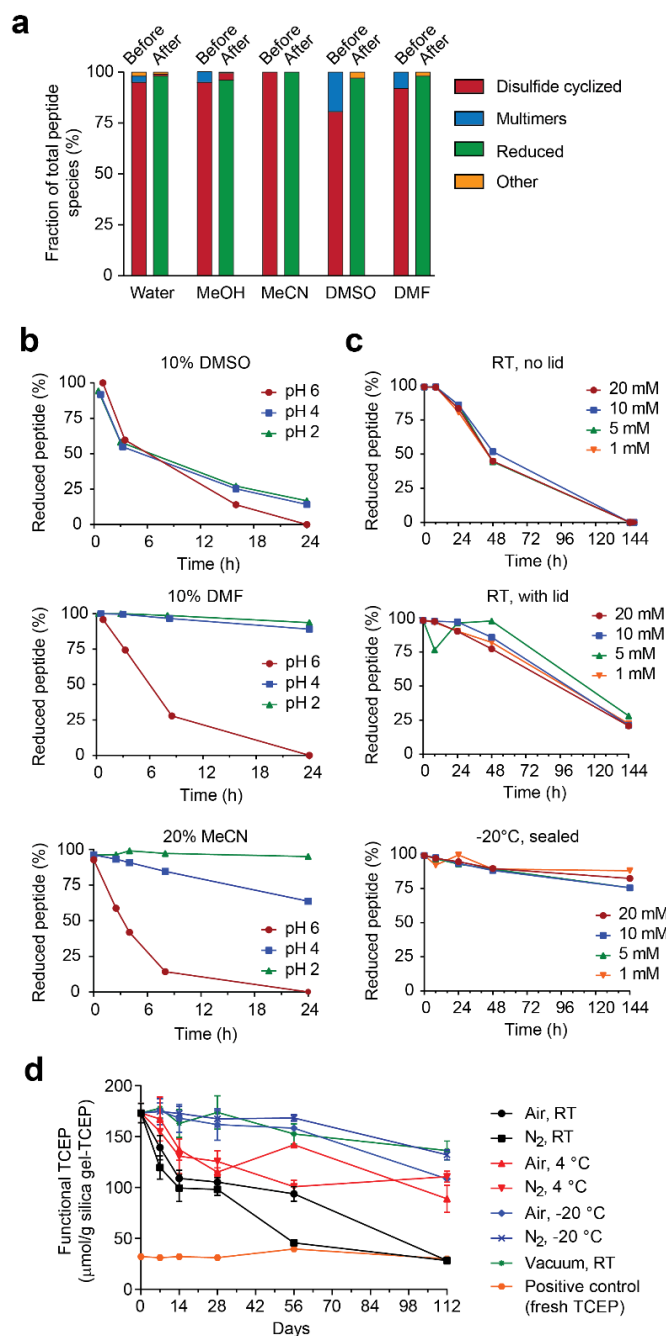


Figure 16: Solvent compatibility, back-oxidation of peptides, and stability of silica gel-TCEP. (a) Reduction of dithiol peptide by silica gel-TCEP in different solvents. Products were identified and quantified (absorbance at 220 nm) by LC-MS before and after reduction. Experiments were performed with peptide A for all solvents except MeCN, for which peptide B was used for solubility reasons. (b) Back-oxidation was assessed with model peptide G (1 mM; Supplementary Figure 2), incubated in mixtures of 60 mM NH_4HCO_3 buffer and the indicated organic solvents at the indicated pH, and monitored over 24 hours. (c) Back-oxidation of model peptide C at different concentrations in DMSO, stored at the indicated temperatures in 384 PP microwell plates covered with the indicated lids and monitored by LC-MS over 7 days. (d) Storage stability of silica gel-TCEP beads. For each time point and condition, vials containing 15

mg of beads ($173 \pm 9 \mu\text{mol/g}$) were stored in triplicate, and the reducing capacity was analyzed at the indicated time points using Ellman's reagent.

4.5 ***Conclusion***

We have developed TCEP beads that have an 8-fold higher reduction capacity than the widely applied and commercially used agarose-TCEP. We achieved this by immobilizing TCEP on silica gel, which is a highly porous, non-swelling, and cheap solid-phase material that is compatible with a wide range of solvents. We have shown that the silica gel-TCEP beads are suited to efficiently reduce disulfide bridges in peptides. Due to the higher reduction capacity, the new beads allow quantitatively reducing disulfide bridges in peptide samples having concentrations as high as 16 mM. We furthermore showed that the beads are suited to reduce disulfide-cyclized peptides that could, due to the efficient removal of the immobilized TCEP, be immediately cyclized by bis-electrophile linker reagents. The silica gel-TCEP beads were found to be stable and can be stored for several months at -20°C or for days at RT without losing much of their reduced capacity. The silica gel-TCEP bead may be particularly attractive for applications where disulfide bridges at higher millimolar concentrations need to be reduced. The beads may also be applied to recover partially oxidized peptide stock solutions in organic solvents. The broad compatibility with numerous functional groups, solvents, and longer-term storage possibilities are further beneficial aspects of these highly-dense immobilized TCEP beads.

4.6 **Material & methods**

General considerations

Unless otherwise indicated, all reagents were purchased from commercial sources and used without further purification. Solvents were not anhydrous, nor were they dried prior usage. The following abbreviations are used in the manuscript:

MeCN (acetonitrile), APTES (3-aminopropyl)triethoxysilane), DCM (dichlormethane), DMF (dimethylformamide), DMSO (dimethylsulfoxide), EDC (*N*-(3-dimethylaminopropyl)-*N'*-ethylcarbodiimid-hydrochlorid), HATU (1-[bis(dimethylamino)methylene]-1H-1,2,3-triazolo[4,5-b]pyridinium 3-oxide hexafluorophosphate), MES (2-morpholin-4-ylethanesulfonic acid), NMM (*N*-methylmorpholine), NMP (*N*-methylpyrrolidone), TCEP (tris(2-carboxyethyl)phosphine), TFA (trifluoro acetic acid), THF (tetrahydrofuran), TIS (triisopropyl silane), SiO₂ (silica gel)

Quality of chemicals

Ammoniumbicarbonate (Sigma-Aldrich, 99-101%), MeCN (Fisher Chemical, >99.8%), (3-aminopropyl)triethoxysilane (Sigma-Aldrich, 99%), 2,6-bisbromomethyl pyridine (sigma-Aldrich, 98%), dichlormethane (Sigma-Aldrich, >99.9%), DMF (Biosolve Chimie Sarl, >99.5%), DMSO (Sigma-Aldrich, >99.5%), EDC (Carl Roth GmbH + Co KG, >99%), fluorenylmethoxycarbonyl (Fmoc) amino acids and derivatives (GL Biochem Shanghai Ltd, >99%), HATU (GL Biochem Shanghai Ltd, >99%), MES (Apollo Scientific, >99.5%), NMP (VWR, 99.5%), NMM (Sigma-Aldrich, >98%), phenol (Acros Organics, >99%), piperidine (Acros Organics, 99%), potassium cyanide (Sigma-Aldrich, 99%), sodium chloride (Carl Roth GmbH + Co KG, >99.5%), pyridine (Sigma-Aldrich, 99%), TCEP (Chem Scene, >98%), TFA (Sigma-Aldrich, 99%), THF (Fisher Chemical, >99.5%), TIS (Sigma-Aldrich, 98%), silica gel (SiliaFlash® P60, Silicycle).

Peptide synthesis

Peptides were synthesized at a 50 μ mol scale on an Intavis Multi pep RSi synthesizer using 5 ml polypropylene (PP) reactors containing polyethylene (PE) frits (V051PE76, Multisyn tech GmbH) and cysteamine 4-methoxytrityl resin (49.6 mg, 50 μ mol, 1.01 mmol/g, S8066787 106, Novabiochem). The resin in each column was washed with DMF (4 \times 1000 μ l) for resin swelling. Coupling was performed with 417 μ l of Fmoc amino acid (209 μ mol, 4.2 equiv., final conc. 0.22 mM), 392 μ l of HATU (196 μ mol, 4.0 equiv., final conc. 0.21 mM), 125 μ l of NMM (500 μ mol, 10 equiv., final conc. 1.27 M,) and 5 μ l of NMP. All components were premixed for one minute prior to addition to the resin. The reaction mixture was left for one hour without shaking. The final volume of the coupling reaction was 939 μ l. Coupling was performed twice. Then, the resin was washed with 4 \times 1000 μ l of DMF. Fmoc deprotection was performed using 800 μ l piperidine/DMF (1:4, v/v) for 5 minutes and was repeated once. Next, the resin was washed with 4 \times 1000 μ l of DMF. At the end of the peptide synthesis, the resin was washed with 2 \times 1000 μ l of DCM. The resin was deprotected and cleaved using 4 ml TFA/H₂O/TIS (95:2.5:2.5, v/v/v) for 3 h at room temperature. The TFA of the filtrate was evaporated under a continuous stream of nitrogen in a 15 mL canonical PP tube (greiner bio-one, 188271).

Peptide purification

Peptide from a 50 μ mol-scale synthesis was dissolved in 10 ml of a MeCN and H₂O mixture (10:90, v/v), filtered through a teflon (PTFE) syringe filter (25 mm diameter, 0.22 μ m pore size; BGB) and run over a preparative column (XTerra Prep MS C18 OBT 10 μ m, 19 \times 250 mm) using preparative HPLC system (Waters 2535). A flow rate of 16 mL/min and a linear gradient from 0 to 40% solvent B over 39 min (A: 99.9% H₂O and 0.1% TFA; B: 99.9% MeCN and 0.1% TFA) were applied. Absorbance was monitored at 220 nm. Fractions containing the desired peptide were pooled together, frozen (liquid nitrogen), and lyophilized until dry white fluffy powder was obtained.

Disulfide cyclization of peptides

Monomeric disulfide cyclized peptide was formed by incubating a 1 mM solution of purified reduced peptide in 60 mM NH_4HCO_3 (pH 8) containing 50% MeCN (v/v) for three days under rotation (10 rpm) at room temperature. The samples were frozen (liquid nitrogen) and lyophilized again. Oxidized peptides were dissolved in 10 ml solvent mixture of MeCN and H_2O (10:90, v/v) and purified by HPLC. The fractions were frozen (liquid nitrogen) and lyophilized to obtain a fluffy white powder. The purity and identification of disulfide cyclized peptide was confirmed by UHPLC-MS.

LC-MS analysis of peptides

Peptides were analyzed by LC-MS analysis with a UHPLC and single quadrupole MS system (Shimadzu LCMS-2020) using a C18 reversed-phase column (Phenomenex Kinetex 2.1 mm \times 50 mm C18 column, 100 Å pore, 2.6 μM particle) and a linear gradient of solvent B (acetonitrile, 0.05% formic acid) over solvent A (H_2O , 0.05% formic acid) at a flow rate of 1 ml min^{-1} . For all samples, a gradient of 0 to 100% MeCN within 10 min was applied, and UV at 220 nm was used when not otherwise mentioned. Mass analysis was performed in positive ion mode. 100 μl polypropylene (PP) HPLC microvial (Shimadzu, 980-14379) with PP and Teflon caps (Shimadzu, 980-18425) were used for all samples. For the assessment of reduced peptide content, the samples were injected within 3 min after sample preparation to avoid back-oxidation.

For analyzing HPLC-purified peptides (reduced, disulfide-cyclized, and linker-cyclized peptides), a 20 μl sample of the desired fraction was transferred and analyzed using an injection volume of 2 μl .

For analyzing peptides treated with agarose-TCEP beads (around 1 mM peptide), 10 μl of supernatant were transferred into a microvial and 1 μl was injected for analysis.

For analyzing peptides treated with silica gel-TCEP beads (around 10 mM peptide) or peptide cyclized by bis-electrophile reagents, samples of 2 μl were diluted with 18 μl buffer to reach a final buffer concentration of 60 mM NH_4HCO_3 and a DMSO content of 10%. Samples of 3 μl were injected for analysis.

Quantification of functional TCEP of resins

Around 5 mg of immobilized TCEP (dry resin) was added to a well of 96-well PS microtiter plate (Greiner Bio-One, 655061). To the resin, 80 μ l of 150 mM NH_4HCO_3 (pH 8) containing 10% DMSO was added, followed by 20 μ l of 20 mM Ellman's reagent in ammonium bicarbonate buffer (pH 8). An immediate color change from transparent colorless to yellow was observed upon addition if functional TCEP was present. This solution was diluted with ammonium bicarbonate buffer (typically a factor 1 to 12) to reach an absorption value of around 0.5 on a Nanodrop 8000 instrument ($d = 1$ mm, 412 nm, 2 μ l). The concentration of functional TCEP was determined by correlating the absorbance with a calibration curve using the same solvents and procedures and a freshly prepared solution of free TCEP ($A_{412} = 0.1$ -1.0). For quantifying the functional TCEP of commercial agarose-TCEP, lyophilized solid (21.5 mg) from a ~ 1.0 ml of suspension was washed three times with water, filtered on a microscale column filter (Intavis, 35.103) and added about 3 mg to a well of a microtiter plate. The gel was transferred by plastic instead of a metal spatula to avoid risks of TCEP inactivation, as suggested in the product description.

Space occupation of immobilized TCEP

Immobilized TCEP was added to microscale column filters (Intavis, 35.103). In the case of agarose-TCEP (ThermoFisher; 15.3 ± 1.3 $\mu\text{mol/ml}$), 0, 25, 50, 75, 100, 150, 200, and 400 μ l settled beads, corresponding to 0, 0.38, 0.77, 1.1, 1.5, 2.3, 3.1, 6.1 μmol of functional TCEP, were transferred. In the case of dry silica gel-TCEP, 0, 2.7, 5.4, 8.1, 10.8, 16.2, 21.6 or 43.2 mg wet resin, corresponding to 0, 0.4, 0.8, 1.2, 1.6, 2.4, 3.2, 6.4 μmol of functional TCEP (batch loading = 149 ± 19 $\mu\text{mol/g}$), were transferred and wetted with DMSO (200 μ l). The solvent was removed by positive pressure (rubber suction cup) and the different wet beads amounts were placed into the eight tubes containing 40 μ l of DMSO (silica gel-TCEP) or water (agarose-TCEP). The resin was settled by gravity and a picture from the “hanging” samples (Olympus OMD EM-5, Olympus M. Zuiko Premium 60/2.8 ED Macro lens) was taken on a black background.

Preparation of silica gel-TCEP

Silica gel (15.2 g, 230-400 mesh) was transferred into a dry round bottom flask (250 ml) and suspended in toluene (150 ml) followed by the addition of APTES (30 ml, 129 mmol). The suspension was refluxed for 2 h, cooled down, and filtered using reduced pressure. The filter cake was washed with toluene (3 × 30 ml) and DCM (3 × 30 ml) before drying it at air and under reduced pressure overnight (room temperature, 0.15 mbar). Afterward, the functionalized silica beads were grafted by heating for 2 h at 120 °C before cooling down for drying under vacuum (RT, 0.10 mbar). The grafted beads showed purple coloration in the Kaiser test, and the total mass increased by 3.25 g, which corresponds to roughly 2 mmol/g primary amines if fully grafted.

In a 50 ml PP canonical falcon tube (Greiner Bio-One), TCEP*HCl (3.30 g, 11.4 mmol, 2.9 eq.), MES (0.651 g, 3.34 mmol), and NaCl (0.585 g, 10.0 mmol) were dissolved in millipore water (23 ml) and the pH was adjusted from 1.6 to 6.8 using 10 M NaOH solution. The solution was adjusted to the final volume (33 ml) with millipore water. Afterward, EDC*HCl (0.730 g, 3.81 mmol, 0.95 equiv.) was added to the TCEP buffer solution, quickly dissolved the solid by shaking the tube vigorously, and added the amino-functionalized silica beads (2.00 g, 4.00 mmol, 1.0 equiv.) into the solution. The suspension was incubated for 3 h at room temperature under rotation (20 rpm) before filtering in a 20 mL reaction column (CEM, 99.278). The resin was washed with water (3 × 10 ml) and THF (3 × 10 ml). The resin was dried inside the syringe using a nitrogen stream before placing it under reduced pressure overnight (RT, 0.05 mbar) to afford dry immobilized TCEP silica beads.

Several different attempts were undertaken to increase the reducing capacity. The use of a smaller mesh size (625-2500, increased surface area), larger excess of TCEP*HCl over EDC*HCl (3:1) in respect to the maximal theoretical primary amine loading, the addition of hydroxysulfosuccinimide (1.6 equiv.) and variation of the pH (6.5, 7.5, 8.0) did led to a higher reducing capacity. The reducing capacity of all batches of silica gel-TCEP ranged from 107 ± 9.5 to 151 ± 8 $\mu\text{mol/ml}$ wet resin (Supplementary Table 3).

Immobilization of TCEP on diverse supports

NovaPEG-NH₂ (188 mg, 100 μ mol, 0.53 mmol/g, S7256726 833 Novabiochem), ChemMatrix-AM-NH₂ (100 mg, 100 μ mol, 1.0 mmol/g, BCBW3297, Sigma Aldrich), PEGA-NH₂ (238 mg (F = 8.2), 100 μ mol, 0.42 mmol/g, S7786915, Novabiochem), TentaGel S-NH₂ (385 mg, 100 μ mol, BCBX7246, Sigma Aldrich), NovaGel-AM-NH₂ (145 mg, 100 μ mol, 0.69 mmol/g, S529238425, Novabiochem), PS-AM-NH₂ (71.9 mg, 100 μ mol, 1.39 mmol/g, 9952639, apptec), SiO₂-APTES-NH₂ (84 mg, 1.2 mmol/g, 230-400 mesh, 100 μ mol) or high-density AM agarose gel (2.0 ml, 50 μ M/ml suspension, I123R-1005, ABT) were added into pre-weighed disposable 5 ml PP syringes with PE filters (Multisyntech GmbH) followed by the addition of a buffer solution (2.6 ml) containing 0.34 M TCEP·HCl (260 mg, 900 μ mol) in 0.1 M MES and 0.3 M NaCl at an adjusted pH of 6.8. In case of the agarose ABT gel, the storage buffer was filtered off, and the gel was washed with water (3 \times 3 ml). EDC·HCl (58 mg, 300 μ mol) was added to each reaction container and dissolved through shaking. The coupling reaction was performed by incubating the tubes for 3 h at room temperature under rotation (20 rpm) before filtration. Each syringe was washed with water (3 \times 3 ml) and THF (except agarose) prior to drying overnight under a high vacuum (0.08 mbar, room temperature). The net dry weight of each resin inside the syringe was determined to calculate the reductive capability per unit of mass.

Determination of resin swelling factor

The swelling factor was determined with water for Thermo Scientific Pierce agarose gel, G-Biosciences agarose gel, ABT agarose gel, and Tentagel S as well as SiO₂-APTES-NH₂ (230-400 mesh). Between 100 and 500 mg of dried resin or gel was added into a 5 ml PP syringe reactor with PE frit (Multisyntech GmbH). The occupying volume was calculated by the height of the solid inside the column and the syringe's inner diameter. The dried resin was swollen by adding 3 ml of water and one hour of incubation at room temperature. The water was filtered off, and the level of wet swollen resin was

determined. The swelling factor was calculated by dividing the swollen wet resin volume by the initial dry solid volume.

Quantifying disulfide reduction in peptides

Agarose-TCEP gel suspension (ThermoFisher; reducing capacity of 15.3 ± 1.3 $\mu\text{mol/ml}$ wet beads as determined using Ellman's reagent) was pipetted into a microscale column filter (Intavis, 35.103) and washed with millipore water ($3 \times 100\text{-}800$ μl) by applying positive pressure. The added volumes of wet agarose-TCEP gel were 0, 50, 100, 200 and 400 μl , corresponding to 0, 0.8, 1.5, 3.1, and 6.1 μmol and around 0, 2, 4, 8 and 16 equiv. respectively compared to the peptide sample (40 μl , 0.400 μmol , 1 equiv). Wet resin was added to 1 mM of oxidized peptide in 400 μl of solvent composed of 90% aqueous buffer (66 mM NH_4HCO_3 in ddH₂O, pH 8.0) and 10% DMSO (0.4 μmol peptide). The 1.5 ml PP tubes were gently rotated (20 rpm, Stuart rotator). At one and three hours of incubation, 10 μl supernatant (UHPLC-MS samples) were taken and immediately analyzed by LC-MS.

Silica gel-TCEP beads (reducing capacity of 149 ± 19 $\mu\text{mol/g}$ wet beads) were weighed out into a microscale column filter (Intavis, 35.103) and acidified using HCl proportional to the amount of beads. For example, 2.7 mg dry silica gel-TCEP beads were suspended with a solution of 100 μl of 40 mM HCl in 1,4-dioxane. The quantity of beads used were 0, 2.7, 5.5, 11, and 22 mg of dry beads, having 0, 400, 800, 1600, and 3200 nmol functional TCEP. The solvent was removed by positive pressure and washed with DMSO (3×100 μl). The DMSO wet silica resin was transferred to 200 μl PP tubes containing 10 mM of oxidized peptide in 40 μl of DMSO (0.4 μmol peptide). The 1.5 ml PP tubes were gently rotated (20 rpm, Stuart rotator). At one and three hours of incubation, 2 μl supernatant (UHPLC-MS samples) were taken, diluted, and immediately analyzed by LC-MS. It is worth mentioning that the TCEP silica beads have an optimal reduction time (about 3 h). They should not be used for more than about six hours since a start of the slow decrease in peak intensity (LC-MS) was observed from six hours on.

Cyclization of reduced peptide by alkylating agents

Solvents and reagents were added to a 0.3 ml PP microvial (Shimadzu, 980-18425) in the following order. A volume of 14 μl reaction solution containing 71% of NH_4HCO_3 (85.7 mM) and 29% DMSO (pH 8), 4 μl of 20 mM 2,6-bis(bromomethyl)pyridine (BBP) in DMSO (4 equiv.), and 2 μl of 10 mM reduced peptide in DMSO (20 nmol, 1 equiv.). The final concentrations in the reactions were 1 mM peptide, 4 mM BBP, 60 mM NH_4HCO_3 and 50% DMSO. The reaction mixture was well mixed with a pipette and incubated for 3 hours at room temperature. The reaction mixture was analyzed by UHPLC-MS.

Testing disulfide reduction in different solvents

To each test solution inside a 200 μl PCR tube (TreffLab, 96.09852.9.01), acidified immobilized TCEP silica beads (10.1 mg/sample, $\sim 1.6 \mu\text{mol}$, 4 equiv., loading = 158 $\mu\text{mol/g}$) were added and incubated for 3 hours at room temperature under rotation (20 rpm). Samples of 2 μl were diluted with 18 μl aqueous 150 mM NH_4HCO_3 buffer containing 10% DMSO and analyzed by UHPLC-MS.

Storage stability determination of silica gel-TCEP

A single uniform batch of immobilized TCEP on silica (1.0 g, $173 \pm 9.5 \mu\text{mol/g}$ dry resin) was split (15 mg) into 6 \times 7 (42) HPLC glass vials (Schmidlin Labor, LPP 11 09 0500) with septum based screw caps (Brown, 155630) for tight closing. Seven different storage conditions were tested, and for each storage condition, six vials with silica were stored together. The conditions parameters included either room temperature, 4 or -20°C with either nitrogen or air atmosphere. One condition consisted of keeping the beads at vacuum ($< 0.1 \text{ mbar}$) at room temperature. The nitrogen atmosphere was introduced by placing all appropriate samples into a desiccator and the septum caps untightened. By pulling a vacuum and refilling the atmosphere with a nitrogen balloon (3 \times), the air atmosphere in the vials was exchanged by nitrogen. Afterward, the lids were closed quickly and tightly, right after opening the desiccator and before storage. For each time point, one sample vial was taken for analysis. Before the functional immobilized TCEP

was determined, the silica beads were homogenized by gently shaking the vial. The functional TCEP quantification of the beads was realized using Ellman's procedure.

4.7 *Supplementary information*

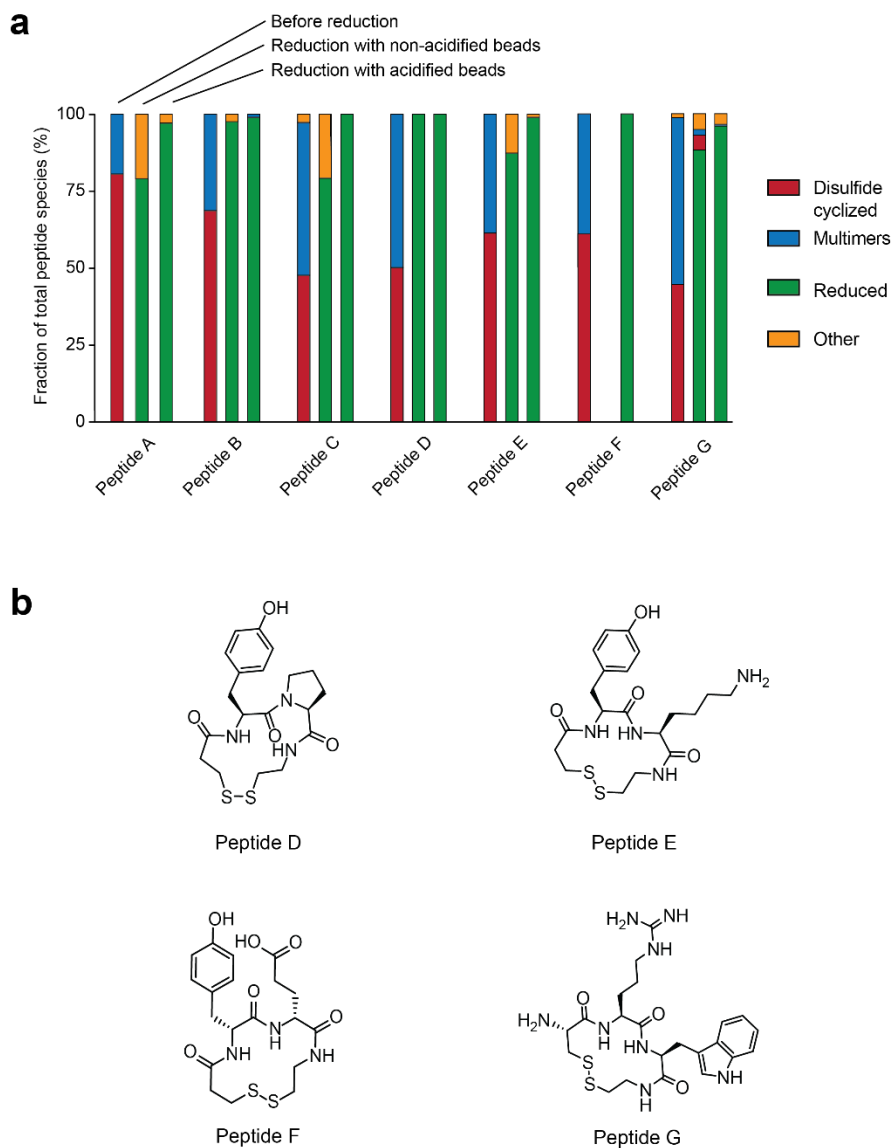
SUPPLEMENTARY TABLE

Supplementary Table 3: Reduction capacity of nine different TCEP-functionalized solid supports. Six of the solid supports are peptide synthesis resins, one is silica gel, and two are based on agarose beads. The capacity is indicated as μmol of functional TCEP per mg dry resin and μmol of functional TCEP per mL wet resin, determined using Ellman's reagent and using free TCEP as a reference. The swelling factors of each different solid support for water is indicated. DMSO swelling factor was determined only for silica gel-TCEP beads and not for the others (N.D.). For agarose-TCEP, the DMSO swelling factor could not be determined due to solubilization (not compatible, n.c.)

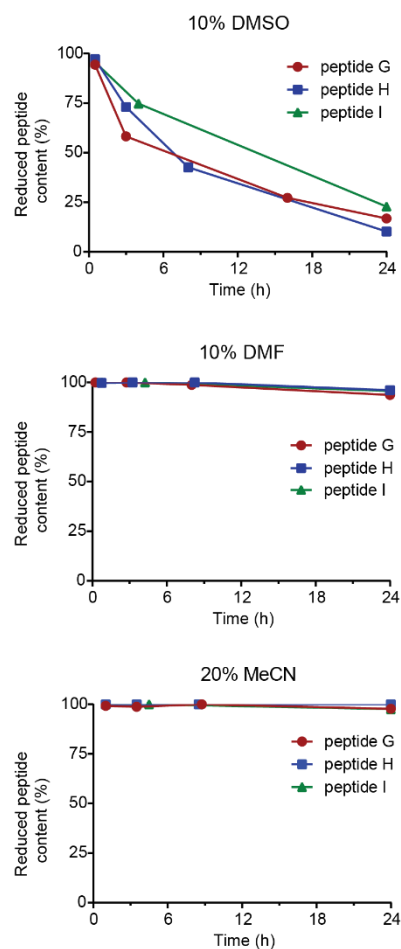
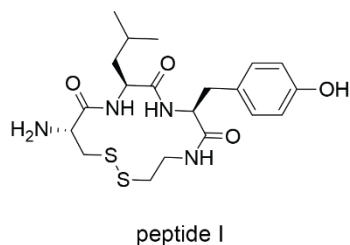
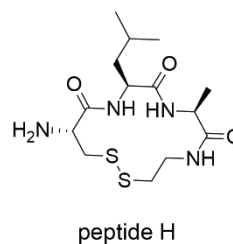
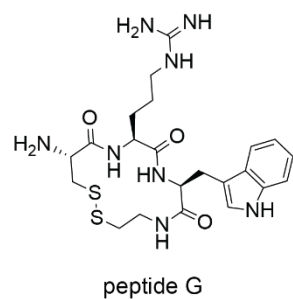
Solid support	Reducing capacity ($\mu\text{mol/g}$ dry resin)	Reducing capacity ($\mu\text{mol/mL}$ wet resin)	Swelling (H_2O)	Swelling (DMSO)
NovaPEG	63 ± 7.2	5.7 ± 0.7	11	N.D.
ChemMatrix	27 ± 1.9	2.5 ± 0.2	11	N.D.
PEGA	62 ± 13	3.9 ± 0.8	16	N.D.
TentaGel S	12 ± 0.4	3.4 ± 0.1	3.6	N.D.
NovaGel	40 ± 2	20 ± 2.5	2	N.D.
PS	0 ± 1	0.4 ± 1.0	1	N.D.
Silica gel (batch 1)	122 ± 11	107 ± 9.5	1.1	1.1
Agarose (Pierce)	230 ± 19	15 ± 1.3	15	n.c.
Agarose (G-Biosciences)	156 ± 56	10 ± 3.7	15	n.c.

Silica gel (batch 2)	134 ± 16	118 ± 14	1.1	1.1
Silica gel (batch 3)	149 ± 19	131 ± 16	1.1	1.1
Silica gel (batch 4)	158 ± 5	139 ± 4	1.1	1.1
Silica gel (batch 5)	173 ± 9	151 ± 8	1.1	1.1

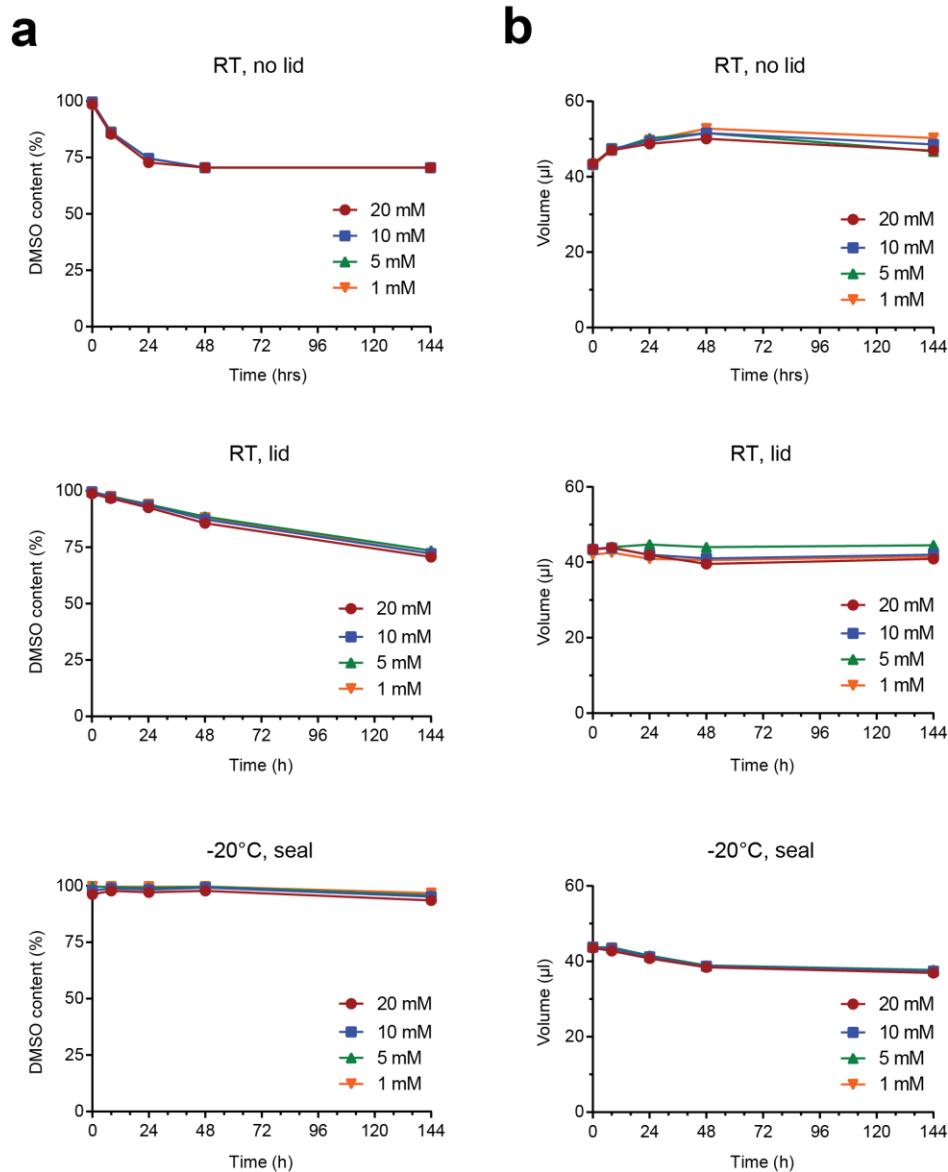
SUPPLEMENTARY FIGURES



Supplementary Figure 1: Acidification of silica gel-TCEP. (a) Disulfide bridges of seven model peptides were reduced using either non-acidified TCEP beads or acidified TCEP beads (40 μ l samples, 10 mM peptide, 4 equiv. TCEP beads, 3 h, RT). The products were analysed by UHPLC-MS and quantified by the peak area at 220 nm. (b) Chemical structures of model peptides (D to G) are shown in main figures and model peptides A to C in Figure 13d.

a**b**

Supplementary Figure 2: Back-oxidation of peptides in different solvents and different pH. (a) Model peptides were incubated in mixtures of water and the indicated organic solvents at pH 2 and monitored over 24 hours. (b) Chemical structures of model peptides applied.



Supplementary Figure 3: DMSO content and sample volumes of model peptides stored at different concentrations in DMSO and at different conditions. During storage at the indicated temperatures in microwell plates covered with the indicated lids, the samples took up water, which was measured over a time period of 7 days using acoustic waves. (a) DMSO content. (b) Sample volume.

4.8 References

- (79) Sangouard, G.; Zorzi, A.; Wu, Y.; Ehret, E.; Schüttel, M.; Kale, S.; Díaz-Perlas, C.; Vesin, J.; Bortoli Chapalay, J.; Turcatti, G.; Heinis, C. Picomole-Scale Synthesis and Screening of Macrocyclic Compound Libraries by Acoustic Liquid Transfer. *Angew. Chem.* **2021**, 133 (40), 21870–21875. <https://doi.org/10.1002/ange.202107815>.
- (80) Kale, S. S.; Bergeron-Brlek, M.; Wu, Y.; Kumar, M. G.; Pham, M. V.; Bortoli, J.; Vesin, J.; Kong, X.-D.; Machado, J. F.; Deyle, K.; Gonschorek, P.; Turcatti, G.; Cendron, L.; Angelini, A.; Heinis, C. Thiol-to-Amine Cyclization Reaction Enables Screening of Large Libraries of Macrocyclic Compounds and the Generation of Sub-Kilodalton Ligands. *Sci. Adv.* **2019**, 5 (8), eaaw2851. <https://doi.org/10.1126/sciadv.aaw2851>.
- (135) Getz, E. B.; Xiao, M.; Chakrabarty, T.; Cooke, R.; Selvin, P. R. A Comparison between the Sulfhydryl Reductants Tris(2-Carboxyethyl)Phosphine and Dithiothreitol for Use in Protein Biochemistry. *Anal. Biochem.* **1999**, 273 (1), 73–80. <https://doi.org/10.1006/abio.1999.4203>.
- (136) Gray, W. R. Disulfide Structures of Highly Bridged Peptides: A New Strategy for Analysis. *Protein Sci.* **1993**, 2 (10), 1732–1748. <https://doi.org/10.1002/pro.5560021017>.
- (137) Burns, J. A.; Butler, J. C.; Moran, J.; Whitesides, G. M. Selective Reduction of Disulfides by Tris(2-Carboxyethyl)Phosphine. *J. Org. Chem.* **1991**, 56 (8), 2648–2650. <https://doi.org/10.1021/jo00008a014>.
- (138) Rüegg, U. Th.; Rudinger, J. [10] Reductive Cleavage of Cystine Disulfides with Tributylphosphine. In *Methods in Enzymology*; Elsevier, 1977; Vol. 47, pp 111–116. [https://doi.org/10.1016/0076-6879\(77\)47012-5](https://doi.org/10.1016/0076-6879(77)47012-5).
- (139) Han, J. C.; Han, G. Y. A Procedure for Quantitative Determination of Tris(2-Carboxyethyl)Phosphine, an Odorless Reducing Agent More Stable and Effective Than Dithiothreitol. *Anal. Biochem.* **1994**, 220 (1), 5–10. <https://doi.org/10.1006/abio.1994.1290>.
- (140) Shafer, D. E.; Inman, J. K.; Lees, A. Reaction of Tris(2-Carboxyethyl)Phosphine (TCEP) with Maleimide and α -Haloacyl Groups: Anomalous Elution of TCEP by Gel Filtration. *Anal. Biochem.* **2000**, 282 (1), 161–164. <https://doi.org/10.1006/abio.2000.4609>.

- (141) Miralles, G.; Verdié, P.; Puget, K.; Maurras, A.; Martinez, J.; Subra, G. Microwave-Mediated Reduction of Disulfide Bridges with Supported (Tris(2-Carboxyethyl)Phosphine) as Resin-Bound Reducing Agent. *ACS Comb. Sci.* **2013**, *15* (4), 169–173. <https://doi.org/10.1021/co300104k>.
- (142) Kirley, T. L.; Greis, K. D.; Norman, A. B. Selective Disulfide Reduction for Labeling and Enhancement of Fab Antibody Fragments. *Biochem. Biophys. Res. Commun.* **2016**, *480* (4), 752–757. <https://doi.org/10.1016/j.bbrc.2016.10.128>.
- (143) Zwysig, A.; Schneider, E. M.; Zeltner, M.; Rebmann, B.; Zlateski, V.; Grass, R. N.; Stark, W. J. Protein Reduction and Dialysis-Free Work-Up through Phosphines Immobilized on a Magnetic Support: TCEP-Functionalized Carbon-Coated Cobalt Nanoparticles. *Chem. - Eur. J.* **2017**, *23* (36), 8585–8589. <https://doi.org/10.1002/chem.201701162>.
- (144) Alzahrani, E.; Welham, K. Fabrication of a TCEP-Immobilised Monolithic Silica Microchip for Reduction of Disulphide Bonds in Proteins. *Anal Methods* **2014**, *6* (2), 558–568. <https://doi.org/10.1039/C3AY41442F>.

5. Solid-phase peptide synthesis in 384-well plates

5.1 *Work contribution*

Solid-phase peptide synthesis in 384-well plates

Mischa Schüttel,^{1,2} Edward Jeffrey Will,^{1,2} Gontran Sangouard,¹ Anne Sofie Luise Zarda,¹ Sevan Habeshian¹, Alexander Lund Nielsen and Christian Heinis^{1,*}

¹Institute of Chemical Sciences and Engineering, School of Basic Sciences, École Polytechnique Fédérale de Lausanne (EPFL), CH-1015 Lausanne, Switzerland.

²Authors contributed equally

KEYWORDS

384-well plate, combinatorial chemistry, peptide library, peptide synthesis, SPPS

Author contribution: I, Edward Will (E.J.W.) and Gontran Sangouard (G.S.) conceptualized the idea to realize 384-well plate SPPS synthesis. Initial plate evaluation experiments were conducted by me, E.J.W. and G.S.. Iterative design drafting (paper & electronic) of the critical pieces (solid dispensers, size tester, prototypes of 16-channel manifold, reagent rack, adapters) and managing the communication between mechanical workshop was realized by me. Various prototype testing, experimental designs, performing multiple 96 and 384-well plate syntheses and post-synthesis processing as well as analysis were performed by me (60%) and E.J.W. (40%). The mechanical workshop adapted the designs so that they were compatible with their CNC machines for manufacturing. The workshop incorporated important design changes in the second prototype version of the 16-channel manifold. Edward Will adapted the software to make it compatible with 384-well plate synthesis and developed, along with me, the critical calibration procedure. E.J.W. maintained and implemented the upgrade into our daily laboratory synthesis routine. Sevan Habeshian proposed the idea of using deep well plates as a derivative reservoir. Anne Sofie Luise Zarda wrote the python script for

randomizing peptides used in the proof-of-concept synthesis. Alexander Lund Nielsen optimized the resin preparation procedure and provided critical feedback to the manuscript. The manuscript (text and figures) was drafted and edited by me and Christian Heinis. E.J.W. provided the text for the calibration procedure and one figure (supplementary Figure 10).

Acknowledgment: We are grateful to Guillaume Francey, Florian Pattiny and André Fattet from the mechanical workshop of the Institute of Chemical Sciences and Engineering for helping with producing the synthesizer hardware components.

This chapter is based on a manuscript prepared for publication and the project was supported by the Swiss National Science Foundation (grant: 192368).

5.2 *Abstract*

Recently developed solid-phase peptide synthesis and release strategies allow production of short peptides with higher than 90% purity that do not require chromatographic purification, enabling direct screening for desired bioactivities. However, the maximal number of peptides that can currently be synthesized per microtiter plate reactor is 96, allowing the parallel synthesis of 384 peptides in the most performant instrument that has space for four microwell plate reactors. To synthesize larger numbers of peptides per run, we reconstructed a commercial peptide synthesizer to enable production of peptides in 384-well plates (4 × 384 peptides), which allowed synthesizing 1,536 peptides in one go. We report and describe the new hardware components that we developed and software that was adapted and present the synthesis of 1,536 short peptides that were obtained in high concentration ($\sim 18 \pm 3$ mM) and purity ($\sim 82 \pm 6\%$) without the need of purification. The high-throughput peptide synthesis that we established with peptide drug development applications in mind may be broadly applied for large-scale peptide library synthesis and screening, antibody epitope scanning, epitope mimetic development, or protease/kinase substrate screening.

5.3 Introduction

Peptides offer an attractive modality for drug development due to their advantageous properties, such as the ability to engage with challenging targets, high target specificity, low inherent toxicity and ease of development by automated synthesis. Today, more than 80 peptides are used as therapeutics, nearly all derived from naturally occurring bioactive peptides, and many are in pre-clinical and clinical development, including several that were developed *de novo* by screening random libraries of peptides by phage display or mRNA display.¹⁴⁵ The development of peptide therapeutics has been enabled and steadily facilitated by powerful techniques and methods introduced over several decades, including solid-phase peptide synthesis (SPPS),⁸⁷ automation of synthesis,⁸⁸ Fmoc chemistry,⁸⁹ reversed-phase HPLC purification, and most recently the development of techniques for the *in vitro* evolution of peptide ligands such as phage display¹⁴⁶ and mRNA display.¹⁴⁷ Over the years, the development of peptides was much facilitated also by steadily lowered prices for amino acid building blocks and other reagents and the growing number of commercially available reagents such as hundreds of affordable unnatural Fmoc amino acids.

With the long-term goal of developing membrane-permeable or even orally available peptide-based therapeutics, our laboratory is taking advantage of many of the above mentioned techniques to synthesize and screen large combinatorial libraries. We are using SPPS for producing large libraries of short peptides that are subsequently cyclized and screened in microwell plates. For omitting a throughput-limiting purification step, we have developed methods that allow both, deprotecting side chains of peptides on solid phase (so that they can be washed away from the still bound peptides) and selectively releasing the peptides with reagents that do not interfere with subsequent bioassays. With these methods, we obtained large numbers of peptides at purities approaching or exceeding 90%.^{91, 106} We further developed methods for combinatorially diversifying short peptides in combinatorial reactions, for example by acylating 196 short cyclic peptides at a peripheral amino group with 100 diverse carboxylic acids, yielding a library of nearly 20,000 cyclic peptide compounds.⁸¹ Screening these libraries in functional assays in 384- and 1,536-well plates led to the identification of nanomolar binders to a range of targets, including thrombin, KLK5 and MDM2.^{80, 81} For synthesizing hundreds of peptides, we

performed peptide synthesis in a 96-well format using four 96-well plate reactors in the MultiPep 2 from CEM/Intavis (384 peptides in one run). Other parallel peptide synthesizers that can synthesize similar numbers of peptides in one go are the Syro I (4 × 96 peptides) and Syro II (6 × 96 peptides) from Biotage, and the Vantage (96 peptides) and Apex 396 (4 × 96 peptides) from aapptec. Solid-phase peptide synthesis in 384-well format was so far only reported by Maric and co-workers who had synthesized peptides on laser-cut membrane discs placed into a 384 CelluSpots frame using a MultiPep 2 synthesizer (CEM/Intavis).^{148, 149} Synthesis with this method yielded around 30 nmol peptide per well, which was sufficient for their protein-protein interaction (low μ M) activity screening.¹⁴⁸ In case the peptides need to be cyclized⁸⁰ or diversified in a combinatorial fashion by chemical modification of lateral groups,⁹¹ the quantity of peptide synthesized on membrane disks would likely be too small, especially for repetitive usage of peptide and library stock solution.

A range of techniques were developed that allow the synthesis of peptides in more dense arrays on membranes, wherein the peptides are not released but applied in their membrane-bound form for binding assays similar to immunoblots.¹⁵⁰ Mostly applied is SPOT synthesis, where peptides and synthesis reagents are applied in droplets to individual spots on a nitrocellulose membrane, and excess is removed by filtration.^{151,152} For example, the MultiPep 2 synthesizer together with a 384 CelluSpots frame (CEM/Intavis) can produce up to 1536 peptides that are synthesized in spots of approximately 2–3 mm on four membranes (100 × 150 mm each). Sophisticated techniques were developed to synthesize peptide arrays at higher density, for example, based on noncontact inkjet printers that eject pico- to nanoliter volumes of liquid onto a solid support in a predefined pattern¹⁵³ and photolithography that uses light to activate selective regions of the solid support for coupling reactions, usually by removing a photoactive protecting group to allow further synthesis.¹⁵⁴ Release of peptides from membranes to obtain soluble peptide libraries was reported, as for example, for developing antibacterial peptides,¹⁵⁵ but it is challenging due to the technical hurdles in releasing and transferring peptides from dense arrays to microwell plates, and the much smaller quantities of peptide synthesized on membranes (e.g. ~ 100 nmol per 7 mm diameter disc) compared to solid-phase resins (e.g. 2 μ mol per well in a 96-well plate).

Herein, we aim to synthesize peptides in 384-well plates using conventional polystyrene resin as solid phase support that promises high peptide yields. To date, no peptide synthesis on resin in 384 well plates was reported and suitable instrumentation is not available. Towards the SPPS in 384-well reactors, we developed hardware parts and adapt software to convert a standard 96-well plate parallel peptide synthesizer into a device that can synthesize peptides in 4×384 -well plates and thus 1,536 peptides at once.

5.4 ***Results & discussion***

Installation of 384-well synthesis plates

A wide range of 384-well filter plates are commercially offered, mainly for protein and DNA filtration applications, but also for DNA solid-phase synthesis. For peptide synthesis, we chose a plate type that is fabricated with polypropylene (PP) as material and contains a polyethylene (PE) membrane, both materials compatible with the required solvents and reagents, has membrane pores suited for DMF retention, and holds volumes of around 100 μ l per well, that we considered suited for up to 3 mg of polystyrene (PS) resin per well, and thus allowing synthesis of peptides at a scale of around 3 μ mol. Of four plates evaluated, we found a 384 PP filter plate with a 25 μ m pore PE frit most suited (PN 201035-100 with PE 25 UM; Agilent). The 384-well plates could not directly be mounted to our CEM/Intavis MultiPep 2 peptide synthesizer using the standard reactor holder of the MultiPep 2 synthesizer (Figure 17a) because they have a height of only 14 mm, which is 17 mm less compared to the 96-well synthesis plates that we used (OF1100, Orochem). In order to compensate for the height difference, we designed and produced adapter frames so that the top of the 384-microwell plates reached the same height as the 96-well ones (Figure 17b). We produced the adapter frames using the chemical-resistant material polytetrafluoroethylene (PTFE) (Supplementary Figure 4). For mounting the plates to the holders, we used stainless screws with shorter heads compared to the standard screws with black plastic heads, to avoid clashes between the screw heads and the mobile dispensing manifold that we aimed to have as close as possible to the wells of the 384-well plates.

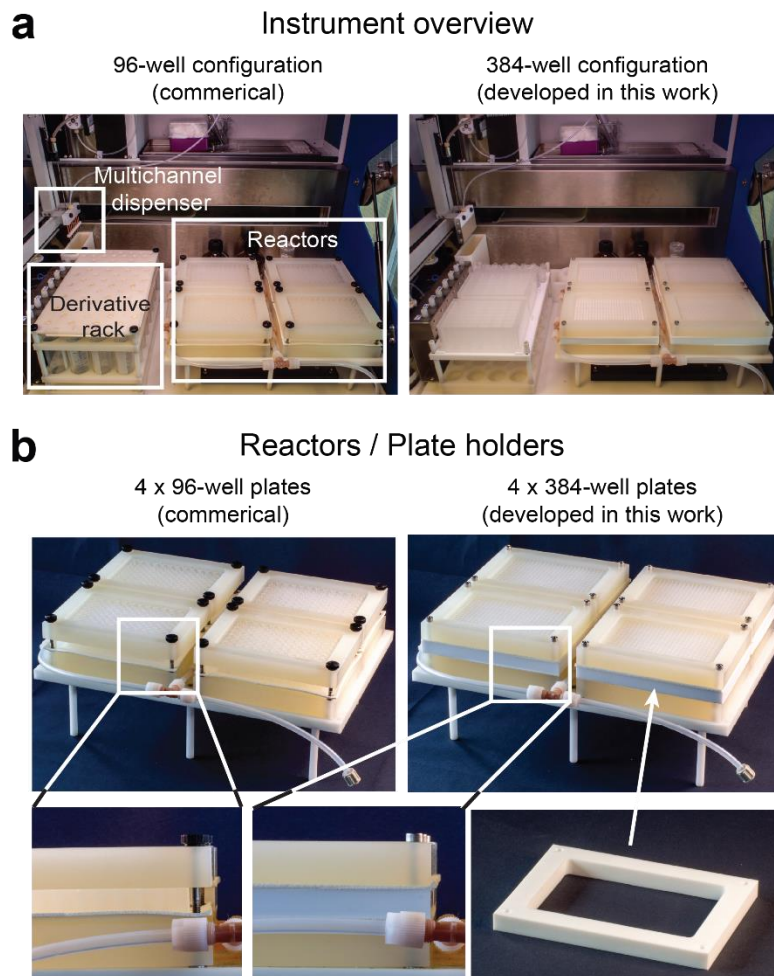


Figure 17: Peptide synthesizer working space overview and microwell plate reactors. (a) Synthesizer working space. Left: Commercial peptide synthesizer MultiPep 2 from CEM/Intavis for peptide synthesis in 4 × 96-well plates. Right: Modified instrument for the synthesis in 4 × 384-well plates. (b) Comparison of synthesis reactors. Left: Commercial plate holders for 96-well plates. Right: modified plate holders for 384-well plates. An adapter frame (lower right corner) was fabricated to compensate for the smaller height of 384-well synthesis plates. Screws with smaller heads (silver) were used to allow a smaller distance between dispensing devices and reactor plate surface.

Dispensing manifold with 16 channels

The CEM/Intavis MultiPep 2 peptide synthesizer offers a 16-channel manifold for SPOT peptide synthesis. However, the outlets of this manifold are too distant from the installed 384-well plates (18 mm), risking the splashing of reagents to neighboring wells. Instead of using the commercial manifold, we designed and produced a new manifold that has 16 channels and releases solvents closer to the 384-well plate surface (11 mm; Figure 18a). The more precise dispensing allowed to use of the manifold also for dispensing

piperidine, a process that needs much precision due to the potential contamination of neighboring wells. Using the multichannel manifold instead of a single-channel needle for piperidine dispensing allowed reducing the time needed for Fmoc deprotection by around 16-fold, which was important to achieve similar reaction times in the first and last well of the 384-well plates, and shortened the total time needed for peptide synthesis. We built the 16-channel manifold using PTFE and polyether ether ketone (PEEK) material as housing and 16 non-sharp (cut) disposable needles (0.8 mm × 40 mm) made of stainless steel (Supplementary Figure 5). The robotic arm mounting specifications were kept the same as for the commercial 8-channel manifold. Optimal dispensing was achieved at a flow rate of 45 ml/min.

Reagent racks

The commercial peptide synthesizer has a reagent rack for 24 × 50-ml tubes and seven 11-ml tubes (and the same number of pre-activation tubes), which allows the use of 31 different amino acids at maximum. In order to offer space for more different building blocks needed for the generation of structurally and chemically highly diverse combinatorial peptide libraries, we constructed a reagent rack that has space for four 50-ml tubes, seven 11-ml tubes (and the same number of 6 ml pre-activation tubes), and a holder for two polypropylene (PP) microwell plates (Figure 18b). In the position of the holders, suitable deep-well plates can be positioned that contain 48 4-ml wells, 96 2-ml wells, or 384 0.3-ml wells (Supplementary Figure 6). One of the two plates is used as a reagent holder, and one for amino acid pre-activation. We produced the new reagent rack using parts of the CEM/Intavis rack and a top plate that we manufactured using the chemical-resistant material PTFE (Supplementary Figure 7).

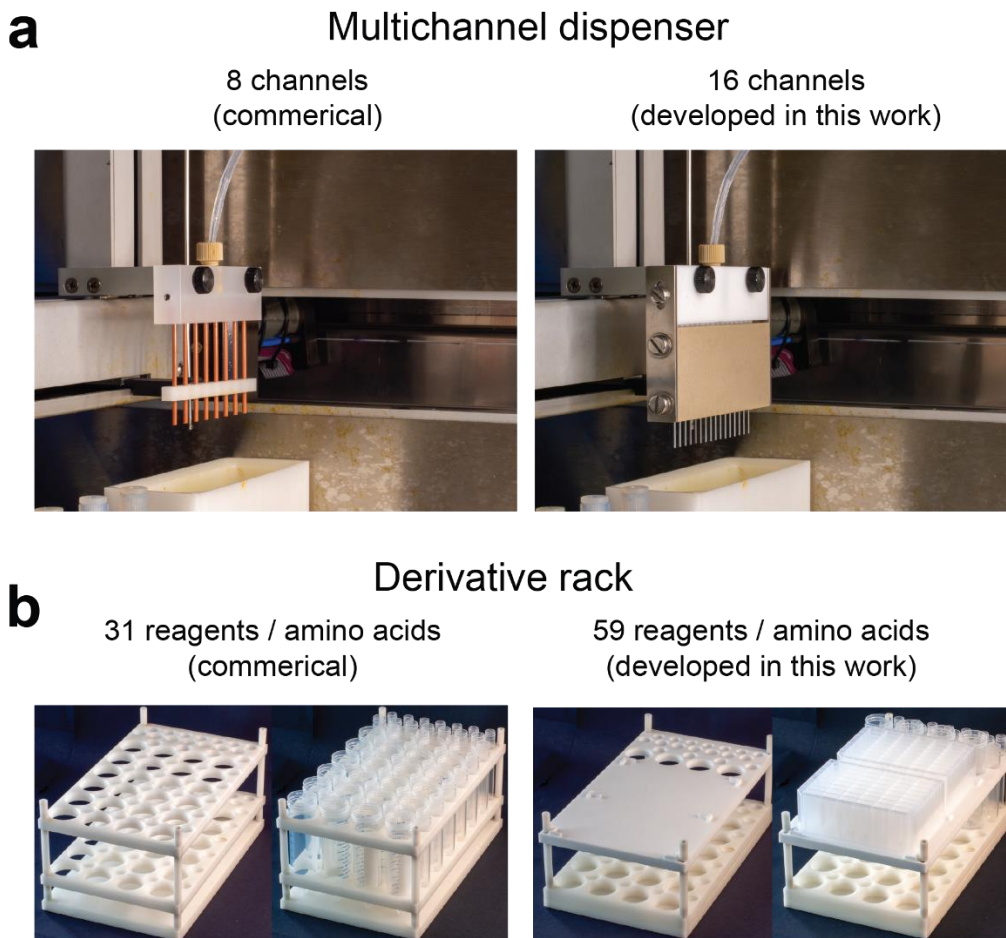


Figure 18: Multichannel dispenser and derivative rack. (a) Comparison of multichannel dispensers. Left: Commercial 8-channel dispenser. Right: Custom-made 16-channel dispenser. (b) Comparison of derivative racks. Left: Commercial rack for 24 large volumes (50 ml reagent tubes and 11 ml pre-activation tubes) and 7 medium volumes (11 ml reagent tubes and 6 ml pre-activation tubes). Right: Newly built reagent rack for 48 small volumes (4 ml volumes in 48-deep well plates), 4 large volumes (50 ml reagent tubes and 11 ml pre-activation tubes), and 7 medium volumes (11 ml reagent tubes and 6 ml pre-activation tubes). Alternatively, 96-deep well plates can be used that hold 2 ml per well.

Software adjustments

The coordinates of the 384-well reactor plates and the new reagent rack were defined in the MultiPep 2 peptide-synthesis control software version 4.4.17 (Supplementary Configuration File 1). Before starting a synthesis, the positions of the reactor plates and the reagent rack are calibrated (see instrument calibration procedure further below).

Peptide synthesis in 384-well plates

We tested the new peptide synthesizer configuration by synthesizing 384 short peptides in a 384-well plate reactor. In order to directly test the synthesis of 1,536 peptides in one run, we synthesized the 384 peptides four times, each time in one of four 384-well reactors that were mounted to the modified CEM/Intavis MultiPep 2 synthesizer (Supplementary Table 4). For comparison, we synthesized the same 384 peptides in four 96-well plates using the original peptide synthesizer configuration (Supplementary Table 5). As model peptides, we chose short random sequences that all contain at the N-terminus a mercaptopropionic acid (Mpa) and at the C-terminus a mercaptoethylamine (Mea) group. These terminal thiol-containing groups can efficiently be cyclized by bis-electrophilic reagents for accessing large libraries of macrocyclic compounds (Figure 19a). In each of the four 384-well reactors, we synthesized 96 random peptide sequences that contain two random canonical amino acids (four building blocks in total) and 288 random peptides that contain three canonical amino acids (five building blocks in total). All peptides were synthesized on a PS resin carrying a disulfide-linker Mea group (Mea-SS-PS; Figure 19b) and synthesized as described before.¹⁰⁶ In contrast to our previous work in which we used PS A SH resin (Rapp Polymere), we prepared thiol-functionalized resin by coupling S-trityl-3-mercaptopropionic acid (Trt-MPA) aminomethyl PS resin (100-130 mesh; Aapptec). The new resin had the advantage that it could be loaded more easily into the 384-well synthesis plates with a procedure described in the following.

In order to efficiently transfer equal amounts of Mea-SS-PS resin to wells of 384-well plates, we developed resin dispenser devices that are based on PTFE plate having small conical holes with volumes corresponding to the desired amount of resin, arrayed exactly as the wells of a 384-well plate (Figure 19c). The resin was placed onto the device, distributed by spreading with a blank PTFE plate to fill the arrayed holes and to remove the excess of resin. Next, the reactor plate was placed upside-down on top, and the sandwich was turned to transfer the resin to the reactor wells by centrifugation as illustrated in the video (supplementary video file). The optimal amount of resin was assessed using a "size-tester" resin dispenser having holes of different sizes (Figure 19c, left and 19d right). For the 384-well synthesis, we used resin for a 3 μ mol-scale synthesis (around 3 mg resin per well), and for the 96-well reference synthesis, we used resin for a 5 μ mol scale synthesis (5 mg resin per well). For all transfers of resin with resin dispenser

devices, the dry resin was first swollen in DMF, the DMF filtered away, and the resin used in wet form. We produced the resin dispenser devices using the PTFE as material (Supplementary Figure 8).

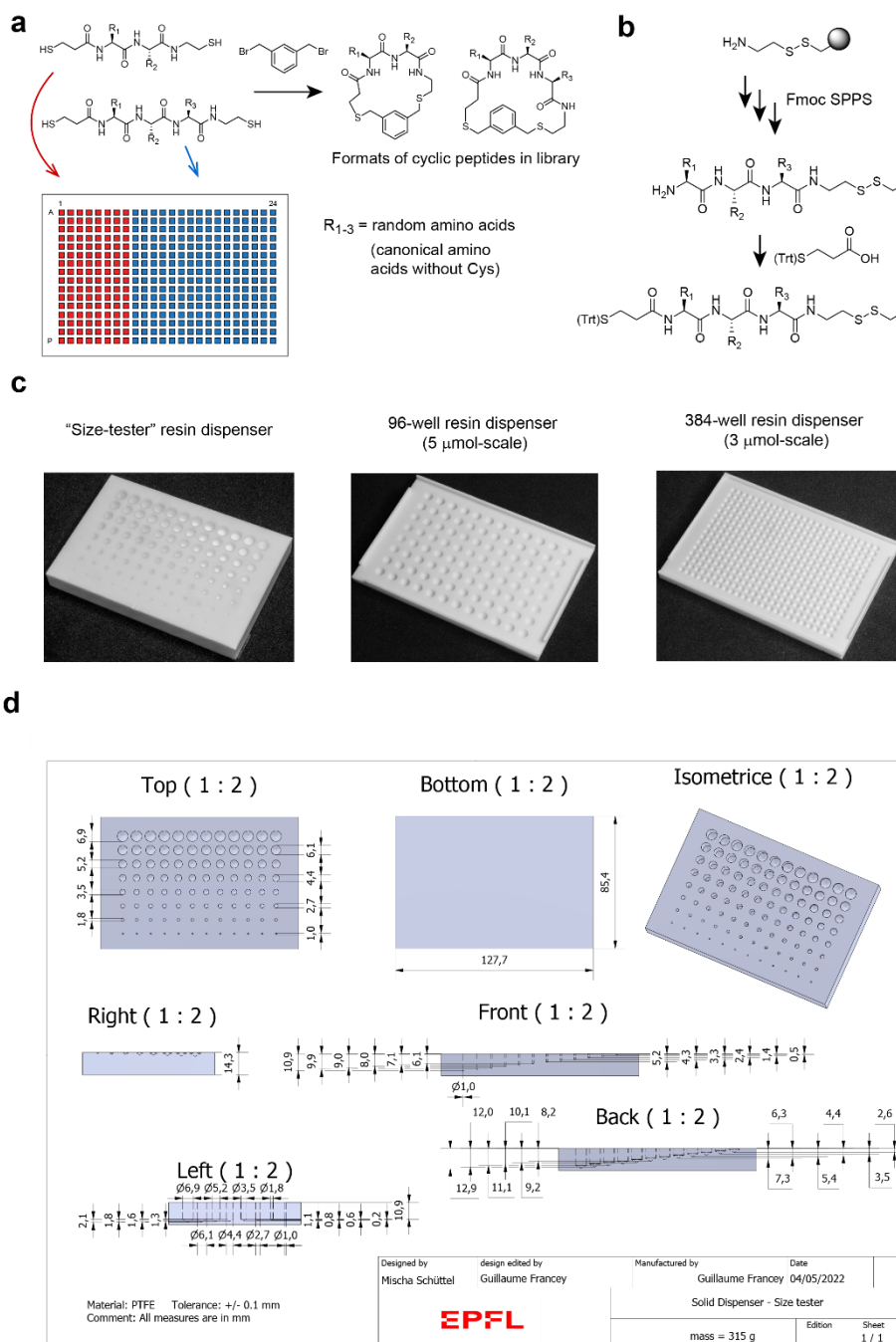


Figure 19: Synthesis of 1,536 peptides in four 384-well plate reactors. (a) Design of peptides. All peptides contain two or three random canonical amino acids (excluding cysteine) and thiol groups at both ends that allow efficient cyclization by bis-electrophilic reagents such as the indicated 1,3-bis(bromomethyl)benzene. The layout of the 384-well

reactor plate is shown. (b) Strategy for the solid phase synthesis of dithiol peptides. The peptides are synthesized via a disulfide linker which allows on-resin amino acid sidechain deprotection and peptide release by reduction. (c) Self-made resin dispenser used for loading of resin into 96 and 384-well synthesis plates. (d) Technical drawing of size-tester.

For the synthesis in the 384-well reactor format, pre-activated Fmoc amino acids were applied in volumes of 61 μl (205 mM final concentration, 5-fold molar excess) and coupled twice (45 min each time). The resin was washed with 70 μl volumes of DMF dispensed through the 16-channel manifold. Fmoc deprotection was performed twice, each time adding 35 μl volumes of piperidine in DMF (1/4, v/v) dispensed also through the 16-channel manifold. For removing on-resin the side chain protecting groups, we removed the 384-well plates from the synthesizer, closed the pointy outlet tips by pressing the plates onto a soft ethylene vinyl acetate (EVA) pad, added twice 52 μl TFA solution to each well for one hour. The wells were then washed three times with 52 μl DCM, allowed to dry at room temperature overnight, and the peptides released by disulfide cleavage, adding twice 30 μl DMSO containing 1,4-butanedithiol (BDT; 400 mM) and triethylamine (TEA, 400 mM) to each well for one hour. DMSO, BDT and TEA were removed by rotational vacuum evaporation. Prior to this evaporation, the solutions were acidified with aqueous TFA (6.5 M, 7.4 μl /well; 2.0 equivalent relative to TEA) to avoid dimer formation. In addition to this, the plate was protected beforehand by applying pierced aluminum seals (homemade puncher, Supplementary Figure 11 and 12) to prevent cross-contamination during the evaporation process. The oily or solid residues after evaporation was dissolved in DMSO (30 μl /well) to form the desired peptide stock solutions of around 10 mM.

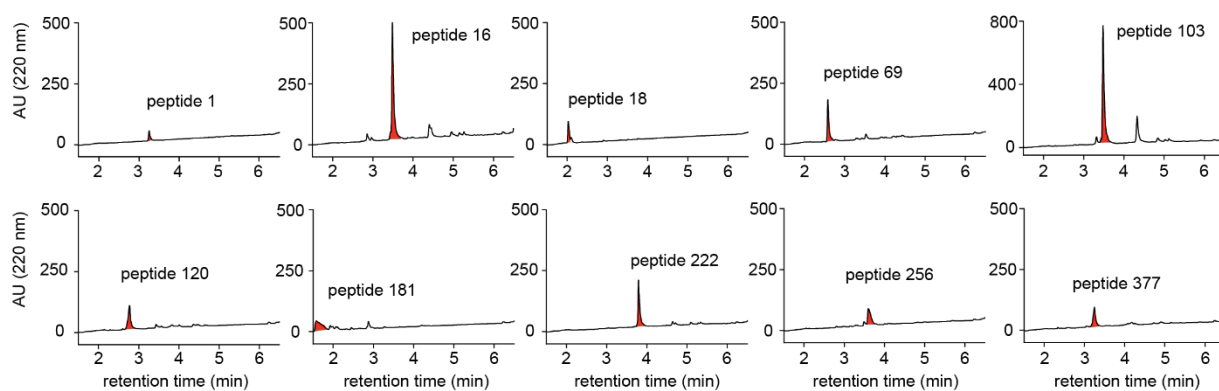
Purity and yield of peptides synthesized in 384-well plates

Analysis of ten randomly picked peptides by LC-MS showed that all peptides were correctly synthesized and that they had a good purity ($82 \pm 6.1\%$) (Figure 20a). Analysis of the same 10 peptide sequences synthesized in the other three 384-well plates (a total of 30 peptides) showed comparable purities (Supplementary Table 6). The main impurities (0 to 17%, average: 6%) were the corresponding *t*Bu capped peptides. Analysis of the peptides synthesized in the 96-well plates as a reference showed a purity in the same range ($87 \pm 5.9\%$) (Supplementary Figure 9a and Supplementary Table 7) with *t*Bu capping impurities ranging from 0 to 16% (average: 5%). We quantified the peptide

concentrations and yields using Ellman's reagent and measured absorbance. Peptides synthesized in the 384-well plates had concentrations of 18 ± 8.4 mM (30 μ l elution volume, 3 μ mol scale, 18% yield (Figure 20b), which was comparable to the concentrations obtained for the 96-well plate synthesis, which was 20 ± 4.6 mM (50 μ l elution volume, 5 μ mol scale, 96-well plate, 20% yield) (Supplementary Figure 9b, Supplementary Table 3). A comparison of the time required for the entire liquid handling of the synthesis process showed that 3.3 times less time is required per peptide if produced

in the 384-well format without considering synthesizer preparation time (Supplementary Figure 10).

a



b

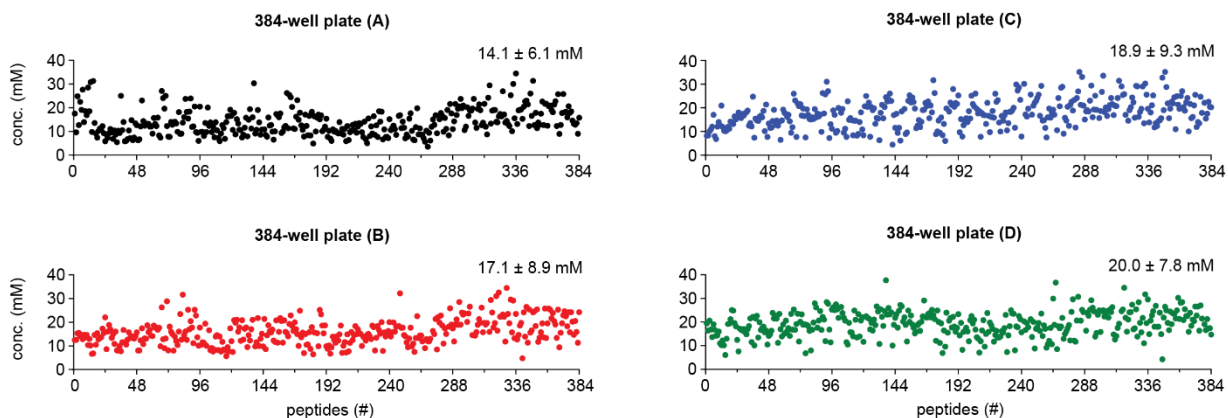


Figure 20: Quantity and purity of peptides. (a) HPLC chromatograms of 10 randomly picked peptides. (b) Concentrations of peptides quantified by reacting the thiol groups of the peptide with Ellman's reagent and measuring absorbance.

Table 3: Comparison of yield and purity of peptide synthesized in 96- and 384-well reactor plates, respectively.

The purity was determined by HPLC analysis measuring absorbance at 220 nm. Two of the 10 peptides synthesized in 96-well plates showed a small absorbance and were not included for quantifying the purity. The concentration was quantified by reacting the thiol groups of the peptide with Ellman's reagent and measuring the absorbance.

Reactor plate	Scale ($\mu\text{mol}/\text{well}$)	Number of peptides synthesized	Number of peptides analyzed	Average purity (%)	Concentration (mM)	Elution volume (μl)
4 x 96-well plate	5	384	10	87 ± 5.9	20 ± 4.6	50
4 x 384-well plate	3	1,536	10	82 ± 6.1	18 ± 8.4	30

5.5 Conclusion

In summary, we have successfully implemented and tested a 384-well plate SPPS upgrade for the commonly used CEM/Intavis MultiPep 2 synthesizer, which usually performs its synthesis in 96-well plates. Now, we can synthesize 4×384 peptides in one run, in not much more time than needed for the synthesis of 4×96 peptides in a commercially offered synthesizer. The achieved quality and quantity allow us to implement this upgrade in our daily SPPS routine for our combinatorial libraries, hopefully increasing our hit rates against challenging targets. Along the way, practical tools (resin dispenser, piercer) were developed to significantly facilitate our laboratory work to a meaningful throughput by maintaining peptide quality. We think this work might be helpful for other fields, such as antibody epitope scanning, epitope mimetic development, peptide ligand development, and peptide-substrate screening.

5.6 **Material & methods**

Design and fabrication of adapter frame and installation of 384-well synthesis plate

Adapter frames were designed with the computer-aided design (CAD) software Autodesk Inventor Professional 2023. The frames with the dimensions shown in Supplementary Figure 4 were produced by chip removal and utilization of a computerized numerical controlled milling machine and PTFE as material (8000943348, APSOparts). The 384-well plates (PN 201035-100 with PE 25 UM; Agilent) were installed by placing the following hardware parts to one of the four reactor positions of the CEM/Intavis MultiPep 2: 1) standard bottom plate (from 96-well reactor setting), 2) silicon pad (32.402, CEM), 3) newly produced adapter frame, 4) silicon pad (32.402, CEM), 5) PTFE foam pad (32.406, CEM), 6) 384-well synthesis plate, 7) standard top plate (from 96-well reactor setting). The components of the pile were mounted by four non-standard screws with the following dimensions: $l = 40$ mm, $d = 3.9$ mm (M4), socket cap screw head: $h = 4.0$ mm, $d = 7.8$ mm).

Design, fabrication, and installation of a 16-channel dispenser

The 16-channel dispenser was designed with the CAD software and produced by chip removal using a computerized numerical controlled (CNC) milling machine and PTFE (piece a, supplementary figure 5), stainless steel (pieces b and c, supplementary figure 5), and PEEK (piece d, supplementary figure 5) as materials (0253000103, APSOparts), respectively. In addition, 16 needles (0.8 mm \times 40 mm) made of stainless steel were prepared. The parts were assembled by inserting the needles into the holes of piece a (depth: middle of 7 mm) and mounting the other parts with four larger ($l = 7.3$ mm, $d = 3.9$ mm (M4), head $h = 2.5$ mm, $d = 6.9$ mm) and two smaller ($l = 7.3$ mm, $d = 2.9$ mm (M3), head $h = 2.3$ mm, $d = 6.0$ mm) stainless button head screws. For all six screws, stainless washers were used (four larger: $d1 = 9.0$ mm, $d2 = 4.2$ mm, $w = 0.75$ mm; two smaller: $d1 = 6.7$ mm, $d2 = 3.2$ mm, $w = 0.5$ mm). Each needle is sealed and fixed through the mechanical force upon assembly by the underlying channel support. The robotic arm mounting specifications were kept the same as for the commercial 8-channel manifold. Optimal dispensing was achieved at a flow rate of 45 ml/min.

Design, fabrication, and installation of reagent rack

The top plate of the reagent rack was designed with CAD software and produced by chip removal and utilization of a computerized numerical controlled milling machine and PTFE as material. The top plate was assembled outside the peptide synthesizer with parts of the standard reagent rack of the CEM/Intavis MultiPep 2 by assembling the following parts from bottom to top: 1) new socket head cap screws ($l = 30$ mm, $d = 3.9$ mm (M4), head: $h = 4.8$ mm, $d = 7.8$ mm), 2) standard bottom plate with openings oriented to the back (from CEM/Intavis MultiPep 2), 3) standard middle plate (from CEM/Intavis MultiPep 2), 4) 5.5 cm standard long spacers (from CEM/Intavis MultiPep 2) with standard grub screws ($d = 3.9$ mm (M4), $l = 20$ mm), 5) new top plate, and 6) 2 cm standard small spacers (from CEM/Intavis MultiPep 2). The following tubes can be added to the derivative rack: 4×50 ml canonical flat bottom PP tubes (210261, greiner bio-one), 11×11 ml round bottom PP tubes (60610, Sarstedt), 7×6 ml round bottom PP tubes (38.035, CEM/Intavis), and two of either 48-well (43001-0062, Ritter), 96-well (260252, Thermo Scientific,) or 384-well (CLS3342, Corning) PP deep well plates. Optionally, the derivative solutions were covered with pre-pierced adhesive aluminum lid (Silverseal 676090, greiner bio-one).

Design of resin loader

The motivation to design a new type of resin loader was to overcome the limited density to the 96-well format of resin loaders. We would need at least 384-well plate format. Commercial providers of 96-well resin loaders are Biotage (Z125HZ096), LabTie by Molgen (TitanTM resin loader) and Interchim/radleys (96-well Powder Dispenser). Additionally, we noticed that resin is often heterogenous but dry loading often requires a high quality of homogeneity of beads. Furthermore, we noticed that wet resin allowed a more rapid and non-invasive loading of resin. Therefore, we thought that Teflon (PTFE) might be very suitable as a device material since it has very desirable properties (hydrophobic) to spread wet resin (e.g. polystyrene resin) but also high chemical compatibility to many types of solvents. A compact device shape with limited weight was also important so that wet resin can be transferred inside a centrifuge (plate rotor/buckets) using centrifugal force. Centrifugation instrumentations are commonly available and accessible in many laboratories. The basic rectangle dimensions of the resin loader are

based on the dimensions of the utilized synthesis plates. The volume of the hole corresponds to the volume of DMF-swollen and filtered resin (aminomethly-PS; aapptec) for the desired synthesis scale per well for automated high throughput SPPS. The position of the holes were chosen so that the resin fell into the wells of the 384-well reactor plate. On all four sites of the loader, edges were added to facilitate aligning of the loader holes to the wells of the reactor plate and to stabilize movements in x and y-axis direction. The edges were designed to contain small gaps allowing facile removal of excess of wet resin during the resin spreading process using a blank PTFE remnant piece.

Definition of new hardware parts in software

The newly designed and produced hardware requires adaptations in the software (configuration file, *.MPC) to allow synthesis in the 384-well plates. The MultiPep software (version 4.4.17) allows custom modification of the reagent rack and reactors. The user manual of the CEM/Intavis MultiPep synthesizer describes how to create and define customized zones for the reagent rack and the reactors to establish customized configuration files. We provide configuration files for the set-ups used in this work as supplementary files shown in Table 4:

Table 4: List of prepared configuration files using custom-made pieces in many variations.

File name	Reactor	Derivative rack
MultiPepPlates_4x96_31Derivs.MPC	4 × 96-well synthesis plate	31 reagents
MultiPepPlates_4x96_59Derivs.MPC	4 × 96-well synthesis plate	59 reagents
MultiPepPlates_4x96_107Derivs.MPC	4 × 96-well synthesis plate	107 reagents
MultiPepPlates_4x384_31Derivs.MPC	4 × 384-well synthesis plate	31 reagents
MultiPepPlates_4x384_59Derivs.MPC	4 × 384-well synthesis plate	59 reagents
MultiPepPlates_4x384_107Derivs.MPC	4 × 384-well synthesis plate	107 reagents

Installation of 384-synthesis setting and calibration of the syringe needle and 16-channel manifold

The hardware parts needed for peptide synthesis in 384-well plates were installed as follows. The 16-channel manifold was mounted to the robot arm by two screws (without the solvent line being connected). The robot arm was then moved to the front right corner of the workspace to connect the solvent line as follows. The tubing was held behind the robotic arm, and the solvent line was gently screwed into the manifold. This procedure was chosen to ensure that the solvent line was not pinched or dragged by the robotic arm's movements. The robotic arm was then moved in all dimensions to verify that the tubing was moving freely. The 384-well filter plates were inserted in the following order:

top left, bottom left, top right, and bottom right (to match the order of peptide #). Wells of a 384-well synthesis plate that was not used for peptide synthesis were covered with an adhesive aluminum foil to retain sufficient vacuum pressure for the positions in use. If a synthesis was performed with fewer than four reactor plates, the non-used positions were occupied with 96-well reactor plates that were covered with silicon pads from CEM/Intavis. The new reagent rack was placed into the synthesizer, and all positions were filled with empty tubes or deep well plates.

Before each synthesis, the syringe needle and the 16-channel manifold needed to be calibrated so that they were well aligned with the derivative rack and reactor plates. The service software was opened (via "*MultiPep_Service.bat*"), where the previously programmed XYZ-coordinates ("X-Pos.", "Y-Pos", "Z-Pos") can be found for all the locations available to the software in the "Vials" page ("*Tray Editor*" → "*Vials*"). On the bottom toolbar is the actual XYZ-coordinates of the current position of the needle tip ("actual XYZ:"). At each step described below for a particular position, the previously programmed XYZ-coordinates were compared with the actual XYZ-coordinates observed on manual positioning of the needle tip to the corresponding position. The differences between these two sets of coordinates were then used to "calibrate" the configuration file by changing the previously programmed XYZ-coordinates.

For the derivative rack, actual XYZ-coordinates were recorded by moving the needle to the XY-center of the tube/well opening, then gently pressing the needle down until the tip was in contact with the plastic bottom. For tubes, actual coordinates were recorded for the left and rightmost tubes in every row. The average of the XY-coordinate differences observed in these two tubes was then added to all the previously programmed XY-coordinates of that row (which were changed individually via "*Racks*" → **click corresponding rack** → **click blue protractor icon** → "*Vials List (fix)*"; Y-coordinates can be set at once by highlighting all positions and clicking the header "Y"). The Z-coordinate for all tubes in the row was set to the average actual Z-coordinate observed in the left and rightmost tubes minus a pre-defined offset value (see following table 5).

For deep well plates, actual coordinates were recorded for the four corner wells of each plate. The average of the XY-coordinate differences observed in these four wells

was then added to all the previously programmed XY-coordinates of that plate (which were changed at once via “*Racks*” → **click corresponding rack** → *home position:*). The Z-coordinate for all wells in the microplate was set to the average actual Z-coordinate observed in the four corners minus a pre-defined offset value. The predefined Z-coordinate offset values are subtracted from the actual plastic bottom coordinate to prevent needle collisions and needle bending. The quality of calibration was checked by commanding the needle to move to some of the reagent rack positions (via “*Vials*” → **click any vial position** → **click green walking man button**). The needle should not contact any solid surface and, when pressed down manually, have 1-2 mm of dead volume room between the needle and the actual plastic bottom.

Table 5: Z-offset settings applied to adjust the needle to an appropriate height depending on which container is used.

Z-offsets (reagent rack)	
Container	Z-offset (1 unit = 0.1 mm)
Small tube (6 ml)	10
Medium tube (11 ml)	10
Large tube (50 ml)	20
48 deep-well plate (4 ml)	15
96 deep-well plate (2 ml)	15

For the reactor plates, actual XYZ-coordinates were recorded by moving the needle to the XY-center of the well opening, then gently pressing the needle down until the tip was flush with the opening plane of the well. Actual coordinates were recorded for the four corner wells of each plate. The average of the XY-coordinate differences observed in these four wells was then added to all the previously programmed XY-coordinates of that plate (which were changed at once via “*Racks*” → **click corresponding rack** → “*home position:*”). The Z-coordinate for all wells in the synthesis microplate was set to the average actual Z-coordinate observed in the four corners. The quality of calibration was checked by commanding the needle to move to the middle H12 well of each reactor plate

(via “*Vials*” → *click *H12 position** → *click green walking man button*). The needle should not contact any solid surface, be nearly perfectly centered in the XY-plane (to within 1 mm), and flush with the opening of the well. If a significant off-centering was observed, it should be confirmed that it was not systematic in all four corners of the plate (if so, the calibration should be repeated until the centering improves).

For the 16-channel manifold, an accurate dispensing of liquid into the center of reactor plate wells was essential to reduce contamination of the working area with excess piperidine (which will quench following coupling reactions leading to failed synthesis). The manifold was calibrated simply by initiating a *WashResin* command and then observing the dispensing of liquid droplets (via “*Run Synthesis*” → *click any *WashResin* task* → *click the green start button*). The liquid droplets should land in the XY-coordinate center of the well of all plates. The experiment was aborted after dispensing to all reactor plates (via “*Pause*” → *click red *Abort Run* button*). If the droplets were not centered, the approximate correction was added to the previously programmed XY-coordinates of the 16-channel manifold (via “*Tray Editor*” → “*Racks*” → *click any reactor plate* → “*Manifold dX/dY :*”). These changes reposition the 16-channel manifold independently of the needle. The quality of calibration was checked by restarting any *WashResin* task and again observing the dispensing of liquid droplets. Once the calibration is complete, the experiment was aborted and restarted from the first task to run the actual 384-well plate SPPS synthesis run.

Reagent abbreviations

All reagents were purchased from commercial sources and used with no additional purification. The solvents were not anhydrous, nor were they dried prior to use. The following abbreviations are used in this article: Ac₂O (acetic anhydride), MeCN (acetonitrile), BDT (1,4-butanedithiol), d = diameter, DCM (dichloromethane), DIPEA (diisopropyl ethyl amine), 5,5'-dithiobis(2-nitrobenzoic acid) (Ellman's reagent), DMF (dimethyl formamide), DMSO (dimethylsulfoxide), DWP (deep well plate), EVA (ethylene-vinyl acetate), FEP (tetrafluorethylen-hexafluorpropylen-copolymer), FFKM (perfluoroelastomer), Fmoc (fluorenylmethoxycarbonyl), l = length, HATU (1-

[bis(dimethylamino)methylene]-1H-1,2,3-triazolo[4,5-b]pyridinium-3-oxide hexafluorophosphate), Mea (2-mercaptoethylamine), MeOH (methanol), Mpa (3-mercaptopropionic acid), NMM (N-methylmorpholine), NMP (N-methylpyrrolidone), PE (polyethylene), PEEK, (polyetheretherketone), PP (polypropylene), PS (polystyrene), PTFE (polytetrafluoroethylene), pyridyl-S-S-Mea (2-[2-pyridinyldithio]-ethanamine), TEA (triethyl amine), TFA (trifluoro acetic acid), TIS (triisopropyl silane), Trt (trityl).

Quality of chemicals

Ac₂O (Sigma-Aldrich, >99%), ammoniumbicarbonate (Sigma-Aldrich, 99-101%), BDT (Sigma-Aldrich, >97%), MeCN (Fisher Chemical, >99.8%), DCM (Sigma-Aldrich, >99.9%), 2,6-dimethylpyridine (Sigma-Aldrich, >99%), DIPEA (Carl Roth GmbH + Co KG, >99.5%), DMF (Sigma-Aldrich, >99.8%), DMSO (Sigma-Aldrich, >99.5%), Ellman's reagent (Sigma-Aldrich, 99%), Fmoc amino acids and derivatives (GL Biochem Shanghai Ltd, >99%), HATU (GL Biochem Shanghai Ltd, >99%), Mea (abcr, 95%), MeOH (Fisher Scientific, >99.9%), Mpa(Trt) (CombiBlock, 95%), NMP (Thermo Scientific, 99%), NMM (Sigma-Aldrich, >98%), piperidine (Acros Organics, 99%), amino methyl PS resin (aapptec, 100-150 mesh, 1.39 mmol/g), TEA (Fluka Analytical, >98%), water (MilliQ).

Cysteamine-S-S-polystyrene resin preparation

The amino methyl PS resin (12.8 g, 17.8 mmol, 1.39 mmol/g) was washed using MeOH (2 × 200 ml), DCM (3 × 200 ml), 1% TFA in DCM (2 × 100 ml), 5% DIPEA in DCM (2 × 100 ml, with incubation for 5 min each), DCM (2 × 200 ml) and DMF (2 × 200 ml) by gently stirring the solvent/resin mixture with a plastic spatula and removing the solvent with a vacuum over a sealed sinter glass filter on a feeding bottle.

The thiol source was coupled to the resin by mixing the pre-washed resin with a pre-activated solution containing Mpa(Trt) (18.6 g, 53.4 mmol, 3.0 equiv.), HATU (20.3 g, 53.4 mmol, 3.0 equiv.) and DIPEA (18.2 ml, 107 mmol, 6.0 equiv.) in DMF (250 ml). The reaction mixture was incubated for 1 h at room temperature and horizontal shaking (200 rpm, IKA KS 260 basic). The resin was washed with DMF (3 × 150 ml). The coupling step

and the washing steps were repeated once more. The resin was dried over two days at room temperature and under vacuum (~1 mbar). The loading of Mpa(Trt) was determined by weight and amounted to 1.08 mmol/g. This loading is an estimation of maximum on resin thiol loading possible and was used as a basis. As a consequence of this, computed yields might be actually higher than indicated in the experiments (conservative estimation). The absence of free primary amino groups was confirmed using the ninhydrin test. Potentially remaining amino groups were inactivated by capping using 200 ml capping solution (5% Ac₂O, 6% 2,6-lutidine in DMF) and incubation for 5 min at room temperature. The resin was washed with DMF (3 × 150 ml) and DCM (3 × 150 ml) before continuing with the Trt deprotection.

Deprotecting solution (250 ml, 10% TFA in DCM with 2% TIS) was added, and the resin was incubated for 1 h at room temperature while horizontally shaking (150 rpm, IKA KS 260 basic). The resin was washed with DCM (3 × 150 ml). The deprotecting and washing step was repeated once more. The resin was dried overnight under vacuum (~1 mbar) and stored in the freezer at -20°C.

For resin stored for more than two months (-20°C), full reduction of the thiol groups was ensured by treating the resin with TCEP. For example, for 100 mg of resin (~1.0 mmol/g, 100 mmol, 1.0 equiv.) a solution (1.5 ml) containing TCEP (268 mM, 400 mmol, 4.0 equiv.) and DIPEA (536 mM, 800 mmol 8.0 equiv.) in solvent (NMP/MeOH, 2:1, v/v) was incubated for one hour at room temperature. The TCEP-treated resin was washed with MeOH (5 × 10 ml), NMP (5 × 10 ml), and THF (5 × 10 ml) followed by a qualitative Ellman's reagent test of the washing filtrates.

The disulfide exchange reaction with pyridyl-S-S-Mea was performed to introduce the disulfide-linked amino group to the resin. The reaction was performed in 20 ml PP syringes with PE filters (99.278, CEM) and on a 0.44 mmol scale (~0.4 g dry resin, 1.1 mmol/g) as follows. Per syringe, a solution of 19.5 ml pyridyl-S-S-Mea disulfide (0.42 g, 1.22 mmol, 2.2 equiv., MeOH/DCM, 3:7; the pyridyl-S-S-Mea disulfide was difficult to dissolve but good solubility was achieved by first adding MeOH and then DCM) was added followed by the addition of DIPEA (0.415 ml, 2.45 mmol, 4.4 equiv.). A yellow color appeared upon the addition of the base. The reaction solution was stirred for 3 h at room

temperature and rotation (15 rpm, Stuart rotator). The resin was washed with solvent (MeOH/DCM, 3:7, 2 × 10 ml), DMF (2 × 10 ml), 1.2 M DIPEA in DMF (1 × 10 ml with incubation for 5 min), DMF (3 × 10 ml) and DCM (2 × 10 ml). The DCM wet resin was kept overnight under reduced pressure for drying and stored at -20°C. A qualitative ninhydrin test was performed to ensure the successful introduction of the amino group. An Ellman's test was performed to ensure the absence of thiol groups.

Resin transfer into well plates using a solid dispenser

The resin was filled to synthesis plates using resin dispenser devices, wherein a device with a suitable number of wells (96 or 384) and cavity size was chosen using a size tester. The resin was filled to the wells of the dispenser in wet form. Attempts to apply resin in dry form led to problems due to clump formation. Resin was introduced into a 20 ml syringe (99.278, CEM) containing a PE filter and swelled with DMF for 15 min at room temperature. The excess of solvent was discarded, and the syringe without piston and cap was centrifuged ($216 \times g$) inside a closed 50 ml canonical tube for 1 min to standardize the DMF content. The wetted resin was placed onto the appropriate solid dispenser. The resin was distributed, and the excess was gently wiped off with another PTFE plate so that all wells were evenly filled. The synthesis plate was inversely placed on top of it, aligned, and fixed by tape. The assembly was turned around and moved into suitable rotor buckets with walls (75006449, Thermo Scientific) containing a 10 mm thick ethylene-vinyl acetate (EVA) foam pad (78 263 01, Rayher Hobby GmbH) underneath to protect the synthesis plate's tip during centrifugation. Alternatively, centrifugation buckets with less supporting walls, such as from Sigma (13421, Sigma), could also be applied but require thinner (3 mm) EVA pads. The resin was transferred from the solid dispenser to the synthesis plate by centrifugation at different speeds (900 or $1400 \times g$) depending on the microtiter plate format (96 or 384-well) and amount (~ 5 or $\sim 3 \mu\text{mol/well}$). The loading and transfer of two plates took about 5-10 min. The amount of resin loaded into the wells by using the solid dispenser (Supplementary Figure 8c & 8e) was determined by weighing the individual amounts of wet loaded resin inside the cavities of the solid dispenser itself. In total, 10 wells (A6, B7, C8, D9, E10, F11, G12, H13, I14 and J15 for solid dispenser

Supplementary Figure 8e and A1, B2, C3, D4, E5, F6, G7, H8, G9, F10 for solid dispenser Supplementary Figure 8c) were analyzed. It was easier to remove the resin by spatula from the solid dispenser (known DMF content) than at the later stage from inside the well after transfer due to unknown DMF content after centrifugation. The averaged transferred resin per well for solid dispenser (Supplementary Figure 8e) amounted to $\sim 4.2 \pm 0.25$ mg/well ($\pm 6.0\%$) and 1.6 ± 0.09 $\mu\text{mol/well}$ (wet corrected) respectively. For the other solid dispenser at larger scale (Supplementary Figure 8c), the averaged amount of transferred resin was determined to be $\sim 14 \pm 1.6$ mg/well ($\pm 11\%$) and 4.2 ± 0.47 $\mu\text{mol/well}$ (wet corrected) respectively.

Peptide synthesis with CEM/Intavis MultiPep 2 in 384-well plates

Automated solid-phase peptide synthesis was performed on an Intavis Multiprep RSi synthesizer (equivalent to CEM MultiPep 2) using the above-described hardware adaptations. Commercial 384-well filter plates were used (201035-10 PE 25 UM, Agilent). Around 1.1 g/plate of dry cysteamine-S-S-polystyrene resin (loading of cysteamine = 1.08 mmol/g assuming that thiol groups were quantitatively modified) were loaded onto the plate (~ 3 $\mu\text{mol/well}$) using the solid dispenser as described above. The resin in each well was washed with 6×70 μl DMF (16-manifold). Coupling was performed with 25 μl of Fmoc amino acid (500 mM, 4.0 equiv.), 27 μl HATU (500 mM, 4.5 equiv.), 6 μl of *N*-methylmorpholine (4 M, 8.0 equiv.), and 3 μl *N*-methylpyrrolidone. All components were premixed for 1 min, then added to the appropriate well-containing resin, and incubated for 45 min without shaking. The final volume of the coupling reaction was 61 μl , and the final concentrations of reagents were 205 mM amino acid, 221 mM HATU, and 393 mM *N*-ethylmorpholine. Coupling was performed twice followed by resin washing with 6×70 $\mu\text{l/well}$ of DMF. Fmoc deprotection was performed twice, each time using 35 $\mu\text{l/well}$ of piperidine in DMF (1:4, v/v) for 5 min. After Fmoc deprotection, the resin was washed with 8×70 μl DMF. At the end of the peptide synthesis, the resin was washed with 2×70 $\mu\text{l/well}$ of DCM using the needle and not the manifold due to dripping caused by the high density of DCM.

Deprotection of peptides in 384-well plates

After DCM washing, the 384-well plates were dried (4 h, room temperature at air), and the side chains of the peptides were deprotected by incubation with 3×1 h deprotecting solution (TFA/TIS/ddH₂O, 38:1:1, 40 μ l/well). The cocktail was transferred using a multichannel pipette (8 channels, 30-300 μ l, VWR) with active coal-protected tips (5469, MBP 200 Solvent Safe TM) while the outlet of the wells was blocked by pressing (whole body weight, by hands or stepping on it, sealed first to avoid contamination) the tips of the plate onto a 10 mm thick EVA foam pad (76899, Creotime). During incubation, the 384-well plate synthesis was covered with a PP adhesive lid (G070-N, Kisker Biotech GmbH & Co.). The deprotection solution was removed using a manual plate vacuum filtration station, and the resin was washed with DCM (3×60 μ l/well) and dried at the air for a few hours before continuing with the reductive release. It was important to efficiently remove traces of TFA by fully evaporating DCM, in order to prevent base neutralization in the next step of reductive release.

Reductive release of library peptides and concentration

The 384-well reactor plates containing the deprotected peptides on resin (theoretical: ~ 3 μ mol/well, 1.0 equiv.) were stacked onto 384-well deep well plates (CLS3342, Corning). The peptides were released by applying release solution (30 μ l/well, 400 mM TEA and 400 mM BDT, 4.0 equiv.) using a multichannel pipette (8 channels, 30-300 μ l, VWR) with active coal protected tips (5469, MBP 200 Solvent Safe TM). Upon base addition, it was verified that no white smoke developed that would have indicated incomplete TFA removal. The plate stacks were placed into food-grade PP zipper bags (15387154, M-Classic) to avoid the strong smell of BDT during incubation, transport, and centrifugation. The plate stacks were incubated overnight at room temperature and centrifuged ($485 \times g$, 1 min, room temperature). The release was repeated once more (5 hours incubation only), the two release filtrates combined, and the combined filtrates (60 μ l/well) acidified with 50% TFA solution in water (7.4 μ l/well, 6.5 M, 2.0 equiv. compared to TEA) for avoiding disulfide oxidation during concentration. The 384-well deep well plates were sealed using an adhesive aluminum lid (silverseal 676090, greiner bio-one)

and pierced with a homemade aluminum 384-well piercer (Supplementary Figure 11) to form 0.3 mm diameter holes into each well to minimize risks of spillovers during rotational vacuum concentration. The solvents were removed using a rotational vacuum concentrator (RVC 2-33 CDplus IR and Alpha 2-4 LSCbasic, Christ) at ~30°C for 5 h and 1750 rpm (24700, Christ plate rotator 1 and 124708 plate buckets) with a gradient of vacuum down to 0.5 mbar within 20 min. The residues formed after the removal of solvent inside each well were dissolved in DMSO (40 μ l/well), covered with PS lid (greiner bio-one, Easyseal 676001), sonicated, and centrifuged (485 \times g, 1 min, room temperature) before determining the concentration using Ellman's reagent.

LC-MS analysis of peptides

Peptide samples were analyzed by LC-MS analysis with a UHPLC and single quadrupole MS system (Shimadzu LCMS-2020) using a C18 reversed-phase column (Phenomenex Kinetex 2.1 mm \times 50 mm C18 column, 100 Å pore, 2.6 μ m particle) and a linear gradient of solvent B (MeCN, 0.05% formic acid) over solvent A (H₂O, 0.05% formic acid) at a flow rate of 1 ml min⁻¹. For all samples, a gradient of 0 to 60% MeCN within 10 min was applied, and UV at 220 nm was used when not otherwise mentioned. Mass analysis was performed in positive ion mode. 100 μ l polypropylene (PP) HPLC microvial (Shimadzu, 980-14379) with PP and Teflon caps (Shimadzu, 980-18425) were used for all samples.

For analyzing peptides after reductive release and final linear peptide stock solutions in DMSO, a 2 μ l sample was transferred into 198 μ l solvent (MeCN/water/TFA, 50:49.9:0.1%, v/v/v) and analyzed using an injection volume of 2 μ l.

Peptide library quantification by absorption using Ellman's reagent

The final linear peptide stock solution concentrations in DMSO were determined by using Ellman's reagent absorption assay in a 384-well plate format. Aqueous 150 mM ammonium bicarbonate buffer (pH 8.0) in 10% DMSO (23.84 μ l/well) and 10 mM Ellman's reagent in buffer (6.00 μ l/well) were transferred by bulk dispenser (Certus Flex, Fritz Gyger

AG) into a 384-well plate (781096, Greiner bio-one) followed by the addition of ~10 mM linear peptide stock solutions in DMSO (135 nl) by acoustic droplet ejection (ECHO 650, Labcyte/Beckman Coulter) amounting to a total volume of 30.0 μ l/well. ECHO Qualified 384-well source plates (PP-0200, Beckman Coulter) were used, and transfers were realized with the standard DMSO calibration. The positive control was composed of aqueous 150 mM ammonium bicarbonate buffer at pH 8.0 (23.9 μ l/well), 10 mM Ellman's reagent in buffer (6.00 μ l/well) and 10 mM TCEP in buffer (90 nl/well). The negative control contained aqueous 150 mM ammonium bicarbonate buffer at (24 μ l/well) and 10 mM Ellman's reagent in buffer (6.00 μ l/well) only. The assay plate was sealed by an adhesive PS lid (Easyseal, 676001), centrifuged (485 \times g, 1 min, room temperature) and analyzed by absorption at 412 nm using a Tecan M200 Pro. The obtained absorption values were compared to a calibration curve established with the same conditions and a purified linear dithiol model peptide.

Peptide synthesis with CEM/Intavis MultiPep 2 in 96-well plates

Automated solid-phase peptide synthesis was performed on an Intavis MultiPep RSi synthesizer (equivalent to CEM MultiPep 2) with 4 \times 96 well plates (Orochem, OF 1100). For the synthesis of peptide in 4 \times 96-well plates, ~0.45 g/plate of dry cysteamine-S-S-polystyrene resin (loading of cysteamine = 1.08 mmol/g assuming that thiol groups were quantitatively modified) were loaded onto the plate (~5 μ mol/well) using a suitable solid dispenser. The resin in each well was washed with 6 \times 225 μ l/well DMF (8-manifold). Coupling was performed with 50 μ l of Fmoc amino acid (500 mM, 5.0 equiv.), 53 μ l HATU (500 mM, 5.3 equiv.), 12.5 μ l of *N*-methymorpholine (4 M, 10 equiv.), and 5 μ l *N*-methylpyrrolidone. All components were remixed for 1 min, then added to the appropriate well containing resin for 45 min reaction without shaking. The standard derivative rack (24 \times 50 ml canonical and 7 \times 11 ml tubes) was used. The final volume of the coupling reaction was 121 μ l/well and the final concentrations of reagents were 207 mM Fmoc amino acid, 219 mM HATU and 413 mM *N*-ethylmorpholine. Coupling was performed twice followed by resin washing with 6 \times 225 μ l/well of DMF. Fmoc deprotection was performed twice, each time using 150 μ l/well of piperidine in DMF (1:4, v/v) for 5 min. After Fmoc

deprotection, the resin was washed with $8 \times 225 \mu\text{l/well}$ DMF. At the end of the peptide synthesis, the resin was washed with $2 \times 300 \mu\text{l/well}$ of DCM. Solvent removal was realized through vacuum filtration, which is integrated into the synthesis plate holder module.

Deprotection of peptide libraries in 96-well plates

The same deprotecting procedure was applied as for 384-well synthesis plates, except that a larger volume of deprotecting solution (TFA/TIS/ddH₂O, 38:1:1, 300 $\mu\text{l/well}$) was added with an 8-multichannel pipette.

Reductive release of peptide libraries in 96-well plates

The same release and concentration procedure was applied as for 384-well synthesis plates, except that larger volumes of release (50 $\mu\text{l/well}$, 400 mM TEA and 400 mM BDT, 4.0 equiv.) and acidification (12.3 $\mu\text{l/well}$, 6.5 M TFA in water, 2.0 equiv. compared to TEA) solutions were used transferred by multichannel pipette (VWR). The combined release solutions were concentrated in 1.2 ml 96-well PP DWP (260252, Thermo Scientific) using pierced seals (silverseal 676090, greiner bio-one) with the developed device (Supplementary Figure 12).

Determination of peptide synthesis duration in 96 and 384-well plates

The simultaneously created log files from the performed syntheses were evaluated to determine the required time to process the individual peptide synthesis steps (pre-activation and distribution, washing, deprotection, etc.) using the CEM/Intavis MultiPep 2 synthesizer in either 96- or 384-well plates together with 31 or 59 derivative racks.

5.7 Supplementary information

Supplementary tables

Supplementary Table 4: Peptides synthesized in a 384-well plate on the modified CEM/Intavis MultiPep 2 peptide synthesizer. EM = exact mass.

C-term										N-term										C-term										N-term										C-term										N-term									
ID	coordinate	plate	ID	5	4	3	2	1	EM	ID	coordinate	plate	ID	5	4	3	2	1	EM	ID	coordinate	plate	ID	coordinate	plate	ID	5	4	3	2	1	EM																											
1	B1	1	MPA	S	Q	380.13	98	B7	2	MPA	T	K	384.18	194	B13	3	MPA	Q	M	H	380.24	290	B18	4	MPA	D	I	A	354.20																														
2	C1	1	MPA	N	P	376.14	99	C7	2	MPA	T	K	384.18	195	C13	3	MPA	K	N	D	322.22	291	C18	4	MPA	Q	P	I	353.24																														
3	D1	1	MPA	V	K	459.14	100	D7	2	MPA	K	N	407.16	196	D13	3	MPA	M	F	T	354.17	292	D18	4	MPA	Q	F	M	357.26																														
4	E1	1	MPA	G	H	358.12	101	E7	2	MPA	A	K	384.17	197	E13	3	MPA	Q	Y	D	351.20	293	E18	4	MPA	S	H	P	386.18																														
5	F1	1	MPA	W	R	507.93	102	F7	2	MPA	N	R	435.18	198	F13	3	MPA	I	L	P	322.20	294	F18	4	MPA	V	L	E	358.19																														
6	G1	1	MPA	S	W	438.87	103	G7	2	MPA	S	W	430.87	199	G13	3	MPA	M	W	P	379.03	295	G18	4	MPA	Q	T	N	437.15																														
7	H1	1	MPA	F	W	458.90	104	H7	2	MPA	N	W	465.88	200	H13	3	MPA	S	N	I	350.20	296	H18	4	MPA	D	I	A	384.20																														
8	I1	1	MPA	F	I	425.19	105	I7	2	MPA	K	E	422.15	201	I13	3	MPA	Y	N	L	355.23	297	I18	4	MPA	W	Q	360.96																															
9	J1	1	MPA	S	N	395.12	106	J7	2	MPA	D	E	450.13	202	J13	3	MPA	N	V	A	346.19	298	J18	4	MPA	Q	R	T	355.25																														
10	K1	1	MPA	K	L	450.22	107	K7	2	MPA	K	D	450.18	203	K13	3	MPA	S	P	N	353.17	299	K18	4	MPA	V	T	V	358.22																														
11	L1	1	MPA	P	K	440.20	108	L7	2	MPA	I	M	450.16	204	L13	3	MPA	P	A	A	354.17	300	L18	4	MPA	W	W	N	459.87																														
12	M1	1	MPA	Q	D	426.14	109	M7	2	MPA	S	G	359.06	205	M13	3	MPA	V	S	G	358.16	301	M18	4	MPA	S	R	G	423.11																														
13	N1	1	MPA	M	I	450.16	110	N7	2	MPA	Y	W	514.90	206	N13	3	MPA	G	N	T	357.15	302	N18	4	MPA	R	R	T	378.29																														
14	O1	1	MPA	K	L	450.22	111	O7	2	MPA	G	T	323.11	207	O13	3	MPA	I	R	T	355.27	303	O18	4	MPA	K	L	M	510.20																														
15	P1	1	MPA	Y	M	459.14	112	P7	2	MPA	V	L	377.19	208	P13	3	MPA	K	A	L	377.26	304	P18	4	MPA	Q	A	N	478.18																														
16	Q1	1	MPA	I	L	391.21	113	Q7	2	MPA	G	A	358.10	209	Q13	3	MPA	Y	I	V	354.24	305	Q18	4	MPA	G	E	A	422.11																														
17	R1	1	MPA	Q	H	438.16	114	R7	2	MPA	P	D	377.14	210	R13	3	MPA	P	M	N	328.17	306	R18	4	MPA	Q	T	E	358.21																														
18	S1	1	MPA	Q	Y	456.16	115	S7	2	MPA	Q	N	407.14	211	S13	3	MPA	P	N	I	350.22	307	S18	4	MPA	H	I	F	358.23																														
19	T1	1	MPA	F	D	427.15	116	T7	2	MPA	S	Y	415.14	212	T13	3	MPA	T	H	W	359.04	308	T18	4	MPA	R	S	W	354.97																														
20	U1	1	MPA	Q	I	455.17	117	U7	2	MPA	K	I	450.22	213	U13	3	MPA	L	H	A	358.22	309	U18	4	MPA	V	D	H	358.23																														
21	V1	1	MPA	T	T	357.14	118	V7	2	MPA	Y	W	514.90	214	V13	3	MPA	G	Q	F	357.19	310	V18	4	MPA	F	L	S	352.22																														
22	W1	1	MPA	D	A	357.15	119	W7	2	MPA	V	S	351.14	215	W13	3	MPA	H	S	G	357.19	311	W18	4	MPA	F	W	I	351.99																														
23	X1	1	MPA	Y	M	459.14	120	X7	2	MPA	I	F	381.14	216	X13	3	MPA	G	S	T	355.14	312	X18	4	MPA	V	Q	W	357.06																														
24	Y1	1	MPA	I	E	395.13	121	Y7	2	MPA	S	A	353.11	217	Y13	3	MPA	A	I	Y	354.21	313	Y18	4	MPA	L	Q	S	353.21																														
25	Z1	1	MPA	W	A	422.87	122	Z7	2	MPA	N	T	380.13	218	Z13	3	MPA	M	S	T	355.18	314	Z18	4	MPA	Q	P	S	477.18																														
26	AA1	1	MPA	M	A	357.15	123	AA7	2	MPA	I	T	423.13	219	AA13	3	MPA	I	W	M	355.96	315	AA18	4	MPA	R	G	N	534.26																														
27	AB1	1	MPA	S	N	395.12	124	AB7	2	MPA	L	Y	441.19	220	AB13	3	MPA	D	T	D	356.17	316	AB18	4	MPA	V	G	N	498.17																														
28	AC1	1	MPA	M	R	452.18	125	AC7	2	MPA	G	H	378.15	221	AC13	3	MPA	Y	A	C	356.16	317	AC18	4	MPA	M	U	Q	355.21																														
29	AD1	1	MPA	R	F	458.21	126	AD7	2	MPA	P	I	375.18	222	AD13	3	MPA	A	Y	L	352.22	318	AD18	4	MPA	S	P	A	350.15																														
30	AE1	1	MPA	R	F	458.21	127	AE7	2	MPA	H	W	450.05	223	AE13	3	MPA	I	T	I	356.21	319	AE18	4	MPA	G	O	M	453.21																														
31	AF1	1	MPA	N	E	380.13	128	AF7	2	MPA	K	N	407.16	224	AF13	3	MPA	L	S	C	358.21	320	AF18	4	MPA	P	T	E	357.26																														
32	AG1	1	MPA	G	H	358.12	129	AG7	2	MPA	L	R	I	581.20	225	AG13	3	MPA	G	F	S	356.16	321	AG18	4	MPA	E	L	T	358.21																													
33	AH1	1	MPA	D	Q	458.14	130	AH7	2	MPA	P	L	A	440.21	226	AH13	3	MPA	T	W	A	358.17	322	AH18	4	MPA	K	N	K	355.27																													
34	AI1	1	MPA	F	I	425.19	131	AI7	2	MPA	P	P	M	450.16	227	AI13	3	MPA	K	Y	N	355.26	323	AI18	4	MPA	V	Q	E	355.19																													
35	AJ1	1	MPA	H	V	451.17	132	AJ7	2	MPA	Q	A	N	478.19	228	AJ13	3	MPA	A	W	H	352.22	324	AJ18	4	MPA	G	I	P	432.20																													
36	AK1	1	MPA	K	D	450.18	133	AK7	2	MPA	E	A	W	551.91	229	AK13	3	MPA	V	I	N	355.21	325	AK18	4	MPA	M	G	H	458.18																													
37	AL1	1	MPA	Q	I	455.17	134	AL7	2	MPA	N	W	I	375.05	230	AL13	3	MPA	R	W	M	356.07	326	AL18	4	MPA	L	R	E	355.27																													
38	AM1	1	MPA	Y	P	425.16	135	AM7	2	MPA	Y	F	M	551.91	231	AM13	3	MPA	Y	I	T	354.24	327	AM18	4	MPA	E	M	P	340.20																													
39	AN1	1	MPA	K	K	422.18	136	AN7	2	MPA	V	H	471.25	232	AN13	3	MPA	Q	J	S	355.16	328	AN18	4	MPA	W	M	I	453.82																														
40	AO1	1	MPA	F	R	458.21	137	AO7	2	MPA	D	E	Y	572.19	233	AO13	3	MPA	I	R	K	356.22	329	AO18	4	MPA	N	S	H	575.82																													
41	AP1	1	MPA	S	Q	395.13	138	AP7	2	MPA	V	M	P	450.25	234	AP13	3	MPA	L	N	A	353.20	330	AP18	4	MPA	M	P	P	521.19																													
42	AQ1	1	MPA	N	E	380.13	139	AQ7	2	MPA	V	A	F	450.25	235	AQ13	3	MPA	V	S	L	354.26	331	AQ18	4	MPA	T	V	A	357.04																													
43	AR1	1	MPA	A	S	323.11	140	AR7	2	MPA	D	L	G	450.19	236	AR13	3	MPA	N	L	R	350.26	332	AR18	4	MPA	P	E	S	478.17																													
44	AS1	1	MPA	H	I	415.18	141	AS7	2	MPA	K	N	W	550.97	237	AS13	3	MPA	G	F	M	350.17	333	AS18	4	MPA	Q	V	M	520.23																													
45	AT1	1	MPA	S	D	397.12	142	AT7	2	MPA	V	F	M	542.27	238	AT13	3	MPA	K	D	H	355.24	334	AT18	4	MPA	T	M	R	553.23																													
46	AU1	1	MPA	S	F	358.14	143	AU7	2	MPA	Q	H	T	531.21	239	AU13	3	MPA	N	R	Q	353.24	335	AU18	4	MPA	W	P	S	355.82																													
47	AV1	1	MPA	I	P	375.15	144	AV7	2	MPA	N	N	A	454.16	240	AV13	3	MPA	S	H	M	354.15	336	AV18	4	MPA	M	I	S	496.20																													
48	AW1	1	MPA	L	W	450.22	145	AW7	2	MPA	Q	F	M	554.21	241	AW13	3	MPA	E	G	R	357.21	337	AW18	4	MPA	V	V	A	354.21																													
49	AX1	1	MPA	N	K	457.16	146	AX7	2	MPA	Y	F	V	574.24	242	AX13	3	MPA	W	F	F	357.04	338	AX18	4	MPA	Q	D	L	351.23																													
50	AY1	1	MPA	A	S	323.11	147	AY7	2	MPA	W	R	M	438.97	243	AY13	3	MPA	Q	M	T	355.19	339	AY18	4	MPA	V	V	V	480.23																													
51	AZ1	1	MPA	V	C	321.13	148	AZ7	2	MPA	A	M	E	456.16	244	AZ13	3	MPA	Q	I	K	355.20	340	AZ18	4	MPA	C	I	T	470.18																													
52	BA1	1	MPA	T	H	423.15	149	BA7	2	MPA	S	R	L	521.20	245	BA13	3	MPA	S	F	A	356.18	341	BA18	4	MPA	Q	K	K	470.25																													
53	BB1	1	MPA	N	P	376.14	150	BB7	2	MPA	R	I	A	570.24	246	BB13	3	MPA	R	N	N	358.27	342	BB18	4	MPA	K	K	K	470.25																													
54	BC1	1	MPA	L	M	42																																																					

Supplementary Table 5: Peptides synthesized in 96-well plates on the CEM/Intavis MultiPep 2 peptide synthesizer. EM = exact mass.

C-term										N-term										C-term										C-term										C-term									
ID	coordinate	plate	ID	5	4	3	2	1	EM	ID	coordinate	plate	ID	5	4	3	2	1	EM	ID	coordinate	plate	ID	5	4	3	2	1	EM	ID	coordinate	plate	ID	5	4	3	2	1	EM										
1	A1	1								97	A7	2								193	A13	3								289	A19	4																	
2	B1	1								98	B7	2								194	B13	3								290	B19	4																	
3	C1	1								99	C7	2								195	C13	3								291	C19	4																	
4	D1	1								100	D7	2								196	D13	3								292	D19	4																	
5	E1	1								101	E7	2								197	E13	3								293	E19	4																	
6	F1	1								102	F7	2								198	F13	3								294	F19	4																	
7	G1	1								103	G7	2								199	G13	3								295	G19	4																	
8	H1	1								104	H7	2								200	H13	3								296	H19	4																	
9	I1	1								105	I7	2								201	I13	3								297	I19	4																	
10	J1	1								106	J7	2								202	J13	3								298	J19	4																	
11	K1	1								107	K7	2								203	K13	3								299	K19	4																	
12	L1	1								108	L7	2								204	L13	3								300	L19	4																	
13	M1	1								109	M7	2								205	M13	3								301	M19	4																	
14	N1	1								110	N7	2								206	N13	3								302	N19	4																	
15	O1	1								111	O7	2								207	O13	3								303	O19	4																	
16	P1	1								112	P7	2								208	P13	3								304	P19	4																	
17	A2	1								113	A8	2								209	A14	3								305	A20	4																	
18	B2	1								114	B8	2								210	B14	3								306	B20	4																	
19	C2	1								115	C8	2								211	C14	3								307	C20	4																	
20	D2	1								116	D8	2								212	D14	3								308	D20	4																	
21	E2	1								117	E8	2								213	E14	3								309	E20	4																	
22	F2	1								118	F8	2								214	F14	3								310	F20	4																	
23	G2	1								119	G8	2								215	G14	3								311	G20	4																	
24	H2	1								120	H8	2								216	H14	3								312	H20	4																	
25	I2	1								121	I8	2								217	I14	3								313	I20	4																	
26	J2	1								122	J8	2								218	J14	3								314	J20	4																	
27	K2	1								123	K8	2								219	K14	3								315	K20	4																	
28	L2	1								124	L8	2								220	L14	3								316	L20	4																	
29	M2	1								125	M8	2								221	M14	3								317	M20	4																	
30	N2	1								126	N8	2								222	N14	3								318	N20	4																	
31	O2	1								127	O8	2								223	O14	3								319	O20	4																	
32	P2	1								128	P8	2								224	P14	3								320	P20	4																	
33	A3	1								129	A9	2								225	A15	3								321	A21	4																	
34	B3	1								130	B9	2								226	B15	3								322	B21	4																	
35	C3	1								131	C9	2								227	C15	3								323	C21	4																	
36	D3	1								132	D9	2								228	D15	3								324	D21	4																	
37	E3	1								133	E9	2								229	E15	3								325	E21	4																	
38	F3	1								134	F9	2								230	F15	3								326	F21	4																	
39	G3	1								135	G9	2								231	G15	3								327	G21	4																	
40	H3	1								136	H9	2								232	H15	3								328	H21	4																	
41	I3	1								137	I9	2								233	I15	3								329	I21	4																	
42	J3	1								138	J9	2								234	J15	3								330	J21	4																	
43	K3	1								139	K9	2								235	K15	3								331	K21	4																	
44	L3	1								140	L9	2								236	L15	3								332	L21	4																	
45	M3	1								141	M9	2								237	M15	3								333	M21	4																	
46	N3	1								142	N9	2								238	N15	3								334	N21	4																	
47	O3	1								143	O9	2								239	O15	3								335	O21	4																	
48	P3	1								144	P9	2								240	P15	3								336	P21	4																	
49	A4	1								145	A10	2								241	A16	3								337	A22	4																	
50	B4	1								146	B10	2								242	B16	3								338	B22	4																	
51	C4	1								147	C10	2								243	C16	3								339	C22	4																	
52	D4	1								148	D10	2								244	D16	3								340	D22	4																	
53	E4	1								149	E10	2								245	E16	3								341	E22	4																	
54	F4	1								150	F10	2								246	F16	3								342	F22	4																	
55	G4	1								151	G10	2								247	G16	3								343	G22	4																	
56	H4	1								152	H10	2								248	H16	3								344	H22	4																	
57	I4	1								153	I10	2								249	I16	3								345	I22	4																	
58	J4	1								154	J10	2								250	J16	3								346	J25																		

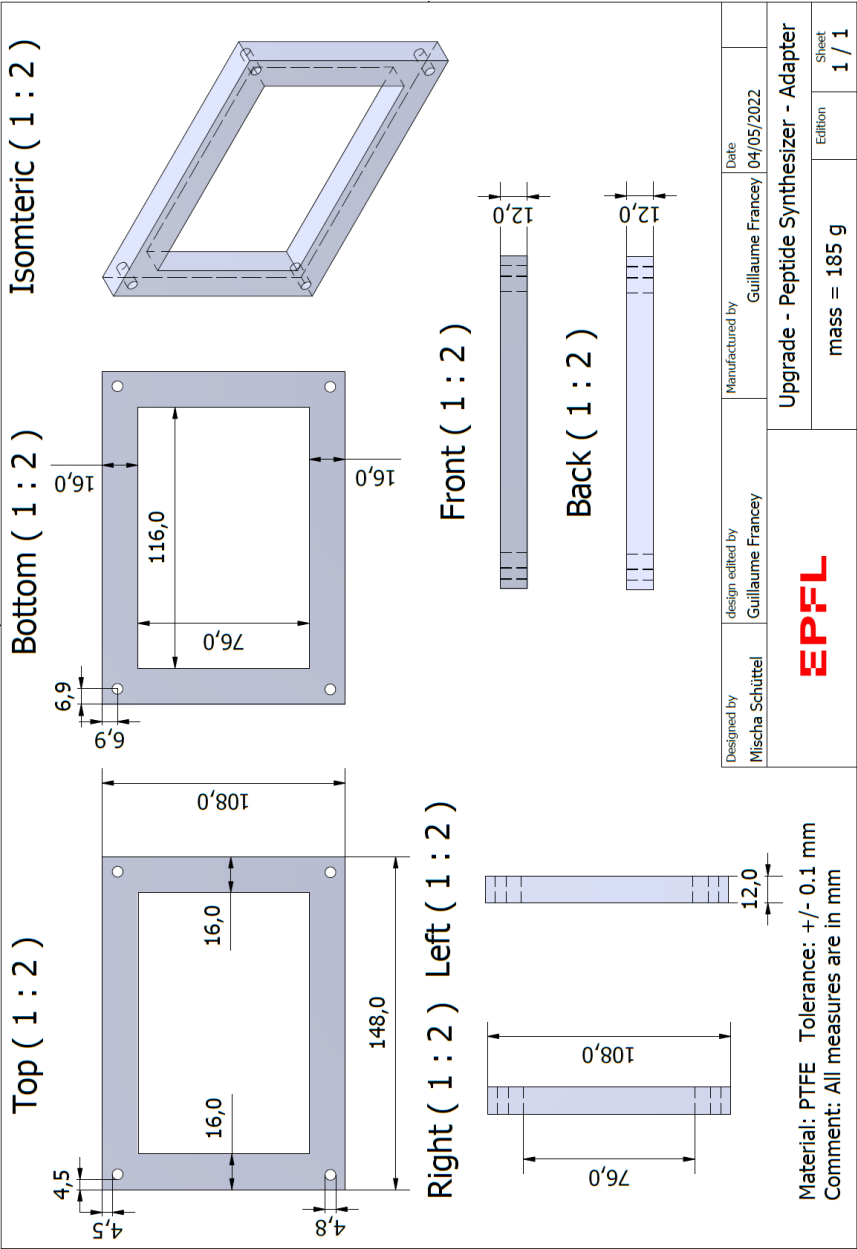
Supplementary Table 6: Analysis of peptides from the synthesis in 384-well plates using the CEM/Intavis modified MultiPep 2 synthesizer. The indicated peptides were randomly picked (the same well in each one of the four 384-well plates). The italic marked peptides correspond to the peptide represented in the chromatogram (Figure 20a)
*) No peptide found.

Peptide	Plate	Coordinate	Retention time (min)	[M+H] ⁺ (m/z)	Peak area at 220 nm (%)
<i>1</i>	A	<i>A1</i>	3.26	699.1	93
<i>1</i>	B	<i>A1</i>	3.26	699.3	89
<i>1</i>	C	<i>A1</i>	3.26	699.2	89
<i>1</i>	D	<i>A1</i>	3.02*	699.3	93
<i>16</i>	A	<i>P1</i>	3.49	460.1	79
<i>16</i>	B	<i>P1</i>	3.49	460.1	82
<i>16</i>	C	<i>P1</i>	3.48	460.1	83
<i>16</i>	D	<i>P1</i>	3.48	460.1	84
<i>18</i>	A	<i>B2</i>	2.03	431.0	76
<i>18</i>	B	<i>B2</i>	-	-	*
<i>18</i>	C	<i>B2</i>	2.03	431.0	72
<i>18</i>	D	<i>B2</i>	2.03	431.0	73
<i>69</i>	A	<i>E5</i>	2.58	392.0	88
<i>69</i>	B	<i>E5</i>	2.59	392.0	86
<i>69</i>	C	<i>E5</i>	2.58	392.0	88
<i>69</i>	D	<i>E5</i>	2.58	392.0	69
<i>103</i>	A	<i>G7</i>	3.48	439.1	77
<i>103</i>	B	<i>G7</i>	3.48	439.1	76
<i>103</i>	C	<i>G7</i>	3.48	439.1	77
<i>103</i>	D	<i>G7</i>	3.48	439.1	77
<i>120</i>	A	<i>H8</i>	2.77	392.1	85
<i>120</i>	B	<i>H8</i>	2.77	392.1	75
<i>120</i>	C	<i>H8</i>	2.64	392.1	84
<i>120</i>	D	<i>H8</i>	2.77	392.1	91
<i>181</i>	A	<i>E12</i>	1.58	532.2	72
<i>181</i>	B	<i>E12</i>	1.52	532.2	72
<i>181</i>	C	<i>E12</i>	1.64	532.2	83
<i>181</i>	D	<i>E12</i>	1.61	532.2	65
<i>222</i>	A	<i>N14</i>	3.8	513.3	83
<i>222</i>	B	<i>N14</i>	3.79	513.2	79
<i>222</i>	C	<i>N14</i>	3.79	513.2	85
<i>222</i>	D	<i>N14</i>	3.79	513.3	80
<i>256</i>	A	<i>P16</i>	3.6	529.3	80
<i>256</i>	B	<i>P16</i>	3.62	529.3	83
<i>256</i>	C	<i>P16</i>	3.61	529.3	80
<i>256</i>	D	<i>P16</i>	3.58	529.3	81
<i>377</i>	A	<i>I24</i>	3.25	463.1	83
<i>377</i>	B	<i>I24</i>	3.24	463.1	87
<i>377</i>	C	<i>I24</i>	3.25	463.1	90
<i>377</i>	D	<i>I24</i>	3.25	463.2	83

Supplementary Table 7: Analysis of peptides from the synthesis in 96-well plates. The indicated peptides were randomly picked. Peptides 18 and 181 showed no peak (n.d.) in the chromatogram.

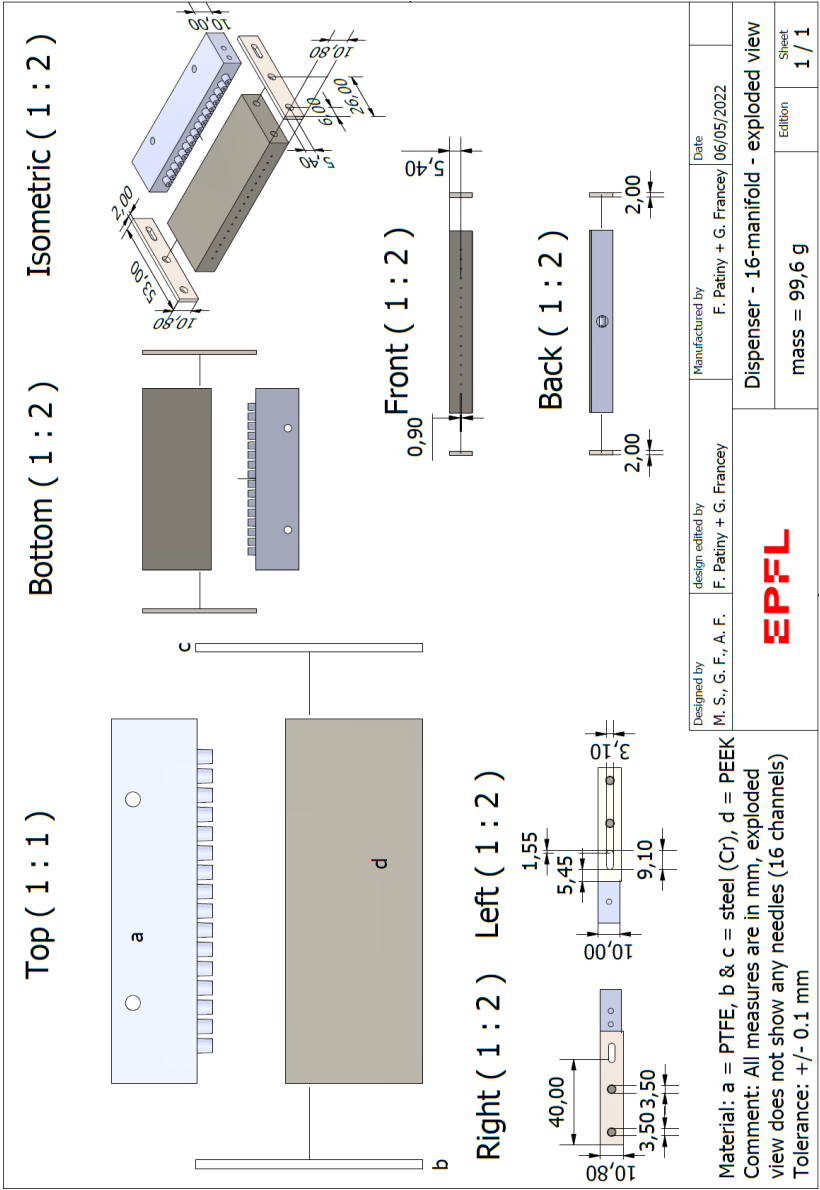
Peptide	Plate	Coordinate	Retention time (min)	[M+H] ⁺ (m/z)	Peak area at 220 nm (%)
1	A	A1	3.29	350.1	93.8
16	A	H2	3.5	460.1	80.3
18	A	B3	n.d.	n.d.	n.d.
69	A	E3	2.7	392	89.5
103	B	G1	3.5	439.1	78.1
120	B	H3	2.85	392	92.2
181	B	E11	n.d.	n.d.	n.d.
222	C	F4	3.79	513.3	92.9
256	C	H8	3.64	529.6	86.7
377	D	A12	3.27	463.2	84.8

Supplementary figures



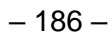
Supplementary Figure 4: Technical drawing of 384-well synthesis plate adapter.

a

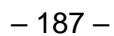


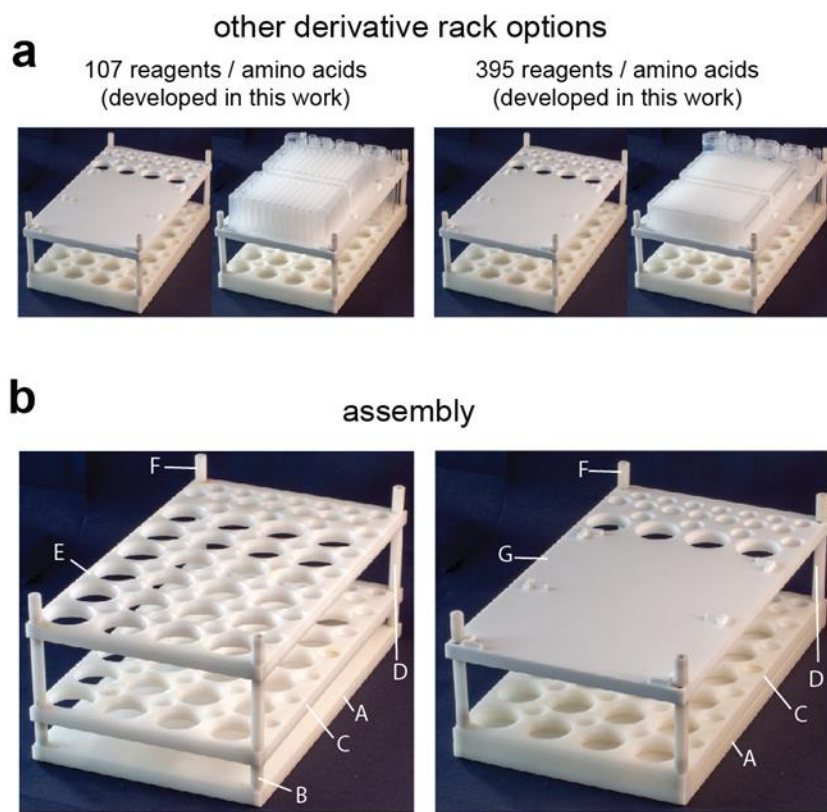
Supplementary Figure 5: Liquid dispensing manifold. (a) Exploded view of the manufactured pieces required for the 16-channel liquid dispensing manifold. The individual blunt needles (Braun, 4657527) for each channel are not visualized. (b) Technical drawing of piece a. (c) Technical drawing of piece d.

Supplementary Figure 5: Continued.

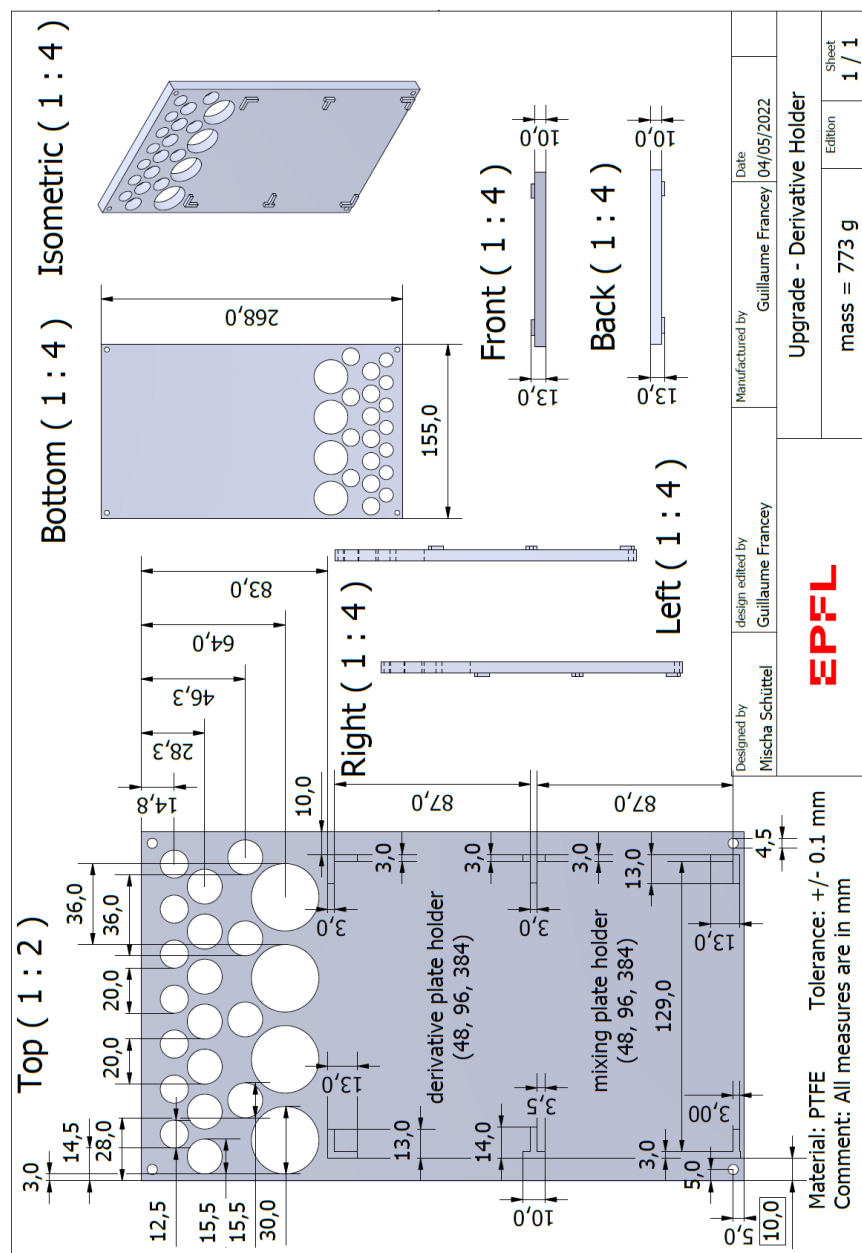


Supplementary Figure 5: Continued.





Supplementary Figure 6: Detailed description of the new amino acid rack. (a) The newly developed derivative rack provides space for 4 × 50 ml PP canonical tubes (greiner bio-one, 210261), 7 × 15 ml PP tubes (Sarstedt, 60610), and two 96-well (Thermo Scientific, 260252) or two 384-well deep well plates (Corning, CLS3342). One of the deep well plates is used for storing the amino acids (upper), and the other for pre-activation of the amino acids (bottom). (b) The standard (left) and the newly designed derivative rack (right) are assembled differently using the same pieces. A = Standard base plate, B and F = short spacer (2.0 cm), C = bottom tube support plate, D = long spacer (4.0 cm), E = upper tube support plate, G = newly designed tube and deep well plate holder plate.



Supplementary Figure 7: Technical drawing of the new amino acid rack. For mounting the new rack, four longer socket head cap screws (30 vs 16 mm, M4) were used with a cylindrical head (h = 4 mm) containing an allen key fit (3 mm). See Supplementary Figure 3 for assembly.

Top (1 : 2)

Bottom (1 : 2)

Front (1 : 2)

Back (1 : 2)

Right (1 : 2)

Left (1 : 2)

Isometric (1 : 2)

Material: PTFE Tolerance: ± 0.1 mm
 Comment: All measures are in mm

EPFL

Designed by
 Mischa Schüttel

Design edited by
 Guillaume Francy

Manufactured by
 Guillaume Francy

Date
 04/05/2022

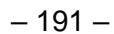
Solid Dispenser - Size tester

Sheet
 1 / 1

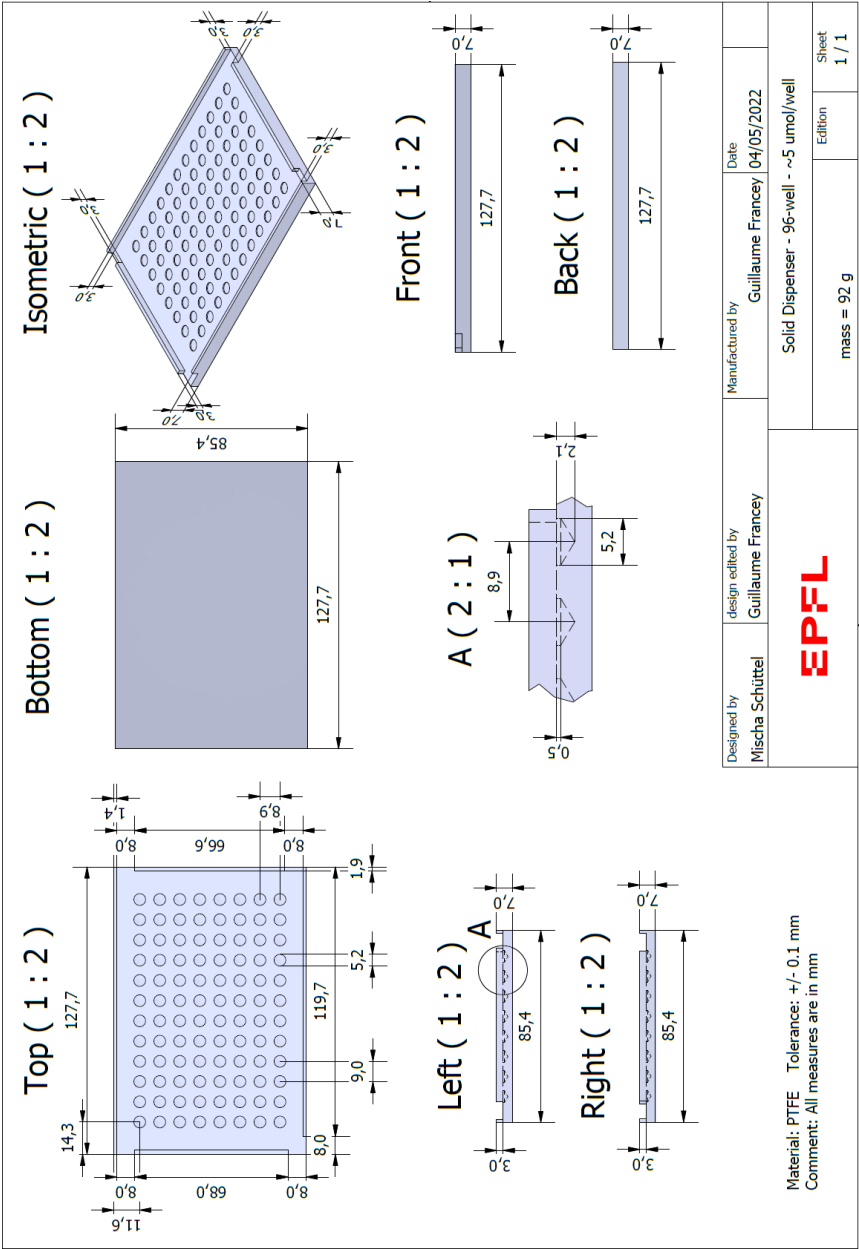
Edition
 mass = 315 g

– 190 –

Supplementary Figure 8: Continued.

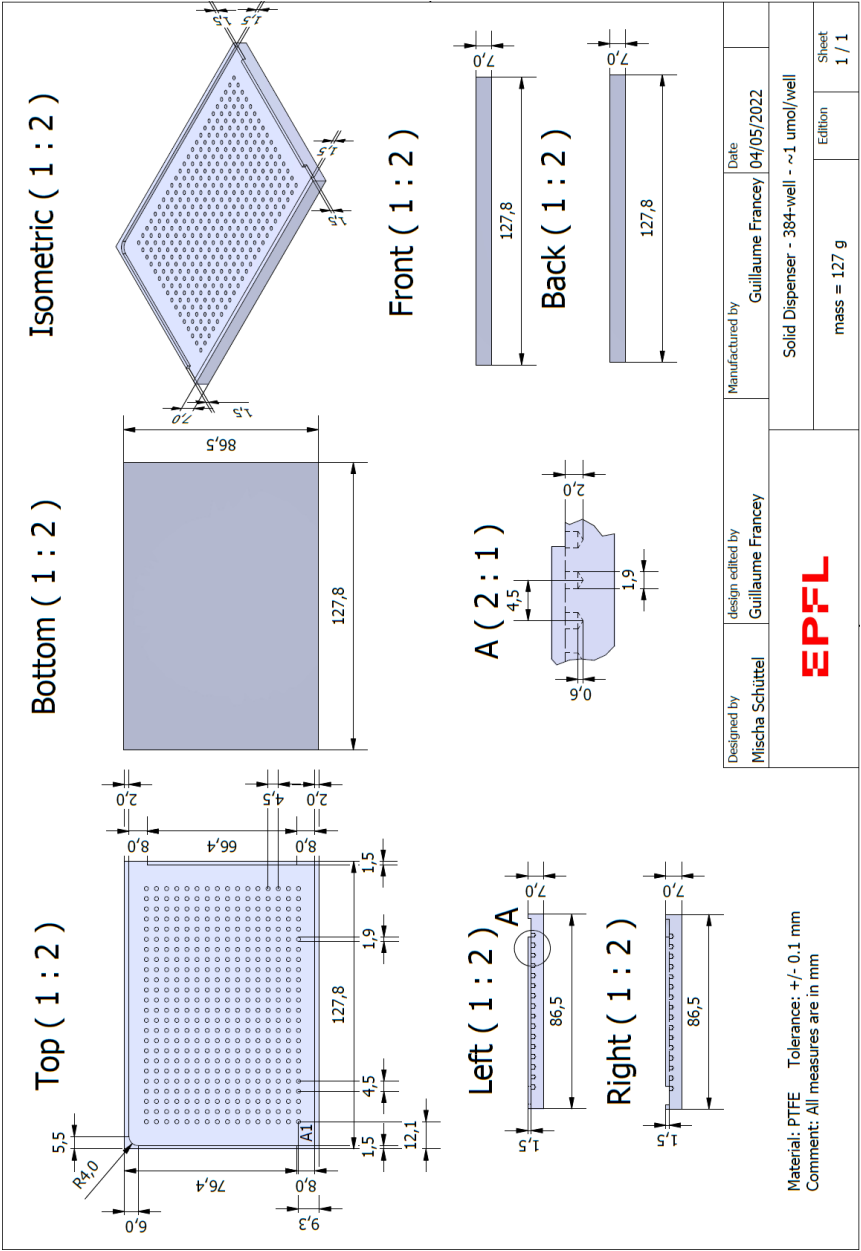


C

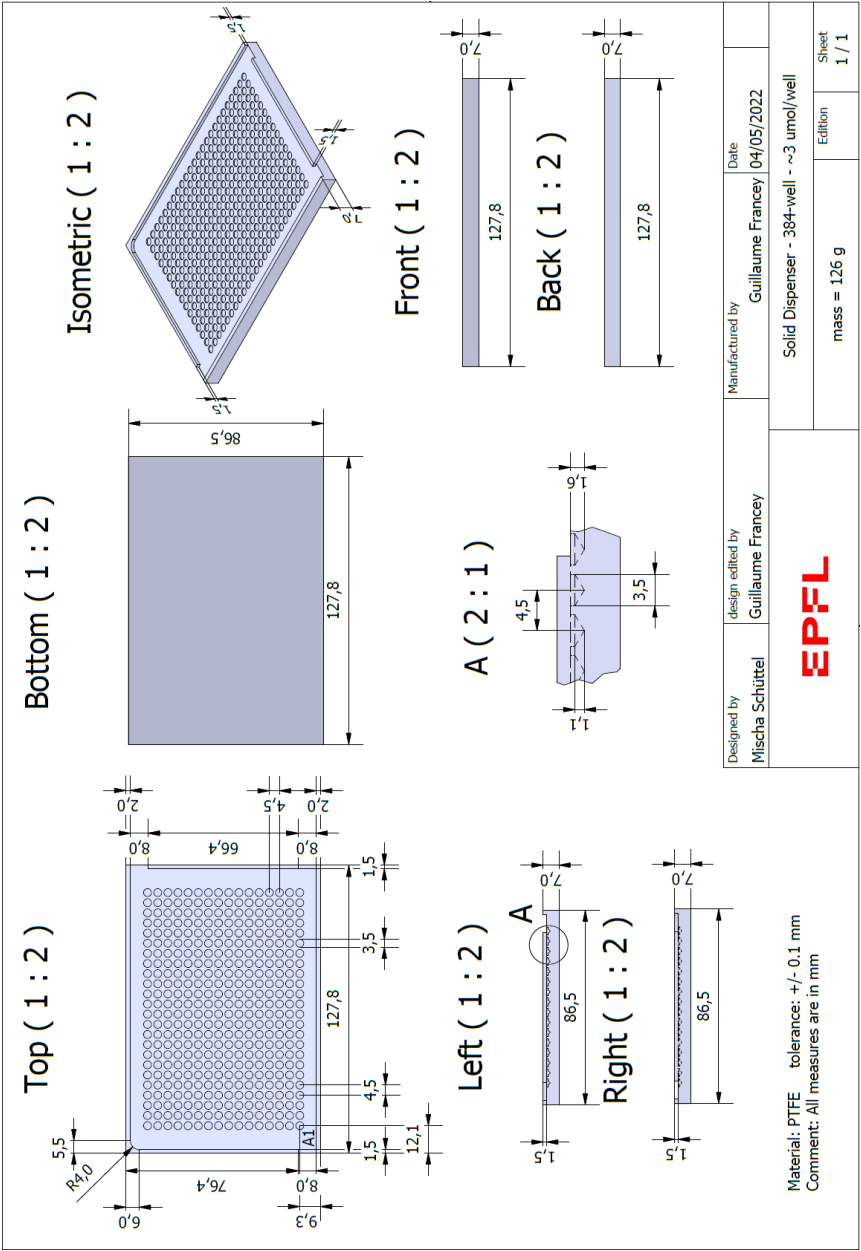


Supplementary Figure 8: Continued.

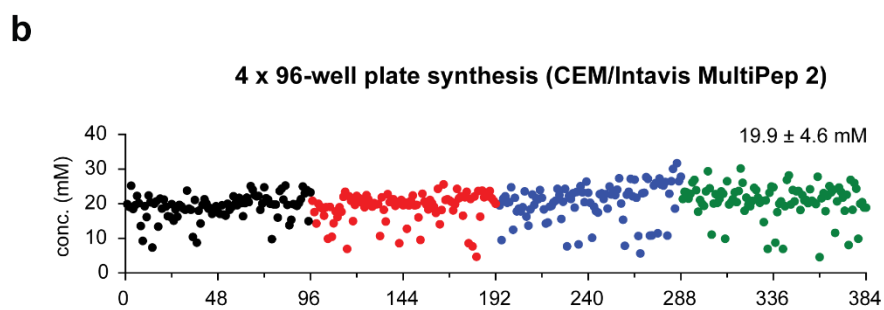
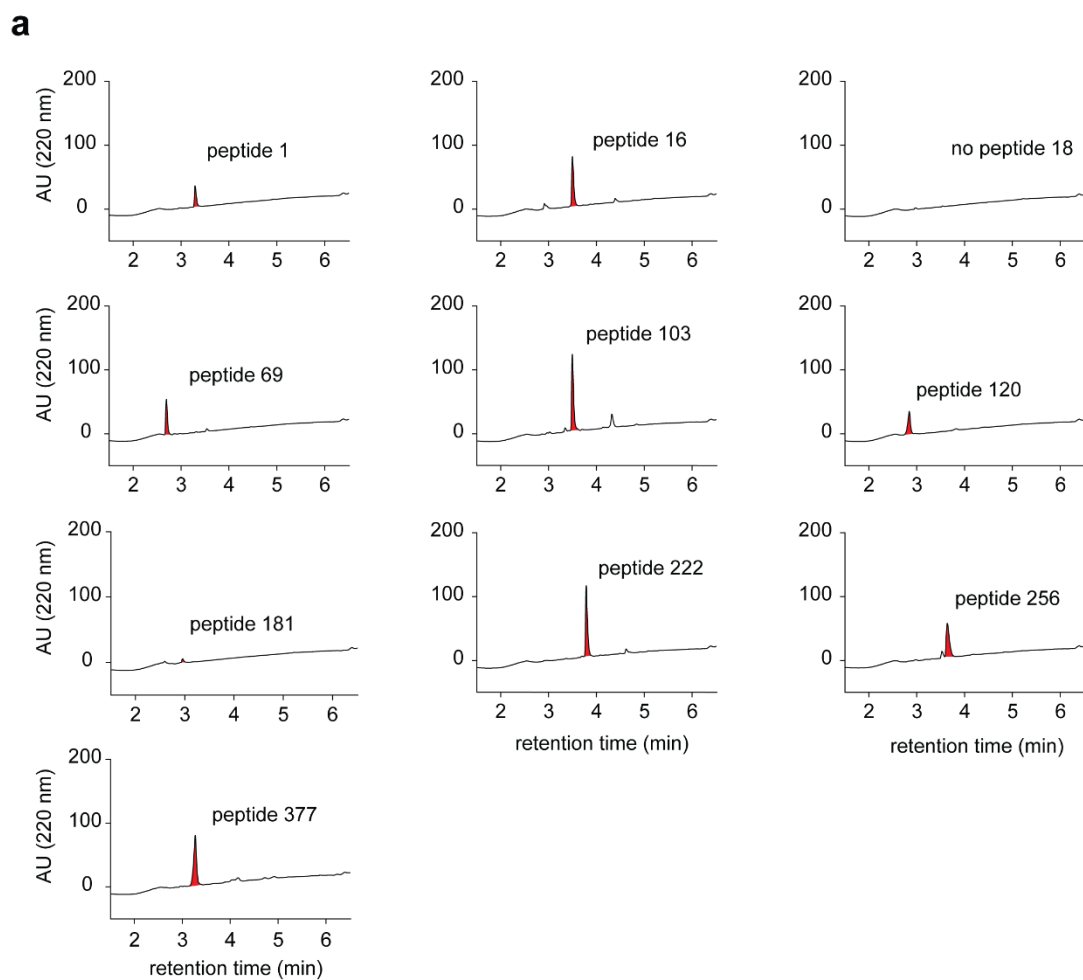
d



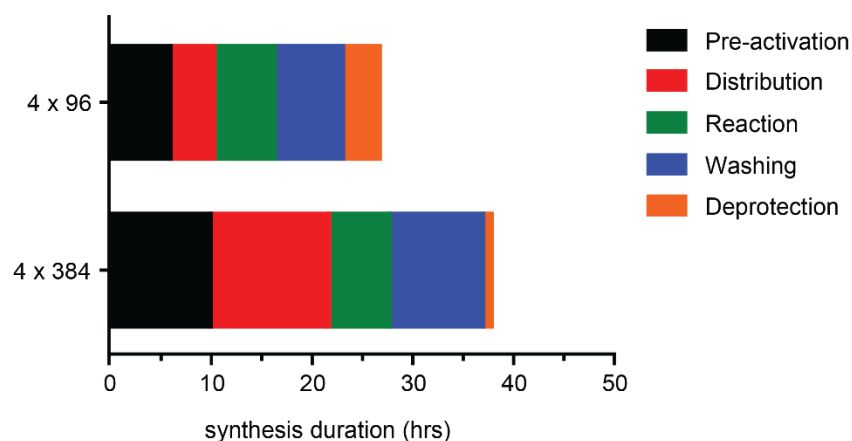
Supplementary Figure 8: Continued.



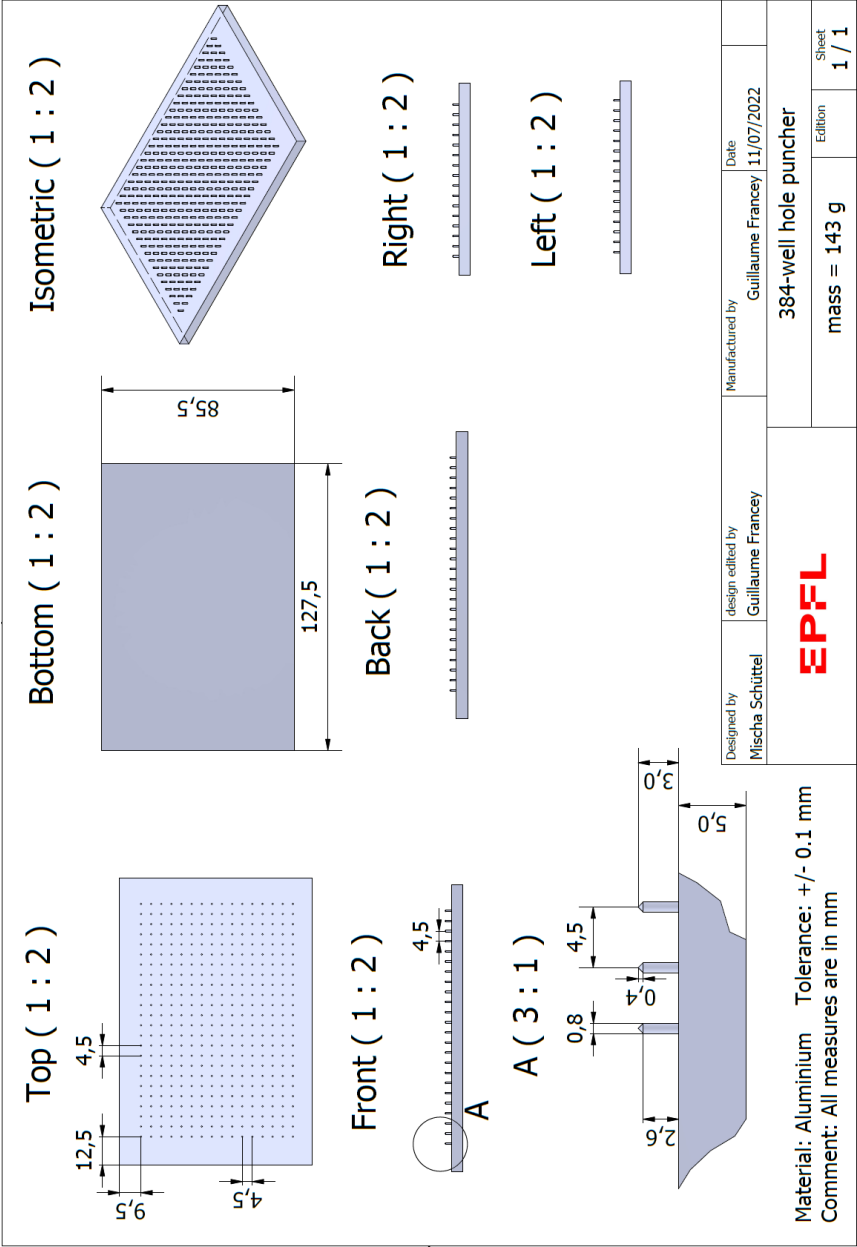
Supplementary Figure 8: Continued.



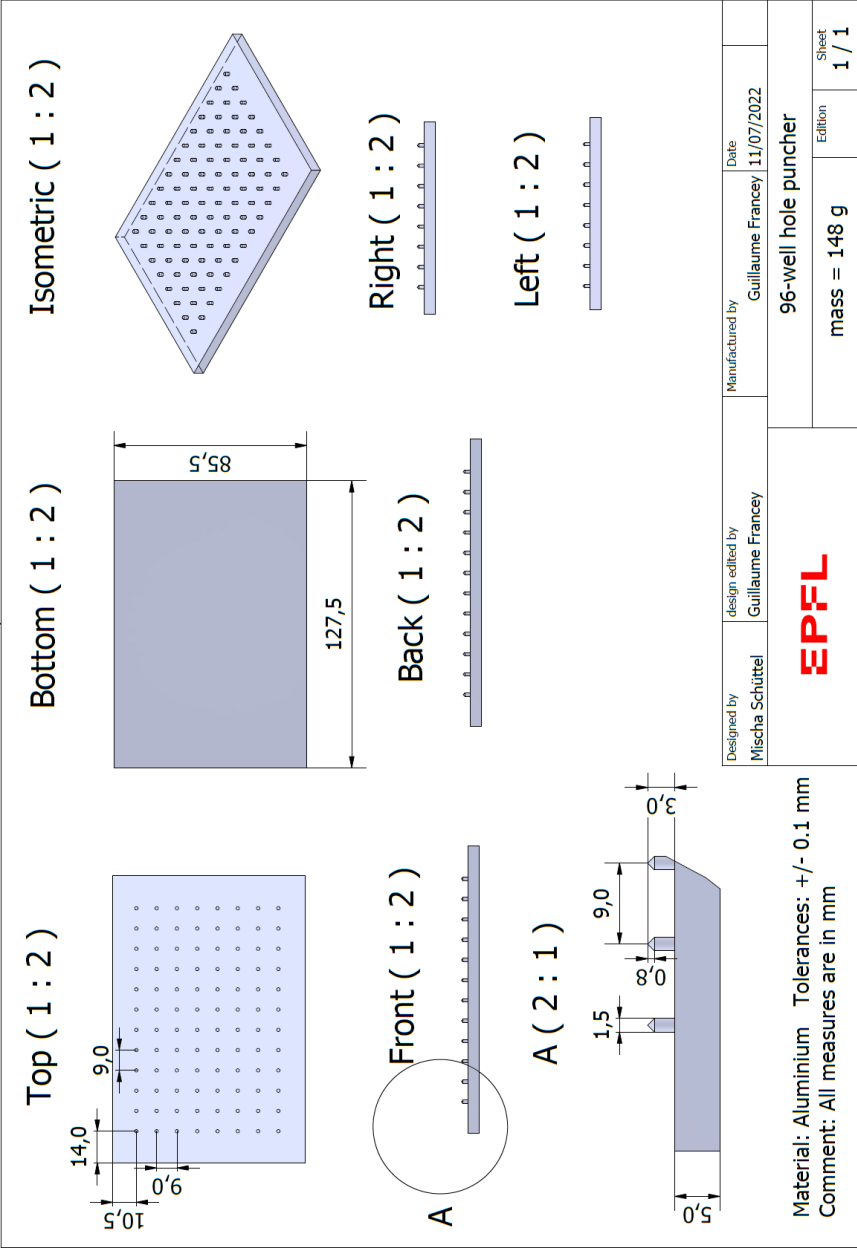
Supplementary Figure 9: Peptides synthesized with the CEM/Intavis MultiPep 2 in 96-well plates. (a) HPLC chromatograms of 8 randomly picked peptides. (b) Concentrations of peptides were quantified by reacting the thiol groups of the peptide with Ellman's reagent and measuring the absorbance.



Supplementary Figure 10: Time required for peptide synthesis in 96- and 384-well plates. The time required (~27 h) for the synthesis of 4 × 96 peptides (384 peptides in total) on a conventional peptide synthesizer (CEM/Intavis MultiPep 2) is compared to the time required (~38 h) for the synthesis of 4 × 384 peptides (1,536 peptides in total) on the herein modified synthesizer (modified CEM/Intavis MultiPep 2). The indicated data is shown for the short random peptides described in Figure 3. Cumulative required execution time of each individual task for 4 × 96-well / 4 × 384-well plate synthesis: Pre-activation (5.9 h / 9.9 h), distribution (4.3 h / 12 h), reaction (6.0 h / 6.0 h), washing (6.8 h / 9.3 h) and deprotection (3.7 h / 0.9 h).



Supplementary Figure 11: Technical drawing of the manual 384-well hole puncher. The pins ($d = 0.75$ mm, $h = 3.0$ mm) have sharpened tips and are made from aluminum.



Supplementary Figure 12: Technical drawing of manual 384-well hole punch. The pins ($d = 0.75$ mm, $h = 3.0$ mm) have sharpened tips and are made form aluminum.

Supplementary configuration files

The following configuration files can be used on a CEM/Intavis MultiPep 2 instrument to define the positions of the 384-well plate reactors and the reagent racks. For the manufacturing of hardware objects presented in this work, 3D files (STEP, STL) are available upon request.

1. Configuration files from synthesizer for 4 × 384 with 31 derivative rack
2. Configuration files from synthesizer for 4 × 384 with 57 derivative rack
3. Configuration files from synthesizer for 4 × 384 with 107 derivative rack
4. Configuration files from synthesizer for 4 × 384 with 395 derivative rack

Supplementary videos

A short visual illustration of the resin loading process is shown in a supplementary video file.

5.8 Reference

- (80) Kale, S. S.; Bergeron-Brlek, M.; Wu, Y.; Kumar, M. G.; Pham, M. V.; Bortoli, J.; Vesin, J.; Kong, X.-D.; Machado, J. F.; Deyle, K.; Gonschorek, P.; Turcatti, G.; Cendron, L.; Angelini, A.; Heinis, C. Thiol-to-Amine Cyclization Reaction Enables Screening of Large Libraries of Macrocyclic Compounds and the Generation of Sub-Kilodalton Ligands. *Sci. Adv.* **2019**, *5* (8), eaaw2851. <https://doi.org/10.1126/sciadv.aaw2851>.
- (81) Habeshian, S.; Merz, M. L.; Sangouard, G.; Mothukuri, G. K.; Schüttel, M.; Bognár, Z.; Díaz-Perlas, C.; Vesin, J.; Bortoli Chapalay, J.; Turcatti, G.; Cendron, L.; Angelini, A.; Heinis, C. Synthesis and Direct Assay of Large Macrocyclic Diversities by Combinatorial Late-Stage Modification at Picomole Scale. *Nat. Commun.* **2022**, *13* (1), 3823. <https://doi.org/10.1038/s41467-022-31428-8>.
- (87) Merrifield, R. B. Solid Phase Peptide Synthesis. I. The Synthesis of a Tetrapeptide. *J. Am. Chem. Soc.* **1963**, *85* (14), 2149–2154. <https://doi.org/10.1021/ja00897a025>.
- (88) Merrifield, R. B.; Stewart, J. M. Automated Peptide Synthesis. *Nature* **1965**, *207* (4996), 522–523. <https://doi.org/10.1038/207522a0>.
- (89) Carpino, L. A.; Han, G. Y. 9-Fluorenylmethoxycarbonyl Amino-Protecting Group. *J. Org. Chem.* **1972**, *37* (22), 3404–3409. <https://doi.org/10.1021/jo00795a005>.
- (91) Habeshian, S.; Sable, G. A.; Schüttel, M.; Merz, M. L.; Heinis, C. Cyclative Release Strategy to Obtain Pure Cyclic Peptides Directly from the Solid Phase. *ACS Chem. Biol.* **2022**, *17* (1), 181–186. <https://doi.org/10.1021/acscchembio.1c00843>.
- (106) Bognar, Z.; Mothukuri, G. K.; Nielsen, A. L.; Merz, M. L.; Pânzar, P. M. F.; Heinis, C. Solid-Phase Peptide Synthesis on Disulfide-Linker Resin Followed by Reductive Release Affords Pure Thiol-Functionalized Peptides. *Org. Biomol. Chem.* **2022**, *20* (29), 5699–5703. <https://doi.org/10.1039/D2OB00910B>.
- (145) Muttenthaler, M.; King, G. F.; Adams, D. J.; Alewood, P. F. Trends in Peptide Drug Discovery. *Nat. Rev. Drug Discov.* **2021**, *20* (4), 309–325. <https://doi.org/10.1038/s41573-020-00135-8>.
- (146) Smith, G. P. Filamentous Fusion Phage: Novel Expression Vectors That Display Cloned Antigens on the Virion Surface. *Science* **1985**, *228* (4705), 1315–1317. <https://doi.org/10.1126/science.4001944>.

- (147) Wilson, D. S.; Keefe, A. D.; Szostak, J. W. The Use of mRNA Display to Select High-Affinity Protein-Binding Peptides. *Proc. Natl. Acad. Sci.* **2001**, *98* (7), 3750–3755. <https://doi.org/10.1073/pnas.061028198>.
- (148) Schulte, C.; Khayenko, V.; Gupta, A. J.; Maric, H. M. Low-Cost Synthesis of Peptide Libraries and Their Use for Binding Studies via Temperature-Related Intensity Change. *STAR Protoc.* **2021**, *2* (3), 100605. <https://doi.org/10.1016/j.xpro.2021.100605>.
- (149) Schulte, C.; Khayenko, V.; Nordblom, N. F.; Tippel, F.; Peck, V.; Gupta, A. J.; Maric, H. M. High-Throughput Determination of Protein Affinities Using Unmodified Peptide Libraries in Nanomolar Scale. *iScience* **2021**, *24* (1), 101898. <https://doi.org/10.1016/j.isci.2020.101898>.
- (150) Szymczak, L. C.; Kuo, H.-Y.; Mrksich, M. Peptide Arrays: Development and Application. *Anal. Chem.* **2018**, *90* (1), 266–282. <https://doi.org/10.1021/acs.analchem.7b04380>.
- (151) Frank, R. Spot-Synthesis: An Easy Technique for the Positionally Addressable, Parallel Chemical Synthesis on a Membrane Support. *Tetrahedron* **1992**, *48* (42), 9217–9232. [https://doi.org/10.1016/S0040-4020\(01\)85612-X](https://doi.org/10.1016/S0040-4020(01)85612-X).
- (152) Hilpert, K.; Winkler, D. F.; Hancock, R. E. Peptide Arrays on Cellulose Support: SPOT Synthesis, a Time and Cost Efficient Method for Synthesis of Large Numbers of Peptides in a Parallel and Addressable Fashion. *Nat. Protoc.* **2007**, *2* (6), 1333–1349. <https://doi.org/10.1038/nprot.2007.160>.
- (153) Stadler, V.; Felgenhauer, T.; Beyer, M.; Fernandez, S.; Leibe, K.; Güttler, S.; Gröning, M.; König, K.; Torralba, G.; Hausmann, M.; Lindenstruth, V.; Nesterov, A.; Block, I.; Pipkorn, R.; Poustka, A.; Bischoff, F. R.; Breitling, F. Combinatorial Synthesis of Peptide Arrays with a Laser Printer. *Angew. Chem. Int. Ed.* **2008**, *47* (37), 7132–7135. <https://doi.org/10.1002/anie.200801616>.
- (154) Legutki, J. B.; Zhao, Z.-G.; Greving, M.; Woodbury, N.; Johnston, S. A.; Stafford, P. Scalable High-Density Peptide Arrays for Comprehensive Health Monitoring. *Nat. Commun.* **2014**, *5* (1), 4785. <https://doi.org/10.1038/ncomms5785>.

- (155) Hilpert, K.; Volkmer-Engert, R.; Walter, T.; Hancock, R. E. W. High-Throughput Generation of Small Antibacterial Peptides with Improved Activity. *Nat. Biotechnol.* **2005**, 23 (8), 1008–1012. <https://doi.org/10.1038/nbt1113>.

6. Use of microvalves for reagent dispensing in solid-phase peptide synthesis

6.1 *Work contribution*

Use of microvalves for reagent dispensing in solid-phase peptide synthesis

Mischa Schüttel,¹ Pamela Canjura Rodriguez,¹ Edward Will,¹ Gontran Sangouard¹ and Christian Heinis^{1,*}

¹Institute of Chemical Sciences and Engineering, School of Basic Sciences, École Polytechnique Fédérale de Lausanne (EPFL), CH-1015 Lausanne, Switzerland.

*Correspondence should be addressed to C.H. E-mail: christian.heinis@epfl.ch

KEYWORDS

384-well plate, 1536-well plate, combinatorial chemistry, microvalve, peptide library, peptide synthesis, solenoid valve

Author contribution: I conceptualized the idea of using microvalves for solid phase peptide synthesis and initiated and maintained the collaboration between EPFL and Fritz Gyger AG for simple feasibility studies of SPPS synthesis with the Certus Flex device. I and Christian Heinis conceptualized the experimental designs. All experimental executions and analysis were realized by me. Pamela del Carmen Rodriguez provided the filter inserts for the homemade 1536-well PP filter plate. Edward Will designed the library described in figure 23. Gontran Sangouard was involved in early-stage discussion for developing the idea. I wrote the first draft of the manuscript, and contributed to editing. Christian Heinis reviewed and edited the manuscript including figures.

Acknowledgment: We are grateful to Guillaume Francey and André Fattet from the mechanical workshop of the Institute of Chemical Sciences and Engineering for help with producing the 1,536-well resin loader device. The authors would like to thank Fritz Gyger AG for lending us the Certus Flex instrument essential for conducting our experimentation.

This chapter is based on a manuscript for publication and was supported by an SNSF grant (192368).

6.2 *Abstract*

The parallel synthesis of large numbers of peptides offers new opportunities in drug development, such as the rapid diversification and improvement of bioactive peptides or the generation and screening of vast libraries of random peptides. Up to 96 peptides can be produced by solid-phase peptide synthesis (SPPS) in microwell plate reactors using commercial synthesizers. Recently, the synthesis scale was increased by establishing SPPS in 384-well plates, but a challenge with classical SPPS equipment is the reagent transfer by syringes that prevents accurate and rapid dispensing of small reagent volumes. In particular, the transfer of small volumes of trifluoroacetic acid (TFA) to 384-well plates has been difficult and needed to be performed manually by multichannel pipettes. Herein, we have applied microvalves for reagent dispensing to 384-well plates, which allowed efficient transfer of solvents and reagents to 384-well reactors used in peptide synthesis, including the corrosive acid TFA. As a proof-of-principle, we synthesized a library of 384 short peptides using microvalve dispensing. In a pilot trial, we were able to apply microvalve dispensing even for the synthesis of peptides in a custom-fabricated 1,536-well plate reactor. The high-throughput microvalve-based peptide synthesis overcomes a limit of syringe-based synthesizers and enables the facile synthesis of large number of peptides.

6.3 Introduction

Peptides offer an attractive modality for drug development due to their ability to bind to challenging targets, usually high specificity, a modular structure, and the availability of powerful chemical synthesis and development techniques. The process of generating a new peptide drug typically requires the synthesis of large numbers of peptides, often several hundreds or thousands of peptides for a single drug. Usually, natural bioactive peptides or *de novo* developed peptides identified by phage or mRNA display serve as starting points that are then improved in iterative cycles of synthesizing and screening peptide variants. Even larger peptide synthesis capacities are required if peptide drugs are to be developed *de novo* by synthesizing and screening random libraries of peptides. For example, our laboratory recently identified inhibitors of thrombin and ligands of MDM2 by screening random libraries of short cyclic peptides, which required the chemical synthesis of thousands of random peptides.⁹¹ While the major bottleneck in accessing large numbers of peptides has been the purification for a long time, several recently developed methods have enabled the purification-free production of short peptides. Such methods rely on the synthesis of peptides on solid phase via a TFA-stable linker to remove side chain protecting groups while the peptide is on solid phase, and subsequent selective release of unprotected, rather pure peptide.^{91, 106} The upper limit of peptides that today be accessed essentially depends on how many peptides can be synthesized.

Automated solid-phase peptide synthesis (SPPS) can produce large numbers of synthetic peptides in which reagents are transferred from source tubes to reactor wells following a sequence that can be programmed and performed unattended. In most parallel peptide synthesizer systems, reagents and solvents are transferred by a syringe pump and a needle that can be moved in all three dimensions (Figure 21a). Commercially offered automated peptide synthesizers can produce peptides in 96-well formats, including Syro I and II (Biotage), MultiPep 1 and 2 (CEM, formerly Intavis), and Apex 396 (Aapptec). Some of these synthesizers can accommodate four 96-well plate reactors and thus synthesize 384 peptides in one run. Our laboratory has recently modified a MultiPep 2 synthesizer with hardware to enable synthesis in 384-well plates, which allows now the synthesis of 1,536 peptides in one run (chapter 5). A bottleneck in the 384-well synthesis of peptides has been the protection group removal by TFA that cannot be done in the

peptide synthesizer due to corrosion by TFA and has to be performed manually by an 8-line multi-channel pipette that is protected by charcoal filter tips. Other limitations in 384-well synthesis are the need for x- and y-position calibration of the dispensing needle of the instrument due to the small diameter of the wells, and the limited speed of syringe-based liquid dispensing (Figure 21a). To synthesize even larger numbers of peptides, SPPS could potentially be performed in 1,536-well plates. However, the precision and speed of syringe-based dispensing offered by current instruments are not sufficiently good.

Highly precise and rapid reagent and solvent transfer can be achieved by various technologies ranging from valve-based systems, over micro pipetting, to acoustic liquid transfer. In valve-based devices, reagents under positive pressure pass a valve that regulates the volume delivered through the time it is kept open.¹⁵⁶ For example, the SMLD microvalves of the Certus Flex (Fritz Gyger AG) can dispense accurate nano- and microliter volumes to 96-, 384- and 1,536-well plates.¹⁵⁷ Mosquito dispensing (SPT Labtech) offers the transfer of 500 nl to 5 μ l volumes by disposable micropipettes by positive pressure displacement.¹⁵⁸ Acoustic droplet ejection (ADE) allows the transfer of liquids by applying a pulse of ultrasound to the bottom of a microwell plate to move low volumes of fluid to a plate that is placed upside-down above, all without any physical contact.¹⁵⁹ For example, ECHO systems (Beckman Coulter, formerly developed by Labcyte) can transfer 2.5 nl volume increments to dispense nanoliter to microliter volumes. Another non-contact dispensing system, the I.Dot or Flex DropTM iQ (Dispendix, PerkinElmer) can transfer droplets of 8 to 50 nl through small holes in wells of a 96-well plate upon application of positive controlled pressure. To our knowledge, none of the above techniques have been applied to transfer reagents and solvents for peptide synthesis. Valve-based liquid dispensing is used for synthesizing DNA in a 384-well plate format by the device Dr. Oligo 768XLc (Biolytic), showing that valve dispensing is suited for solid-phase synthesis and the transfer of small volumes of reagents and organic solvents. Valve-based dispensing was also used in a proof-of-concept study to synthesize oligonucleotides in a 1,536-well plate,¹⁶⁰ further validating valve-dispensing and showing that this technology can be applied for solid-phase synthesis in the small wells of 1,536-well plates.

In this work, we have investigated the applicability of microvalve technology for transferring reagents and solvents in SPPS. We chose to use SMLD microvalves (Fritz Gyger AG) as these valves have a high chemical resistance and promise to be compatible with even highly corrosive reagents such as TFA needed in peptide synthesis (Figure 21b and 21c). We used a Certus Flex system (Fritz Gyger AG) with eight valves that each could be regulated individually to dispense nano- and microliter volumes with high precision and speed to wells of 384- and 1,536-well synthesis plates. We found that the valves are resistant to all reagents and solvents required for peptide synthesis, including TFA; and that short peptides can efficiently be synthesized in 384- and even 1,536-well plates.

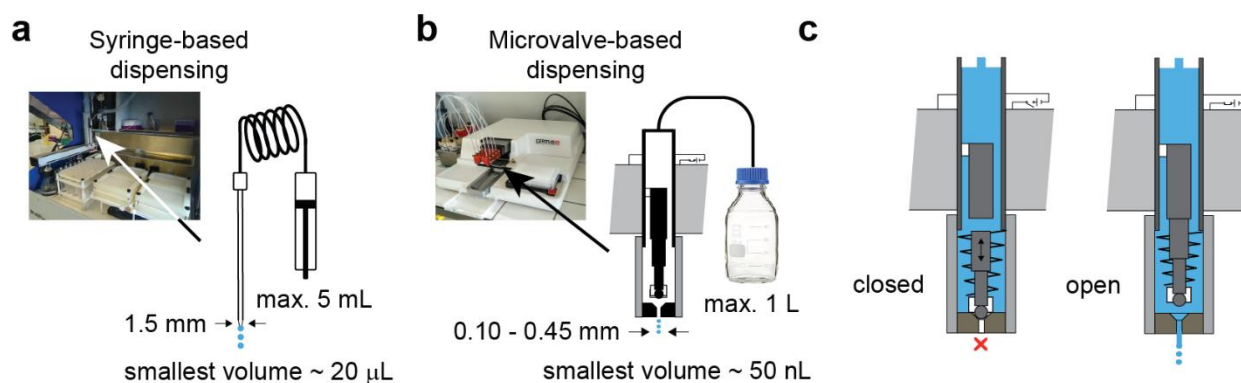


Figure 21: Reagent and solvent transfer in solid phase peptide synthesis. (a) Reagent transfer by a syringe as used in commercially provided parallel peptide synthesizers. As example, the CEM/Intavis MultiPep 2 peptide synthesizer is shown (photo) together with dimensions of the syringe and needle outlet diameter (schematic drawing). (b) Reagent dispensing by microvalves illustrated with a Gyger Certus Flex bulk dispenser. The schematic drawings show a microvalve with the outlet diameter indicated. (c) Schematic drawing of an electromagnetically controlled microvalve in closed and open state. A spring pushes the ball against the opening to close the valve.

6.4 Results & discussion

Microvalve reagent dispensing to 384-well reactor plates

To test the dispensing of reagents and solvents by microvalves, we used the solenoid microvalve liquid dispensing technology of the Certus Flex nanoliter dispenser from Gyger AG (Figure 21a). The SMLD technology allows the transfer of liquids with a smaller than 2% error for a 1 μ l volume and a speed of 11 seconds per 384-well plate if eight channels are used to dispense 5 μ l per well. For the synthesis of peptides in 384-well plates, we planned dispensing volumes between around 10 and 100 μ l. It was important that peptide synthesis reagents dispensed to the synthesis plate did not pass through the polyethylene (PE) frits of the wells by gravity force. Liquids with low surface tensions, such as dimethylformamide (DMF), dichloromethane (DCM), and TFA passed the frits, and the outlets of the reactor plate had thus to be closed. We sealed them by pressing the plates into 1 cm thick ethylene-vinyl acetate (EVA) foam pads (having identical size as the plate) with strong physical force. For steps that did not require long exposure of the resin to the solvent, such as washing steps, we placed the plate onto a 384-deep well plate. The plate with the foam pad or the plate on the deep well plate was then placed onto the Certus Flex plate holder and mechanically fixed by a plate positioner that pressed against one of the corners of the foam pad or deep well plate. The height of the valves was adjusted to be 3 mm above the upper surface of the 384-well plates. We tested microvalve-based liquid transfer by dispensing 10 μ l volumes of DMF and found that the liquid was accurately transferred to all wells.

Solvent and reagent compatibility

We tested the compatibility of the system (SMLD microvalves and accessories, not Certus Flex device) with solvents required in peptide synthesis. For all tests, we used microvalves that were most resistant to corrosive reagents, being the “Gyger Certus Resistant” (GCR) microvalves (Fritz Gyger AG, 24651). For the transfer of volumes between 10 and 100 μ l we used the GCR 0.20/0.10 mm microvalves. For each solvent, we calibrated one microvalve to be used at a pressure of 0.300 bar. By repetitively dispensing different volumes ranging from 60 nl to 140 μ l of DMF, DCM, and TFA, and

weighing the transferred amount, we found that all solvents were efficiently and precisely dispensed. For TFA, we observed impairment at the o-rings of the caps from the Falcon tubes from which TFA was dispensed. The damage to the o-rings could be prevented in subsequent experiments by using chemically resistant o-rings. No damage was caused to the microvalves, indicating that they resisted these harsh chemical conditions. After repetitive use of TFA, we found that TFA caused some corrosion at metal parts of the instrument not related to the microvalves, suggesting that exposure of the instrument to TFA vapor should be minimized.

TFA-deprotection of peptides in 384-well plates

For the deprotection of amino acid side chains of peptides synthesized in 384-well plates, the resin needs to be incubated with TFA. The addition of TFA to wells of 384-well reactor plates cannot be performed by a syringe-based parallel peptide synthesizer due to the corrosion of metal parts by TFA. Consequently, we so far dispensed TFA to wells of 384-well reactor plates manually with 8-line multichannel pipettes protected with charcoal filter tips. The manual transfer of 30 μ l volumes to all wells of 384 well plates is physically demanding to the experimenter due to the large number of repetitive transfers (48 times per 384 well plate and cycle) and difficult as it has to be performed in a fume hood due to the health risks of TFA. The compatibility of the microvalves with TFA was thus of high practical relevance as we could now conveniently and rapidly add TFA to well of 384-well reactor plates. As expected, TFA was accurately dispensed by the Certus Flex instrument and the protecting groups were equally well removed as when the TFA was added by a pipette.

Peptide synthesis in 384-well plates by microvalve dispensing

We next tested if peptides can be synthesized in 384-well plates, dispensing all reagents and solvents by microvalves using the Certus Flex dispenser and standard SPPS conditions. We synthesized the peptides on a disulfide-linker resin that allows on-resin side-chain deprotection and mild release of the peptides by disulfide bond reduction.¹⁰⁶ All peptides contained at the N-terminus a mercaptopropionic acid (Mpa) and at the C-terminus a mercaptoethylamine (Mea) group, and two random amino acids

chosen from Trp, Gln, and Pro, giving nine combinations (Figure 22a). We synthesized the nine different short peptides in 384-well plates, each one 40 times and thus in total 360 peptides (Figure 22b). Of the eight valves we had available in the Certus Flex, two were used to dispense DMF, two for piperidine/DMF, one for each of HATU-activated Fmoc-tryptophane, Fmoc-glutamine, Fmoc-proline, and MPA. We applied standard Fmoc synthesis conditions, wherein the volumes of reagent and solvents used were adapted to the small synthesis scale (3 μ mol) and the small dimension of the 384-reactor plate wells (Figure 22c). To remove solvents and reagents from the wells, we manually transferred the plates to a plate vacuum filtration station (Intavis). For deprotecting amino acid side chains as well as for releasing the peptides, we washed four of the microvalves and used them for resin washing with DCM (one valve), dispensing TFA (one valve), and releasing solution (two valves).

To assess the synthesis's quality and yield, we analyzed peptides synthesized in five different regions of the 384-well plate (Figure 22b). LC-MS analysis of the nine different peptides synthesized in the left top corner of the 384-well plate showed that all peptides were synthesized (Figure 22d). Four of the peptides showed two peaks that corresponded to the expected mass and that were most likely isomers. We analyzed an additional 36 peptides that were synthesized in four different regions of the plate (Figure 22b) and found a similar result, indicating that peptides were efficiently produced in all wells of the plate. For all the analyzed 45 peptides, we found a purity of $72 \pm 11\%$ (Supplementary Table 9) and a concentration of 18.0 ± 4.1 mM (in ~ 30 μ l, Supplementary Figure 13) which corresponded to a yield of around 13%. *t*Bu capped side product varied from 0 to 16 % (average 5%). Taken together, we found that microvalve dispensing is suited to synthesize short peptides in 384-well plates.

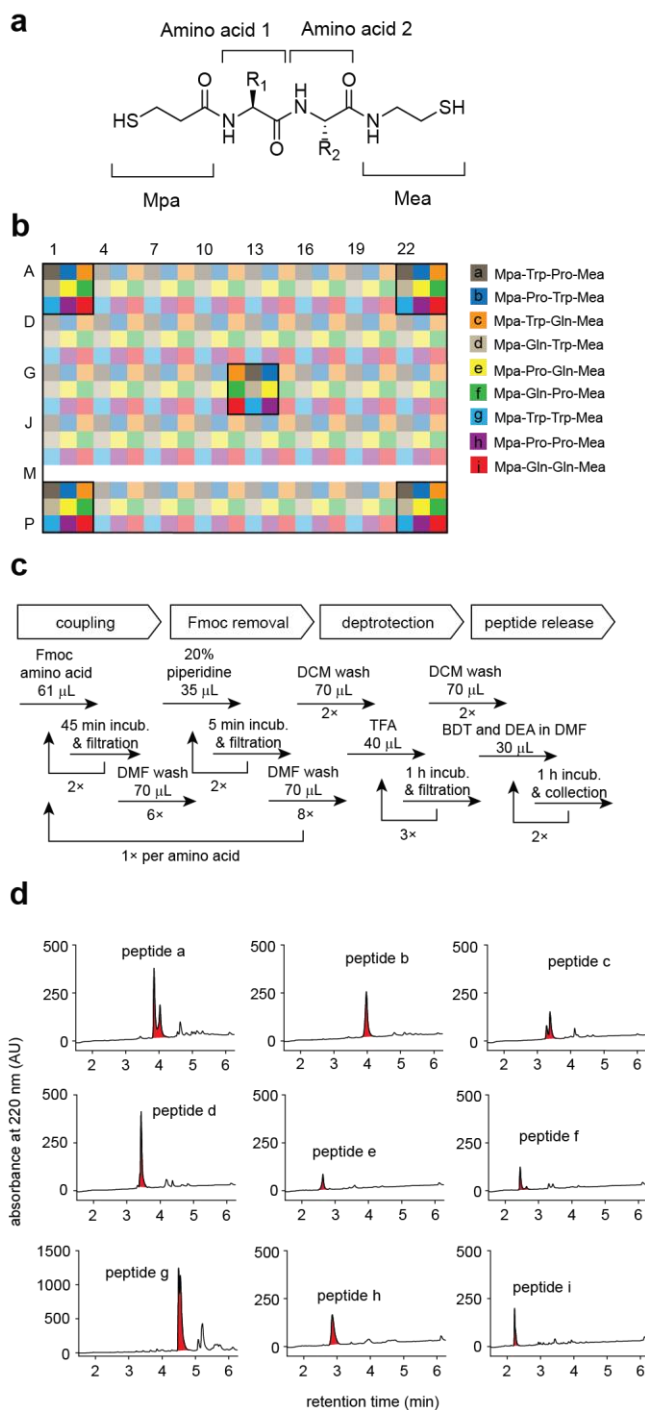


Figure 22: Peptide synthesis is 384-well plate reactor. (a) Format of peptides synthesized. Amino acids 1 and 2 are chosen from Gln, Pro and Trp. Mpa = mercaptopropionic acid, Mea = mercaptoethylamine. (b) 384-well reactor layout. Nine different peptides, each peptide shown by a different color, were synthesized 40 times. The peptides in the five highlighted regions were analyzed by LC-MS. (c) Peptide synthesis procedure indicating the volumes of reagents and solvents dispensed by microvalves. (d) RP-HPLC chromatograms of the nine peptides synthesized in the top left corner of the reactor plate shown in panel (b).

Synthesis of a 384-member peptide library

We next applied microvalve dispensing for the synthesis of a large combinatorial library comprising 384 cyclic 4- or 5-mer peptides (Figure 23a, Supplementary Table 8). For the peptides, we chose semi-random sequences that were tailored for identifying ligands against IL-23 receptor (project being published elsewhere). Amino acids in randomized positions of these peptides were chosen from 51 chemically and structurally diverse Fmoc amino acids (Figure 23b). Given the limited number of eight valves of the applied dispenser, we decided to transfer the 51 amino acid building blocks by syringes of a parallel peptide synthesizer. At the same time, we took advantage of the microvalve dispenser for rapidly transferring solvents for the numerous washing steps (DMF, DCM), reagents for Fmoc deprotection (20% v/v piperidine in DMF), and reagents for amino acid side chain deprotection (TFA). Between the different steps of synthesis, we transferred the 384-well plate manually between the three devices being, the peptide synthesizer (amino acid coupling), the microvalve dispenser (washing and deprotection), and the vacuum device. LC-MS analysis of the product in ten randomly picked wells revealed that peptide was synthesized in all of them, with an average purity of $68 \pm 13\%$ (Figure, 23c). Quantification of yields of all 384 peptides by Ellman's reagent and absorbance measurement showed that peptides were obtained at an average concentration of 17 ± 5.1 mM (in around 30 μ l; Figure 23d), corresponding to 9% relative to the amount of functional group on the resin. The linear dithiol peptides were subsequently cyclized by bis-electrophilic linkers, and the quantity and quality were found suited for activity screens (shown elsewhere).

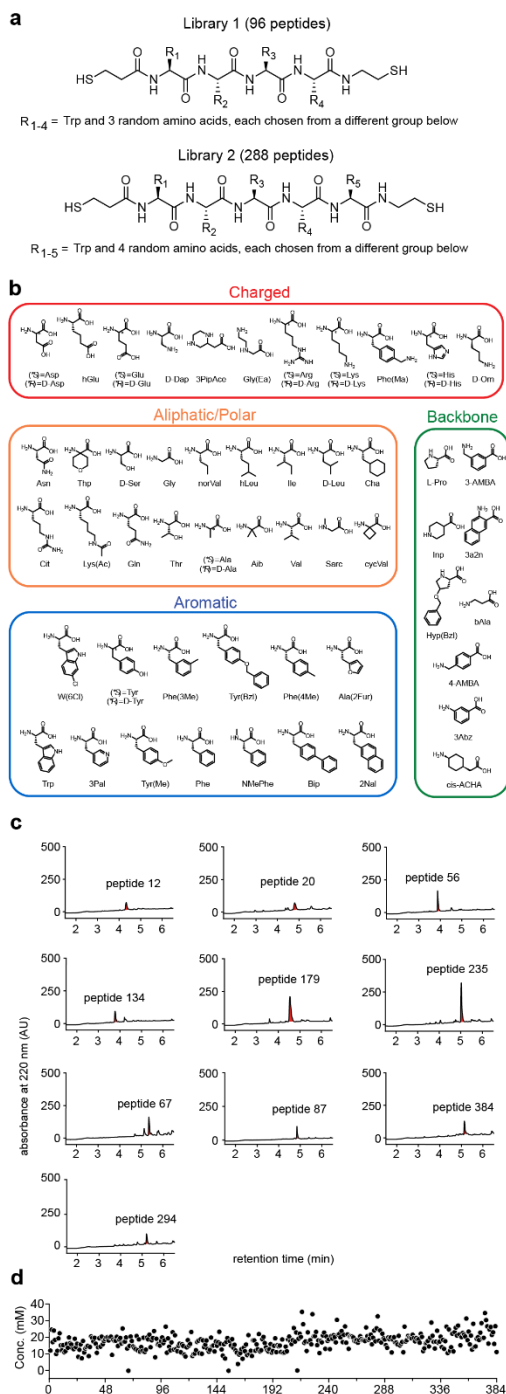


Figure 23: Synthesis of a 384-member peptide library. (a) Format of peptides and strategy for choosing the amino acids in the four or five random positions R1-R5. (b) Amino acids used for the synthesis of the random peptide library. (c) RP-HPLC chromatograms of ten randomly chosen peptides of the library. (d) Concentrations of the 384 peptides, determined by absorbance measurement after reaction the peptides' thiol groups with Ellman's reagent.

Peptide synthesis in 1,536-well plates

The successful synthesis of peptides in 384-well plates using microvalve reagent dispensing encouraged us to try peptide synthesis in 1,536-well plates. Given the lack of commercial PP filter plates in this format, we built a 1,536-well SPPS reactor plate (Figure 24a). In brief, we drilled 0.4 mm holes into the centers of all wells of a 1,536-well PP deep well plate. We then cut 1.9 × 3.0 mm ashless filter paper inserts and plugged them into the wells. To this plate, we transferred resin using a solid dispenser device as follows. We prepared a polytetrafluoroethylene (PTFE) plate having small conical cavities with volumes corresponding to a desired amount of resin, arrayed exactly as the wells of a 1,536-well plate (Figure 24b and Supplementary Figure 13). The resin was then swollen in DMF, the DMF filtered away, and the resin was placed onto the device and distributed by spreading with a blank PTFE plate to fill the arrayed holes and to remove the excess of resin. Next, the reactor plate was placed upside-down on top, and the sandwich turned to transfer the resin to the reactor wells by centrifugation (Figure 24c). The optimal amount of resin was assessed beforehand using a "size-tester" resin dispenser having holes of different sizes as previously described (chapter 5). For the synthesis in 1,536-well plates, we used resin for a 1 μ mol-scale synthesis (around 1 mg resin per well). For testing SPPS in the 1,536-well reactor plate, we synthesized the same nine short peptides as shown in Figure 2, but due to the larger number of wells in a 1,536-plate, we synthesized each peptide 160 times (and some 172 times) (Figure 24d). Given the smaller volumes in wells of 1,536-plates, we adapted the volumes of reagents and solvents (Supplementary Figure 14a). The dispensing of the small volumes was fast and accurate and the filtration of excess reagents and solvents applied in the washing steps worked well. For some of the wells, we observed that the filter paper inserts ruptured or loosened during the synthesis, indicating that better 1,536-well filter plates are needed (Figure 24e). For the release of peptides, it was not possible to stack the synthesis plate onto a receiver plate because the custom-made synthesis lacked conical well outlets. We therefore transferred the released peptide by manual pipetting from the reactor plate to tubes. Nine peptide sample chromatograms (UHPLC-MS) show that SPPS in 1536-well plates is possible. They have an average purity of $82 \pm 7.3\%$ (Supplementary Figure 15b). The major side product in the shown chromatograms was *t*Bu capped product ranging from 0-12% (average 5%).

For many other peptide samples (45 total, Supplementary Table 10) some cross-contamination and lower peptide quality was observed and it was mainly due to the absent of integrated reactor plate outlet welltips. The overall determined peptide purity was determined to be $72 \pm 7.3\%$ for all 45 samples (Supplementary Table 10). While the fabrication of the filter reactor plate requires improvement to prevent detachment of the filter frits (e.g. increasing yield), the experiment showed that microvalve dispensing is suited for the SPPS in a 1,536-well format.

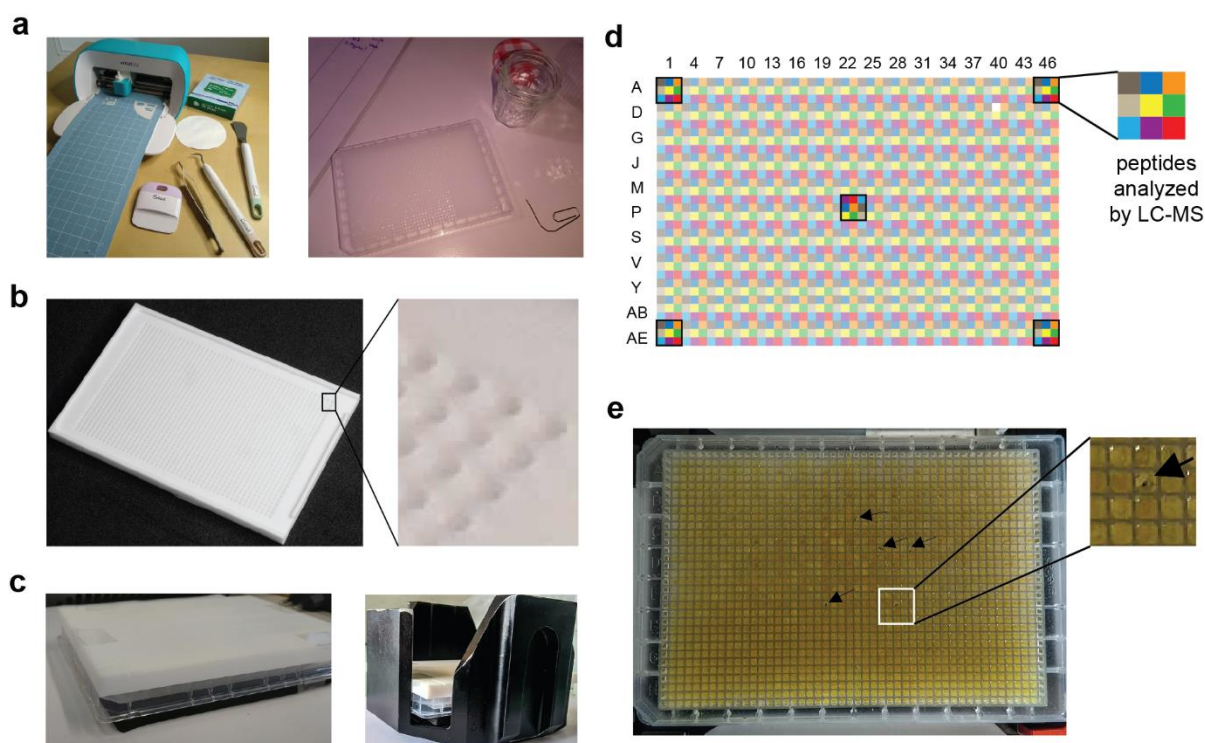


Figure 24: Peptide synthesis in 1,536-well plate reactor. (a) Production of 1,536 well filter plate by drilling holes into a commercial PP plate and inserting filters cut to have the size and shape of the wells. (b) Resin dispenser device for 1,536 well reactor. The enlarged region shows conical cavities. (c) Resin dispenser placed upside-down on 1,536 well reactor (left). Sandwich is placed in swing-out centrifugation buckets to spin and transfer the resin (right). (d) Layout of 1,536 well plate with colors indicating the nine different peptides synthesized. Peptides of highlighted regions were analyzed by LC-MS. (e) Reactor after SPPS. In wells indicated with an arrow, the filter frit was detached during the synthesis process.

6.5 *Conclusion*

We have tested the use of microvalves for transferring small volumes of reagents and solvents in SPPS and found that this technology is highly suited. Using a bulk dispenser, we were able to transfer any reagent and solvent of choice to 384- and 1,536-well reactor plates, all with high precision and speed. Applying valves with high chemical resistance allowed even the transfer of TFA that we had so far to transfer manually due to its corrosive nature. In proof-of-principle studies, we show that microvalve dispensing is suited for synthesizing large number of peptides in 384- and 1,536-well plates. For the synthesis of a diverse library of 384 different peptides formed of more than 50 different amino acids, we had to use a conventional peptide synthesizer for the amino acid coupling as the dispenser did not have enough valves, but this problem may be solved with instruments that have a larger number of microvalves. In addition to this, an integrated filtration station would be of great value. For the synthesis in 1,536-well plates, we faced the problem that filter plates were not available commercially, but such plates will likely be fabricated by commercial providers, particularly if instruments become available that can synthesize peptides in such plates. The integration into a continuous work flow procedure involving automatized infrastructure, which the Certus Flex is build for, could even further boost high-throughput SPPS synthesis.

6.6 *Material & methods*

Reagent abbreviations

Unless otherwise noted, all reagents were purchased from commercial sources and used with no additional purification. The solvents were not anhydrous nor were they dried prior use. The following abbreviations are used in this article: MeCN (acetonitrile), BDT (1,4-butanedithiol), d= diameter, DCM (dichloromethane), DIPEA (diisopropyl ethyl amine), 5,5'-dithiobis(2-nitrobenzoic acid) (Ellman's reagent), DMF (dimethylformamide), DMSO (dimethylsulfoxide), DWP (deep well plate), EVA (ethylene-vinyl acetate), FEP (Tetrafluoroethylen-Hexafluorpropylen-Copolymer), FFKM (perfluoroelastomer), Fmoc (Fluorenylmethoxycarbonyl), l = length, HATU ((1-[bis(dimethylamino)methylene]-1H-1,2,3-triazolo[4,5-b]pyridinium-3-oxide hexafluorophosphate, Mea (2-mercaptoethylamine), MeOH (methanol), Mpa (3-mercaptopropionic acid), NMM (N-methylmorpholine), NMP (N-methylpyrrolidone), PE (polyethylene), PEEK, (polyetheretherketone), PP (polypropylene), PS (polystyrene), PTFE (polytetrafluoroethylene), TEA (triethyl amine), TFA (trifluoro acetic acid), TIS (triisopropyl silane), Trt (trityl).

Quality of chemicals

Ammoniumbicarbonate (Sigma-Aldrich, 99-101%), BDT (Sigma-Aldrich, >97%), MeCN (Fisher Chemical, >99.8%), DCM (Sigma-Aldrich, >99.9%), DIPEA (Carl Roth GmbH + Co KG, >99.5%), DMF (Sigma-Aldrich, >99.8%), DMSO (Sigma-Aldrich, >99.5%), Ellman's reagent (Sigma-Aldrich, 99%), Fmoc amino acids and derivatives (GL Biochem Shanghai Ltd, >99%), HATU (GL Biochem Shanghai Ltd, >99%), Mea (abcr, 95%), Mpa(Trt)-OH (CombiBlock, 95%), NMP (Thermo Scientific, 99%), NMM (Sigma-Aldrich, >98%), piperidine (Acros Organics, 99%), amino methyl PS resin (aapptec, 100-150 mesh, 1.39 mmol/g), TEA (Fluka Analytical, >98%).

Disulfide-linked cysteamine resin preparation

As described in chapter 5 (Material & methods).

Resin transfer into well plates using a solid dispenser

A device for loading resin to 1,536-well plates was fabricated as described before for 96- and 384-well plates in chapter 5. The dimensions for the new resin loading device are shown in Supplementary Figure 14. To transfer all resin efficiently, a centrifugation speed of $\sim 3000 \times g$ was used. It was important to place the 1536 deep well plate onto a 6 mm thick EVA foam pad to distribute the weight across a larger area preventing cracking of the plate's Xyz during centrifugation. The 1536-well resin dispenser does not need centrifugation buckets with high walls (Thermo Scientific, 75006449 P), also other buckets such as these from Sigma (13421) work as well since the resin dispenser is designed to lock x and y-axis movement during centrifugation. The loading of resin (AM PS NH₂, aapptech, RAZ001, Lot: 9952639, 100-150 mesh) was tested (10 samples, A6, B7, C8, D9, E10, F11, G12, H13, I14 & J15) by weighing the transferred amount of resin inside the well for the specifically used cavity dimensions of the 1536-well plate solid dispenser (Supplementary Figure 14). The to be transferred resin amount (DMF wet, dry vs wet factor = 3.4) was 1.9 ± 0.2 mg/well ($\pm 11\%$) leads to a general loading per well of 0.56 ± 0.06 μ mol/well ($\pm 11\%$) when assuming a loading of 1.0 mmol/g.

Configuration of Certus Flex

For all experimentation with Certus Flex, a eight-channel dispensing head (2 x 4 channels, 21285, Fritz Gyger AG) was applied.

For the peptide synthesis in 384-well plates using microvalve (0.20/0.10 mm SMLD 300 GCR) dispensing, the following fluid configuration was used in the Certus Flex: Each HATU-activated building block occupied one, piperidine (1:4, v/v) two and DMF (washing) two of the total eight available microvalve positions. The used accessories for building blocks, piperidine, and DMF were the corresponding 50 ml canonical tube (standard O-ring) and 250 ml glass bottles (one bottle per fluid with two outlets, standard O-rings), respectively, offered officially by Fritz Gyger AG. In a second installation step for pursuing with DCM washing, TFA deprotection and peptide release (reductive release solution), all mounted accessories and microvalves were removed. New accessories and microvalves

were replaced by the same types of accessories (only 50 ml canonical tube), and microvalves (0.20/0.10 mm SMLD 300 GCR) were installed, and for each of three fluids (DCM, TFA, and release solution) only one position was occupied. For DCM and TFA, more chemical-resistant O-rings offered by Fritz Gyger AG (25428) were necessary either due to degradation (TFA) or extreme swelling (DCM).

For peptide synthesis of the 384-membered peptide library, where the Certus Flex was used to pursue repetitive washing (DMF) and Fmoc deprotection (piperidine, 1:4, v/v) but no couplings, four microvalves (0.20/0.10 mm SMLD 300 GCR) of each fluid were installed using two sources (250 ml glass bottle for each fluid with four outlets each). No special O-rings were required. Deprotection and release of peptides were executed as already mentioned above.

For the peptide synthesis in 1536-well plates, the same set-up as for the peptide synthesis in 384-well plates was applied. The only change conducted was the exchange of the microvalves from SMLD 300 GCR (0.20/0.10 mm) to SMLD 300 GCR (0.15/0.03 mm) since the narrower diameter was more suitable for precise dispensing into 1536-well plates.

Stability study of microvalves

Full exposure of the microvalves (SMLD 300 GCR, 0.20/0.10 and 0.15/0.03 mm) in multiple fluids (DMF, DCM, 95% TFA, 0.5 M HATU, 20% piperidine in DMF, NMP) for one week (covered with liquid) did not cause any visual impairments and it did not even compromise the glaze of the material itself. Therefore, it was concluded that the microvalves could be used for peptide synthesis.

TFA deprotection of peptides in 384-well plates

The 384-well plates containing DCM washed and dried (4 h, room temperature at air) peptide resin was deprotected using 3×1 h deprotecting solution (TFA/TIS/ddH₂O, 38:1:1, 40 μ l/well). The cocktail was transferred using a multichannel pipette (8 channels, 30-300 μ l, VWR) with active coal-protected tips (MBP 200 Solvent Safe TM, 5469), while

the outlet of the wells was blocked using a 10 mm thick EVA foam pad (Creotime, 76899). During incubation, the 384-well plate synthesis was covered with a PP adhesive lid. A manual plate vacuum filtration station removed the liquid, and the resin was washed with DCM (3 x 60 μ l/well) and dried at the air for a few hours before continuing with the reductive release. For the experiments involving the bulk dispenser (Certus Flex, Fritz Gyger AG), the deprotection was realized using chemical-resistant microvalves (0.20 mm / 0.10 mm GCR, Fritz Gyger AG) at 0.300 bar and 50 ml canonical PP containers (greiner bio-one, 227 261) with suitable FEP tubing (Fritz Gyger AG, 21706). The dispensation time of TFA (40 μ l/well) and DCM (70 μ l/well) using one microvalve was 4 min 04 s/plate and 3 min 26 s/plate, respectively. One plate refers to 384 wells.

Peptide synthesis in 384-well plates

The semi-automated solid-phase peptide synthesis approach was performed on a Certus Flex to simultaneously distribute pre-activated Fmoc amino acid derivatives and all other liquids required for SPPS. A manual plate vacuum filtration station realized liquid removal. The liquids were prevented from dripping out of the 384 PP filter plate (Agilent, 201035-10 PE 25 μ M) by squeezing the tips of the filter plate into a 10 mm thick ethylene-vinyl acetate foam pad (Creotime, 76899) with ANSI standardized dimensions. Eight highly chemical resistant microvalves (0.20 mm / 0.10 mm GCR, Fritz Gyger AG) were used to re-distribute all liquids (DMF-based solutions, DCM, 95% TFA) at 0.300 bar either using compatible 50 mL canonical tubes (PP, greiner bio-one, 227 261) or 250 ml glass bottles as solvent containers with appropriate tubing (Fritz Gyger AG, 21794). Each 0.5 M Fmoc amino acid derivative solution (20.0 ml; 10 mmol; 4.5 equiv.) in DMF was mixed with 0.5 M HATU (18.5 ml, 9.25 mmol, 4.2 equiv.) in DMF, 4 M NMM (4.40 ml, 17.8 mmol, 8.0 equiv.) in DMF and NMP (2.22 ml, 5%). The pre-activation was incubated for 1 min before dispensing over the synthesis plate. All the pre-activated solutions were kept the same (no fresh preparation) throughout the whole synthesis duration since Trp, Pro & Gln are used in all of the three couplings. 61 μ L/well of each activated amino acid was dispensed into the appropriate wells, in which \sim 3 μ mol/well resin was previously transferred using the 384-well solid dispenser (Figure 19c). The coupling reaction's incubation time was 45 min at room temperature and was performed twice per synthesis

cycle. The final concentrations of reagents were 207 mM Fmoc amino acid (12.6 $\mu\text{mol/well}$, 4.2 equiv.), 219 mM HATU (13.4 $\mu\text{mol/well}$, 4.5 equiv.), and 413 mM *N*-ethyl morpholine (25.2 $\mu\text{mol/well}$, 8.4 equiv.). To each liquid, one (pre-activated derivatives, TFA, release solution) or two (20% piperidine, DMF) valves were assigned to dispense the desired amount of liquid. The same volumes were transferred for all the other liquids, and the same amount of deprotection and washing cycles were conducted as previously mentioned in the 384-well plate synthesis using the upgraded Intavis MultiPep synthesizer. Dispensation (simultaneous) speeds for one full 384-well plate and process steps were as follows: pre-activated derivatives (2 min 35 s to 3 min 2 s/plate, 61 $\mu\text{l/well}$), DMF (1 min 46 s/plate, 70 $\mu\text{l/well}$), 20% piperidine (1 min 12 s/plate, 35 $\mu\text{l/well}$) and DCM (3 min 26 s, 70 $\mu\text{l/well}$).

Reductive release of library peptides and concentration

The deprotected peptide on resin inside the 384-well plates (theoretical: ~3 $\mu\text{mol/well}$, 1.0 equiv.) was released by applying a release solution (30 $\mu\text{l/well}$, 400 mM TEA and 400 mM BDT, 4.0 equiv.) using a multichannel pipette (8 channels, 30-300 μl , VWR) with active coal protected tips (MBP 200 Solvent Safe TM, 5469) placed over a 384-well DWP (Corning, CLS3342). The plate was incubated overnight at room temperature, and the plates were centrifuged (485 x g, 1 min, room temperature) together (384-well filter plate and DWP) with a food-grade PP zipper bag to avoid the strong smell of BDT during transport and centrifugation. The release was repeated once more (5 hours only), and the combined release filtrates were concentrated using a rotational vacuum concentrator (RVC 2-33 CDplus IR and Alpha 2-4 LSCbasic, Christ) at ~30°C for 5 h and 1750 rpm (Christ plate rotator 124700 and 124708 buckets) with a gradient of vacuum down to 0.5 mbar within 20 min. Before concentration, the combined filtrates (60 ml) were acidified with 50% TFA solution in water (7.4 ml/well, 6.5 M, 2.0 equiv. compared to TEA) to minimize disulfide oxidation during concentration. In addition to this, the 384-well DWP were sealed using an adhesive aluminum lid (greiner bio-one, silverseal 676090) and pierced with a homemade aluminum 384-well piercer to form 0.3 mm diameter holes into each well to minimize risks of spillovers during rotational vacuum concentration. The

residues formed after the removal of solvent inside each well were dissolved in DMSO (40 μ l/well), covered with PS lid (greiner bio-one, Easyseal 676001), sonicated, and centrifuged (485 x g, 1 min, room temperature) before determining the concentration of free thiol by absorption (Ellman's reagent).

LC-MS analysis of peptides

Peptide samples were analyzed by LC-MS analysis with a UHPLC and single quadrupole MS system (Shimadzu LCMS-2020) using a C18 reversed-phase column (Phenomenex Kinetex 2.1 mm \times 50 mm C18 column, 100 Å pore, 2.6 μ M particle) and a linear gradient of solvent B (acetonitrile, 0.05% formic acid) over solvent A (H₂O, 0.05% formic acid) at a flow rate of 1 mL min⁻¹. For all samples, a gradient of 0 to 60% MeCN within 10 min was applied, and UV at 220 nm was used when not otherwise mentioned. Mass analysis was performed in positive ion mode. 100 μ L polypropylene (PP) HPLC microvial (Shimadzu, 980-14379) with PP and teflon caps (Shimadzu, 980-18425) were used for all samples. For analyzing peptides after reductive release and final linear peptide stock solutions in DMSO (from MultiPep Synthesizer & Certus Flex), a 2 μ l sample was transferred into 198 μ l solvent (MeCN:water: TFA, 50:50:0.1%, v/v/v) and analyzed using an injection volume of 2 μ l.

Peptide library quantification by absorption using Ellman's reagent

The final linear peptide stock solution concentrations in DMSO were determined by using Ellman's reagent absorption assay in a 384-well plate format. Aqueous 150 mM ammonium bicarbonate buffer (pH 8.0) in 10% DMSO (23.84 μ l/well) and 10 mM Ellman's reagent in buffer (6.00 μ l/well) were transferred by bulk dispenser (Certus Flex, Fritz Gyger AG) into a 384-well plate (greiner bio-one, 781096) followed by the addition of ~10 mM linear peptide stock solutions in DMSO (135 nl) by acoustic droplet ejection (ECHO 650, Labcyte/Beckman Coulter) amounting to a total volume of 30.0 μ l/well. 384-well PP 2.0 Microplates ECHO Qualified source plates (PP-0200, Beckman Coulter) were used and transfer were realized with the standard DMSO calibration. The positive control was

composed of aqueous 150 mM ammonium bicarbonate buffer at pH 8.0 (23.91 μ l/well), 10 mM Ellman's reagent in buffer (6.00 μ l/well) and 10 mM TCEP in buffer (90 nl/well). The negative control contained aqueous 150 mM ammonium bicarbonate buffer at (24.00 μ l/well) and 10 mM Ellman's reagent in buffer (6.00 μ l/well) only. The assay plate was sealed by an adhesive PS lid (Easyseal, 676001), centrifuged (485 x g, 1 min, room temperature), and analyzed by absorption at 412 nm using a Tecan M200 Pro. The obtained absorption values were negative control corrected and compared to a calibration curve established with the same conditions and a purified linear dithiol model peptide.

Preparation of home-made 1536-well synthesis filter plate

An improvised 1536-well PP deep well synthesis plate (max volume = 12.5 μ l/well) with filters was prepared in-house since no suitable commercially available 1536-well filter plate was found. Into each bottom of the 1536-well PP DWP (greiner bio-one, 782261) was drilled a centered 0.4 mm hole. Appropriate-sized paper filters (Macherey-Nagel MN 615, 4310045) were cut (~1700 pieces) by the precise home crafting machine "Cricut" in the dimensions of 1.9 mm x 3.0 mm using specific tools as shown in Figure 24a. Each rectangle filter was inserted into each well (manually) by lifting the filter at the center on a wetted tip of an unfolded office paper clip.

Peptide synthesis with Certus Flex in 1536-well plates

The semi-automated solid-phase peptide synthesis proof of concept (1536-well SPPS) was performed on a Certus Flex for the simultaneous distribution of pre-activated Fmoc amino acid derivatives and all other liquids required for SPPS. The removal of liquid was realized by hand, on a plate vacuum filtration station. The holes diameter of 0.4 mm was sufficiently small to prevent leaking of DMF and containing liquids out of the well during the preliminary tests. Eight highly chemical resistant microvalves (0.15 mm / 0.03 mm SMLD 300 GCR, Fritz Gyger AG) were used to re-distribute all liquids (DMF-based solutions, DCM, 95% TFA) at 0.300 bar either using compatible 50 ml canonical tubes (PP, greiner bio-one, 227 261) or 250 ml glass bottles as solvent containers with appropriate tubing (Fritz Gyger AG, 21794). Each 0.5 M Fmoc amino acid derivative solution (20.0 ml; 10 mmol; 4.5 equiv.) in DMF was mixed with 0.5 M HATU (18.5 ml, 9.25

mmol, 4.2 equiv.) in DMF, 4 M NMM (4.40 ml, 17.8 mmol, 8.0 equiv.) in DMF and NMP (2.22 ml, 5%). The pre-activation was incubated for 1 min before dispensing over the whole plate. All the pre-activated solutions were kept the same (no fresh preparation) throughout the whole synthesis duration since Trp, Pro & Gln are used in all of the three couplings. Mpa was prepared freshly just before the last coupling step. 10 μ l/well of each activated amino acid was dispensed into the appropriate wells, in which \sim 1 μ mol/well resin was previously transferred using the 1536-well solid dispenser (Supplementary Figure 13). The coupling reaction's incubation time was 45 min at room temperature and was performed twice per synthesis cycle. The final concentrations of reagents were 207 mM Fmoc amino acid (2.1 μ mol/well, 2.1 equiv.), 219 mM HATU (2.2 μ mol/well, 2.2 equiv.) and 413 mM *N*-ethyl morpholine (4.1 μ mol/well, 4.1 equiv.). To each liquid, one (pre-activated derivatives, TFA, release solution) or two (20% piperidine, DMF) microvalves were assigned to dispense the desired amount of liquid. The same volumes were transferred for all the other liquids, and the same amount of deprotection and washing cycles were conducted as previously mentioned in the 384-well plate synthesis using the upgraded Intavis MultiPep RSi synthesizer. Dispensation (simultaneous) speeds for one full 1536 well plate and process steps were as follows: pre-activated derivatives (4 min 11 s to 5 min 41 s/plate, 10 μ l/well), DMF (3 min 7 s/plate, 11 μ l/well), 20% piperidine (2 min 7 s/plate, 5.7 μ l/well) and DCM (3 min 26 s, 11 μ l/well). An overall comparison of synthesis time using microvalves and the multi pep 2 SPPS synthesizer (with & without upgrade) is shown in Supplementary Figures 16.

6.7 Supplementary information

Supplementary tables

Supplementary Table 8: Peptides synthesized in a 384-well plate on the modified CEM/Intavis MultiPep 2 peptide synthesizer (amino acid coupling) and the Gyger Certus Flex microvalve dispenser (washing and deprotection steps). EM = exact mass.

ID	coordinate	plate	ID	C-term	6	5	4	3	2	N-term	EM
1	A1	1	Mpa	2FurAla	Trp	bAla	DGAP				Mea 842.25
2	B1	1	Mpa	Arg	Trp	imp	Tyr				Mea 781.35
3	C1	1	Mpa	Trp	Trp	3AABA					Mea 825.35
4	D1	1	Mpa	bAla	3PAl	Trp	Arg				Mea 725.32
5	E1	1	Mpa	Dlys	Trp	HyP(B)	DTyr				Mea 845.37
6	F1	1	Mpa	3Abz		Phe(4-CH2NH2)	Trp	Tyr(B)			Mea 899.36
7	G1	1	Mpa	Trp	HyP(B)	Trp	Phe(4-CH2NH2)				Mea 915.39
8	H1	1	Mpa	DHis	Tyr	CSAChA	Trp				Mea 790.34
9	I1	1	Mpa	Trp	DArg	4AABA					Mea 853.34
10	J1	1	Mpa	Trp	2Nal	HyP(B)	Phe(4-CH2NH2)				Mea 822.35
11	K1	1	Mpa	Trp	imp	Phe(4-Me)	Dlys				Mea 751.37
12	L1	1	Mpa	HyP(B)	Trp	Gly(ENH2)	DTyr				Mea 817.34
13	M1	1	Mpa	Bip	Trp	4AABA	Trp				Mea 857.34
14	N1	1	Mpa	HyP(B)	Trp	Bip	Gly(ENH2)				Mea 877.38
15	O1	1	Mpa	3amino2naph	DGAP	Tyr	Trp				Mea 759.23
16	P1	1	Mpa	Trp	DTyr	3AABA	Dlys				Mea 775.33
17	A2	1	Mpa	Phe(3-Me)	Trp	DGAP	bAla				Mea 659.29
18	B2	1	Mpa	Phe	His	Trp	CSAChA				Mea 774.35
19	C2	1	Mpa	DGAP	Trp	2Nal	Trp				Mea 722.29
20	D2	1	Mpa	HyP(B)	Phe(4-Me)	3PAl	Trp				Mea 840.37
21	E2	1	Mpa	Arg	3Abz	Trp	W(6-Cl)				Mea 845.30
22	F2	1	Mpa	bAla	Trp	NMePhe	Dom				Mea 897.32
23	G2	1	Mpa	imp	Trp	3PAl	Trp				Mea 773.34
24	H2	1	Mpa	Trp	Trp	3AABA	DHis				Mea 784.29
25	I2	1	Mpa	His	Trp	3amino2naph	Phe(3-Me)				Mea 816.31
26	J2	1	Mpa	DTyr	Trp	3amino2naph					Mea 797.31
27	K2	1	Mpa	Trp	Phe(3-Me)	3Abz	DArg				Mea 787.34
28	L2	1	Mpa	Trp	DTyr	3PAl	3amino2naph				Mea 858.31
29	M2	1	Mpa	Trp	Phe(3-Me)	4AABA	Gly(ENH2)				Mea 745.32
30	N2	1	Mpa	2FurAla	HyP(B)	Trp	His				Mea 828.32
31	O2	1	Mpa	DGAP	2FurAla	CSAChA	Trp				Mea 713.31
32	P2	1	Mpa	Bip	Arg	bAla	Trp				Mea 851.35
33	A3	1	Mpa	Phe(4-CH2NH2)	Trp	bAla	Tyr(Me)				Mea 775.33
34	B3	1	Mpa	Phe(4-Me)	Trp	HyP(B)	His				Mea 852.39
35	C3	1	Mpa	Trp	DArg	NMePhe	imp				Mea 775.37
36	D3	1	Mpa	3PAl	Pro	Trp	Gly(ENH2)				Mea 659.35
37	E3	1	Mpa	Glu	HyP(B)	Trp	Phe(3-Me)				Mea 871.34
38	F3	1	Mpa	Trp	imp	3PAl	Glu				Mea 755.29
39	G3	1	Mpa	DGlu	Trp	3PAl	Pro				Mea 752.28
40	H3	1	Mpa	3amino2naph	Trp	hGlu	NMePhe				Mea 681.29
41	I3	1	Mpa	Trp	Tyr(B)	DGAP	3amino2naph				Mea 888.31
42	J3	1	Mpa	2Nal	Trp	4AABA	Trp				Mea 827.30
43	K3	1	Mpa	DArg	Trp	2Nal	Pro				Mea 750.28
44	L3	1	Mpa	Tyr(B)	DGAP	3amino2naph	Trp				Mea 888.31
45	M3	1	Mpa	HyP(B)	3PAl	DGlu	Trp				Mea 858.32
46	N3	1	Mpa	Trp	DGlu	Tyr(Me)	3AABA				Mea 817.29
47	O3	1	Mpa	4AABA	Trp	Arg	Tyr(B)				Mea 852.31
48	P3	1	Mpa	Phe(3-Me)	Trp	4AABA	Phe(4-Me)				Mea 845.28
49	A4	1	Mpa	Trp	DGlu	3AABA	DTyr				Mea 803.28
50	B4	1	Mpa	DGlu	4AABA	Trp	Tyr				Mea 803.28
51	C4	1	Mpa	2FurAla	Trp	Pro	DGlu				Mea 741.25
52	D4	1	Mpa	CSAChA	DGAP	Trp	Phe(4-Me)				Mea 755.33
53	E4	1	Mpa	Glu	3PAl	Trp	HyP(B)				Mea 858.32
54	F4	1	Mpa	DTyr	DGAP	Trp	3amino2naph				Mea 798.25
55	G4	1	Mpa	Trp	W(6-Cl)	DArg	3Abz				Mea 850.22
56	H4	1	Mpa	Glu	2FurAla	Trp	bAla				Mea 715.25
57	I4	1	Mpa	DArg	3Abz	NMePhe	Trp				Mea 745.27
58	J4	1	Mpa	Glu	Pro	NMePhe	Trp				Mea 755.30
59	K4	1	Mpa	3PAl	Trp	Pro	Trp				Mea 711.29
60	L4	1	Mpa	Trp	3amino2naph	NMePhe	hGlu				Mea 681.29
61	M4	1	Mpa	HyP(B)	DGlu	DTyr	Trp				Mea 875.32
62	N4	1	Mpa	2Nal	imp	Trp	hGlu				Mea 659.27
63	O4	1	Mpa	Glu	Pro	Tyr(B)	Trp				Mea 857.32
64	P4	1	Mpa	imp	DTyr	Arg	Trp				Mea 742.28
65	A5	1	Mpa	Trp	Tyr(B)	Arg	4AABA				Mea 852.31
66	B5	1	Mpa	Bip	Trp	CSAChA	Glu				Mea 859.35
67	C5	1	Mpa	W(6-Cl)	hGlu	3amino2naph	Trp				Mea 745.21
68	D5	1	Mpa	3Abz	Tyr	DGlu	Trp				Mea 750.25
69	E5	1	Mpa	Arg	Trp	Tyr(B)	3AABA				Mea 852.31
70	F5	1	Mpa	2FurAla	Trp	DGlu	Trp				Mea 777.25
71	G5	1	Mpa	Trp	HyP(B)	Trp	DArg				Mea 832.30
72	H5	1	Mpa	DArg	Trp	2Nal	Trp				Mea 795.28
73	I5	1	Mpa	DArg	Trp	2Nal	Dlys				Mea 817.39
74	J5	1	Mpa	Dlys	Trp	Phe(4-Me)	Trp				Mea 753.35
75	K5	1	Mpa	His	NMePhe	Trp	DArg				Mea 735.29
76	L5	1	Mpa	Dlys	Tyr	Arg	Trp				Mea 873.41
77	M5	1	Mpa	DHis	Glu	NMePhe	Trp				Mea 777.32
78	N5	1	Mpa	Trp	Phe	DHis	Trp				Mea 755.35
79	O5	1	Mpa	Glu	2Nal	His	Trp				Mea 813.32
80	P5	1	Mpa	His	2FurAla	cycVal	Trp				Mea 722.28
81	A6	1	Mpa	Trp	Arg	Dlys	3PAl				Mea 755.37
82	B6	1	Mpa	Trp	Phe(4-CH2NH2)	Arg	2FurAla				Mea 775.30
83	C6	1	Mpa	Gly(ENH2)	Trp	DArg	3PAl				Mea 685.28
84	D6	1	Mpa	DGAP	Glu	Trp	3PAl				Mea 713.29
85	E6	1	Mpa	NMePhe	DArg	Trp	DGlu				Mea 755.28
86	F6	1	Mpa	Phe	Trp	DAla	Trp				Mea 684.25
87	G6	1	Mpa	Phe(4-Me)	DGlu	Trp	DArg				Mea 751.33
88	H6	1	Mpa	Trp	DGlu	Trp	NMePhe				Mea 725.31
89	I6	1	Mpa	Phe(4-Me)	Arg	Trp	Cha				Mea 750.35
90	J6	1	Mpa	Phe(4-Me)	Trp	DArg	Trp				Mea 742.31
91	K6	1	Mpa	Glu	Trp	Val	Trp				Mea 752.31
92	L6	1	Mpa	Arg	W(6-Cl)	Trp	DArg				Mea 773.22
93	M6	1	Mpa	Nleu	Trp	DGlu	2FurAla				Mea 771.31
94	N6	1	Mpa	Arg	Cha	Tyr(B)	Trp				Mea 875.37
95	O6	1	Mpa	Tyr	Arg	CE	Trp				Mea 758.29
96	P6	1	Mpa	CE	Trp	hGlu	Trp				Mea 671.27
97	A7	1	Mpa	Glu	W(6-Cl)	Trp	3amino2naph	Arg			Mea 1024.37
98	B7	1	Mpa	2Nal	3AABA	DGAP	CE				Mea 824.39
99	C7	1	Mpa	Trp	W(6-Cl)	Glu	3PAl				Mea 895.39
100	D7	1	Mpa	Gly(ENH2)	Trp	CSAChA	Arg				Mea 857.39
101	E7	1	Mpa	HyP(B)	Tyr(B)	Phe(4-CH2NH2)	Trp				Mea 1110.48
102	F7	1	Mpa	3Abz	Ala	Trp	2Nal				Mea 894.36
103	G7	1	Mpa	DArg	Nleu	2FurAla	CSAChA				Mea 910.47
104	H7	1	Mpa	Trp	Cha	W(6-Cl)	HyP(B)				Mea 1263.47
105	I7	1	Mpa	Ala	3Abz	2FurAla	Trp				Mea 775.30
106	J7	1	Mpa	3PAl	CSAChA	Trp	Arg				Mea 907.47
107	K7	1	Mpa	imp	Glu	2FurAla	DArg				Mea 883.39
108	L7	1	Mpa	3AABA	Gly(ENH2)	Trp	Trp				Mea 833.35
109	M7	1	Mpa	Trp	Phe	3Abz	DHis				Mea 811.31
110	N7	1	Mpa	Trp	Arg	Phe(3-Me)	cycVal				Mea 895.41
111	O7	1	Mpa	Trp	imp	Gly(ENH2)	Ala				Mea 895.42
112	P7	1	Mpa	Glu	Trp	Tyr(Me)	Trp				Mea 950.37
113	A8	1	Mpa	3AABA	Lys(AC)	Tyr(B)	His				Mea 1044.45
114	B8	1	Mpa	Phe(4-Me)	3PAl	Trp	HyP(B)				Mea 811.41
115	C8	1	Mpa	bAla	Trp	Tyr(B)	DHis				Mea 883.35
116	D8	1	Mpa	CSAChA	3PAl	2Nal	Trp				Mea 955.49
117	E8	1	Mpa	DHis	Trp	3amino2naph	Phe(3-Me)				Mea 931.42
118	F8	1	Mpa	HyP(B)	cycVal	NMePhe	DGAP				Mea 895.42
119	G8	1	Mpa	DArg	Trp	3PAl	Dom				Mea 811.35
120	H8	1	Mpa	Arg	HyP(B)	W(6-Cl)	CE				Mea 1087.44
121	I8	1	Mpa	cycVal	DArg	3Abz	NMeGly				Mea 844.35
122	J8	1	Mpa	Lys(AC)	Trp	3PAl	3Abz				Mea 920.42
123	K8	1	Mpa	Nleu	Trp	HyP(B)	Phe(4-CH2NH2)				Mea 1043.49
124	L8	1	Mpa	cycVal	Trp	Dom	3amino2naph				Mea 854.42
125	M8	1	Mpa	Nleu	Trp	Tyr(B)	Trp				Mea 952.43
126	N8	1	Mpa	Dom	Cha	Trp	4AABA				Mea 885.41
127	O8	1	Mpa	3PAl	DArg	Trp	HyP(B)				Mea 855.45
128	P8	1	Mpa	Lys	Trp	Phe(4-Me)	Trp				Mea 920.41
129	A9	1	Mpa	Glu	Trp	Gly(ENH2)	Phe				Mea 895.36
130	B9	1	Mpa	Trp	Phe(3-Me)	Arg	HyP(B)				Mea 957.44
131	C9	1	Mpa	Trp	Phe(4-CH2NH2)	Trp	Trp				Mea 1085.52
132	D9	1	Mpa	2FurAla	Trp	Nleu	Pro				Mea 814.38
133	E9	1	Mpa	Alb	3PAl	Trp	Trp				Mea 849.39
134	F9	1	Mpa	3PAl	CSAChA	Trp	Trp				Mea 853.39
135	G9	1	Mpa	Lys(AC)	Phe(4-Me)	DArg	Trp				Mea 957.45
136	H9	1	Mpa	Tyr(Me)	Trp	Gly(ENH2)	cycVal				Mea 795.35
137	I9	1	Mpa	3AABA	DGAP	2Nal	Cha				Mea 920.42
138	J9	1	Mpa	3Abz	Trp	3PAl	Trp				Mea 895.37
139	K9	1	Mpa	3PAl	bAla	DArg	Trp				Mea

C-term										N-term												
ID	coordinate	plate	ID	7	8	9	10	11	12	ID	coordinate	plate	ID	7	8	9	10	11	12			
190	A13	1	Mpa	Tyr	DGsr	Trp	Sabz	Mea	853.32	290	A10	1	Mpa	Dasp	Bip	bala	Trp	Dau	Mea	873.37		
194	B13	1	Mpa	3AMBA	Gly(ETNH2)	Trp	Cit	Trp	Mea	827.40	290	B10	1	Mpa	Tyr(Bzl)	Trp	Gly	Asp	Imp	Mea	887.35	
195	C13	1	Mpa	cycVal	His	Hy(Bzl)	Phe	Trp	Mea	903.39	291	C10	1	Mpa	3AMBA	Asp	Alb	W(6-Cl)	Trp	Mea	904.20	
196	D13	1	Mpa	DQsp	2FurAla	Trp	norVal	Hy(Bzl)	Mea	913.33	292	D10	1	Mpa	NMeGly	2Nal	DGlu	Trp	3AMBA	Tyr	Mea	920.34
197	E13	1	Mpa	Lys	cisACHA	Trp	norVal	2FurAla	Mea	854.43	293	E10	1	Mpa	Tyr(Me)	Hy(Bzl)	Trp	Asp	Gln	Mea	974.38	
198	F13	1	Mpa	Hy(Bzl)	Alb	Trp	Phe(3-Me)	Dlys	Mea	928.45	294	F10	1	Mpa	Glu	Tyr(Me)	Trp	cycVal	3aminoznaph	Mea	950.35	
199	G13	1	Mpa	Hy(Bzl)	Trp	Dleu	His	Tyr(Bzl)	Mea	1057.47	295	G10	1	Mpa	Trp	Tyr(Me)	3AMBA	NMeGly	Glu	Mea	888.33	
200	H13	1	Mpa	Pro	Trp	DOm	Gln	NMePhe	Mea	861.35	296	H10	1	Mpa	Dleu	Phe	Trp	Sabz	Dasp	Mea	845.34	
201	I13	1	Mpa	3aminoznaph	Phe(3-Me)	Trp	NMeGly	His	Mea	889.35	297	I10	1	Mpa	Glu	Hy(Bzl)	Trp	ile	Tyr	Mea	968.40	
202	J13	1	Mpa	Tyr(Me)	Pro	Trp	DHS	hLeu	Mea	869.41	298	J10	1	Mpa	bala	Val	Trp	Trp	DGlu	Mea	893.35	
203	K13	1	Mpa	His	Hy(Bzl)	Trp	Lys(AC)	Trp	Mea	1055.46	299	K10	1	Mpa	Lys(AC)	Trp	DGlu	3AMBA	Tyr	Mea	973.36	
204	L13	1	Mpa	Cit	Bip	DOsp	3AMBA	Trp	Mea	920.42	300	L10	1	Mpa	Thr	Asp	Phe(4-Me)	Trp	Pro	Mea	925.33	
205	M13	1	Mpa	Glu	Trp	Phe	Dleu	3AMBA	Mea	900.37	301	M10	1	Mpa	Imp	DGlu	Trp	2Nal	ile	Mea	926.40	
206	N13	1	Mpa	Dasp	Pro	Trp	Phe	NMeGly	Mea	781.30	302	N10	1	Mpa	Pro	Dleu	Trp	Trp	Glu	Mea	903.38	
207	O13	1	Mpa	Trp	Asp	Pro	Ala	Mea	797.30	303	O10	1	Mpa	Asp	Tyr(Me)	Trp	bala	Asn	Mea	923.31		
208	P13	1	Mpa	Trp	Glu	cycVal	3AMBA	DTyr	Mea	900.33	304	P10	1	Mpa	Asp	2FurAla	3aminoznaph	Dleu	Trp	Mea	885.33	
209	A14	1	Mpa	Trp	2FurAla	Alb	Imp	hGlu	Mea	884.29	305	A20	1	Mpa	cisACHA	Phe(4-Me)	Trp	Asp	Gln	Mea	894.39	
210	B14	1	Mpa	Gly	Trp	Dasp	Tyr	Pro	Mea	783.28	306	B20	1	Mpa	Ala	Sabz	Trp	Tyr(Me)	hGlu	Mea	715.27	
211	C14	1	Mpa	DGlu	Hy(Bzl)	hLeu	Trp	Phe	Mea	964.42	307	C20	1	Mpa	Trp	2Nal	Glu	hLeu	Imp	Mea	942.41	
212	D14	1	Mpa	Asp	Alb	bala	2Nal	Trp	Mea	819.32	308	D20	1	Mpa	Phe(3-Me)	Alb	bala	Trp	Dasp	Mea	783.32	
213	E14	1	Mpa	Phe	Thr	cisACHA	DGlu	Trp	Mea	884.38	309	E20	1	Mpa	Trp	Glu	2FurAla	3AMBA	Thr	Mea	878.31	
214	F14	1	Mpa	Val	Imp	Asp	Tyr(Me)	Trp	Mea	883.38	310	F20	1	Mpa	Trp	Phe(3-Me)	Val	4AMBA	Asp	Mea	850.35	
215	G14	1	Mpa	Trp	4AMBA	Glu	Lys(AC)	DTyr	Mea	907.38	311	G20	1	Mpa	Trp	Phe(4-Me)	Lys(AC)	Asp	cisACHA	Mea	906.44	
216	H14	1	Mpa	Glu	Phe	Trp	Val	Imp	Mea	864.37	312	H20	1	Mpa	hLeu	Phe	Glu	3AMBA	Trp	Mea	914.38	
217	I14	1	Mpa	Phe(4-Me)	Val	Imp	hGlu	Trp	Mea	723.34	313	I20	1	Mpa	Trp	Lys(AC)	Arg	Dleu	Phe(3-Me)	Mea	951.40	
218	J14	1	Mpa	W(6-Cl)	Val	DGlu	Trp	Pro	Mea	923.32	314	J20	1	Mpa	Trp	3Pspace	Trp	Trp	NMeGly	Mea	930.38	
219	K14	1	Mpa	Trp	NMePhe	Sabz	Ala	Asp	Mea	817.30	315	K20	1	Mpa	Arg	Dsr	Trp	Tyr	Gln	Mea	888.37	
220	L14	1	Mpa	Trp	3aminoznaph	Tyr(Bzl)	Gly	DGlu	Mea	869.35	316	L20	1	Mpa	DHS	Dsr	norVal	Trp	2FurAla	Mea	811.33	
221	M14	1	Mpa	3aminoznaph	Dasp	Phe	Phe	Trp	Mea	882.35	317	M20	1	Mpa	Phe(4-Me)	Asn	DGlu	Lys(AC)	Trp	Mea	925.45	
222	N14	1	Mpa	Trp	Lys(AC)	Tyr	3AMBA	Glu	Mea	973.38	318	N20	1	Mpa	Trp	DOm	Dsr	DTyr	Pro	Mea	820.33	
223	O14	1	Mpa	Hy(Bzl)	2Nal	Trp	Asp	Mea	904.38	319	O20	1	Mpa	Val	Trp	Alb	Phe	Gly(ETNH2)	Mea	782.37		
224	P14	1	Mpa	Trp	NMePhe	hGlu	Sabz	Dleu	Mea	744.32	320	P20	1	Mpa	2FurAla	His	Trp	cycVal	THP	Mea	849.34	
225	A15	1	Mpa	Glu	Sabz	3PAl	ile	Mea	887.33	321	A21	1	Mpa	Dlys	NMePhe	Trp	norVal	Trp	Mea	924.42		
226	B15	1	Mpa	DGlu	Sabz	Trp	Gln	Phe(4-Me)	Mea	915.34	322	B21	1	Mpa	W(6-Cl)	Asn	Lys	hLeu	Trp	Mea	940.40	
227	C15	1	Mpa	Tyr(Me)	Trp	Gly	Asp	bala	Mea	771.28	323	C21	1	Mpa	Trp	Phe	Gln	Gly(ETNH2)	Ala	Mea	797.35	
228	D15	1	Mpa	Pro	DGlu	Trp	Tyr(Bzl)	THP	Mea	984.39	324	D21	1	Mpa	Ala	Trp	cycVal	Darg	Trp	Mea	891.39	
229	E15	1	Mpa	3PAl	Sabz	Glu	Trp	Asn	Mea	888.31	325	E21	1	Mpa	Cit	cycVal	Trp	His	Trp	Mea	903.40	
230	F15	1	Mpa	Glu	Trp	Val	bala	Bip	Mea	900.37	326	F21	1	Mpa	Gly(ETNH2)	Tyr	THP	Trp	hLeu	Mea	868.41	
231	G15	1	Mpa	Gln	Tyr	Trp	3aminoznaph	DGlu	Mea	987.34	327	G21	1	Mpa	W(6-Cl)	3Pspace	Gly	Lys(AC)	Trp	Mea	923.36	
232	H15	1	Mpa	Trp	Val	Trp	3aminoznaph	Asp	Mea	897.38	328	H21	1	Mpa	Trp	Gln	DHS	Asn	Tyr	Mea	993.34	
233	I15	1	Mpa	Dsr	Sabz	Asp	Phe	Trp	Mea	819.28	329	I21	1	Mpa	Dsr	Trp	Dlys	Dala	2Nal	Mea	854.37	
234	J15	1	Mpa	Bip	Trp	norVal	Dasp	Arg	Mea	907.37	330	J21	1	Mpa	ile	2Nal	Trp	Lys(AC)	Arg	Mea	987.40	
235	K15	1	Mpa	Dala	3PAl	Trp	DGlu	cisACHA	Mea	855.36	331	K21	1	Mpa	Phe(4-Me)	DOsp	Alb	Trp	Alb	Mea	756.36	
236	L15	1	Mpa	Ala	Trp	2FurAla	hGlu	bala	Mea	902.41	332	L21	1	Mpa	Lys	Trp	Ala	Gly	ile	Mea	982.36	
237	M15	1	Mpa	Tyr(Bzl)	Cha	DGlu	3aminoznaph	Trp	Mea	1052.44	333	M21	1	Mpa	Trp	DHS	3PAl	Lys(AC)	THP	Mea	933.41	
238	N15	1	Mpa	Ala	Trp	Glu	W(6-Cl)	cisACHA	Mea	907.34	334	N21	1	Mpa	Gly(ETNH2)	Trp	Arg	hLeu	Phe	Mea	882.44	
239	O15	1	Mpa	NMeGly	Trp	hGlu	W(6-Cl)	Mea	811.25	335	O21	1	Mpa	Tyr(Bzl)	Alb	Trp	Arg	Val	Mea	922.44		
240	P15	1	Mpa	Trp	bala	2Nal	Dala	DGlu	Mea	945.32	336	P21	1	Mpa	cycVal	Alb	3PAl	Trp	Phe	Mea	837.39	
241	A16	1	Mpa	Tyr	norVal	Dasp	Trp	3AMBA	Mea	851.33	337	A22	1	Mpa	cycVal	Thr	Bip	DHS	Trp	Mea	907.43	
242	B16	1	Mpa	Trp	Cit	bala	2Nal	Asp	Mea	891.35	338	B22	1	Mpa	Trp	Asn	2Nal	Dlys	Cit	Mea	947.43	
243	C16	1	Mpa	Tyr(Bzl)	Trp	Hy(Bzl)	Dasp	Trp	Mea	903.39	339	C22	1	Mpa	hLeu	Trp	norVal	Phe(4-Me)	Lys	Mea	894.47	
244	D16	1	Mpa	Trp	DGlu	bala	Alb	Tyr(Bzl)	Mea	910.36	340	D22	1	Mpa	Gly(ETNH2)	Dleu	Trp	Trp	norVal	Mea	849.41	
245	E16	1	Mpa	cycVal	Pro	Dasp	Trp	Mea	880.29	341	E22	1	Mpa	Darg	Ala	3PAl	Trp	Cit	Mea	883.41		
246	F16	1	Mpa	Tyr(Me)	Ala	Trp	hGlu	3AMBA	Mea	752.29	342	F22	1	Mpa	Alb	Gly(ETNH2)	Cit	3PAl	Trp	Mea	841.38	
247	G16	1	Mpa	Glu	Trp	Asn	Trp	Mea	1018.41	343	G22	1	Mpa	Trp	Dala	Ala	Trp	DOm	Trp	Mea	793.35	
248	H16	1	Mpa	bala	Dasp	ile	Trp	Mea	839.35	344	H22	1	Mpa	cycVal	Trp	Lys	NMePhe	Cha	Mea	860.47		
249	I16	1	Mpa	Trp	4AMBA	hLeu	Asp	Phe	Mea	873.37	345	I22	1	Mpa	Phe	DHS	Trp	Cha	Dleu	Mea	901.45	
250	J16	1	Mpa	Trp	Gly	cisACHA	hGlu	2Nal	Mea	744.22	346	J22	1	Mpa	NMeGly	Lys	Asn	Trp	2Nal	Mea	951.35	
251	K16	1	Mpa	Gly	Dasp	Pro	Bip	Trp	Mea	943.32	347	K22	1	Mpa	Gly(ETNH2)	Cit	Gln	Bip	Trp	Mea	959.43	
252	L16	1	Mpa	Trp	Asp	cisACHA	Dala	Bip	Mea	899.38	348	L22	1	Mpa	Trp	Lys(AC)	hLeu	DTyr	Gly(ETNH2)	Mea	911.45	
253	M16	1	Mpa	bala	Thr	hGlu	DTyr	Trp	Mea	988.27	349	M22	1	Mpa	3PAl	Trp	Glu	Asn	NMeGly	Mea	840.31	
254	N16	1	Mpa	bala	Glu	Trp	Ala	W(6-Cl)	Mea	869.28	350	N22	1	Mpa	Bip	Dala	Trp	Ala	Asp	Mea	831.32	
255	O16	1	Mpa	Asn	Trp	3aminoznaph	Asp	Bip	Mea	972.34	351	O22	1	Mpa	Glu	hLeu	DTyr	Trp	ile	Mea	910.41	
256	A17	1	Mpa	NMePhe	3abz	Tyr(Me)	Lys(AC)	Trp	Mea	949.38	352	P22	1	Mpa	2FurAla	Gly	Dasp	ile	Trp	Mea	773.30	
257	B17	1	Mpa	NMePhe	Sabz	Trp	Lys(AC)	Trp	Mea	910.37	353	A23	1	Mpa	Trp	Cha	Tyr(Bzl)	DGlu	NMeGly	Mea	984.42	
258	C17	1	Mpa	Val	Bip	Trp	Glu	Pro	Mea	920.38	354	B23	1	Mpa	Glu	Trp	THP	3PAl	Alb	Mea	987.34	
259	D17	1	Mpa	2Nal	Gln	Hy(Bzl)	Dasp	Trp	Mea	904.38	355	C23	1	Mpa	hLeu	Ala	Trp	Phe(4-Me)	Asp	Mea	825.37	
260	E17	1	Mpa	Trp	Asp	Trp	bala	Asn	Mea	837.31	356	D23	1	Mpa	Glu	Dleu	NMePhe	Trp	Asn	Mea	895.37	
261	F17	1	Mpa	Bip	3AMBA	cycVal	Trp	DGlu	Mea	900.37	357	E23	1	Mpa	Phe(4-Me)	Alb	Dasp	Dala	Trp	Mea	783.32	
262	G17	1	Mpa	W(6-Cl)	hGlu	3AMBA	cycVal	Trp	Mea	891.27	358	F23	1	Mpa	Trp	Alb	Dala	Trp	Dasp	Mea	808.32	
263	H17	1	Mpa	2Nal	3aminoznaph	Trp	hGlu	Dala	Mea	788.29	359	G23	1	Mpa	Val	Trp	Bip	Asn	Asp	Mea	902.36	
264	I17	1	Mpa	THP	Trp	Asp	Imp	2Nal	Mea	901.35	360	H23	1	Mpa	THP	Asp	Trp	Alb	Tyr(Me)	Mea	855.34	
265	J17	1	Mpa	DTyr	Trp	Dasp	NMeGly	Imp														

Supplementary Table 9: Analysis of peptides from the synthesis in a 384-well plate using the Gyger Certus Flex microvalve dispenser. The indicated (*italic*) peptides were picked and shown in Figure 22.

Peptide	Coordinate	Retention time (min)	[M+H] ⁺ (m/z)	Exact mass	Peak area at 220 nm (%)
A	A1	3.85 + 4.03	449.3	448.1603	79
A	A22	3.85 + 4.03	449.3	448.1603	78
A	G13	3.84 + 4.02	449.3	448.1603	82
A	N1	3.84 + 4.02	449.3	448.1603	63
A	N22	3.85 + 4.02	449.3	448.1603	79
<i>B</i>	<i>A2</i>	3.97	449.2	448.1603	87
B	A23	3.97	449.4	448.1603	83
B	G14	3.97	449.3	448.1603	82
B	N2	3.97	449.4	448.1603	89
B	N23	3.97	449.4	448.1603	83
C	A3	3.28 + 3.38	480.1	479.1661	77
C	A24	3.35 + 3.44	480.3	479.1661	74
C	G12	3.36 + 3.45	480.2	479.1661	80
C	N3	3.35 + 3.44	480.2	479.1661	84
C	N24	3.35 + 3.44	480.3	479.1661	78
<i>D</i>	<i>B1</i>	3.43	480.3	479.1661	78
D	B22	3.42	480.3	479.1661	74
D	H13	3.42	480.2	479.1661	72
D	O1	3.42	480.3	479.1661	78
D	O22	3.42	480.3	479.1661	76
<i>E</i>	<i>B2</i>	2.64	391.2	390.1395	71
E	B23	2.63	391.2	390.1395	50
E	H14	2.63	391.1	390.1395	61
E	O2	2.63	391.1	390.1395	76
E	O23	2.64	391.2	390.1395	71
<i>F</i>	<i>B3</i>	2.45 + 2.64	391.1	390.1395	66
F	B24	2.45 + 2.64	391.1	390.1395	59
F	H12	2.44 + 2.63	391.1	390.1395	59
F	O3	2.44 + 2.64	391.1	390.1395	76
F	O24	2.44 + 2.64	391.1	390.1395	61
G	C1	4.5	538.5	537.1868	68
G	C22	4.50 + 4.55	538.2	537.1868	78
G	I13	4.50 + 4.55	538.2	537.1868	77
G	P1	4.50 + 4.55	538.2	537.1868	57
G	P22	4.50 + 4.55	538.2	537.1868	78
<i>H</i>	<i>C2</i>	2.86	360.3	359.1337	72
H	C23	2.86	360.1	359.1337	68
H	I14	2.85	360.1	359.1337	72

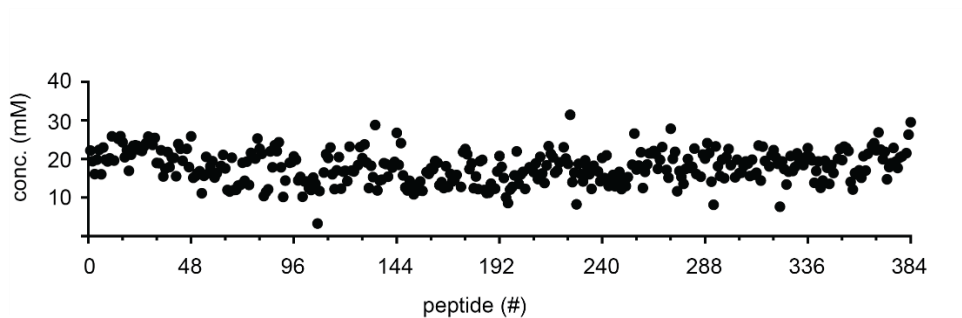
H	P2	2.85	360.1	359.1337	73
H	P23	2.85	360.2	359.1337	67
I	C3	2.22	422.1	421.1454	69
I	C24	2.22	422	421.1454	70
I	I12	2.22	422.1	421.1454	81
I	P3	2.23	422.1	421.1454	25
I	P24	2.22	422	421.1454	68

Supplementary Table 10: Analysis of peptides from the synthesis in a 1536-well plate using the Fritz Gyger AG's Certus Flex microvalve dispenser. The indicated peptides were picked (*italic*) and shown in Supplementary Figure 15. The indicated peptides with an asterisk (*) were wells found with ruptured filters. The capital letters in brackets within the peak area column refer to specific found cross-contaminations of indicated peptide.

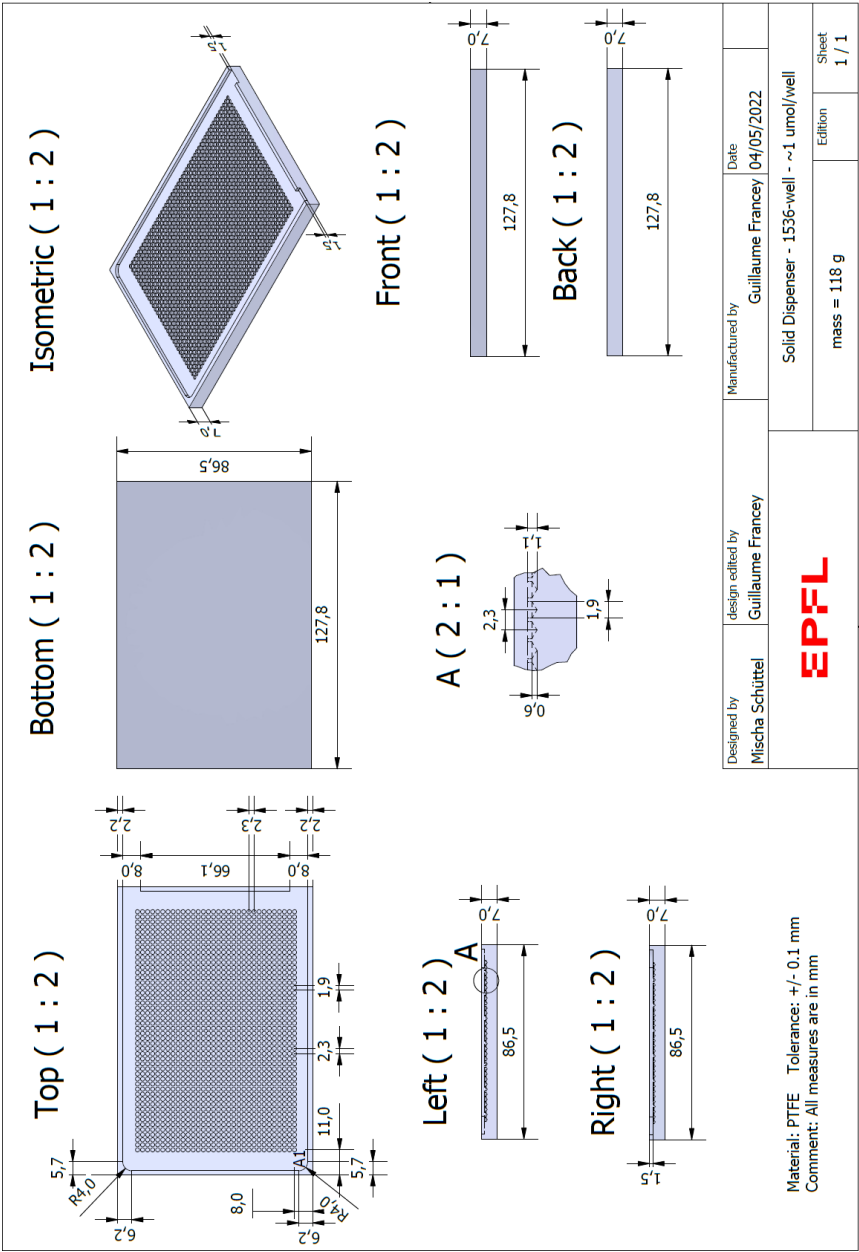
Peptide	Coordinat	Retention time (min)	[M+H] ⁺ (m/z)	Exact mass	Peak area at 220 nm (%)
A	A1	3.85 + 4.03	449.3	448.1603	78
A	<i>A46</i>	<i>3.85 + 4.03</i>	<i>449.2</i>	<i>448.1603</i>	86
A	P25	3.84 + 4.03	449.2	448.1603	84
A	AD1	No peaks	-	448.1603	No peaks
A	AD46	3.85 + 4.01	449.2	448.1603	79
B	A2	3.97	449.3	448.1603	87
B	A47	3.98	449.2	448.1603	95
<i>B</i>	<i>P23</i>	<i>3.97</i>	<i>449.2</i>	<i>448.1603</i>	95
B	AD2	3.97 (3.85)	449.2	448.1603	76, 18 (A) *
B	AD47	3.97	449.2	448.1603	74
C	A3	3.37 + 3.44	480.2	479.1661	83
C	A48	3.37 + 3.46	480.2	479.1661	87
<i>C</i>	<i>P24</i>	<i>3.37 + 3.46</i>	<i>480.2</i>	<i>479.1661</i>	85
C	AD3	3.37 + 3.45	480.2	479.1661	72
C	AD48	3.37 + 3.44	480.3	479.1661	42 *
<i>D</i>	<i>B1</i>	<i>3.43</i>	<i>480.3</i>	<i>479.1661</i>	80
D	B46	3.44	480.3	479.1661	62
D	Q25	3.43	480.2	479.1661	80
D	AE1	3.42 (4.49)	480.1	479.1661	12, 70 (G) *
D	AE46	3.42	480.2	479.1661	62
<i>E</i>	<i>B2</i>	<i>2.65</i>	<i>391.1</i>	<i>390.1395</i>	72
E	B47	2.65	391.0	390.1395	83
E	Q23	2.65	391.0	390.1395	73
E	AE2	2.63 (3.44)	391.1	390.1395	44, 28 (D) *
E	AE47	2.64	391.1	390.1395	14 *
F	B3	2.45 + 2.64	391.0	390.1395	70 *
<i>F</i>	<i>B48</i>	<i>2.45 + 2.64</i>	<i>391.1</i>	<i>390.1395</i>	87
F	Q24	2.44 + 2.63	391.1	390.1395	86
F	AE3	2.39 + 2.58	391.0	390.1395	80
F	AE48	2.44 + 2.64	391.1	390.1395	28 *
G	C1	4.50 + 4.55	538.2	537.1868	76
G	C46	4.50 + 4.55	538.2	537.1868	77
G	O25	4.50 + 4.56	538.2	537.1868	76
G	<i>AF1</i>	<i>4.49 + 4.55</i>	<i>538.4</i>	<i>537.1868</i>	77

G	AF46	no peaks	538.2	537.1868	no peaks
H	C2	2.87	360.1	359.1337	56 *
H	C47	2.86	360.1	359.1337	88
<i>H</i>	O23	2.85	360.1	359.1337	93
H	AF2	2.87	360.1	359.1337	82
H	AF47	2.88	360.1	359.1337	12*
I	C3	2.24	422.0	421.1454	54 *
I	C48	2.24	422.1	421.1454	47 *
<i>I</i>	O24	2.23	422.1	421.1454	73
I	AF3	2.23	422.1	421.1454	35 *
I	AF48	2.24	422.1	421.1454	21 *

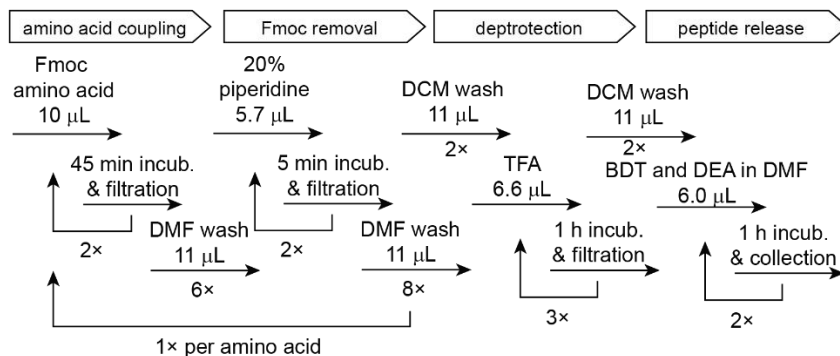
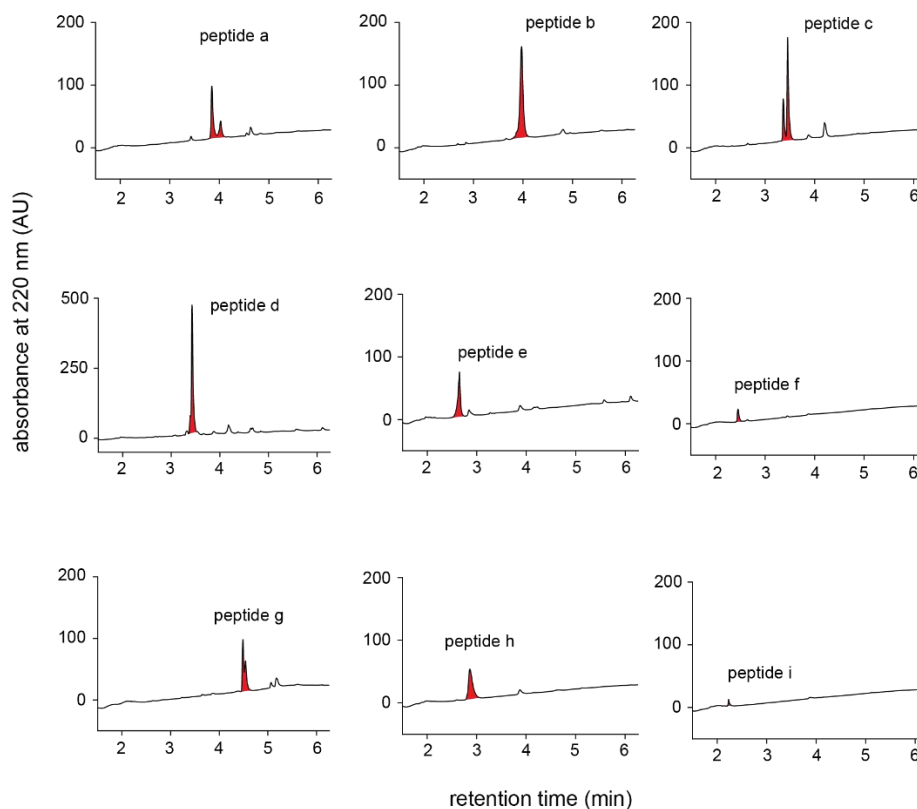
Supplementary Figures



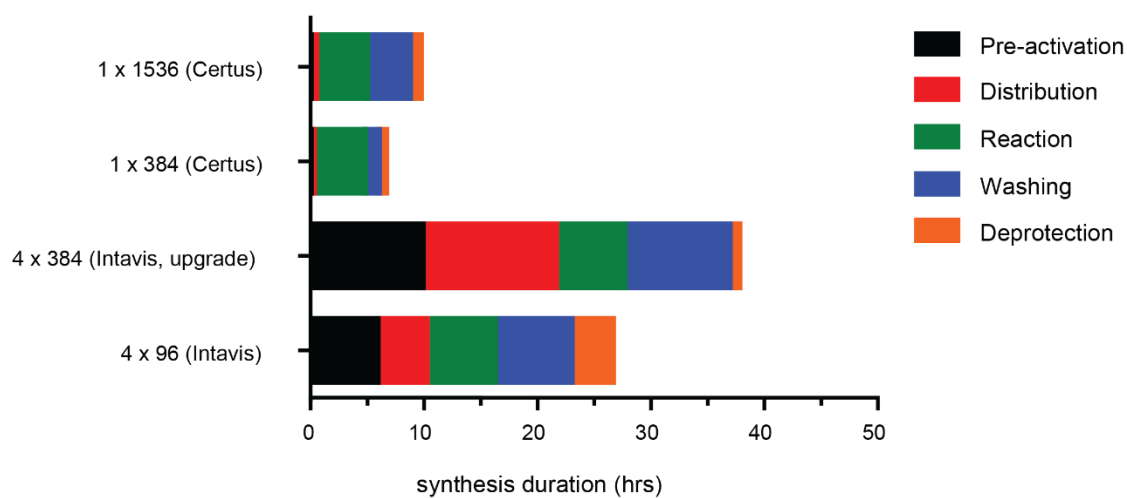
Supplementary Figure 13: Quantity of peptide. Concentrations of peptides synthesized by Certus Flex inside 384-well reactor plate and quantified by reacting the thiols groups of the peptide with Ellman's reagent and measuring absorbance.



Supplementary Figure 14: Technical drawing of the 1,536-well plate resin dispensing tool (for around 1 μ mol resin per well).

a**b**

Supplementary Figure 15: Peptide synthesis in 1,536-well plates. (a) Peptide synthesis procedure indicating the volumes of reagents and solvents dispensed by microvalves. (b) Selected RP-HPLC chromatograms of peptides synthesized in the 1,536 well reactor plate. The nine shown peptide chromatograms are marked as *italic* in supplementary Table 10, where all 45 analyzed peptides are listed.



Supplementary Figure 16: Synthesis time overview of four different SPPS methods. The commercial state of the art parallel peptide synthesizer (needle-piston based dispensation, sequential work flow, chapter 5) using microplates as reactors (4 x 96, Intavis), our home made synthesizer upgrade capable of using denser micropaltes as reactors (4 x 384, Intavis, upgrade, chapter 5) and the proof of conept SPPS synthesis using microvalves in either 384-well or 1536-well microplate reactors (chapter 6).

6.8 References

- (91) Habeshian, S.; Sable, G. A.; Schüttel, M.; Merz, M. L.; Heinis, C. Cyclative Release Strategy to Obtain Pure Cyclic Peptides Directly from the Solid Phase. *ACS Chem. Biol.* **2022**, 17 (1), 181–186. <https://doi.org/10.1021/acscchembio.1c00843>.
- (106) Bogнар, Z.; Mothukuri, G. K.; Nielsen, A. L.; Merz, M. L.; Pânzar, P. M. F.; Heinis, C. Solid-Phase Peptide Synthesis on Disulfide-Linker Resin Followed by Reductive Release Affords Pure Thiol-Functionalized Peptides. *Org. Biomol. Chem.* **2022**, 20 (29), 5699–5703. <https://doi.org/10.1039/D2OB00910B>.
- (156) Niles, W. D.; Coassin, P. J. Piezo- and Solenoid Valve-Based Liquid Dispensing for Miniaturized Assays. *ASSAY Drug Dev. Technol.* **2005**, 3 (2), 189–202. <https://doi.org/10.1089/adt.2005.3.189>.
- (157) Butendeich, H.; Pierret, N. M.; Numao, S. Evaluation of a Liquid Dispenser for Assay Development and Enzymology in 1536-Well Format. *SLAS Technol.* **2013**, 18 (3), 245–250. <https://doi.org/10.1177/2211068212472184>.
- (158) Manjunath, H. S.; Kalikiri, M. K. R.; Kabeer, B. S. A.; Tomei, S. When Mosquito HV Bites Biomark HD: An Automated Workflow for High-Throughput QPCR. *SLAS Technol.* **2022**, 27 (3), 219–223. <https://doi.org/10.1016/j.slast.2021.12.007>.
- (159) Ellson, R.; Mutz, M.; Browning, B.; Leejr, L.; Miller, M.; Papen, R.; Picoliterinc. Transfer of Low Nanoliter Volumes between Microplates Using Focused Acoustics?Automation Considerations. *J. Assoc. Lab. Autom.* **2003**, 8 (5), 29–34. [https://doi.org/10.1016/S1535-5535\(03\)00011-X](https://doi.org/10.1016/S1535-5535(03)00011-X).
- (160) Jensen, M.; Roberts, L.; Johnson, A.; Fukushima, M.; Davis, R. Next Generation 1536-Well Oligonucleotide Synthesizer with on-the-Fly Dispense. *J. Biotechnol.* **2014**, 171, 76–81. <https://doi.org/10.1016/j.jbiotec.2013.11.027>.

7. General Conclusion

The research of my PhD project aimed at developing methods for accessing large libraries of structurally highly diverse macrocyclic compounds. In this work, I have built on a general procedure established by former members of the lab, in which a large number of "*m*" peptides containing two thiol groups are combinatorially cyclized in microwell plates with a number of "*n*" bis-electrophilic cyclization reagents to obtain $m \times n$ macrocyclic compounds, that are subsequently screened as crude products for identifying binders of disease targets. I have followed in total four projects that all aimed at improving the throughput and library size of this general method. From today's point of view, the established procedure for peptide synthesis in 384-well plates and reagent dispensing by microvalves will likely have most value of all the results of my thesis, and I thus start discussing this outcome and the potential impact. Results of the other two thesis results chapter may be used by others too, and their potential future will be discussed afterwards.

The developed hardware parts and procedures for parallel peptide synthesis in 384-well plates opened up new opportunities to our research group. While peptide synthesis was restricted to 4×96 peptides before, we can now produce 4×384 peptides in almost the same time or a bit longer time. The developed tools for SPPS in the 384-well format, along with the microvalve dispensing enormously facilitated practical work to synthesize large numbers of peptides. Much of the structural and chemical diversity of macrocycles generated by di-thiol peptide cyclization is contained in the peptide region. It was thus very important to access larger number of di-thiol peptides. I would say that the diversities that our lab can generate now are 4-times larger than before. Over the course of less than one year, the peptide synthesis in the 384-well plates has been applied to more than twenty synthesis runs using more than fifty 384-well micro plates amounting to a total of over 20,000 synthesized small linear peptides. They were all being further used and modified at nanoliter scale to finally screen hundred-thousands of macrocycles. It is expected that the 384-well synthesis format will be used at the same intensity in the coming years in our lab, and hopefully also by other research groups.

Other results obtained in my PhD project have less impact on practical work in our lab but may have once they get published. The comparison of bis-electrophilic reagents and

presentation in a "periodic table" may provide a simple guide for other labs to choose such reagents for diverse applications, ranging from peptide stapling to macrocycles library generation and screening. The developed high density immobilized TCEP beads are not further used in our laboratory because an alternative procedure was found that is more suited for macrocycle library generation (a volatile reducing agent that can be removed with a speedvac). However, the beads are still useful and complementary to existing commercially available TCEP agarose beads by having almost an order of magnitude higher reductive capacity, suitable for low throughput applications and double-digit millimolar concentrated disulfide peptide solutions with or without high organic solvent required to maintain peptide's solubility. The beads may be used by other labs for different applications once published.

Overall, this work has led to the establishment of several techniques and tools that facilitate the generation of large peptide-based macrocycle libraries. These methods will likely allow the development of macrocyclic ligands against therapeutically important targets, and hopefully, they will contribute to the development of new macrocycle-based therapeutics.

8. Curriculum Vitae

Curriculum Vitae

Personal Data

Last name: Schüttel
First name: Mischa

Nationality: Swiss
E-Mail: mischa.schuettel@gmx.ch
mischa.schuettel@epfl.ch

Education

- 09/2018 - 03/2023 **PhD in Chemical Biology**
École Polytechnique Fédérale de Lausanne (EPFL) in Ecublens (VD), Switzerland
- 09/2016 - 08/2018 **MSc in Molecular and Biological Chemistry**
École Polytechnique Fédérale de Lausanne (EPFL) in Ecublens (VD), Switzerland
- Research stay at Harvard University in Cambridge (MA), USA (5 months)
- 09/2015 - 02/2017 **Preparatory year for MSc in Molecular and Biological Chemistry**
École Polytechnique Fédérale de Lausanne (EPFL) in Ecublens (VD), Switzerland
- 09/2010 - 09/2013 **BSc in Chemistry**
Zurich University of Applied Sciences (ZHAW) in Wädenswil (ZH), Switzerland
- Academic exchange semester at Worcester Polytechnic Institute (WPI) in Worcester (MA), USA
- 08/2006 - 08/2009 **Apprenticeship as a chemical lab technician (synthesis) with Vocational Matura**
Novartis Pharma AG in Basel (BS), Switzerland

Professional Experience

- 04/2014 - 07/2015 **Bachem AG** in Bubendorf (BL), Switzerland
Project Chemist: Synthesis of catalogue products (amino acids and small peptides) in liquid phase from grams to kilograms including process development (e.g. reaction optimization, up-scaling, purification, characterization).
- 09/2009 - 08/2010 **Novartis Institute for BioMedical Research (NIBR)** in Cambridge (MA), USA
Chemical laboratory technician: Synthesis of lipids and macromolecules for oligonucleotide based medicine.

Internships & Projects

- 09/2018 - 03/2023 **PhD Thesis:** *École Polytechnique Fédérale de Lausanne (EPFL)*, Group of Prof. Christian Heinis.
Title: "Development of methods for the synthesis of large combinatorial libraries of macrocyclic compounds"
- 02/2018 - 07/2018 **Master Thesis:** *École Polytechnique Fédérale de Lausanne (EPFL)*, Group of Prof. Nicolai Cramer.
Towards a "Synthetic Approach to the Phalloidin Class of Natural Products" with late-stage modifications.
- 09/2017 - 01/2018 **Research Internship:** *Harvard University*, Group of Prof. Andrew G. Myers.
Synthetic contribution to the development of a fully component-based synthesis platform for 1N-HABA gentamicin C1 amino glycoside antibiotics.
- 09/2013 - 10/2013 **Internship:** *Zurich University of Applied Sciences*, Group of Prof. Christiane Zaborosch.
Up- and downstream processing of glutathione-s-transferase.
- 05/2013 - 07/2013 **Bachelor Thesis:** *Zurich University of Applied Sciences*, Group of Prof. Christian Adlhart.
"Development of an *in vivo* screening method for moisturizers by Raman spectroscopy" involving a human pre-clinical study.
- 01/2013 - 02/2013 **Internship:** *Swiss Federal Institute of Technology in Zurich (ETHZ)*, Group of Prof. Peter Walde.
Enzymatic polymerization of conductive polyaniline with surfactant vesicles.
- 08/2012 - 12/2012 **Independent Study Project:** *Worcester Polytechnic Institute*, Group of Prof. Shawn C. Burdette
Synthesis of light sensitive azobenzene derivatives.

Languages

Swiss German: Mother tongue
English: C1 level

German: Mother tongue
French: B2 level

Other Competencies

- 10/2013 - 05/2021 **Compulsory military duty (CH):** Service in nuclear, biological and chemical (NBC) defence
Functions: Chemical, biological, radiological and nuclear (CBRN) detection and sampling
C1 driver
Rank: Gefreiter
Military training school: ABC Abw RS 58-3 in Spiez (BE), Switzerland
Served days: 245/245

Workshops: bench2biz - Workshop for young and aspiring entrepreneurs in science and technology

Innosuisse Buisness Concept
MINTT: Management of Innovation and Technology Transfer
Europe and US Drug/Device Product Development and Regulations

Teaching: Supervised two Master theses
Instructed three times the laboratory course "Experimental Biochemistry and Biophysics" (undergraduate course)
Corrected exams and occasionally supervised students in exercise hours for Biochemistry I (undergraduate course)

Conferences: SCS Therapeutic Peptide Seminar 2020, Basel, Switzerland (participation for conference report)
SCS Peptide Therapeutic Forum 2022, Basel, Switzerland (poster presentation)
SCS Fall meeting 2022, Zürich, Switzerland (oral presentation)
59th Japanese Peptide Symposium 2022, Sendai, Japan (oral presentation)

Others: CEM Webinars - Synthetic Peptide Libraries, 26.01.2023 (oral presentation)

Extracurricular Activities

Sports: Soccer, floorball, ping-pong, snowboarding, swimming, hiking and diving
University: Bachelor class of 2013 representative (2 years)
Jobs: Junior Enterprise EPFL - Performing a market study (Meili Technology SA) and document translation (E/G)
20% as a curry sausage vendor during my Master's (Wurst & Moritz, Bern, CH)
Summer job as a waiter (Aarequai 66, Thun, CH) and dishwasher (Pier 17, Oberhofen, CH)
Summer job as a laundry employee (Hotel Regina, Mürren, CH)
Interests: Reading (Economy), 3D printing, Blockchain, Arduino, travel and photography

Awards & Honourable mentions

04/10/2018: 1st place poster award (master thesis)
06/07/2009: Graduation with honours (chemical lab technician, Novartis Pharma AG)

Publications (7) & Patent (1)

- 8) Sevan Habeshian, Manuel Leonardo Merz, Gontran Sangouard, Ganesh Kumar Mothukuri, **Mischa Schüttel**, Zsolt Bognár, Cristina Díaz-Perlas, Jonathan Vesin, Julien Bortoli Chapalay, Gerardo Turcatti, Laura Cendron, Alessandro Angelini & Christian Heinis, Synthesis and direct assay of large macrocycle diversities by combinatorial late-stage modification at picomole scale, *Nat. Commun.* **2022**, 13, 3823 (co-author, research article).
- 7) Patrick Gonschorek, Alessandro Zorzi, Tamara Maric, Mathilde Le Jeune, **Mischa Schüttel**, Mathilde Montagnon, Rebeca Gómez-Ojea, Denis Patrick Vollmar, Chantal Whitfield, Luc Reymond, Vanessa Carle, Hitesh Verma, Oliver Schilling, Alain Hovnanian, and Christian Heinis, Phage Display Selected Cyclic Peptide Inhibitors of Kallikrein-Related Peptidases 5 and 7 and Their In Vivo Delivery to the Skin, *J. Med. Chem.* **2022**, 65 (14), 9735-9749 (co-author, research article, cover page).
- 6) Sevan Habeshian, Ganesh Sable, **Mischa Schüttel**, Manuel Merz and Christian Heinis, Cyclative Release Strategy to Obtain Pure Cyclic Peptides Directly from the Solid Phase, *ACS Chem. Biol.* **2022**, 17 (1), 181-186 (co-author, research article).
- 5) Gontran Sangouard, Alessandro Zorzi, Yufeng Wu, Edouard Ehret, **Mischa Schüttel**, Sangram Kale, Cristina Diaz Perlas, Jonathan Vesin, Julien Bortoli Chapalay, Gerardo Turcatti and Christian Heinis, Picomole-scale synthesis and screening of macrocyclic compound libraries by acoustic liquid transfer, *Angew. Chem. Int. Ed.* **2021**, 60 (40), 21702-21707 (co-author, research article).
- 4) World patent WO 2022242993 (A1) "Method for preparing a library of peptides and peptide (co-inventor, priority date: 17.05.2021).
- 3) Sevan Habeshian and **Mischa Schüttel**, 2nd Anglo-Swiss Symposium on 'Using Chemical Biology to Identify New Targets for Medicinal Chemistry, *Chimia* **2020**, 74 (4), 303 - 304 (conference report).
- 2) Jingjing Yan, Liam Wilbraham, Prem N. Basa, **Mischa Schüttel**, John C. MacDonald, Ilaria Ciofini, François-Xavier Coudert, and Shawn C. Burdette, Emissive Azobenzenes Delivered on a Silver Coordination Polymer, *Inorg. Chem.* **2018**, 57, 23, 15009–15022 (co-author, research article).
- 1) Katja Junker, Sandra Luginbühl, **Mischa Schüttel**, Louis Bertschi, Reinhard Kissner, Lukas D. Schuler, Boris Rakvin and Peter Walde, Efficient Polymerization of the Aniline Dimer p-Aminodiphenylamine (PADPA) with *Trametes versicolor* Laccase/O₂ as Catalyst and Oxidant and AOT Vesicles as Templates, *ACS Catal.* **2014**, 4 (10), 3421–3434 (co-author, research article).